Instituto de Investigación
en Recursos Cinegéticos

Characterization of the immune response to alpha-Gal antigen and possibilities for the control of infectious diseases

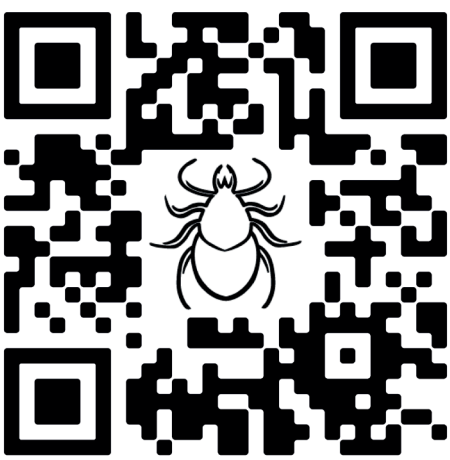

Iván Pacheco Carrillo

PhD Thesis

2022

La realización de esta tesis ha sido posible gracias a las siguientes entidades y proyectos:

Consejería de Educación, Cultura y Deportes, JCCM: proyecto CCM17-PIC-036 (SBPLY/17/180501/000185) cofinanciado por parte de la Junta de Castilla-La Mancha y del Fondo Europeo de Desarrollo Regional (FEDER), respetando lo dispuesto en el anexo XII del reglamento (UE) 1303/2013.

Ministerio de Ciencia e Innovación: Identificación y caracterización de biomoléculas en la saliva de garrapatas y mecanismos asociados con la respuesta inmune frente a alpha-Gal (BIOGAL); PID2020-116761GB-I00.

Characterization of the immune response to alpha-Gal antigen and possibilities for the control of infectious diseases

Caracterización de la respuesta inmune frente al antígeno alfa-Gal y posibilidades para el control de enfermedades infecciosas

Iván Pacheco Carrillo

PhD Thesis

Ciudad Real, 2022

Instituto de Investigación en Recursos Cinegéticos (IREC)
Grupo de Sanidad y Biotecnología, SaBio (Health and Biotechnology)
(CSIC-UCLM-JCCM)

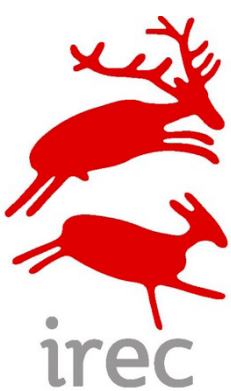

Universidad de Castilla-La Mancha
CAMPUS DE EXCELENCIA INTERNACIONAL

Characterization of the immune response to alpha-Gal antigen and possibilities for the control of infectious diseases

Trabajo de investigación presentado por
Iván Pacheco Carrillo
para optar al grado de Doctor
por la Universidad de Castilla-La Mancha

Vº Bº de los Directores

Dr. José de la Fuente García Dra. Margarita Villar Rayo Dr. Alejandro Cabezas-Cruz.

INSTITUTO DE INVESTIGACIÓN EN RECURSOS CINEGÉTICOS
CSIC-UCLM-JCCM
UNIVERSIDAD DE CASTILLA-LA MANCHA
DEPARTAMENTO DE CIENCIA Y TECNOLOGÍA AGROFORESTAL Y GENÉTICA
PROGRAMA DE DOCTORADO "CIENCIAS AGRARIAS Y AMBIENTALES"

"No tienes que ser grande para comenzar,
pero tienes que comenzar para ser grande".

Hilary Hinton "Zig" Ziglar

A mis padres y hermano,
la razón de mi existencia.

Summary

Abstract / Resumen

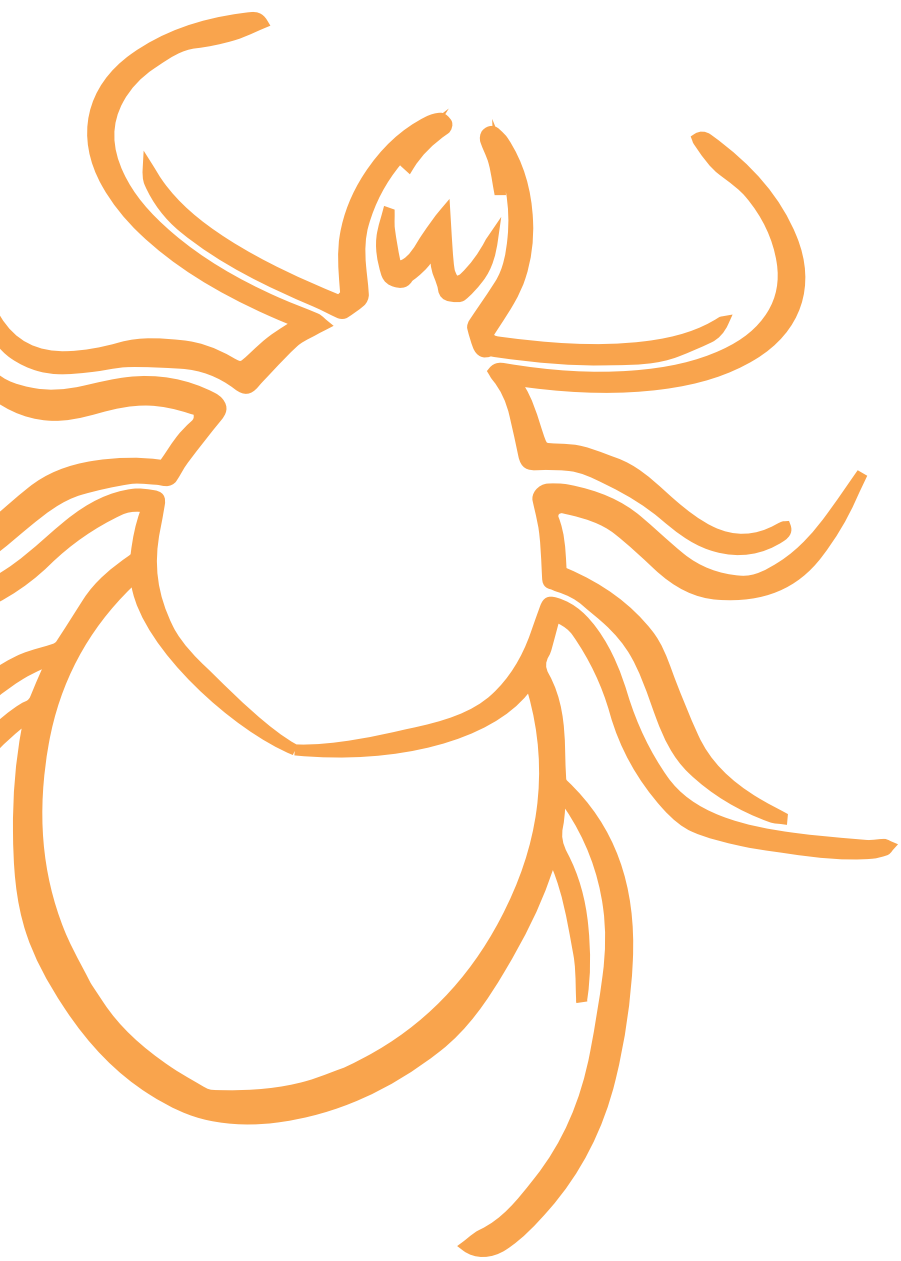

Abstract

Ticks are blood-feeding arthropod ectoparasite vectors of pathogens affecting human and animal health worldwide by increasing the prevalence of infectious diseases and allergic reactions such as the Alpha-Gal Syndrome (AGS).

Actually, tick-borne pathogens (TBPs) implicated in infestations and disease development are controlled mainly using chemical acaricides, with the harmful causes they generate on the environment and the selection of resistant ticks.

Vaccines are considered the most effective and eco-sustainable solution to control pathogen infection, multiplication and transmission, which is why omics technologies and bioinformatic tools have been optimized at the molecular and physiological level, identifying possible candidate protective antigens.

This doctoral thesis focuses on the characterization of the role of the carbohydrate alpha-Gal in vector-host-pathogen molecular interactions and the AGS. The results support alpha-Gal as candidate antigen to develop vaccines for the control of major infectious diseases and reduce the use of acaracides in support of the One Health approach.

Chapter 1:
Alpha-Gal content and origin in ticks

This chapter highlights the importance, variety and modifications that alpha-Gal presents in tick cementome and sialome proteins, being able to modulate the host´s immune system.

In **Chapter 1A**, a proteomics approach is used for the identification and characterization of proteins from tick species associated with the AGS in the United States (*Amblyomma americanum*) and Australia (*Ixodes holocyclus*) analyzing tick salivary glands (sialome SG), secreted saliva (sialome SA) and identifying those proteins with alpha-Gal modifications (alphagalactome SG and SA).

Thus, we provided candidate proteins such as cytoglobin-1, 14-3-3 family chaperone and vitellogenin-1 to advance in the characterization of the function of tick glycoproteins with alpha-Gal modifications in tick immune-mediated mechanisms and possible targets for diagnostic, prevention and control of the AGS.

Similarly, in **Chapter 1B** a proteomics approach is used to characterize the proteome of tick *Rhipicephalus microplus* salivary glands (sialome) and cement (cementome) together with their physical and chemical properties at different adult female parasitic stages.

We propose that some identified proteins and other biomolecules such as alpha-Gal may modulate the biochemical properties of cement in its formation, solidification, maintenance and function, changing the tick´s feeding adaptation.

Chapter 2: Immune response to alpha-Gal and implications for the Alpha-Gal Syndrome (AGS).

This chapter provides a broad overview of the allergic reactions triggered by the alpha-Gal carbohydrate present in glycoproteins from tick saliva. These glycoproteins with alpha-Gal modifications can induce in some individuals the production of high levels of anti-alpha-Gal IgE antibodies, which in most cases confirms the development of AGS symptoms.

However, the classical diagnosis of the AGS only measures anti-alpha-Gal IgE levels without considering all co-factors related to the clinical history that may affect the outcome of disease symptoms in alpha-Gal sensitized patients. Therefore, **Chapter 2A** proposes to include a complementary approach that also integrates the quantitation of tick sialome immunoreactive proteins and immune response markers such as interleukins (IL) IL-1 and IL-4 serum and/or mRNA levels for a more effective diagnosis of AGS.

Chapter 2B addresses this proposal by focusing on a dataset that compares cofactors such as blood group, age and sex on the IgE/IgM/IgG/IgA anti-alpha-Gal antibody response in healthy individuals and patients diagnosed with AGS, tick-borne allergies, GBS and COVID-19. This approach could provide insights into the role of anti-alpha-Gal antibody response in disease symptomatology and possible protective mechanisms.

In **Chapter 2C** we highlight a differential regulation in the antibody response to alpha-Gal in individuals with GBS compared to patients with allergic reactions in response to tick bites. The immune pathways of anti-alpha-Gal IgM/IgG and IgE production are independent and there are differences in the correlation analysis with respect to the different cases of GBS and allergy-type reactions to tick bites providing a new pipeline into the immune-mediated mechanisms associated with GBS.

We close this section by establishing a new animal model using zebrafish for the study of allergic reactions and the immune mechanisms in response to *Rhipicephalus sanguineus* saliva and its biogenic substances such as alpha-Gal and PGE_2 as well as red meat consumption (**Chapter 2D**).

We suggest evidence of similarities in alpha-Gal content and anti-alpha-Gal antibody response in humans and zebrafish after inoculation of these compounds in this animal model. Finally, basophils and some zebrafish immune response and food allergy markers such as interleukin-1beta perform a key role in the regulation of allergic reactions associated to tick saliva in tissue-specific Toll-like receptor (TLR) mediated responses in T helper cells.

Chapter 3: Protective capacity and mechanisms in response to alpha-Gal.

This chapter assesses the capacity of alpha-Gal to be used as a vaccine for the control of tuberculosis caused by *Mycobacterium marinum* in zebrafish model.

It provides a different perspective according to the proteomic approach used where alpha-Gal now also acts by inducing immune responses for the control of infections and multiplication of pathogens containing the alpha-Gal modification on their surface.

Chapter 3A addresses the protective effectiveness of vaccination with alpha-Gal using adjuvated and not adjuvated vaccine formulations. Results provided evidence that vaccination was effective developing protective mechanisms including B-cell maturation, antibody-mediated opsonization of mycobacteria, Fc receptor-mediated phagocytosis, macrophage response, interference with the alpha-Gal antagonistic effect of the TLR2/NF-kB-mediated immune response, and upregulation of pro-inflammatory cytokines.

In **Chapter 3B**, we propose a new model of vaccines using probiotics prepared with bacteria from the gut microbiota with high alpha-Gal content as an alternative to the use of antibiotics due to pathogens resistance and water contamination that they generate, among many other serious consequences. Probiotics containing *Aeromonas veronii* or *Pseudomonas entomophila* are biosafe and effective for the control of fish mycobacteriosis and are suggested, alone or in combination with alpha-Gal, for the control of infectious and/or allergic diseases.

Identically to **Chapter 3A**, we observe all the protective mechanisms that we mentioned above including beneficial effects on nutrient metabolism and reduced oxidative stress.

Resumen

Las garrapatas son ectoparásitos artrópodos que se alimentan de sangre. Actúan como vectores de patógenos, afectando la salud humana y animal por todo el mundo al aumentar la prevalencia de enfermedades infecciosas y reacciones alérgicas como es el síndrome de alfa-Gal (AGS).

Actualmente, los patógenos transmitidos por garrapatas (TBPs) implicados en infestaciones y desarrollo de enfermedades son controlados principalmente mediante acaricidas químicos, con los efectos nocivos que éstos pueden generar tanto sobre el medio ambiente, como por la selección de garrapatas resistentes.

Las vacunas son consideradas como la solución más eficaz y ecosostenible para controlar la infección, multiplicación y transmisión de patógenos, por lo que las tecnologías ómicas y herramientas bioinformáticas se han optimizado a nivel molecular y fisiológico, identificando posibles candidatos como antígenos protectores.

Esta tesis doctoral se centra en la caracterización del papel del carbohidrato alfa-Gal en las interacciones moleculares vector-hospedador-patógeno y el AGS. Los resultados respaldan como antígeno candidato a la molécula de alfa-Gal para el desarrollo de vacunas para el control de las principales enfermedades infecciosas y, con ello, reducir el uso de acaricidas en apoyo del concepto de "Una Salud".

Capítulo 1: Contenido y origen de alfa-Gal en garrapatas.

En este capítulo se destaca la importancia, variedad y modificaciones que presenta el alfa-Gal en las proteínas del cementoma y sialoma de la garrapata, siendo capaz de modular el sistema inmunológico del hospedador.

En el **Capítulo 1A**, se usa un enfoque proteómico para la identificación y caracterización de proteínas de especies de garrapatas asociadas con el AGS en los Estados Unidos (*Amblyomma americanum*) y Australia (*Ixodes holocyclus*), analizando las glándulas salivales de las garrapatas (sialoma SG) y la saliva secretada (sialoma SA) e identificando aquellas proteínas con modificaciones de alfa-Gal (alfagalactoma SG y SA).

Así, proporcionamos proteínas candidatas como son la citoglobina-1, la chaperona de la familia 14-3-3 y la vitelogenina-1 para avanzar en la caracterización de la función de las glicoproteínas de garrapata con modificaciones de alfa-Gal sobre los mecanismos inmunes mediados por garrapatas, así como posibles dianas para el diagnóstico, prevención y control del AGS.

De manera similar, en el **Capítulo 1B** se utiliza un enfoque proteómico para caracterizar el proteoma de las glándulas salivales (sialoma) y el cemento (cementoma) de la garrapata *Rhipicephalus microplus* junto con sus propiedades físicas y químicas en diferentes etapas parasitarias de hembras adultas.

Proponemos que algunas de las proteínas identificadas, y otras biomoléculas tales como el alfa-Gal, pueden modular las propiedades bioquímicas del cemento en su formación, solidificación, mantenimiento y función, cambiando la adaptación a la alimentación de la garrapata.

Capítulo 2: Respuesta inmune frente a alfa-Gal e implicaciones en el síndrome de alfa-Gal (AGS).

Este capítulo ofrece una amplia descripción general de las reacciones alérgicas desencadenadas por el carbohidrato alfa-Gal presente en las glicoproteínas de la saliva de las garrapatas. Estas glicoproteínas con modificaciones

alfa-Gal pueden inducir, en algunos individuos, la producción de altos niveles de anticuerpos anti-alfa-Gal IgE, lo que en la mayoría de los casos confirma el desarrollo de síntomas de AGS.

Sin embargo, el diagnóstico clásico de AGS sólo mide los niveles de IgE anti-alfa-Gal, sin considerar todos los cofactores relacionados con el historial clínico que pueden afectar el resultado de los síntomas de la enfermedad en pacientes sensibilizados al alfa-Gal. Así, el **Capítulo 2A** propone incluir un enfoque complementario, que integra también la cuantificación de proteínas inmunorreactivas del sialoma de garrapatas y los marcadores de respuesta inmunitaria, como son las interleucinas (IL) IL-1 e IL-4 en suero y/o los niveles de ARNm, para un diagnóstico más eficaz del AGS.

El **Capítulo 2B** aborda esta propuesta centrándose en una base de datos que compara cofactores como el grupo sanguíneo, la edad y el sexo en la respuesta de anticuerpos IgE/IgM/IgG/IgA anti-alfa-Gal en individuos sanos y pacientes diagnosticados con AGS, con alergias transmitidas por picaduras de garrapatas, con el síndrome de Guillain-Barré (GBS) y, finalmente, con pacientes con COVID-19. Este enfoque podría proporcionar información sobre el papel de la respuesta de anticuerpos anti-alfa-Gal en la sintomatología de la enfermedad y los posibles mecanismos de protección asociados.

En el **Capítulo 2C,** destacamos una regulación diferencial en la respuesta de anticuerpos frente a alfa-Gal en individuos con GBS en comparación con los pacientes que presentaban reacciones alérgicas como respuesta a picaduras de garrapatas. Las vías inmunitarias de producción de IgM/IgG e IgE anti-alfa-Gal son independientes, y existen diferencias en el análisis de correlación en los diferentes casos de GBS y aquellos con reacciones alérgicas a las picaduras de garrapatas, lo que proporciona una nueva fuente de información sobre los mecanismos inmunológicos asociados con el GBS.

Cerramos esta sección estableciendo un nuevo modelo animal, utilizando el pez cebra, para el estudio de las reacciones alérgicas y los mecanismos inmunológicos en respuesta a la saliva de *Rhipicephalus sanguineus* y determinadas

sustancias biogénicas que presenta, como son el alfa-Gal y la prostaglandina E2 (PGE_2), así como tras el consumo de carne roja (**Capítulo 2D**).

Hay evidentes similitudes en el contenido de alfa-Gal y la respuesta de anticuerpos anti-alfa-Gal en humanos y pez cebra tras la inoculación de estos compuestos en este modelo animal. Finalmente, los basófilos y algunos marcadores de respuesta inmune y de alergia alimentaria del pez cebra, como la interleucina-1beta, desempeñan un papel clave en la regulación de las reacciones alérgicas asociadas a la saliva de la garrapata, en respuestas mediadas por receptores tipo Toll (TLR) específicos de tejido en células Th.

Capítulo 3: Capacidad protectora y mecanismos en respuesta a alfa-Gal.

Este capítulo evalúa la capacidad de alfa-Gal para ser utilizado como vacuna para el control de la tuberculosis causada por *Mycobacterium marinum* en el modelo de pez cebra.

Proporciona una perspectiva diferente de acuerdo al enfoque proteómico utilizado, donde ahora el alfa-Gal también actúa induciendo respuestas inmunes para el control de infecciones y la multiplicación de patógenos que contienen una modificación de alfa-Gal en su superficie.

El **Capítulo 3A** aborda la eficacia protectora de la vacunación con alfa-Gal utilizando diferentes formulaciones de vacunas, con y sin adyuvantes. Los resultados proporcionaron evidencias de que la vacunación fue eficaz en el desarrollo de mecanismos de protección, entre los que se incluyen la maduración de células B, la opsonización de micobacterias mediada por anticuerpos, la fagocitosis mediada por receptores Fc, la respuesta de macrófagos, la interferencia con el efecto antagonista del alfa-Gal en la respuesta inmune mediada por TLR2/NF-kB y la regulación positiva de citocinas proinflamatorias.

En el **Capítulo 3B,** proponemos un nuevo modelo de vacunas utilizando probióticos preparados con bacterias de la microbiota intestinal con alto con-

tenido en alfa-Gal, como alternativa al uso de antibióticos, debido a la resistencia de los patógenos y a la contaminación del agua que generan, entre otras consecuencias graves. Los probióticos que contienen *Aeromonas veronii* o *Pseudomonas entomophila* son bioseguros y efectivos para el control de la micobacteriosis en peces y se recomienda su uso, sólos o en combinación con alfa-Gal, para el control de enfermedades infecciosas y/o alérgicas.

De manera idéntica al **Capítulo 3A**, observamos todos los mecanismos de protección que mencionamos anteriormente, incluyendo efectos beneficiosos sobre el metabolismo de los nutrientes y la reducción del estrés oxidativo.

General Introduction

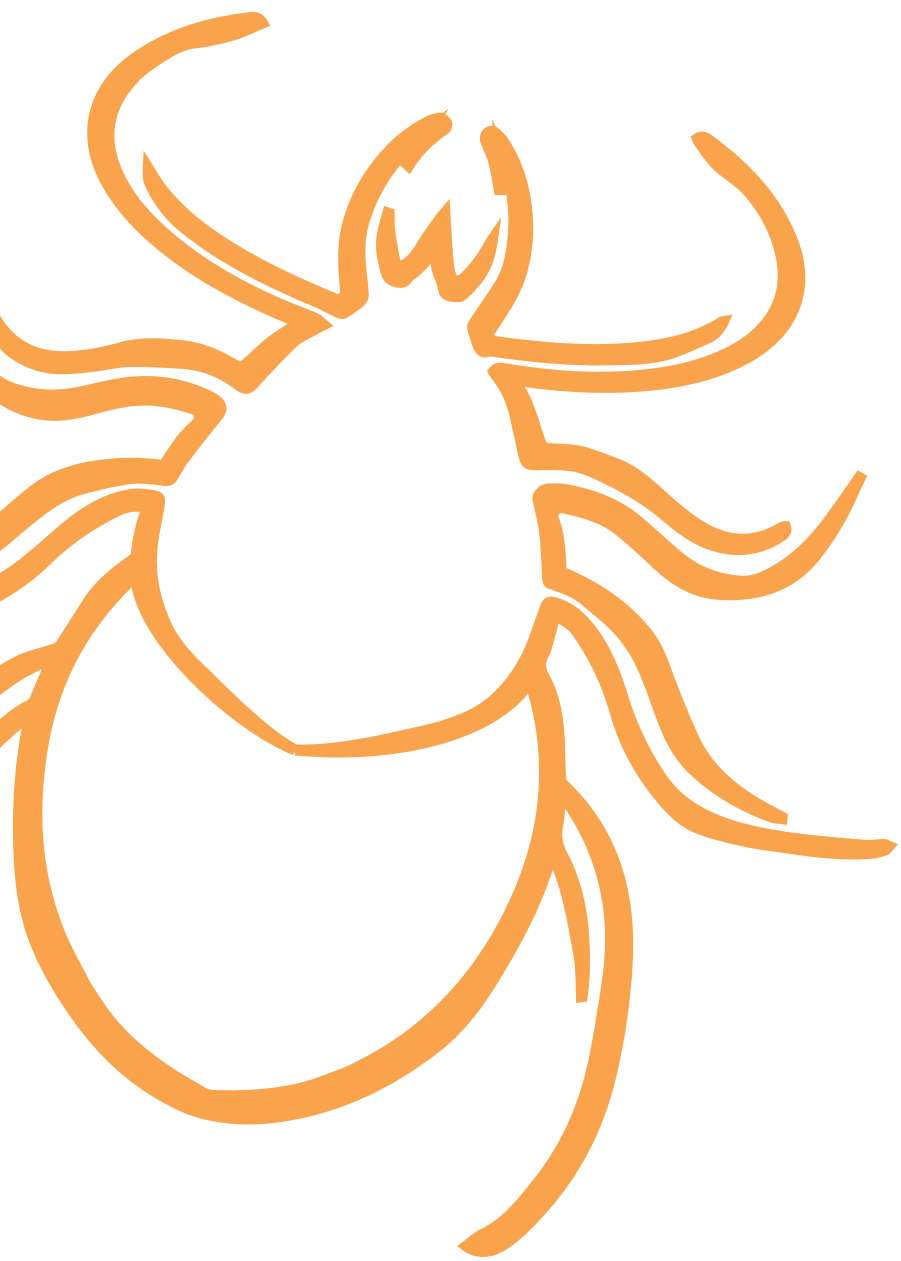

General Introduction

de la Fuente, J., **Pacheco, I.,** Villar, M., Cabezas-Cruz, A. (2019). The alpha-Gal syndrome: new insights into the tick-host conflict and cooperation. Parasites & Vectors 12, 154. https://doi.org/10.1186/s13071-019-3413-z

de la Fuente *et al. Parasites Vectors* (2019) 12:154
https://doi.org/10.1186/s13071-019-3413-z

Parasites & Vectors

PRIMER Open Access

The alpha-Gal syndrome: new insights into the tick-host conflict and cooperation

José de la Fuente[1,2*], Iván Pacheco[1], Margarita Villar[1] and Alejandro Cabezas-Cruz[3]

Abstract

This primer focuses on a recently diagnosed tick-borne allergic disease known as the alpha-Gal syndrome (AGS). Tick bites induce in humans high levels of IgE antibodies against the carbohydrate Galα1-3Galβ1-(3)4GlcNAc-R (α-Gal) present on tick salivary glycoproteins and tissues of non-catarrhine mammals, leading to the AGS in some individuals. This immune response evolved as a conflict and cooperation between ticks and human hosts including their gut microbiota. The conflict is characterized by the AGS that mediate delayed anaphylaxis to red meat consumption and certain drugs such as cetuximab, and immediate anaphylaxis to tick bites. The cooperation is supported by the capacity of anti-α-Gal IgM and IgG antibody response to protect against pathogens with α-Gal on their surface. Despite the growing diagnosis of AGS in all world continents, many questions remain to be elucidated on the tick proteins and immune mechanisms triggering this syndrome, and the protective response against pathogen infection elicited by anti-α-Gal antibodies. The answer to these questions will provide information for the evaluation of risks, diagnosis and prevention of the AGS, and the possibility of using the carbohydrate α-Gal to develop vaccines for the control of major infectious diseases.

Keywords: Tick, Allergy, Alpha-Gal syndrome, Vaccine, Immune response

What is the alpha-Gal syndrome (AGS)?

The main objective of our research is the characterization of vector-host-pathogen molecular interactions, and translating this basic biological information into new interventions for the diagnosis, prevention and control of vector-borne diseases [1–3] (see also video at https://youtu.be/DhbBjQSuLYk). Arthropod vector-borne diseases are a growing problem worldwide, and ticks are only second to mosquitoes as vectors of human diseases and the most important vectors in animals [4–6].

The alpha-Gal syndrome (AGS) is triggered by IgE antibody response against the carbohydrate Galα1-3Galβ1-(3)4GlcNAc-R (α-Gal), which is present in glycoproteins from tick saliva and tissues of non-catarrhine mammals [7–13] (Additional file 1: Figure S1). In 2007, van Nunen et al. [7] first described the association between tick bites and the development of mammalian meat allergy. In 2009, Commins et al. [11] confirmed this association and discovered the epitope likely responsible for such allergic reactions, (α-Gal). Old World monkeys, apes and humans evolved with the inactivation of the α-1,3-galactosyltransferase (GalT) gene, which resulted in the recognition of α-Gal to produce high antibody titers against this antigen [12] (Additional file 1: Figure S1). Tick bites induce high levels of anti-α-Gal IgE antibodies in humans that mediate delayed anaphylaxis to red meat consumption, and immediate anaphylaxis to tick bites, xenotransplantation and certain drugs such as cetuximab [13, 14].

The AGS is becoming a global problem with increasing prevalence in all continents, and several tick species have been implicated in these disorders [10, 15] (Additional file 1: Figure S1). Remarkably, most of the patients that become allergic, had tolerated red meat for many years before being sensitized by tick bites [10]. This finding suggests that while IgG and IgM antibody responses to α-Gal produced by some bacteria of the gut microbiota are beneficial as they protect against infection by pathogens such

*Correspondence: jose_delafuente@yahoo.com
[1] SaBio, Instituto de Investigación en Recursos Cinegéticos (IREC), Consejo Superior de Investigaciones Científicas (CSIC), Universidad de Castilla-La Mancha (UCLM)-Junta de Comunidades de Castilla-La Mancha (JCCM), Ronda de Toledo s/n, 13005 Ciudad Real, Spain
Full list of author information is available at the end of the article

as malaria parasites and tuberculosis mycobacteria, anti-α-Gal IgE antibodies induced by tick bites break the oral tolerance to food allergens and induce anaphylactic reactions to tick α-Gal-containing salivary proteins [7–15].

Why only some individuals develop the AGS in response to tick bites?

Tick saliva is a complex mixture of pharmacologically active compounds with a role in tick attachment cement and feeding, pathogen transmission, and the inhibition of host defensive mechanisms through immunomodulatory, anti-hemostatic and anti-inflammatory molecules [16–26]. Transcriptomics, proteomics and metabolomics studies of tick salivary glands, saliva and cement discovered clusters of functionally related proteins with protease inhibitors being the most abundant group of tick salivary secreted proteins in *Ixodes scapularis* [16, 18, 20–26]. The genes coding for some of these proteins are usually expressed sequentially throughout tick feeding, bringing up the question of whether this phenomenon could be a form of antigenic variation [16]. Tick saliva modulates host immunity towards a T helper 2 (Th-2) response and suppresses inflammatory responses [27], thus deviating the host immune response to profiles that are less damaging to the feeding tick and pathogen transmission. Apart from proteins with immunomodulatory activity, ticks also produce non-protein molecules such as prostaglandin E2 (PGE_2), which is synthesized in the tick salivary glands and secreted via the saliva into the feeding lesion [26, 28].

Humans do not synthesize the carbohydrate α-Gal, and therefore all the sources of α-Gal for the human body are from non-human origin [9, 11–13, 29]. Consequently, humans can develop a potent immune response against this carbohydrate [9, 11–13, 29]. Recently, we demonstrated that ticks synthesize α-Gal with functional GalTs with implications of this protein modification in tick feeding and *Anaplasma phagocytophilum* infection [30]. Considering these facts, evidence supports a role for α-Gal-containing tick salivary proteins in the development of the AGS, possibly in conjunction with other tick salivary components [9, 11–13, 29]. At least two possible mechanisms explain the production in humans of anti-α-Gal IgE antibodies after tick bites (Additional file 1: Figure S1). The first mechanism is supported by our current understanding of the host immune modulation by tick saliva, and proposes that α-Gal on tick salivary proteins interacts with antigen-presenting cells (APC) and B lymphocytes in the context of Th2 cell-mediated immunity induced by tick saliva. Basophils and released histamine have been implicated in IgE-mediated acquired protective immunity to tick infestations and chronic itch [31–35]. This mechanism leads to the elevation of the anti-α-Gal IgE response [16, 28]. The second mechanism needs to be demonstrated, and is based on the possibility that tick saliva contains factors that induce class switch recombination (CSR) to anti-α-Gal IgE producing B cells of pre-existing B cell clones producing anti-α-Gal IgM and/or IgG antibodies [28].

Tick salivary proteins with or without α-Gal modifications that may be involved in triggering the AGS have not been identified, but some α-Gal-containing proteins have been shown to be recognized by patients with anaphylactic reaction to tick bite and not by healthy individuals with a record of tick bites [14]. The characterization of tick proteins involved in AGS and the immune mechanisms triggering this syndrome is essential to answer the question of why only some individuals develop the AGS in response to tick bites [36–38] (Additional file 1: Figure S1). Tick sialome and alphagalactome profiles probably change as tick feeding proceeds thus highlighting the importance of the characterization of proteome changes during tick stages on the host to provide information on the abundance and risks associated with these proteins at different tick feeding stages. Furthermore, tick proteins present in the tick sialome and reacting with IgE in patients but not control sera could be used for the diagnosis of a predisposing condition for AGS. Tick sialome proteins with α-Gal modification (alphagalactome) and recognized by patients but not sera from healthy individuals exposed to tick bites could be selected as candidate protective antigens for the treatment and prevention of the AGS.

Risk factors associated to AGS may include genetic/immune mechanisms such as atopy, and ABO blood group composition leading to strong IgE response against α-Gal after tick bite, and ecological components associated to exposure to tick bites [9, 37, 39–44]. Other factors such as alcohol consumption, physical exercise, cat ownership and infection with pet-associated endoparasites, age and use of some medications may also influence the risk of developing the AGS [37, 42]. A conjunction of these and other still unknown factors may affect the development of AGS by some individuals exposed to tick bites.

Can we benefit from the risk of developing the AGS?

Tick-host-pathogen interactions evolved as a conflict and cooperation [45]. In this context, the AGS evolved as a trade-off to benefit humans by providing immunity to pathogens containing α-Gal while increasing the risks to develop this syndrome [12, 39] (Additional file 1: Figure S1).

Some of the major infectious diseases worldwide are caused by pathogens such as *Plasmodium*,

Mycobacterium, *Trypanosoma*, *Borrelia* and *Leishmania* species with a common characteristic of having α-Gal on their surface [39, 46–52]. As proposed for viruses with envelope-exposed α-Gal as the major evolutionary driver for the lack of functional GalT for α-Gal synthesis in humans, the possibility of developing protective antibodies against this carbohydrate resulted in an effective protection against pathogens with α-Gal [12]. This evolutionary advantage of humans relays on anti-α-Gal IgM and IgG antibodies produced in response to gut bacterial microbiota, tick infestations and/or pathogen infection with a protective effect against some infectious diseases [46–52]. However, this evolutionary cooperation between ticks and humans also leads to the conflict of increasing the risks for developing AGS in response to tick bites.

As previously proposed, we may benefit from this tick-host conflict and cooperation [46, 47] (Additional file 1: Figure S1). Gut bacteria with high α-Gal content selected from individuals with protective immune response against pathogens with α-Gal could be used to develop a probiotic-based easy to administer and low-cost vaccine that could by administered by different routes alone or in combination with α-Gal-containing tick proteins to provide protection against multiple pathogens causing major infectious diseases worldwide [46, 47]. If proven true, this would be a major advance in the control of infectious diseases affecting populations in different parts of the world.

Conclusions

The AGS has been associated with tick bites and constitutes a growingly diagnosed disease worldwide. Nevertheless, many questions remain to be elucidated on the tick proteins and immune mechanisms triggering this syndrome, and the protective response against pathogen infection elicited by anti-α-Gal antibodies. Future research should focus at the identification of tick proteins involved in the production of anti-α-Gal IgE antibodies after tick bite, and the immune mechanisms leading to AGS. The relationship between different tick species/developmental stages and the AGS applying Koch's postulates in GalT negative animal models would contribute to a better understanding of the disease and the evaluation of epidemiological risks. Data on blood group type should be included in epidemiological studies to better evaluate the risks for AGS associated with blood type in the population, and the putative role of anti-α-Gal IgM and IgG antibodies in protection against pathogens with α-Gal. Other factors that may affect the AGS such as endoparasite infections and microbiota composition in both humans and ticks should be considered. The answer to these questions will provide information for the evaluation of risks, diagnosis and prevention of the AGS, and the possibility of using the carbohydrate α-Gal to develop vaccines for the control of major infectious diseases.

Additional file

Additional file 1: Figure S1. Poster of tick-host conflict and cooperation in the AGS: facts, challenges and possibilities.

Abbreviations

AGS: alpha-Gal syndrome; α-Gal: Galα1-3Galβ1-(3)4GlcNAc-R; GalT: galactosyltransferase; Th-2: PGE2: T helper 2, prostaglandin E2; APC: antigen-presenting cells; CSR: class switch recombination.

Acknowledgements

We thank members of our laboratories for fruitful discussion.

Funding

The preparation of this manuscript was partially supported by the Consejería de Educación, Cultura y Deportes, JCCM, Spain, project CCM17-PIC-036 (SBPLY/17/180501/000185). MV was supported by the University of Castilla La Mancha, Spain.

Availability of data and materials

Not applicable.

Authors' contributions

JF conceived the primer focus and outline. JF, IP, MV and AC-C contributed to the design of the poster and editing of the manuscript. AC-C contributed images for the figures in the poster. JF and IP prepared the poster. JF and AC-C wrote the manuscript. All authors read and approved the final manuscript.

Ethics approval and consent to participate

Not applicable.

Consent for publication

Not applicable.

Competing interests

The authors declare that they have no competing interests.

Publisher's Note

Author details

[1] SaBio, Instituto de Investigación en Recursos Cinegéticos (IREC), Consejo Superior de Investigaciones Científicas (CSIC), Universidad de Castilla-La Mancha (UCLM)-Junta de Comunidades de Castilla-La Mancha (JCCM), Ronda de Toledo s/n, 13005 Ciudad Real, Spain. [2] Department of Veterinary Pathobiology, Center for Veterinary Health Sciences, Oklahoma State University, Stillwater, OK 74078, USA. [3] UMR BIPAR, INRA, ANSES, Ecole Nationale Vétérinaire d'Alfort, Université Paris-Est, Maisons-Alfort 94700, France.

Received: 13 February 2019 Accepted: 27 March 2019
Published online: 03 April 2019

References

1. de la Fuente J, Contreras M, Estrada-Peña A, Cabezas-Cruz A. Targeting a global health problem: vaccine design and challenges for the control of tick-borne diseases. Vaccine. 2017;35:5089–94.
2. de la Fuente J, Antunes S, Bonnet S, Cabezas-Cruz A, Domingos A, Estrada-Peña A, et al. Tick-pathogen interactions and vector competence:

identification of molecular drivers for tick-borne diseases. Front Cell Infect Microbiol. 2017;7:114.
3. de la Fuente J. Controlling ticks and tick-borne diseases … looking forward. Ticks Tick Borne Dis. 2018;9:1354–7.
4. Jones KE, Patel NG, Levy MA, Storeygard A, Balk D, Gittleman JL, et al. Global trends in emerging infectious diseases. Nature. 2008;2451:990–3.
5. Estrada-Peña A, Ostfeld RS, Peterson AT, Poulin R, de la Fuente J. Effects of environmental change on zoonotic disease risk: an ecological primer. Trends Parasitol. 2014;30:205–14.
6. de la Fuente J, Estrada-Peña A, Venzal JM, Kocan KM, Sonenshine DE. Overview: ticks as vectors of pathogens that cause disease in humans and animals. Front Biosci. 2008;13:6938–46.
7. van Nunen S, O'Connor KS, Clarke LR, Boyle RX, Fernando SL. The association between *Ixodes holocyclus* tick bite reactions and red meat allergy. Intern Med J. 2007;39:A132.
8. Cabezas-Cruz A, Valdés J, de la Fuente J. Cancer research meets tick vectors for infectious diseases. Lancet Infect Dis. 2014;10:916–7.
9. Steinke JW, Platts-Mills TA, Commins SP. The alpha-gal story: lessons learned from connecting the dots. J Allergy Clin Immunol. 2015;135:589–96.
10. Platts-Mills TA, Schuyler AJ, Tripathi A, Commins SP. Anaphylaxis to the carbohydrate side chain alpha-gal. Immunol Allergy Clin North Am. 2015;35:247–60.
11. Commins SP, Satinover SM, Hosen J, Mozena J, Borish L, Lewis BD, et al. Delayed anaphylaxis, angioedema, or urticaria after consumption of red meat in patients with IgE antibodies specific for galactose-alpha-1,3-galactose. J Allergy Clin Immunol. 2009;123:426–33.
12. Galili U. Evolution in primates by "Catastrophic-selection" interplay between enveloped virus epidemics, mutated genes of enzymes synthesizing carbohydrate antigens, and natural anticarbohydrate antibodies. Am J Phys Anthropol. 2018;168:352–63.
13. Hilger C, Fischer J, Wölbing F, Biedermann T. Role and mechanism of galactose-alpha-1,3-galactose in the elicitation of delayed anaphylactic reactions to red meat. Curr Allergy Asthma Rep. 2019;19:3.
14. Mateos-Hernández L, Villar M, Moral A, García Rodríguez C, Alfaya Arias T, De La Osa V, et al. Tick-host conflict: immunoglobulin E antibodies to tick proteins in patients with anaphylaxis to tick bite. Oncotarget. 2017;8:20630–44.
15. Kwak M, Somerville C, van Nunen S. A novel Australian tick *Ixodes* (*Endopalpiger*) *australiensis* inducing mammalian meat allergy after tick bite. Asia Pac Allergy. 2018;8:e31.
16. Chmelař J, Kotál J, Kopecký J, Pedra JHF, Kotsyfakis M. All for one and one for all on the tick-host battlefield. Trends Parasitol. 2016;32:368–77.
17. Nuttall PA. Wonders of tick saliva. Ticks Tick Borne Dis. 2019;10:470–81.
18. Kim TK, Tirloni L, Pinto AF, Moresco J, Yates JR 3rd, da Silva Vaz I, et al. *Ixodes scapularis* tick saliva proteins sequentially secreted every 24 h during blood feeding. PLoS Negl Trop Dis. 2016;10:e0004323.
19. Hajdušek O, Šíma R, Ayllón N, Jalovecká M, Perner J, de la Fuente J, et al. Interaction of the tick immune system with transmitted pathogens. Front Cell Infect Microbiol. 2013;3:26.
20. Anderson JM, Moore IN, Nagata BM, Ribeiro JMC, Valenzuela JG, Sonenshine DE. Ticks, *Ixodes scapularis*, feed repeatedly on white-footed mice despite strong inflammatory response: an expanding paradigm for understanding tick-host interactions. Front Immunol. 2017;8:1784.
21. Kazimírová M, Štibrániová I. Tick salivary compounds: their role in modulation of host defences and pathogen transmission. Front Cell Infect Microbiol. 2013;3:43.
22. Suppan J, Engel B, Marchetti-Deschmann M, Nürnberger S. Tick attachment cement - reviewing the mysteries of a biological skin plug system. Biol Rev Camb Philos Soc. 2018;93:1056–76.
23. Hoxmeier JC, Fleshman AC, Broeckling CD, Prenni JE, Dolan MC, Gage KL, et al. Metabolomics of the tick-*Borrelia* interaction during the nymphal tick blood meal. Sci Rep. 2017;7:44394.
24. Ayllón N, Villar V, Galindo RC, Kocan KM, Šíma R, López JA, et al. Systems biology of tissue-specific response to *Anaplasma phagocytophilum* reveals differentiated apoptosis in the tick vector *Ixodes scapularis*. PLoS Genet. 2015;11:e1005120.
25. Abreu MR, Pereira MC, Simioni PU, Nodari EF, Paiatto LN, Camargo-Mathias MI. Immunomodulatory and morphophysiological effects of *Rhipicephalus sanguineus s.l.* (Acari: Ixodidae) salivary gland extracts. Vet Immunol Immunopathol. 2019;207:36–45.
26. Oliveira CJ, Sá-Nunes A, Francischetti IM, Carregaro V, Anatriello E, Silva JS, et al. Deconstructing tick saliva: non-protein molecules with potent immunomodulatory properties. J Biol Chem. 2011;286:10960–9.
27. Preston SG, Majtán J, Kouremenou C, Rysnik O, Burger LF, Cabezas-Cruz A, et al. Novel immunomodulators from hard ticks selectively reprogramme human dendritic cell responses. PLoS Pathog. 2013;9:e1003450.
28. Cabezas-Cruz A, Mateos-Hernández L, Chmelař J, Villar M, de la Fuente J. Salivary prostaglandin E2: role in tick-induced allergy to red meat. Trends Parasitol. 2017;33:495–8.
29. Cabezas-Cruz A, Mateos-Hernández L, Pérez-Cruz M, Valdés J, Fernández de Mera IG, Villar M, et al. Regulation of the immune response to α-gal and vector-borne diseases. Trends Parasitol. 2015;31:470–6.
30. Cabezas-Cruz A, Espinosa PJ, Alberdi P, Šimo L, Valdés JJ, Mateos-Hernández L, et al. Tick galactosyltransferases are involved in α-Gal synthesis and play a role during *Anaplasma phagocytophilum* infection and *Ixodes scapularis* tick vector development. Sci Rep. 2018;8:14224.
31. Wada T, Ishiwata K, Koseki H, Ishikura T, Ugajin T, Ohnuma N, et al. Selective ablation of basophils in mice reveals their nonredundant role in acquired immunity against ticks. J Clin Invest. 2010;120:2867–75.
32. Karasuyama H, Yamanishi Y. Basophils have emerged as a key player in immunity. Curr Opin Immunol. 2014;31:1–7.
33. Tabakawa Y, Ohta T, Yoshikawa S, Robinson EJ, Yamaji K, Ishiwata K, et al. Histamine released from skin-infiltrating basophils but not mast cells is crucial for acquired tick resistance in mice. Front Immunol. 2018;9:1540.
34. Hashimoto T, Rosen JD, Sanders KM, Yosipovitch G. Possible roles of basophils in chronic itch. Exp Dermatol. 2018. https://doi.org/10.1111/exd.13705.
35. Karasuyama H, Tabakawa Y, Ohta T, Wada T, Yoshikawa S. Crucial role for basophils in acquired protective immunity to tick infestation. Front Physiol. 2018;9:1769.
36. Hamsten C, Tran TAT, Starkhammar M, Brauner A, Commins SP, Platts-Mills TAE, et al. Red meat allergy in Sweden: association with tick sensitization and B-negative blood groups. J Allergy Clin Immunol. 2013;132:1431–4.
37. Fischer J, Lupberger E, Hebsaker J, Blumenstock G, Aichinger E, Yazdi AS, et al. Prevalence of type I sensitization to alpha-gal in forest service employees and hunters. Allergy. 2017;72:1540–7.
38. Bircher AJ, Hofmeier KS, Link S, Heijnen I. Food allergy to the carbohydrate galactose-alpha-1,3-galactose (alpha-Gal): four case reports and a review. Eur J Dermatol. 2017;27:3–9.
39. Cabezas-Cruz A, Mateos-Hernández L, Alberdi P, Villar M, Riveau G, Hermann E, et al. Effect of blood type on anti-α-Gal immunity and the incidence of infectious diseases. Exp Mol Med. 2017;49:e301.
40. Commins SP, James HR, Kelly LA, Pochan SL, Workman LJ, Perzanowski MS, et al. The relevance of tick bites to the production of IgE antibodies to the mammalian oligosaccharide galactose-α-1,3-galactose. J Allergy Clin Immunol. 2011;127(1286–93):e6.
41. van Nunen S. Tick-induced allergies: mammalian meat allergy and tick anaphylaxis. Med J Aust. 2018;208:316–21.
42. Gonzalez-Quintela A, Dam Laursen AS, Vidal C, Skaaby T, Gude F, Linneberg A. IgE antibodies to alpha-Gal in the general adult population: relationship with tick bites, atopy, and cat ownership. Clin Exp Allergy. 2014;44:1061–8.
43. Villalta D, Pantarotto L, Da Re M, Conte M, Sjolander S, Borres MP, et al. High prevalence of SIgE to galactose-α-1,3-galactose in rural pre-alps area: a cross-sectional study. Clin Exp Allergy. 2016;46:377–80.
44. Rispens T, Derksen NI, Commins SP, Platts-Mills TA, Aalberse RC. IgE production to α-Gal is accompanied by elevated levels of specific igg1 antibodies and low amounts of IgE to blood group B. PLoS One. 2013;8:e55566.
45. de la Fuente J, Villar M, Cabezas-Cruz A, Estrada-Peña A, Ayllón N, Alberdi P. Tick-host-pathogen interactions: conflict and cooperation. PLoS Pathog. 2016;12:e1005488.
46. Cabezas-Cruz A, de la Fuente J. Immunity to α-Gal: toward a single-antigen pan-vaccine to control major infectious diseases. ACS Cent Sci. 2017;3:1140–2.
47. Cabezas-Cruz A, de la Fuente J. Immunity to α-Gal: the opportunity for malaria and tuberculosis control. Front Immunol. 2017;8:1733.
48. Galili U, Mandrell RE, Hamadeh RM, Shohet SB, Griffiss JM. Interaction between human natural anti-α-galactosyl immunoglobulin G and bacteria of the human flora. Infect Immun. 1988;56:1730–7.

49. Yilmaz B, Portugal S, Tran TM, Gozzelino R, Ramos S, Gomes J, et al. Gut microbiota elicits a protective immune response against malaria transmission. Cell. 2014;159:1277–89.
50. Almeida IC, Milani SR, Gorin PA, Travassos LR. Complement-mediated lysis of *Trypanosoma cruzi* trypomastigotes by human anti-alpha-galactosyl antibodies. J Immunol. 1991;146:2394–400.
51. Almeida IC, Krautz GM, Krettli AU, Travassos LR. Glycoconjugates of *Trypanosoma cruzi*: a 74 kD antigen of trypomastigotes specifically reacts with lytic anti-alpha-galactosyl antibodies from patients with chronic Chagas disease. J Clin Lab Anal. 1993;7:307–16.
52. Moura APV, Santos LCB, Brito CRN, Valencia E, Junqueira C, Filho AAP, et al. Virus-like particle display of the α-Gal carbohydrate for vaccination against *Leishmania* infection. ACS Cent Sci. 2017;3:1026–31.

Hypothesis and Objectives

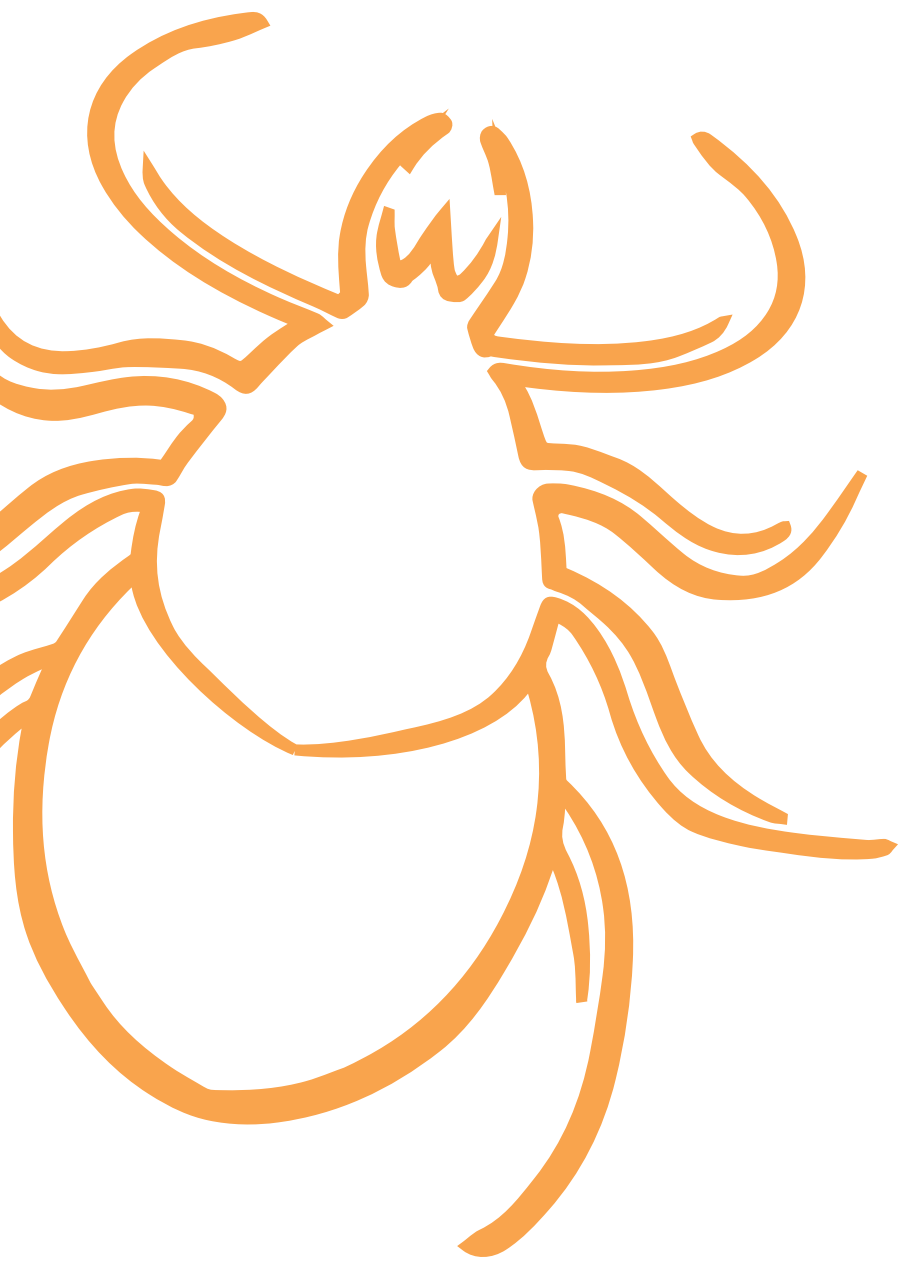

Hypothesis and Objectives

HYPOTHESIS

Humans evolved by losing the capacity to synthesize alpha-Gal because it provides the possibility to control infectious diseases while developing allergic reactions such as the Alpha-Gal Syndrome (AGS).

OBJECTIVES

General objective:

To understand the mechanisms involved in the immune response to glycan alpha-Gal synthesized by ticks and related to the Alpha-Gal Syndrome, and how this information may translate into control interventions for infectious diseases caused by pathogens with this modification on their surface.

Specific objectives:

1. Characterization of the alpha-Gal content and origin in ticks.
2. Characterization of the immune response to alpha-Gal and implications for the Alpha-Gal Syndrome.
3. Characterization of the protective capacity and mechanisms in response to alpha-Gal.

CHAPTER 1.
Alfha-Gal content and origin in ticks

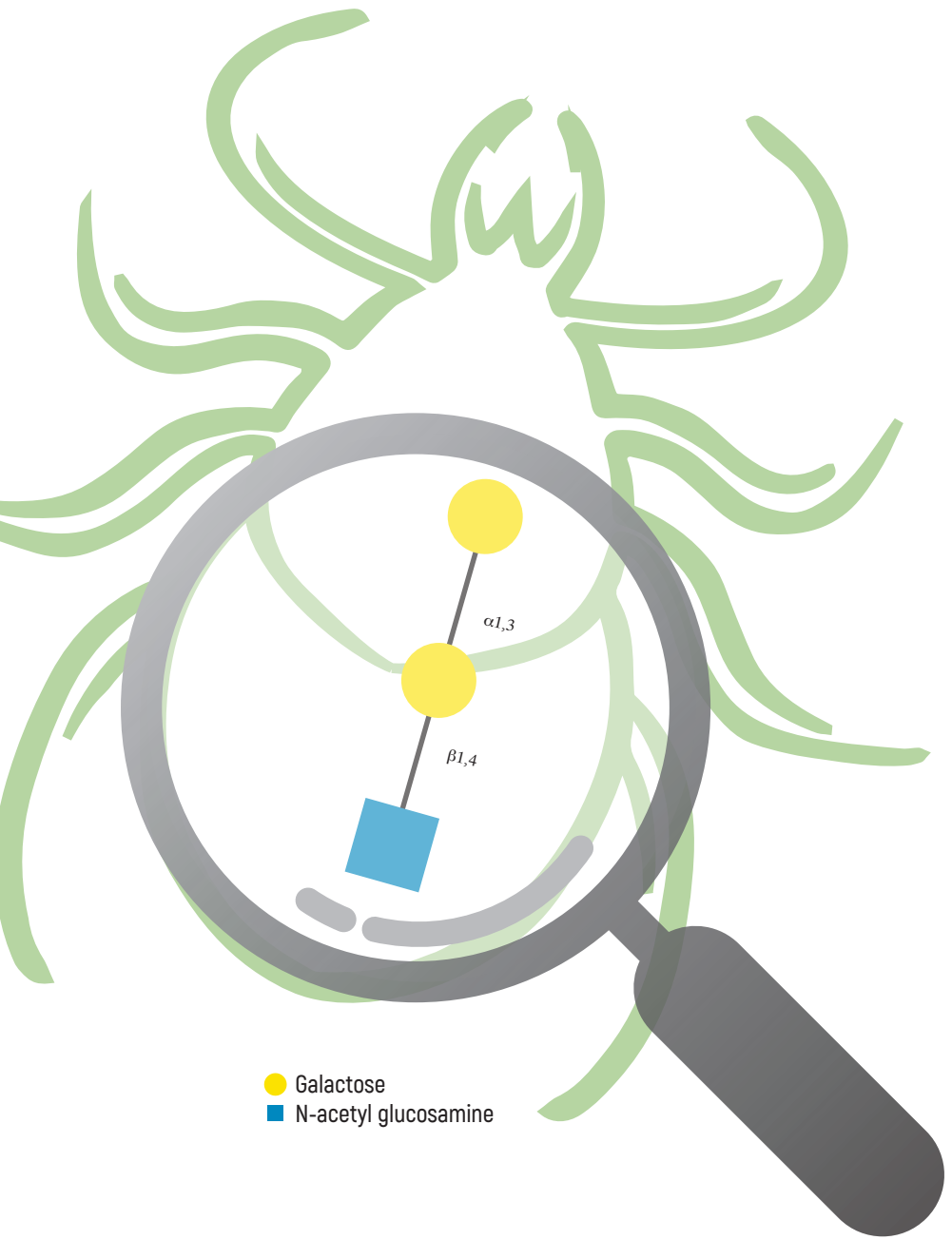

Chapter 1. Alpha-Gal content and origin in ticks

(a) Villar, M., **Pacheco, I.,** Mateos-Hernández, L., Cabezas-Cruz, A., Tabor, A.E., Rodríguez-Valle, M., Mulenga, A., Kocan, K.M., Blouin, E.F., de la Fuente, J. (2021). Characterization of tick salivary gland and saliva alphagalactome reveals candidate alpha-gal syndrome disease biomarkers. Expert Review of Proteomics 18 (12), 1099-1116. https://doi.org/10.1080/14789450.2021.2018305

(b) Villar, M., **Pacheco, I.,** Merino, O., Contreras, M., Mateos-Hernández, L., Prado, E., Barros-Picanco, D.K., Francisco Lima-Barbero, J., Artigas-Jerónimo, S., Alberdi, P., Fernández de Mera, I.G., Estrada-Peña, A., Cabezas-Cruz, A., de la Fuente, J. (2020). Tick and host derived compounds modulate the biochemical properties of the cement complex substance. Biomolecules 10, 555. https://doi.org/10.3390/biom10040555

Chapter 1a. Characterization of tick salivary gland and saliva alphagalactome reveals candidate alpha-gal syndrome disease biomarkers

Villar, M., **Pacheco, I.,** Mateos-Hernández, L., Cabezas-Cruz, A., Tabor, A.E., Rodríguez-Valle, M., Mulenga, A., Kocan, K.M., Blouin, E.F., de la Fuente, J. (2021). Characterization of tick salivary gland and saliva alphagalactome reveals candidate alpha-gal syndrome disease biomarkers. Expert Review of Proteomics 18 (12), 1099-1116. https://doi.org/10.1080/14789450.2021.2018305

EXPERT REVIEW OF PROTEOMICS
2021, VOL. 18, NO. 12, 1099–1116
https://doi.org/10.1080/14789450.2021.2018305

Taylor & Francis
Taylor & Francis Group

ORIGINAL RESEARCH

Characterization of tick salivary gland and saliva alphagalactome reveals candidate alpha-gal syndrome disease biomarkers

Margarita Villar [a,b*], Iván Pacheco[a*], Lourdes Mateos-Hernández[c*], Alejandro Cabezas-Cruz[c], Ala E. Tabor[d,e], Manuel Rodríguez-Valle[d], Albert Mulenga[f], Katherine M. Kocan[g], Edmour F. Blouin[g] and José de La Fuente [a,g]

[a]SaBio, Instituto de Investigación en Recursos Cinegéticos (IREC-CSIC-UCLM-JCCM), Ciudad Real, Spain; [b]Biochemistry Section, Faculty of Science and Chemical Technologies, and Regional Centre for Biomedical Research (CRIB), University of Castilla-La Mancha, Ciudad Real, Spain; [c]UMR BIPAR, INRAE, ANSES, Ecole Nationale Vétérinaire d'Alfort, Université Paris-Est, Maisons-Alfort, France; [d]Queensland Alliance for Agriculture & Food Innovation, Centre for Animal Science, The University of Queensland, Australia; [e]School of Chemistry and Molecular Biosciences, The University of Queensland, Brisbane, Australia; [f]Department of Veterinary Pathobiology, College of Veterinary Medicine, Texas A&M University, College Station, TX, USA; [g]Department of Veterinary Pathobiology, Center for Veterinary Health Sciences, Oklahoma State University, Stillwater, OK, USA

ABSTRACT

Background: Ticks are obligate hematophagous arthropods that synthesize the glycan Galα1-3Galβ1-(3)4GlcNAc-R (α-Gal) associated with the alpha-gal syndrome (AGS) or allergy to mammalian meat consumption.

Research design and methods: In this study, we used a proteomics approach to characterize tick proteins in salivary glands (sialome SG), secreted saliva (sialome SA) and with α-Gal modification (alphagalactome SG and SA) in model tick species associated with the AGS in the United States (*Amblyomma americanum*) and Australia (*Ixodes holocyclus*). Selected proteins reactive to sera (IgE) from patients with AGS were identified to advance in the identification of possible proteins associated with the AGS. For comparative analysis, the α-Gal content was measured in various tick species.

Results: The results confirmed that ticks produce proteins with α-Gal modifications and secreted into saliva during feeding. Proteins identified in tick alphagalactome SA by sera from patients with severe AGS symptomatology may constitute candidate disease biomarkers.

Conclusions: The results support the presence of tick-derived proteins with α-Gal modifications in the saliva with potential implications in AGS and other disorders and protective capacity against tick infestations and pathogen infection. Future research should focus on the characterization of the function of tick glycoproteins with α-Gal in tick biology and AGS.

ARTICLE HISTORY
Received 15 November 2021
Accepted 10 December 2021

KEYWORDS
Tick; saliva; salivary gland; alpha-gal; alpha-gal syndrome

1. Introduction

Ticks (Acari: Ixodida) are blood-feeding ectoparasite vectors of pathogens affecting human and animal health, representing a growing burden worldwide and a control challenge [1-6].

Tick-host-pathogen molecular interactions evolved as both conflict and cooperation with a key role for tick salivary gland (SG) and saliva (SA) proteins and other biomolecules [7–15]. Consequently, tick proteins in salivary glands (sialome SG) have been characterized at the mRNA (transcriptome) and protein (proteome) levels to show their role in host-tick-pathogen interactions with implications for the identification of candidate vaccine protective antigens [7–10,16–21]. Furthermore, recent advances in proteomics technologies and bioinformatics tools including sequence databases have further advanced the characterization of tick sialome SG and secreted saliva (sialome SA) with functional implications [10,17,22–36].

The immunoglobulin IgE-type response to the carbohydrate Galα1-3Galβ1-(3)4GlcNAc-R (α-Gal) mediates the alpha-gal syndrome (AGS) or the allergy to mammalian meat consumption with delayed anaphylaxis and immediate anaphylaxis to tick bites, xenotransplantation and certain drugs such as cetuximab [12,37–52]. Tick SA proteins with α-Gal modifications are hypothesized to be involved in the development of anti-α-Gal IgE-type responses associated with the AGS [48,53,54]. However, the role of other salivary biomolecules and the immune-mediated mechanisms of the AGS are still under investigation [54].

Three possible sources of α-Gal are possible in ticks: its own synthesis, host blood meal and midgut microbiota. Tick species of the genera *Amblyomma* (*A. americanum, A. cajennense, A. testudinarium, A. sculptum, A. variegatum, A. hebraeum), Ixodes* (*I. holocyclus, I. ricinus, I. australiensis, I. cajennense, I. nipponensis), Rhipicephalus* (*R. bursa), Hyalomma* (*H. marginatum*) and *Haemaphysalis* (*H. longicornis*) has been associated with the AGS

CONTACT José de La Fuente jose_delafuente@yahoo.com; josedejesus.fuente@uclm.es SaBio, Instituto de Investigación en Recursos Cinegéticos, Ronda de Toledo s/n, Ciudad Real 13005, Spain
*These authors equally contributed to this work

Supplemental data for this article can be accessed here

Article highlights

- Ticks and associated diseases affecting human and animal health are a growing burden worldwide.
- The IgE-type antibody response to tick proteins with α-Gal modifications may cause allergic reactions to mammalian meat consumption associated with the alpha-gal syndrome (AGS).
- Tick species of different genera are associated with the AGS and synthesize the glycan α-Gal in proteins secreted into saliva during feeding.
- The characterization of tick proteins with α-Gal modifications (alpha-galactome) and recognized by sera from AGS patients but not healthy individuals revealed cytoglobin-1, 14-3-3 family chaperone and vitellogenin-1 as candidate disease biomarkers.
- In addition of being carrier proteins for α-Gal, identified tick proteins may be associated with dysregulation of vascular nitric oxide protective signaling and adaptive cellular response to stress and nutrient availability and increased risk of cerebrovascular disorders.
- These proteins with and without α-Gal modifications may elicit a protective immune response against tick infestations and pathogen infection.
- The results contributed to our understanding of the role of tick proteins in the AGS by providing targets for functional studies to advance diagnostic, prevention and control of AGS and other tick-borne diseases.

syndrome worldwide [54–56]. The presence of host proteins in tick saliva may contribute to its α-Gal content [10] and the possible role of tick microbiota with bacteria containing α-Gal has been discussed [54,57]. Tick-borne pathogens such as *Borrelia burgdorferi* and *Anaplasma phagocytophilum* have been also shown to contain α-Gal [58]. However, how host-derived proteins or tick microbiota contribute to the AGS is still under discussion.

Therefore, the identification of tick proteins with α-Gal modifications (alphagalactome SG and SA) is important for advancement of the identification of the immune-mediated mechanisms and possible targets for diagnostic, prevention and control of the AGS. In this study, we used a proteomics approach to characterize tick proteins in sialome SG and SA and alphagalactome SG and SA in model tick species associated with the AGS in the United States (*A. americanum*) and Australia (*I. holocyclus*). Selected proteins reactive to sera (IgE) from patients with AGS were identified as to advance in the identification of possible proteins associated with the AGS. For comparative analysis, the α-Gal content was measured in SG and midgut combined with other organs (MG) of various tick species of the genera *Hyalomma, Ixodes, Amblyomma* and *Rhipicephalus* and in the cement cones collected from *Rhipicephalus sanguineus* and *Rhipicephalus bursa*. The results further demonstrated the presence tick-derived proteins with α-Gal modifications in the saliva and provided candidate proteins to advance in the characterization of the function of tick glycoproteins with α-Gal modifications in tick biology and the AGS.

2. Materials and methods

2.1. Amblyomma americanum (Linnaeus, 1758) ticks and protein samples used for proteomics analysis

Unfed female ticks were obtained from the laboratory colony maintained at the Oklahoma State University Tick Rearing Facility. Larvae and nymphs were fed on rabbits. Animals were housed at the Tick Rearing Facility with the approval and supervision of the OSU Institutional Animal Care and Use Committee. Off-host ticks were maintained in a 12 h light:12 h dark photoperiod at 22–25°C and 95% relative humidity (RH). Saliva was collected from 100 *A. americanum*. Female ticks were washed with phosphate buffered saline (PBS) and placed dorsal side down on double-sided tape on a glass slide. Salivation was induced by injecting 1–3 µl of 2% pilocarpine hydrochloride (Sigma-Aldrich, St. Louis, MO, USA) in PBS, pH 7.4 on the ventral side adjacent to the fourth leg coxa using a 34 gauge/0.5 inches/45° angle beveled needle on a model 701 Hamilton syringe (Hamilton Company, Reno, NV, USA). Saliva was then collected every 15–30 min using a Hamilton syringe for approximately 4 h at room temperature (RT) and stored at −80°C. A total of 130 µl (3.3 mg/ml protein) SA were obtained. Salivary glands were dissected and pooled from 200 *A. americanum* female ticks (16 ticks/pool). For protein extraction, SG were homogenized with a 27 G needle (20 strokes) in lysis buffer (7 M Urea, 2 M Thiourea, 2% 3- [(3-cholamidopropyl)dimethylammonio]-1-propanesulfonate, CHAPS) supplemented with complete mini protease inhibitor cocktail (Roche, Basel, Switzerland). Samples were boiled for 2 min, mixed in a thermocycler for 1 h and sonicated for 1 min in an ultrasonic cooled bath followed by 10 sec vortexes. After 3 cycles of sonication-vortex, the homogenate was centrifuged at 200 x g for 5 min at 4°C to remove cellular debris. The supernatant was collected, and protein concentration was determined using the RC_DC (BioRad, Hercules, CA, USA) with BSA as standard. The 0.87 mg of salivary gland extract (SGE) were stored at −80°C.

2.2. Ixodes holocyclus (Neumann, 1899) ticks and protein samples used for proteomics analysis

Ticks were collected from paralyzed animal hosts (dogs, cats and some local Australian marsupials) in veterinary clinics from different locations across the known geographic range of *I. holocyclus*. Clinics were recruited and participated in tick collection on a voluntary basis. To facilitate and make similar collection of tick samples, a Tick Collection Pack was sent to each clinic containing screw top vials with holes punched in the lid for ventilation, each containing a piece of sponge cloth, pre-paid and self-addressed Express Post satchels, small round takeaway containers, and a plastic transfer pipette marked for the correct volume of water to be added to each sponge. On the day of receipt of ticks, they were examined using a stereo microscope. All adult female ticks received alive and greater (in length and width, respectively) than 4 mm x 3 mm (i.e. fed for at least 96–120 hrs and thus more likely to be producing toxin) were salivated. Ticks were attached to a microscope slide using sticky tape. A 5 µl drop of 5% pilocarpine (Sigma-Aldrich) in methanol was topically applied to the dorsal scutum of the tick, ensuring that it did not contact the basis capitulum and where possible, the alloscutum. The sticky tape then wicked the pilocarpine across the alloscutum to be absorbed. A 10 µl pipette tip was then mounted onto the slide using plasticine and the hypostome of the tick placed into the mouth of the tip. Ticks on slides were placed in a styrofoam box lined with damp paper towel in an incubator (27°C, 75%

RH; Thermoline Scientific TRH-150, Wetherill Park, Australia), and the secreted SA was aspirated at intervals until salivation ceased. For SA volumes greater than 2 µl, an equal volume of protease inhibitor cocktail (PIC, Sigma-Aldrich) was added before sample storage at −80°C. For SA volumes less than 2 µl, 2 µl of PIC were added before storage at −80°C. A total of 100 µl (1.3 mg/ml protein) SA were obtained. Following salivation, or if live ticks were unable to be salivated, they were dissected. The ventral surface of the ticks' alloscutum was attached to petri dishes using duct tape and super glue (Bostik, Colombes, France). Ticks were completely submerged in PBS. Using a size 11 scalpel and fine tipped forceps (T04-821, T05-822, T6-SS-SS; ProSciTech, Kirwan QLD, Australia) the dorsal alloscutum was removed. The salivary glands were each removed and immediately snap frozen and stored at −80°C. Preparation of SGE was conducted as described by Stone [59] and Hall-Mendelin et al. [60] with volumes scaled according to the number of SG. Twenty-two pairs of SG were homogenised in 1 ml PBS by vortexing with five small and one medium glass beads for two 30 sec bursts. The homogenate was centrifuged at 1,500 x g for 30 min at 4°C and the supernatant removed and placed on ice. The pellet was washed three times in 500 µl PBS, centrifuged at 1,500 x g for 30 min at 4°C and the supernatants pooled on ice. Pooled supernatant was sonicated using 30 sec bursts with two min intervals of ice cooling for a total of ten minutes. The sonicate was then centrifuged at 109,000 x g for 1 h at 4°C, and the SGE collected on ice. Each pellet was washed twice using 500 µl PBS and centrifuged at 109,000 x g for 1 h at 4°C, with all supernatants collected and pooled. Saliva samples in PIC collected throughout the tick season were pooled and the total protein concentration measured using the Bradford Assay (BioRad), before storage of 3 mg SGE at −80°C in aliquots.

2.3. Preparation of the tick alphagalactome SG and SA

Proteins from the tick sialome SG and SA were immunoprecipitated with the anti-α-Gal epitope monoclonal IgM antibody (M86; Enzo Life Sciences, Farmingdale, NY, USA) bound to Dynabeads® Protein G (Invitrogen, Thermo Fisher Scientific, Waltham, MA, USA) following manufacturer recommendations. Two hundred micrograms of *A. americanum* SG and SA protein extracts were added to Dynabeads-M86 and incubated with rotation during 2 h at RT. After supernatant removal, Dynabeads-M86-antibody complex was washed twice with PBST (phosphate buffer saline PBS supplemented with 0.05% Tween-20) and tick alphagalactome SG and SA were eluted with Laemmli sample buffer (BioRad, Hercules, CA, USA) and stored at −20°C. To validate the immunoprecipitation, *A. americanum* SG proteins were eluted with 2 M glycine (Sigma-Aldrich) and neutralized with 1 M NaOH (Sigma-Aldrich). One hundred ng from the eluted proteins were treated with 0.2 µg of Alpha-galactosidase (rhα-Galactoidase A, R&D systems, Minneapolis, MN, USA) for 4 hrs at 37°C and other 100 ng control proteins were incubated without Alpha-galactosidase. Treated and control proteins were then used to coat ELISA plates in carbonate/bicarbonate buffer and incubated overnight at 4°C. Then, 100 µl of blocking buffer (1% HSA-human albumin; Sigma-Aldrich) were added to each well and incubated for 1 h at RT followed by five washes with PBST. The anti-α-Gal epitope M86 antibody (Enzo Life Sciences) was2. added to plates at 1:5 dilution in blocking buffer and incubated for 1 hr at 37°C, followed by five washes with PBST. Goat anti-mouse IgM-peroxidase (Sigma-Aldrich) were added at 1:2000 dilution in blocking buffer (100 µl/well), and plates incubated for 1 h at RT. Plates were then washed five times with PBST, and color developed by the addition of 100 µl of 3,3, ´5,5-tetramethylbenzidine (Promega, Madison, WI, USA) and protected from light for 20 min at RT. Reactions were stopped with the addition of 50 µl sulfuric acid, and the O.D. were measured at 450 nm with an ELISA reader. The α-Gal levels between Alpha-galactosidase treated and untreated samples were compared by One-way ANOVA with post-hoc Tukey HSD (Honestly Significant Difference) test (https://astatsa.com/OneWay_Anova_with_TukeyHSD/) ($p < 0.05$, n = 2 biological replicates with 3 technical replicates each).

2.4. Proteomics analysis of tick sialome and alphagalactome SG and SA

Tick sialome (150 µg) and alphagalactome SG and SA prepared as described above were *on gel* concentrated and trypsin-digested with sequencing grade trypsin (Promega, Madison, WI, USA). The resulting tryptic peptides were desalted onto OMIX pipette tips C18 (Agilent Technologies, Santa Clara, CA, USA), dried down and stored at −20°C until mass spectrometry analysis. The desalted protein digests were resuspended in 2% acetonitrile, 5% acetic acid in water and analyzed by reverse phase liquid chromatography coupled to mass spectrometry (RP-LC-MS/MS) using an Ekspert™ nanoLC 415 system coupled with a 6600 TripleTOF® mass spectrometer (AB SCIEX; Framingham, MA, USA) through Information-Dependent Acquisition (IDA). Peptides were first concentrated in a 0.1 × 20 mm C18 RP precolumn (Thermo Scientific) with a flow rate of 5 µl/min during 10 min in solvent A (0.1% formic acid in water) and then separated in a 0.075 × 250 mm C18 RP column (New Objective, Woburn, MA, USA) with a flow rate of 300 nl/min. Elution was done in a 120-min gradient from 5% to 30% solvent B (0.1% formic acid in acetonitrile) followed by 15-min gradient from 30% to 60% solvent B and directly injected for MS analysis. The mass spectrometer was set to scanning full spectra from 350 m/z to 1400 m/z (250 ms accumulation time) followed by up to 50 MS/MS scans (100–1500 m/z). Candidate ions with a charge state between +2 and +5 and counts per second above a minimum threshold of 100 were isolated for fragmentation. One MS/MS spectra was collected for 100 ms, before adding those precursor ions to the exclusion list for 15s (mass spectrometer operated by Analyst TF 1.6, AB SCIEX). Dynamic background subtraction was turned off. Data were acquired in high sensitivity mode with rolling collision energy on and a collision energy spread of 5.

Quality of proteomics data was controlled at multiple levels. An ISE6 cells digest was used for the evaluation of instrument performance and buffer A samples were run as blanks every three injections to prevent carryover. Three

technical replicates were injected for each sample. The IDA MS raw files for each sample were combined and subjected to database searches in unison using ProteinPilot software v. 5.0.1 (AB SCIEX) with the Paragon algorithm. Spectra identification was performed by searching against the *A. americanum* protein database [27] and the *Ixodes scapularis* Uniprot database (33,058 entries in June 2020) for *A. americanum* and *I. holocyclus* samples, respectively, with the following parameters: iodoacetamide cysteine alkylation, trypsin digestion, gel-based ID as special factor, identification focus on biological modification and thorough ID as search effort. The detected protein threshold was set at 0.05. To assess the quality of identifications, an independent False Discovery Rate (FDR) analysis with the target-decoy approach provided by ProteinPilot (AB SCIEX) was performed. Positive identifications were considered when identified proteins reached a 1% global FDR (Supplementary Data 1 and 2). To guarantee quality of protein identification using these parameters for the analysis of mas spectra, Uniprot *I. scapularis* database was used because only 96 entries are available for *I. holocyclus* (https://www.uniprot.org/uniprot/?query=ixodes+holocyclus&sort=score). The mass spectrometry proteomics data have been deposited to the ProteomeXchange Consortium *via* the PRIDE partner repository with the dataset identifier PXD029536 and 10.6019/PXD029536. Gene Ontology (GO) annotations for biological process (BP) and molecular function (MF) in identified proteins were assigned using the Blast2GO software (version 5; https://www.blast2go.com), manually revised and completed (Supplementary Data 1 and 2).

2.5. Human serum samples

Human sera were obtained from peripheral blood samples collected in 2017 and processed in a previous study [50,61]. In this study, three samples were used collected from Patient 1, a 63 y/o male with history of tick bites (*A. americanum* and *I. scapularis*), delayed anaphylaxis to mammalian meat consumption, positive anti-α-Gal IgE response (8.0 kU/l; ImmunoCAP-250, Phadia, Uppsala, Sweden) and diagnosed with AGS, Patient 2, a 71 y/o female with history of tick bites (*A. americanum* and *I. scapularis*), delayed anaphylaxis to mammalian meat consumption, positive anti-α-Gal IgE response (7.3 kU/l; ImmunoCAP-250) and diagnosed with AGS, and a healthy 59 y/o male with record of tick bites (*A. americanum, I. scapularis, I. ricinus*) and negative anti-α-Gal IgE response (0.02 kU/l; ImmunoCAP-250) (Control) [50,61]. Patients 1 and 2 removed larvae, nymphs and male *A. americanum* from their bodies in the spring and *I. scapularis* in the fall. The blood from each patient and the healthy individual were maintained in standing position in a sterile tube without anticoagulant at RT for clotting (20–30 min) and centrifuged at 1,500 x g for 20 min at RT. Serum was collected and conserved at −20°C until used for analysis. The use of human peripheral blood serum samples from patients and healthy individuals was done with their written informed consent in compliance with the Helsinki Declaration and the approval of the Ethical and Scientific Committees (SESCAM C-73) [50,61].

2.6. Human serum IgE, IgM and IgG antibody titers against α-Gal

Anti-α-Gal IgE, IgM and IgG antibody titers were determined in serum samples from patients and the control healthy individual. ELISA plates were coated with 100 ng of Gal1-3Galβ1-4GlcNAc-Human serum albumin (HSA) (Carbosynth Ltd, Berkshire, UK) in carbonate/bicarbonate buffer and incubated overnight at 4°C. Then, 100 µl of blocking buffer (1% HSA-human albumin, Sigma-Aldrich) were added to each well and incubated for 1 h at RT followed by five washes with PBST. Sera were added to plates at 1:50 dilution in blocking buffer and incubated for 1 h at 37°C, followed by five washes with PBST. Goat anti-human immunoglobulins-peroxidase IgG (FC specific), IgM (µ-chain specific), or IgE (ε-chain specific) (Sigma-Aldrich) were added at 1:1000 dilution in blocking buffer (100 µl/well), and plates incubated for 1 h at RT. Plates were then washed five times with PBST, and color developed by the addition of 100 µl of 3,3´,5,5-tetramethylbenzidine (Promega) at dark for 20 min at RT. Reactions were stopped with the addition of 50 µl sulfuric acid, and the O.D. were measured at 450 nm with an ELISA reader. The average value of the blanks (wells without Galα1-3Galβ1- 4GlcNAc-HSA coating; n = 3) was subtracted from all reads and the average of 3 replicates for each sample was used for analysis. Results were compared between different individual sera by One-way ANOVA with post-hoc Tukey HSD test (https://astatsa.com/OneWay_Anova_with_TukeyHSD/) ($p < 0.05$, n = 6 replicated wells per serum).

2.7. Human serum IgE, IgM and IgG antibody titers against tick and pig kidney proteins

Anti-tick and pig kidney IgE, IgM and IgG antibody titers were determined in serum samples from patients and the control healthy individual. The ELISA tests were performed using *A. americanum* and *I. holocyclus* SGE and pig kidney proteins. Pig kidney proteins were extracted from a piece acquired at a local butcher (Ciudad Real, Spain) with 7 M Urea, 2 M Thiourea, 2% 3-[(3-cholamidopropyl)dimethylammonio]-1-propanesulfonate] CHAPS buffer supplemented with complete mini protease inhibitor cocktail (Roche, Basel, Switzerland). The sample was lysed with a polytron and mixed for 1 h before boiled for 2 min and sonicated for 3 min in an ultrasonic cooled bath. Finally, the homogenate was centrifuged at 200 × g for 5 min at 4°C to remove cellular debris. The supernatant was collected, and protein concentration was determined using the RC_DC (BioRad) with BSA as standard. Plates were coated with 100 ng proteins per well in carbonate/bicarbonate buffer and incubated overnight at 4°C. Following five washes with PBS containing PBST, patients and control sera were added at 1:50 dilution in PBS and incubated for 1 h at 37°C followed by five washes with PBST. For the detection of immunoglobulins, 100 µl of goat anti-human immunoglobulins-peroxidase IgG (FC specific), IgM (µ-chain specific), and IgE (ε-chain specific) (Sigma-Aldrich) were added at 1:1000 dilution in blocking buffer (1% HSA in 100 µl/well PBST). The plates were then incubated for 1 h at 37°C and subsequently washed five times with PBST. Reaction was visualized by

adding 100 µl of 3,3´,5,5-tetramethylbenzidine (Promega) and incubated for 20 min in the dark at RT. Reactions were stopped with the addition of 50 µl sulfuric acid, and the O. D. were measured at 450 nm with an ELISA reader. The average value of the blanks (wells without tick proteins coating; n = 6) was subtracted from all reads and the average of 6 replicates for each sample was used for analysis. Results were compared between different individual sera by One-way ANOVA with post-hoc Tukey HSD test (https://astatsa.com/OneWay_Anova_with_TukeyHSD/) ($p < 0.05$, n = 6 replicated wells per serum).

2.8. 2-D Western blot and proteomics analysis of selected spots

Two hundred micrograms of *A. americanum* SG protein extracts were precipitated with the 2D-Clean up kit (GE Healthcare, Little Chalfont, UK), resuspended in 125 µl of DeStreak Rehydration Solution (GE Healthcare) supplemented with 0.5% of IPG buffer 3–11NL pH range (GE Healthcare) and loaded onto IPG strips (pH 3–11NL Drystrip 7 cm; GE Healthcare). Isoelectrofocusing was performed at 20°C in an Ettan IPGphor 3 (GE Healtcare) with conditions: 30 V for 3 hrs, 60 V for 3 hrs, 60–300 V for 30 min, 300 V for 30 min, 300–1000 V for 1 h, 1000 V for 1 h, 1000–5000 V for 5 hrs and 5000 V for 5 hrs. Prior to second dimension, proteins in focused IPG strips were reduced and alkylated by successive incubations in 50 mM Tris-HCl pH 8.8, 6 M urea, 30% v/v glycerol, 2% w/v SDS, 0.2% bromophenol blue, supplemented with 0.5% w/v dithiothreitol (DTT) for the first incubation or supplemented with 4.5% w/v iodoacetamide for the second incubation, during 15 min each with gentle rocking. For second dimension, IPG strips were placed onto homogeneous 12% SDS polyacrylamide gels and electrophoresis was conducted for 1 h at 120 V. Five 2D gels were performed simultaneously, one was stained with SYPRO Ruby Protein Gel Stain (Thermo Scientific) and the others were transferred to nitrocellulose membranes (Bio-Rad, Hercules, CA, USA). Western blots with patients and control sera (anti-IgE antibodies) and with anti-α-Gal antibodies were performed as described previously [43]. *Amblyomma americanum* protein spots recognized by patients and control sera and by anti-α-Gal antibodies were manually excised from the stained gel and digested with sequencing grade trypsin (Promega). Resulting tryptic peptides were desalted onto OMIX Pipette tips C18 (Agilent Technologies), dried-down and stored at −20ºC until RP-LC-MS/MS analysis of desalted protein digests resuspended in 0.1% formic acid using an Easy-nLCII system coupled to an LTQ mass spectrometer (Thermo Scientific) as described previously [43]. The MS/MS raw data were subjected to database search against the *A. americanum* protein database [27] using the SEQUEST algorithm (Proteome Discoverer 1.4; Thermo Scientific) with the following constraints: tryptic cleavage after Arg and Lys, up to two missed cleavage sites, and tolerances of 1 Da for precursor ions and 0.8 Da for MS/MS fragment ions, and the searches were performed allowing optional methionine oxidation and cysteine carbamidomethylation. Search was performed against a decoy database in an integrated decoy approach. A false discovery rate (FDR) <0.01 was considered as a condition for successful peptide assignments and protein identifications (Supplementary Data 3).

2.9. Tick species and tissue samples used for analysis of α-Gal content

The α-Gal content was measured in SG and MG of various tick species of the genera *Hyalomma, Ixodes, Amblyomma* and *Rhipicephalus* collected from adults feeding on different host species (Table 1). All tick species were collected from naturally infested hosts and morphologically classified according to Dantas-Torres et al. [62,63] and Estrada-Peña et al. [64]. The SG and MG were dissected from individual ticks and used for analysis. Cement cones used here were collected from *Rhipicephalus sanguineus* (Latreille, 1806) and *Rhipicephalus bursa* (Canestrini & Fanzago, 1878) adult ticks obtained from a previous study [65]. Briefly, adult female *R. sanguineus* (n = 20 ticks/pool, 2 pools) were collected from naturally infested dogs at an animal shelter in Ciudad Real, Spain. Adult *R. bursa* female ticks (3 pools of 5–9 ticks/pool collected at 1–2 (T1; slow-feeding period), 4–5 (T2) and 7 (T3; fast-feeding period) days post-attachment (dpa) were collected from experimentally infested Hyla breed rabbits [65]. Cement cones were collected using soft tissue forceps from mouthparts of manually detached adult female ticks and all host-derived skin or hairs attached to the cement were removed [65]. Salivary glands were also extracted from the same dissected *R. bursa* ticks as previously reported [65,66]. Results were compared between different tick samples by One-way ANOVA with post-hoc Tukey HSD test (https://astatsa.com/OneWay_Anova_with_TukeyHSD/) ($p < 0.05$, n = 6 biological replicates).

2.10. Tick SG, MG and cement cone α-Gal content

Tick SG, MG and/or cement cone samples were resuspended in 200 µl 50 mM Tris-HCl pH 7.5 supplemented with 4% sodium dodecyl sulfate (SDS) and 1 mM ditiotreitol (DTT), using a 1 ml syringe with a 40 mm needle (Terumo Europe España SL, Alcalá de Henares, Spain) and were sonicated for 3 min in an ultrasonic cooled bath, followed by vortexing for 10 sec. After three cycles of sonication-vortex, lysates were centrifuged at 12,100 × g for 30 sec. Proteins were homogenized in lysis buffer (8 M urea, 2 M thiourea and 2% CHAPS (3-[(3-cholamidopropyl)dimethylammonio]-1-propanesultonate hydrate), following the same cycles of sonication-vortex and centrifugation, until the samples were completely homogenized. Protein concentration was determined using the Bicinchoninic Acid (BCA) Protein Assay Kit (Thermo Fisher Scientific, Waltham, MA, USA) following manufacture's recommendations. Proteins extracts were methanol/chloroform precipitated and stored at −20°C until analysis. The α-Gal content was analyzed by ELISA in tick protein extracts as described previously [10,53]. Plates were coated with 100 ng of protein per well in carbonate/bicarbonate buffer and incubated overnight at 4°C and blocked with 1% human serum albumin (Sigma-Aldrich) in PBS for 1 h at RT, following three washes with PBST. The anti-α-Gal epitope monoclonal antibody (M86; Enzo Life Sciences) was added at 1:200 dilution in PBS and incubated for 1 h at 37°C followed by three washes with PBST. Then, goat anti-mouse IgM (µ-chain specific) peroxidase-conjugated antibodies (Sigma-Aldrich) were added at 1:10,000 dilution in PBS. The reaction was visualized by adding 100 µl of 3,3´,5,5´- Tetramethylbenzidine (Promega, Madison, WI, USA) and incubated for 20 min in the dark at RT. The optical density (OD) was measured at 450 nm with

Table 1. Tick species and hosts used for analysis of α-Gal content.

Tick spp.	Tick sex	No. ticks[a]	Tick α-Gal[b]	Host	Host α-Gal (n = 3)	Country of origin
Hyalomma lusitanicum	F	4	SG: 0.219 ± 0.069 MG: 0.259 ± 0.033	Deer, *Cervus elaphus*	0.249 ± 0.000	Spain
H. lusitanicum	F	5	SG: 0.340 ± 0.035 MG: 0.188 ± 0.162	Wild boar, *Sus scrofa*	0.378 ± 0.001	Spain
Ixodes ricinus	F	5	SG: 0.717 ± 0.166 MG: 0.137 ± 0.094	Deer	0.249 ± 0.000	Spain
I. ricinus	F	4	SG: 0.537 ± 0.303 MG: 0.191 ± 0.011	Wild boar	0.378 ± 0.001	Spain
Ixodes scapularis	F	5	SG: 0.017 ± 0.002	Sheep,	0.461 ± 0.003	U.S.A.
	M	5	SG: 0.020 ± 0.001 MG: N/A	*Ovis aries*		
Amblyomma variegatum	F	5	SG: 0.043 ± 0.012 MG: 0.035 ± 0.010	Cattle, *Bos taurus*	1.119 ± 0.198	Nigeria
Hyalomma aegyptium	F	5	SG: 0.032 ± 0.020	Tortoise, *Testudo graeca*	0.020 ± 0.000	Morocco
	M	7	SG: 0.042 ± 0.010 MG: 0.021 ± 0.003 MG: 0.027 ± 0.004			
Rhipicephalus sanguineus	F	5	SG: 0.081 ± 0.009 MG: 0.029 ± 0.011	Cattle	1.119 ± 0.198	Mexico
Rhipicephalus bursa	F	3	SG: 1.096 ± 0.073 MG: 0.359 ± 0.115	Deer	0.249 ± 0.000	Spain
R. bursa	F	3	SG: 0.241 ± 0.022 MG: 0.133 ± 0.125	Rabbit, *Oryctolagus cuniculus*	0.113 ± 0.001	Morocco
Rhipicephalus annulatus	F	3	SG: 0.219 ± 0.186 MG: 0.028 ± 0.000	Rabbit	0.113 ± 0.001	Morocco

A calibration curve with 0.0 to 1.0 ng α-Gal and O.D. values at 450 nm was constructed using Microsoft Excel for Mac (v. 16.26) to convert ELISA reader values to α-Gal content per sample (α-Gal content = ($O.D._{450nm}$/0.736)-0.049 ng α-Gal/1 µg protein; R^2 = 0.993). Results in tick samples were compared with human promyelocytic leukemia HL60 cells ATCC CCL-240 (0.029 ± 0.016 ng α-Gal/1 µg protein; n = 2) and pig (*S. scrofa*) kidney (0.274 ± 0.048 ng α-Gal/1 µg protein; n = 2) as negative and positive controls, respectively. [a]Number of ticks per pool; two pools per sample. [b]α-Gal content in ng α-Gal/1 µg protein; average ± S.D. per sample). Abbreviations: SG, salivary gland; MG, midgut combined with other organs; N/A, not available.

a Multiskan FC ELISA reader (Thermo Fisher Scientific). The average value of the blanks (wells without tick protein coating; n = 3) was subtracted from all reads and the average of 3–7 replicates for each sample was used for further analysis.

2.11. Animal host blood α-Gal content

Blood samples were collected from tick feeding animal hosts (n = 3 animals per host) and used for analysis of α-Gal content (Table 1). For separation of serum from total blood, a sterile tube without anticoagulant was used. The blood from each animal was maintained in standing position at RT for clotting (20–30 min) and centrifuged at 1,500 × g for 20 min at RT. Serum was collected and conserved at −20°C until used for analysis. The α-Gal content was analyzed by ELISA in host blood protein extracts as described above for tick samples but adding 100 µl sera in carbonate/bicarbonate buffer per well for coating the plates.

2.12. Statistical analysis of α-Gal content

A calibration curve with 0.0 to 1.0 ng of BSA-α-Gal (Dextra, Shinfield, UK) and O.D. values at 450 nm was constructed using Microsoft Excel for Mac (v. 16.26) to convert ELISA reader values to α-Gal content per sample (α-Gal content = ($O.D._{450nm}$/0.736)-0.049 ng α-Gal/1 µg protein; R^2 = 0.993). Protein extracts from human promyelocytic leukemia HL60 cells (ATCC CCL-240; 0.029 ± 0.016 ng α-Gal/1 µg protein; n = 2) and pig (*Sus scrofa*) kidney (0.274 ± 0.048 ng α-Gal/1 µg protein; n = 2) were included as negative and positive controls, respectively [58]. Results in tick samples were compared with human HL60 cells negative control by Student's t-test ($p < 0.05$, n = 2–7 biological replicates). Differences in α-Gal levels between tick species and independently of feeding host, sex and tissue were compared by One-way ANOVA with post-hoc Tukey HSD (Honestly Significant Difference) test (https://astatsa.com/OneWay_Anova_with_TukeyHSD/) ($p < 0.05$, n = 3–7 biological replicates). Correlation analyses of α-Gal content between tick SG or MG and host blood and between tick SG and MG were conducted by Pearson correlation coefficient calculator (https://www.socscistatistics.com/tests/pearson/default2.aspx) ($p < 0.05$, n = 10–11). Variations in α-Gal levels in *R. bursa* SG and cement cones at different time points (T1-T3) were compared by one-way ANOVA test (https://www.socscistatistics.com/tests/anova/default2.aspx) ($p < 0.05$, n = 3 biological replicates with 3 technical replicates each). Differences in α-Gal levels in *R. bursa* between SG and cement cones were compared by One-way ANOVA with post-hoc Tukey HSD test (https://astatsa.com/OneWay_Anova_with_TukeyHSD/) ($p < 0.05$, n = 3 biological replicates with 3 technical replicates each).

3. Results

3.1. Tick proteins identified by proteomics analysis of sialome and alphagalactome SA and SG

The experimental approach used model tick species associated with the AGS in the United States (*A. americanum*) and Australia (*I. holocyclus*) with a proteomics approach for the characterization of tick proteins in sialome and alphagalactome SG and SA (Figure 1). In *A. americanum*, a total of 1633 and 538 proteins were identified in the sialome SG and SA, respectively (Figure 1, Supplementary Data 1). Of them, 339

were identified in both SG and SA. In the alphagalactome, 372 and 125 proteins were identified in SG and SA, respectively, with 86 proteins identified in both SG and SA (Figure 1). In *I. holocyclus*, fewer proteins were identified in both sialome and alphagalactome SG and SA with a lower percentage of proteins identified in the sialome and alphagalactome of both SG and SA (Figure 1, Supplementary Data 2).

Although some proteins were identified in both tick species (Figure 1), these results suggested differences in tick sialome and alphagalactome SG and SA which may be attributed to multiple factors such as tick species, feeding status (unfed *A. americanum* vs. fed *I. holocyclus*), differences in the methodological approach used for saliva collection and protein content (3.3 vs. 1.3 mg/ml in *A. americanum* vs. *I. holocyclus*) and SG protein extraction or the amount of proteins available and used for proteomics analysis. Nevertheless, the percentage of proteins identified in both sialome and alphagalactome were similar between both tick species (21.2–26.4% and 14.9–15.5% in SG and SA, respectively) (Figure 1). Furthermore, the number of proteins identified only in the alphagalactome and probably associated with protein enrichment after immunoprecipitation were also similar between both tick species (26 and 45 proteins for *A. americanum* SG and SA, respectively and 38 and 30 proteins for *I. holocyclus* SG and SA, respectively) (Figure 1).

3.2. Functional annotation of tick proteins identified in the sialome and alphagalactome SA and SG

The GO analysis of proteins identified in the sialome and alphagalactome SG and SA showed differences between SG and SA, sialome and alphagalactome and tick species (Figure 2). At the BP level, some processes were not represented in *A. americanum* (i.e, sexual reproduction and response to stimulus) or in *I. holocyclus* (i.e. biosynthetic process, cellular and organic substance metabolic process, defense response, immune system process and response to host defenses) while other processes showed similar (e.g. biological regulation and localization) or different (e.g. multicellular organismal process and response to stress) profiles between tick species (Figure 2). At the MF level, the most represented functions (e.g. catalytic activity and binding) showed similar profiles between tick species while other

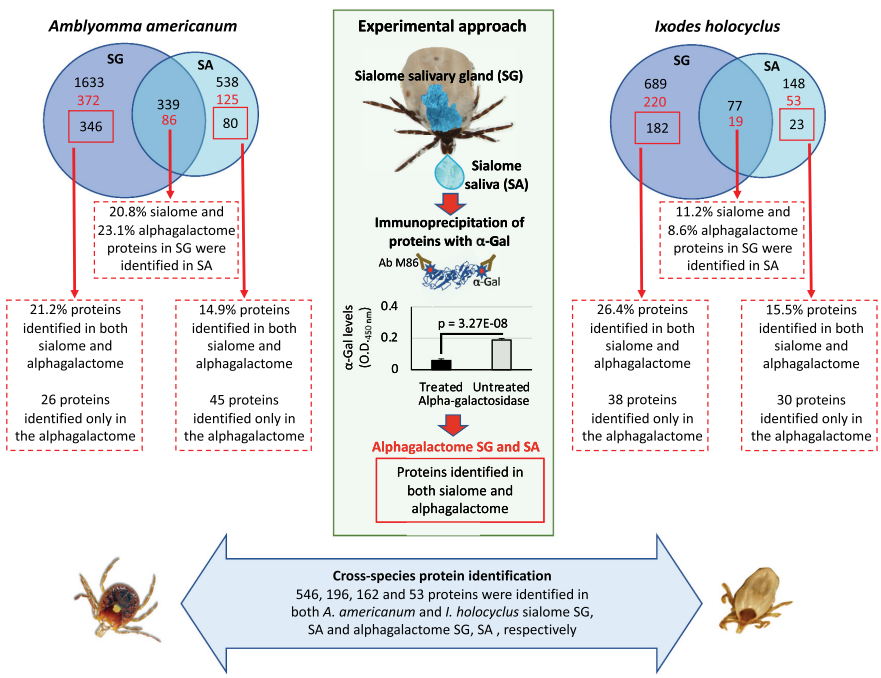

Figure 1. **Identification of tick proteins by proteomics analysis of sialome and alphagalactome SA and SG**. The experimental approach used model tick species associated with the AGS in the United States (*A. americanum*) and Australia (*I. holocyclus*) with a proteomics approach for the characterization of tick proteins in sialome and alphagalactome SG and SA. The α-Gal levels in *A. americanum* SG proteins after immunoprecipitation were compared between Alpha-galactosidase treated and untreated control proteins in ELISA using M86 antiα-Gal monoclonal antibody (Ab) by One-way ANOVA with post-hoc Tukey HSD test (One-way ANOVA p = 3.27E-08, Tukey HSD p = 0.001; n = 2 biological replicates with 3 technical replicates each). The number of proteins identified in the sialome (black numbers), alphagalactome (red numbers) and in both sialome and alphagalactome (black numbers in red square) are shown in the Venn diagram. The percent of proteins identified in SG and SA or in both sialome and alphagalactome and the number of proteins identified only in the alphagalactome are shown in dashed red line squares. Finally, the number of proteins identified in both tick species in shown in the arrow blue panel.

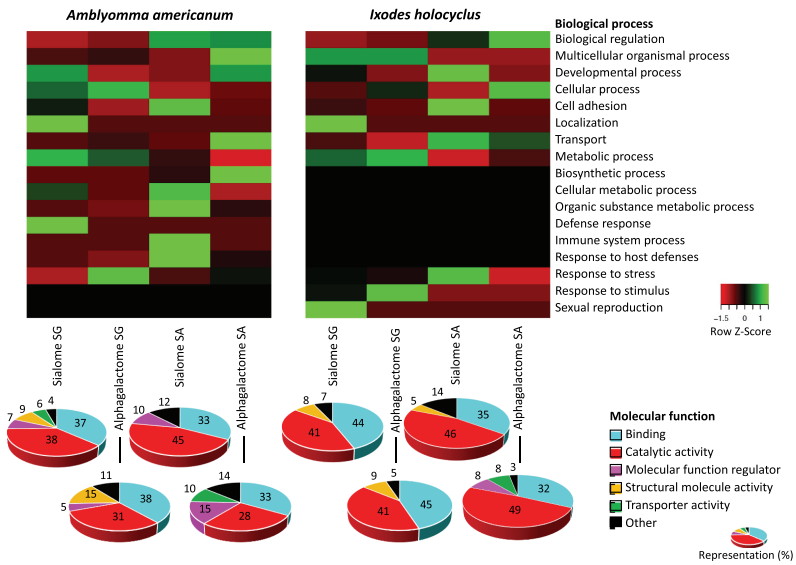

Figure 2. **Functional GO annotations of tick proteins identified in sialome and alphagalactome SA and SG**. Proteins identified by proteomics analysis were annotated for BP and MF. For BP annotations, identified proteins were subjected to heatmap analysis of z-score (http://www.heatmapper.ca/expression/). For MF annotations, 3-D pies were constructed based on percent function representation. All MF with less than 5% representation were grouped and annotated as 'Other.'

were different (e.g. transporter activity and molecular function regulator) (Figure 2). As discussed above, some of these differences may be due to differences in protein identification associated for example to tick feeding which correlates with the absence of sexual reproduction MF in unfed *A. americanum* but not in fed *I. holocyclus*. However, similar profiles suggested an evolutionarily conserved function of tick alphagalactome proteins.

3.3. Identification and characterization of tick sialome SG proteins reactive to patients with AGS

Sera from Patients 1 and 2 diagnosed with AGS in comparison with a healthy control individual, all with record of *A. americanum* tick bites, were used for the identification of tick sialome SG proteins by 2-D Western blot analysis (Figures 3(a-d) and 4). Patient 1 showed more severe symptoms of anaphylaxis, stomach pain, diarrhea, nausea, headaches, and eczema than Patient 2 who had sweats, accelerated gut activity and severe urinary bladder inflammatory response mimicking a urinary tract infection in response to mammalian meat consumption. In correlation with AGS, IgE and IgG antibody titers against α-Gal and pig kidney proteins were significantly higher ($p < 0.01$) in Patients 1 and 2 than in healthy control (Figures 3(a,b)). For *A. americanum* proteins, the IgE, IgM and IgG antibody titers were significantly higher ($p < 0.01$) in Patient 1 than in Patient 2 and healthy control and in Patient 2 when compared to healthy control (Figure 3(c)), reflecting a stronger antibody response to tick proteins in patients with AGS. Although none of the cases included in the study have been exposed to *I. holocyclus*, higher IgM antibody titers ($p < 0.01$) in Patient 2 and healthy control than in Patient 1 (Figure 3(d)) probably reflect a higher exposure to other *Ixodes* tick species (e.g. *I. ricinus* and/or *I. scapularis*) in Patient 2 and healthy control individuals. Alternatively, IgM antibodies may show significant cross-reactivity due to higher avidity while having low affinity to an unrelated antigen.

Selected spots reactive to anti-α-Gal antibodies and/or Patient 1, Patient 2 and healthy control sera were analyzed by proteomics (Figure 4 and Table 2). As expected, all identified proteins were present in the *A. americanum* sialome SG (Table 2). These results validated the presence of proteins with α-Gal modifications in the tick sialome SG (Figure 4 and Table 2). Proteins reactive to anti-α-Gal antibodies in Spots 1 and 2 were also identified by sera from Patient 1 (Spots 1) and Patient 2 and Control (Spots 2). Proteins without α-Gal modifications in Spots 3 were reactive only to serum from Patient 2. Proteins in Spots 2 with α-Gal modifications and reactive to serum from healthy control individual and Patient 2 may be an indicator of exposure to tick bites and included multiple Glycine-rich secreted cement proteins and other structural proteins (Table 2). These proteins were not identified by Patient's 1 serum, which suggests that in cases with more severe AGS symptomatology the antibody response is predominantly directed against candidate disease markers.

3.4. Characterization of α-Gal content in different tick species collected from various animal hosts

To further advance in the characterization of the α-Gal content in different tick species associated or not with the AGS, tick SG

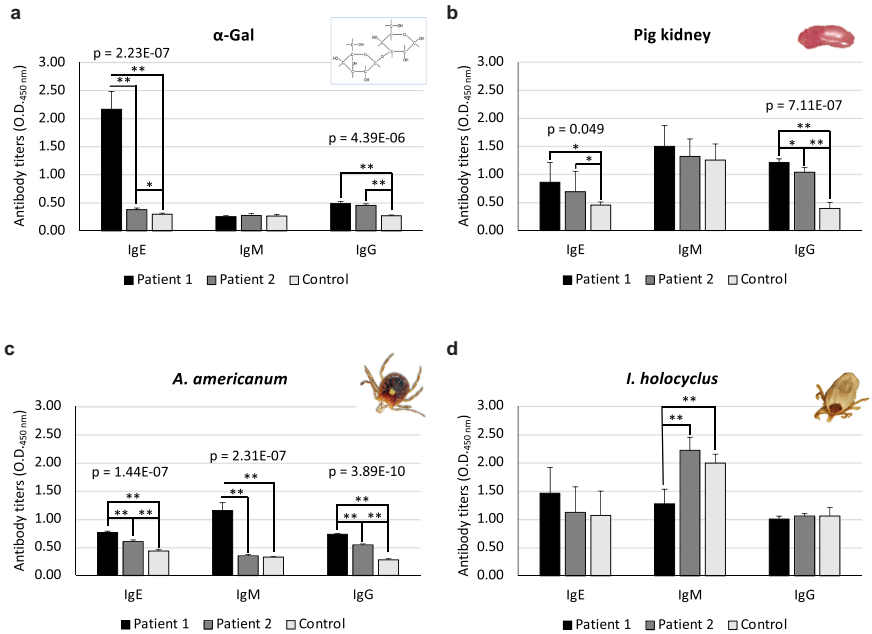

Figure 3. **Antibody response in patients with AGS and healthy control**. The IgE, IgM and IgG antibody titers were determined by ELISA against (a) α-Gal, (b) pig kidney proteins, (c) *A. americanum* SG proteins and (d) *I. holocyclus* SG proteins. Results were compared between different individuals by One-way ANOVA with post-hoc Tukey HSD test (One-way ANOVA p is shown for significant differences with Tukey HSD *p < 0.05, **p < 0.01; n = 6 replicated wells per serum).

and MG extracted proteins were used using a previously validated experimental approach with a calibration curve [10,53] (Figure 5). The results showed significantly higher ($p < 0.05$) α-Gal content in *Hyalomma lusitanicum, Ixodes ricinus, Rhipicephalus sanguineus, Rhipicephalus bursa* and *Rhipicephalus annulatus* SG when compared to human HL60 cells negative control. In MG proteins, only *H. lusitanicum, I. ricinus* and *R. bursa* showed higher α-Gal content than the negative control (Figure 5). Differences in α-Gal levels between tick species and independently of feeding host, sex and SG or MG proteins (groups A-H) were also shown with significant high levels ($p < 0.05$) in *I. ricinus* and *R. bursa* (Figure 5). As an example, proteins from the *R. sanguineus* and *R. bursa* cement cone were also included and showed significantly higher ($p < 0.01$) α-Gal content than the negative control (Figure 5).

To address the possibility that the α-Gal glycans found in tick protein extracts come from the bloodmeal source, sera from the different tick animal hosts were analyzed for α-Gal content (Table 1) and correlated with the α-Gal content in tick SG (Figure 6(a)) and MG (Figure 6(b)). The results showed no significant correlation ($p > 0.2$) while a positive correlation ($p < 0.05$) in the α-Gal content between tick SA and MG was obtained (Figure 6(c)). *Rhipicephalus bursa* female ticks fed on rabbits and with high α-Gal content in SG, MG and cement cones (Figure 5) were used to show that α-Gal levels did not vary during feeding ($p > 0.8$) in both SG and cement cones, which showed higher ($p < 0.01$) α-Gal content than SG (Figure 6(d)).

4. Discussion

Proteomic analysis of the sialome and alphagalactome SG and SA in two tick species and despite methodological differences in sample processing, showed that about 21–26% and 15% of the proteins in the SG and SA, respectively, contain α-Gal modifications in both tick species with some conserved BP and MF GO annotations. This result suggested that α-Gal modifications in tick SG and SA proteins may be evolutionarily conserved and independent of factors such as feeding at least in tick species associated with the AGS such as *A. americanum* and *I. holocyclus* [33,54–56].

Glycans such as α-Gal that are present in tick-derived glycoproteins [10,33,43,53,67] are constituents of matrix proteins, which are important for maintenance of tissue structure, porosity, integrity and matrix organization through binding to other glycoproteins [68]. The results obtained in this study confirmed the presence of α-Gal modifications in *A. americanum, I. holocyclus, I. ricinus, R. bursa*, which has been associated with the AGS [33,54–56] and provided evidence for the presence of this glycan in proteins from *R. sanguineus* and *R. annulatus*. The results also provided additional support for the tick origin of proteins with α-Gal and secreted into the saliva during feeding.

The results showed an anti-α-Gal antibody response with higher IgE and IgG titers in patients with AGS and reflected a stronger antibody response to *A. americanum* tick proteins in

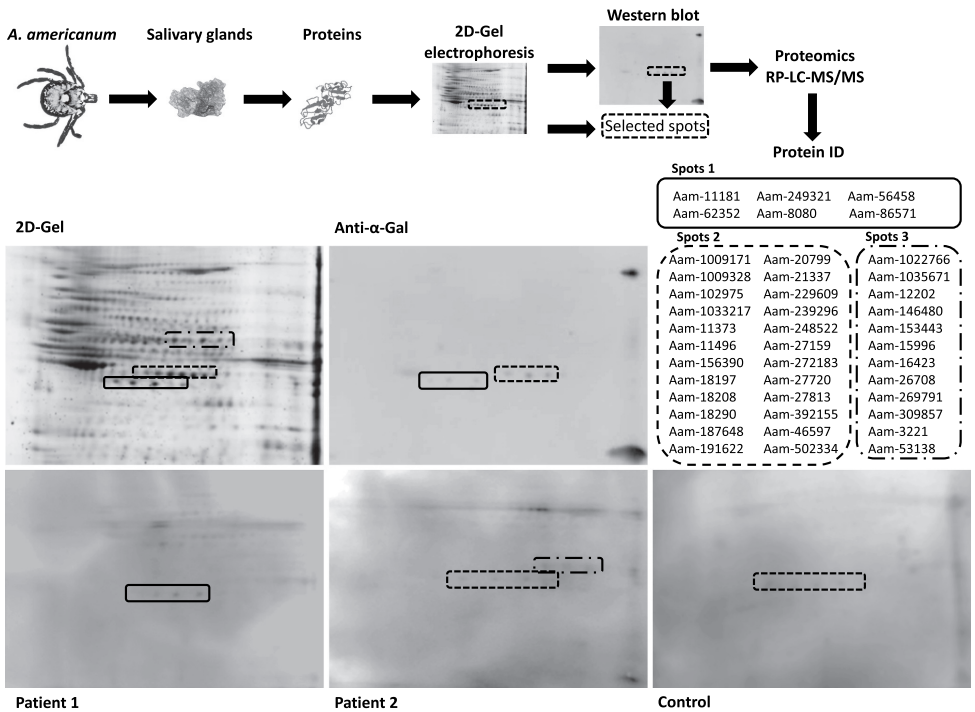

Figure 4. **Identification of *A. americanum* sialome SG proteins reactive to patients with AGS**. The *A. americanum* SG proteins were extracted and analyzed by 2-D Western blot using sera from AGS Patients 1 and 2 and healthy control (anti-IgE antibodies) and anti-α-Gal antibodies. The protein spots of interest recognized by patients or control sera and by anti-α-Gal antibodies were manually excised from the stained gel and used for proteomics analysis. The same settings were used for all four panels in which proteins were resolved by isoelectrical focusing at followed by 12% SDS polyacrylamide gel electrophoresis in the second dimension. Protein spots are marked with boxes using different outlines (solid, dashed, dashed-dot) associated to the proteins grouped with the same outlines.

patients with AGS. As discussed previously, this immune response may be associated with the AGS [33,49,50,69] but anti-α-Gal IgM/IgG antibodies and other immune mechanisms activated in response to α-Gal and tick proteins with and without this modification may be protective against tick infestations and pathogen infection [57,70,71].

Considering the possibility that cases with more severe AGS symptomatology develop an antibody response predominantly directed against candidate disease biomarkers, the analysis was focused on proteins in Spots 1, cytoglobin-1, 14-3-3 family chaperone and vitellogenin-1, reactive only to Patient 1 serum and identified in the *A. americanum* alpha-galactome SA (Table 2). Of these proteins, vitellogenin-1 and 14-3-3 family chaperone were also identified in *I. holocyclus* alphagalactome SA (Supplementary Data 2).

Cytoglobin-1 is a protein functioning in transport by binding to heme, metal ion and oxygen (https://www.uniprot.org/uniprot/B7QHN5). In human cells, cytoglobins are intracellular proteins ubiquitously produced in all tissues with regulation of tissue repair and a protective role against oxidative stress, fibrosis and tumor growth [72–75]. Therefore, upregulation of cytoglobins or its nitric oxide dioxygenase function may reduce vascular nitric oxide levels and its protective signaling that may result for example in liver injury [76]. In arthropods, it has been proposed that cytoglobin-1 is involved in respiration through oxygen transport [77].

The 14-3-3 family chaperone has been suggested to function as a molecular adaptor to promote targeting of misfolded protein aggregates to the aggresome, a cytoplasmic organelle for sequestration and clearance of toxic protein aggregates, with implication in neurological disorders such as Alzheimer disease and Parkinson disease [78,79]. Dynamic 14-3-3 mechanisms drive the adaptive cellular response to stress and nutrient availability [80]. Limited information is available about the function of 14-3-3 family chaperone in arthropods, with evidence of protein interaction with Hsp60 in domestic silk moth *Bombyx mori* larval and adult tissues including brain and silk gland [81]. In ticks, Hsp60 functions as a chaperonin and on antigen-presenting cells (APC) to link innate immune responses and has been suggested as a candidate protective antigen for vaccines against tick infestations [82].

Vitellogenin-1 and other members of the vitellogenin protein family are lipid transporters and precursors of yolk proteins and derivatives mainly synthesized in the liver as a result of coordinated endocrine stimulation that involves brain, ovary, and liver in oviparous and ovoviviparous vertebrates [83]. In Chelicerata, the main function

Table 2. *Amblyomma americanum* SG proteins differentially recognized by IgE in sera from AGS patients and healthy individual and reactive or not to α-Gal.

	Sialome		Alphagalactome		Reactive sera			
Description	SG	SA	SG	SA	α-Gal	P1	P2	C
Spots 1								
Aam-11181. Tropomyosin 1								
Aam-249321. Cytoglobin-1								
Aam-56458. 14-3-3 family chaperone								
Aam-62352. Vitellogenin-1								
Aam-8080. Creatine kinase								
Aam-86571. Prohibitin or B-cell receptor associated protein (BAP) 32								
Spots 2								
Aam-1009171. 1 3-ketoacyl-coa thiolase mitochondrial-like protein								
Aam-1009328. Short-chain acyl-coa dehydrogenase								
Aam-102975. Translocase of outer mitochondrial membrane complex subunit tom40								
Aam-1033217. RNA polymerase I and III subunit								
Aam-11373. F0F1-type ATP synthase alpha subunit								
Aam-11496. Chain A fructose-16-bisphosphate aldolase								
Aam-156390. Synaptic vesicle membrane protein vat-1								
Aam-18197. Glycine-rich secreted cement protein								
Aam-18208. Glycine-rich secreted cement protein								
Aam-18290. Glycine-rich secreted cement protein								
Aam-187648. 26S proteasome regulatory complex subunit								
Aam-191622. Molecular chaperone								
Aam-20799. Actin								
Aam-21337. Cathepsin l-like cysteine proteinase b								
Aam-229609. Translation initiation factor related to eif-2b alpha/beta/delta subunit cig2/idi2								
Aam-239296. 60 kDa chaperonin								
Aam-248522. 26S proteasome regulatory complex ATPase rpt6								
Aam-27159. Small subunit ribosomal protein S22								
Aam-272183. Serine protease inhibitor								
Aam-27720. Elongation factor 1 alpha								
Aam-27813. Molecular co-chaperone sti1								
Aam-392155. Glutamate/aspartate and neutral amino acid transporter								
Aam-46597. 3-hydroxyisobutyryl-CoA hydrolase, mitochondrial								
Aam-502334. Serine protease inhibitor								
Spots 3								
Aam-1022766. Adducin								
Aam-1035671. Tick metalloprotease 1								
Aam-12202. Glucosidase II catalytic alpha subunit								
Aam-146480. Aldehyde dehydrogenase								
Aam-153443. Vesicle coat complex COPII subunit sec23								
Aam-15996. Proline and glutamine-rich splicing factor SFPQ								
Aam-16423. K-similarity type RNA binding protein								
Aam-26708. WD40 repeat stress protein/actin								
Aam-269791. Uncharacterized protein								
Aam-309857. Presequence protease mitochondrial isoform 2 precursor								
Aam-3221. Molecular chaperone dnak								
Aam-53138. Low-density lipoprotein receptor-related protein 1b								

All data are disclosed in Supplementary Data 3. Proteins identified in *A. americanum* sialome and/or alphagalactome SG and SA are shown. Proteins identified in spots reactive to anti-α-Gal antibodies and sera from Patient 1 (P1), Patient 2 (P2) and healthy control individual (C) are shown.

of vitellogenins is in heme-binding hemolymph storage throughout reproduction, blood feeding and development [84]. Human ATP binding cassette (ABC) transporter proteins facilitate the ATP-dependent translocation of lipids or lipid-related compounds such as cholesterol, plant sterols, bile acids, phospholipids and sphingolipids with a positive role in lipid metabolism disorders associated for example with chronic obstructive pulmonary disease, atherosclerosis and severe alcoholic hepatitis [85,86]. However, some ABCA1 variants reduce plasma high-density lipoprotein and correlate with an increased risk of Alzheimer's disease and related dementia and cerebrovascular disease [87]. Recently, Apostolovic et al. [33] using an allergenomics-proteomics approach identified vitellogenins in *I. ricinus* adults and larvae potentially associated with red meat allergy in the AGS.

The function of the candidate disease biomarkers identified here (e.g. cytoglobin-1, 14-3-3 family chaperone and vitellogenin-1) suggest that these proteins may be involved in the AGS and other disorders but also with the possibility of mediating protective immune mechanisms against tick infestations and pathogen infection (Figure 7). Recently, Černý et al. [14] identified by proteomics analysis tick salivary proteins associated with acquired resistance to *I. scapularis* infestations. Interestingly, some of these proteins such as alpha-2-macroglobulin or related alpha-macroglobulins, chitinases, esterases and serpins were identified in our study in the *A. americanum* alphagalactome SA and/or sialome SA (Supplementary Data 1) with representation in *I. holocyclus* for alpha-macroglobulins and chitinases (Supplementary Data 2). These results suggested that some of these proteins may be candidate vaccine protective

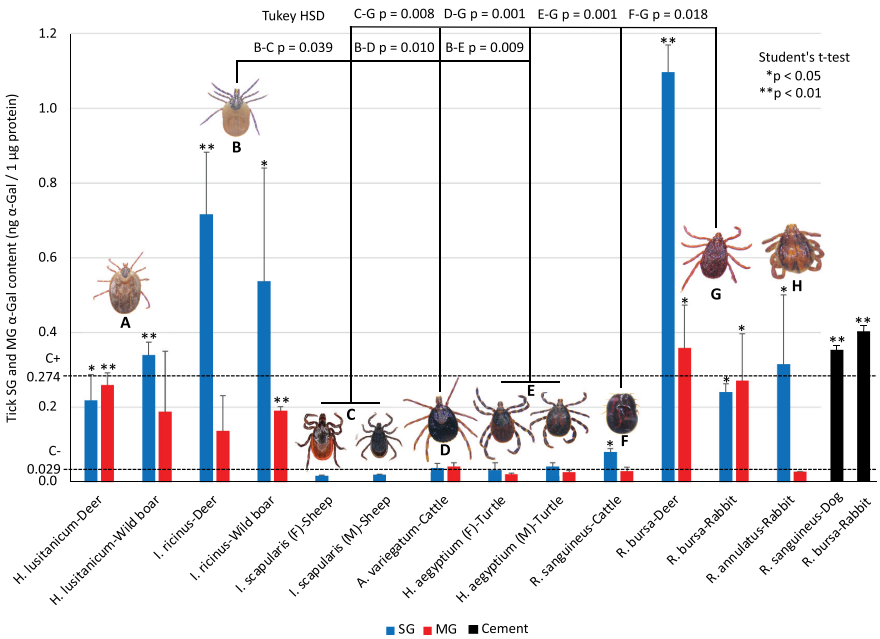

Figure 5. **Glycan α-Gal content in tick SG, MG and cement**. Characterization of α-Gal content in tick protein extracts. Protein extracts from human promyelocytic leukemia HL60 cells (0.029 ± 0.016 ng α-Gal/1 µg protein, n = 2) and pork kidney (0.274 ± 0.048 ng α-Gal/1 µg protein, n = 2) were included as negative (C-) and positive (C+) controls, respectively. Results in tick samples (average + S.D. of α-Gal/1 µg protein) were compared with human HL60 cells negative control by Student's t-test with unequal variance (*p < 0.05, **p < 0.01, n = 2–7 biological replicates). Differences in α-Gal levels between tick species and independently of feeding host, sex and tissue (groups A-H) were compared by One-way ANOVA with post-hoc Tukey HSD test (One-way ANOVA p = 0.0003, Tukey HSD p < 0.05, n = 3–7 biological replicates).

antigens to elicit antibody response against combined tick protein protective epitopes and α-Gal [88].

5. Conclusions

Herein, we confirm that ticks produce proteins with α-Gal modifications which are secreted into saliva during feeding. Proteins identified in tick alphagalactome SA using sera from patients with severe AGS symptomatology may constitute candidate disease biomarkers (Figure 7). Antibodies and other immune response mechanisms activated by tick proteins with and without α-Gal modifications may be a protective response against tick infestations and pathogen infection by interfering with tick respiration, blood feeding, reproduction, immune response and development (Figure 7). The characterization of α-Gal modifications in tick proteins is important to advance research on diagnosis and prevention of the AGS (Box 1). However, in addition of being carrier proteins for α-Gal, the role of tick proteins in the AGS is unknown but may be associated with dysregulation of vascular nitric oxide protective signaling, adaptive cellular response to stress and nutrient availability and increased risk of cerebrovascular disorders (Figure 7). Other biomolecules such as α-Gal-modified glycolipids may be involved in the AGS [89]. To address these possibilities, future experiments should focus on the functional characterization of these, and other candidate proteins and glycolipids associated with the AGS in animal models such as C57BL/6 α1,3-Galactosyltransferase-knockout (α1,3-GalT-KO) mice and zebrafish that like humans do not synthesize α-Gal [53,90,91].

Box 1. Characterization of α-Gal modifications in tick proteins

The characterization of post-translational modifications and associated sites is challenging [92]. Not only the identification of tick proteins with α-Gal modifications, but α-Gal content and where these modifications occur is relevant to better understand the mechanisms associated to the AGS [93–95]. Despite limitations of mass spectrometry-based analyses, it is technically possible to address these questions using proteomics data as illustrated in this example. Two of the proteins identified in *A. americanum* were selected, Aam-55,458 actin-binding cytoskeleton protein filamin and Aam-56,458 14-3-3 protein zeta multifunctional 14-3-3 family chaperone. Aam-55,458 is a cytoskeleton protein identified in sialome SG, sialome SA, alphagalactome SG but not in alphagalactome SA. Aam-56,458 is a multifunctional extracellular exosome protein that was identified in in sialome SG, sialome SA, alphagalactome SG, alphagalactome SA and by serum from AGS Patient 1 (Table 2).

The results of proteomics analysis showed that with similar sequence coverage (50.2% Aam-56,458, 52.3% Aam-55,458), peptides with possible α-Gal binding motifs (length 9 to 34 amino acids) were detected in Aam-55,458 but not in Aam-56,458.

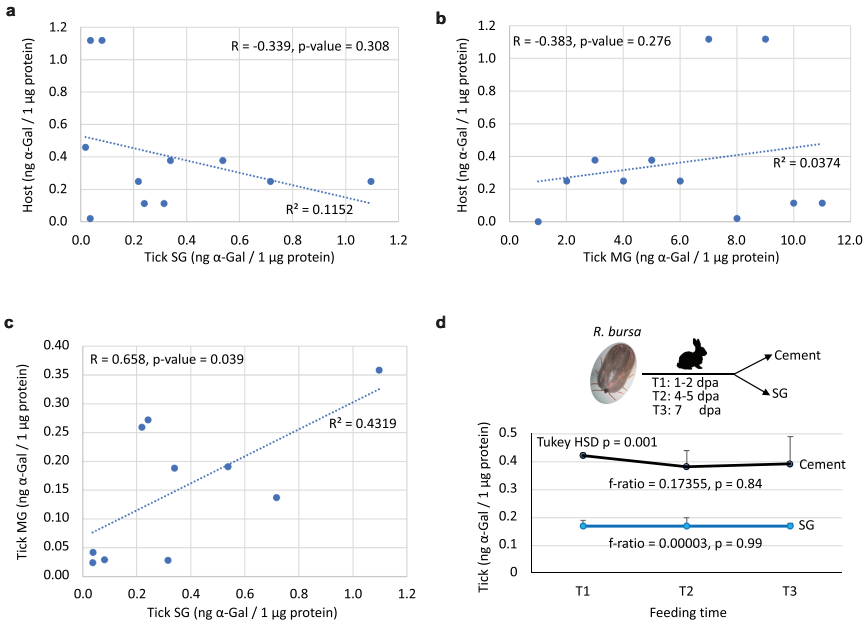

Figure 6. Correlation of α-Gal content in tick tissues with feeding. (a-c) Correlation analyses of α-Gal content between (a) tick SG or (b) tick MG and host blood and between (c) tick SG and MG were conducted by Pearson correlation coefficient (R, $p < 0.05$, n = 10–11). (d) Variations in α-Gal levels in *R. bursa* SG and cement cones (average + S.D. of α-Gal/1 µg protein) at different feeding time points (T1-T3) were compared by One-way ANOVA test ($p < 0.05$, n = 3 biological replicates with 3 technical replicates each). Differences in α-Gal levels in *R. bursa* between SG and cement cones were compared by One-way ANOVA with post-hoc Tukey HSD test (One-way ANOVA p = 4.65E-05, Tukey HSD p = 0.001, n = 3 biological replicates with 3 technical replicates each).

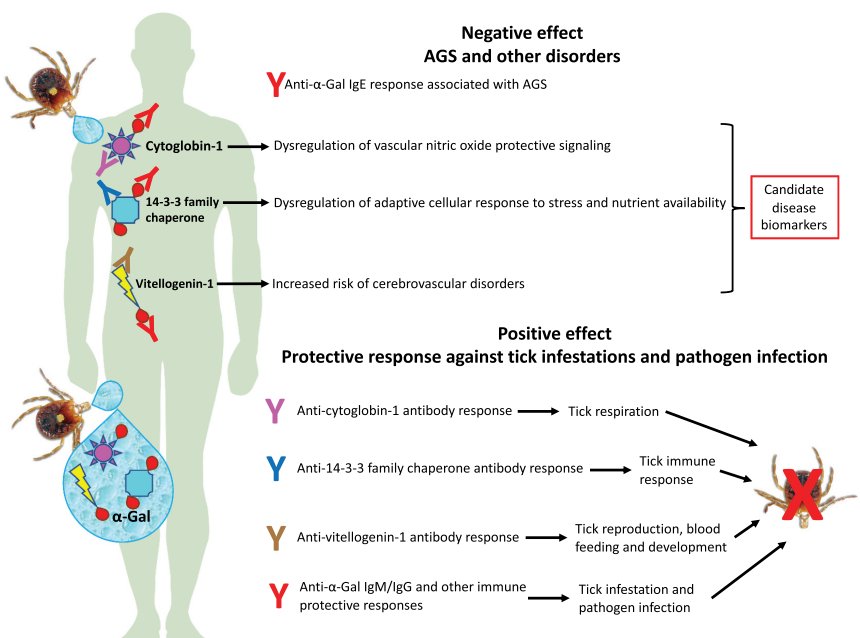

Figure 7. Putative role of tick proteins with α-Gal modifications secreted into saliva. Considering the possibility that cases with more severe AGS symptomatology develop an antibody response predominantly directed against candidate disease biomarkers, the analysis was focused on proteins in Spots 1 reactive only to Patient 1 serum and identified in the *A. americanum* alphagalactome SA. Possible mechanisms associated with the biological activity and the immune response to the biomolecules α-Gal, cytoglobin-1, 14-3-3 family chaperone and vitellogenin-1 with a negative effect in correlation with the AGS and other disorders and a positive effect associated with protective response against tick infestations and pathogen infection are proposed.

Aam-55,458 A0A023FMG5 Actin-binding cytoskeleton protein filamin

Sialome SG (43 peptides)	Sialome SA (4 peptides)	Alphagalactome SG (7 peptides)	Alphagalactom SA (0 peptides)
DIHIPGSPFQFTVGPFR	DIHIPGSPFQFTVGPFR	Not detected	Not detected
VVSPSGHDDDCFVAPLDDDQWALR	VVSPSGHDDDCFVAPLDDDQWALR	Not detected	Not detected
EAAPMAEVGSK	EAAPMAEVGSK	EAAPMAEVGSK	Not detected
ALTEGATQTR	ALTEGATQTR	ALTEGATQTR	Not detected
NLYQVNYVVK	Not detected	NLYQVNYVVK	Not detected
VGKDDADPAAVQAYGPGLR	Not detected	VGKDDADPAAVQAYGPGLR	Not detected
VYVMPQAGDTSK	Not detected	VYVMPQAGDTSK	Not detected
EAGVHTVSVR	Not detected	EAGVHTVSVR	Not detected
IELGSVPEHIQVNKPVAF	Not detected	IELGSVPEHIQVNKPVAF	Not detected
DDADPAAVQAYGPGLR	Not detected	Not detected	Not detected
DGSCYISYVVK	Not detected	Not detected	Not detected
DGTVAVSYLPAAPGEYK	Not detected	Not detected	Not detected
EAGAGSLSISVEGPSK	Not detected	Not detected	Not detected
EAGVAQPEVTVK	Not detected	Not detected	Not detected
EVGEHLINVK	Not detected	Not detected	Not detected
FHVDTIQSGYVTAYGPGLTHGVAGEPSNFTISTK	Not detected	Not detected	Not detected
FNDQHIPDSPFK	Not detected	Not detected	Not detected
FNGYHIAGSPFR	Not detected	Not detected	Not detected
FNHEHVQGSPFR	Not detected	Not detected	Not detected
GIAGESCEFNVWTR	Not detected	Not detected	Not detected
GPCDEVFVK	Not detected	Not detected	Not detected
IVGLDDKPVPASIPQEFTIDAR	Not detected	Not detected	Not detected
KLPNGHLGISFTPR	Not detected	Not detected	Not detected
LPNGHLGISFTPR	Not detected	Not detected	Not detected
MPGTSAFDMAAR	Not detected	Not detected	Not detected
NEFTIDTR	Not detected	Not detected	Not detected
NLSASIVAPSGLEEPCFLK	Not detected	Not detected	Not detected
NLYQVNYVVK	Not detected	Not detected	Not detected
NQISVGHSSEVSLK	Not detected	Not detected	Not detected
TGSHITGSPFK	Not detected	Not detected	Not detected
VDKPVIIDNQNGTVSIQYEPR	Not detected	Not detected	Not detected
VNMDCTEEEEGYK	Not detected	Not detected	Not detected
VSYLPTEPGYYIINLK	Not detected	Not detected	Not detected
VTSPSGSSEDAEIADLEDCSYAVHFVPK	Not detected	Not detected	Not detected
YTPLAPGEYFITVK	Not detected	Not detected	Not detected
HNGIHIPASPFR	Not detected	Not detected	Not detected
FGGQPVPGGTYK	Not detected	Not detected	Not detected
DRGDHVVIVK	Not detected	Not detected	Not detected
LSIAPPTSPETSSMTVDTVVK	Not detected	Not detected	Not detected
WGDDHIPGSPFK	Not detected	Not detected	Not detected
ENGIHQIHIR	Not detected	Not detected	Not detected
VNCTGSVTR	Not detected	Not detected	Not detected
GGLNVAVEGPSK	Not detected	Not detected	Not detected

GTYDVSYMPPPEK-SDCNVRVTYNNK-DIPNSPYK-MK-VR-PTCEPQNVK-IVGLDDK-PVPASIPQEFTIDAR-EAGVAQPEVTVK-GPDNVPR-K-ARVVDNDDGTFR-GQYVLSDVGK-HQINVK-
YGGK-
EVPGSPATVNSVPTGQADK-CK-ISEETK-QEK-VTIGEEYSVTVNAK-QAGK-GAITCTLTNAAG
AEPDVDVQVEDNGDGTYTIFYR-VKEAGEHQVNIK-FGGQPVPGGTYK-ITAVTEQIRQK-TVV
DR-R-FR-SAPPPQGK-FR-PVQLFDIPLQQSAGGQLSAEVIMPSGR-VDK-PVIIDNQ**NGT**VSIQY
EPR-EEGQHELHIK-FNHEHVQGSPFR-FHVDTIQSGYVTAYGPGLTHGVAGEPS**NFT**ISTK-D
AGK-GGLNVAVEGPSK-AEINVHDNK-DGTVAVSYLPAAPGEYK-ISIK-FADK-PIK-GSPFTAK-I
TGEGR-K-R-NQISVGHSSEVSLK-VQEK-DVK-**NLS**ASIVAPSGLEEPCFLK-K-LPNGHLGISFTP
R-EVGEHLINVK-R-TGSHITGSPFK-INVLER-EIGDASK-VK-VQGK-ALTEGATQTR-NEFTIDTR-
EAGYGGLSLSVEGPSK-ADIQCK-DNEDGTLK-VSYLPTEPGYYIINLK-FADHHVTGSPFTVK-
VTGK-GSNIQR-ENIK-K-QR-EAAPMAEVGSK-CTFTYK-MPGTSAFDMTAR-VTSPSGSSEDAEIA
DLEDCSYAVHFVPK-EAGVHTVSVR-NK-DIHIPGSPFQFTVGPFR-DHGAHR-VHAGGPGLER-G
IAGESCEFNVWTR-EAGAGSLSISVEGPSK-AK-IDFK-DRK-DGSCYITYVVK-DPGEYR-VGIK-F
NDQHIPDSPFK-VYVMPQAGDTSK-IELGSVPEHIQVNK-PVAFTISMNGAK-GNLDGK-VVSPS
GHDDDCFVAPLDDDQWALR-FIPR-ENGIHQIHIR-HNGIHIPASPFR-IR-VGK-DDADPAAVQA
YGPGLR-DVK-SGVK-TDFIVDTCNAGAGSMAVTIDGPTK-VNMDCTEEEEGYK-VR-YTPLAPGE
YFITVK-FNGYHIAGSPFR-V**NCT**GSVTR-STGGR-LSIAPPTSPETSSMTVDTVVK-QAAK-K-AD
HLPK-FR-SNAAK-VTSK-GMGLK-R-AVLNK-QNQFTVNCLDAGNNLIYVTVYGPK-GPCDEVFVK-H
LGR-NLYQVNYVVK-DR-GDHVVIVK-WGDDHIPGSPFK-VEVV

Aam-56,458 L7M1Q0 14-3-3 protein zeta multifunctional 14-3-3 family chaperone

Sialome SG(12 peptides)	Sialome SA(6 peptides)	Alphagalactome SG (3 peptides)	Alphagalactome SA (1 peptide)
NLLSVAYK	Not detected	Not detected	NLLSVAYK
YLAEVATGEQR	YLAEVATGEQR	YLAEVATGEQR	Not detected
VISSIEQK	VISSIEQK	VISSIEQK	Not detected
MDKDELVQR	Not detected	MDKDELVQR	Not detected
DSTLIMQLLR	DSTLIMQLLR	Not detected	Not detected
EICYDVLGLLDK	EICYDVLGLLDK	Not detected	Not detected
QVTETGVELSNEER	QVTETGVELSNEER	Not detected	Not detected
QAFDDAIAELDTLNEDSYK	QAFDDAIAELDTLNEDSYK	Not detected	Not detected
AYQEAFDISK	Not detected	Not detected	Not detected
EICYDVLGLLDKYLIPK	Not detected	Not detected	Not detected
YDDMAAAMK	Not detected	Not detected	Not detected
MQPTHPIR	Not detected	Not detected	Not detected

MDK-DELVQR-AK-LAEQAER-YDDMAAAMK-QVTETGVELSNEER-NLLSVAYK-NVVGAR-R-SSWR-
VISSIEQK-TEGSER-K-QQMAR-EYR-EK-VEK-ELR-EICYDVLGLLDK-YLIPK-ASNAESK-VFYLK-
MK-GDYYR-YLAEVATGEQR-NSVVEESQK-AYQEAFDISK-SK-MQPTHPIR-LGLAL**NFS**VFYYE
ILNSPDK-ACQLAK-QAFDDAIAELDTLNEDSYK-DSTLIMQLLR-D**NLT**LWTSDTQGDGDEQQEGGDN

Hyphens (-) represent trypsin protein digestion site (COOH-R/K). Peptides highlighted in grey, green, blue or yellow represent those identified in sialome SG, sialome SA, alphagalactome SG and alphagalactome SA, respectively. Some peptides were detected in multiple samples. Amino acids in bold letters represent the glycan signature possible α-Gal binding motifs (N-X-T/S).

Model of 14-3-3 zeta/phosphopeptide complex homodimer with bi-antennary α-Gal N-glycans in predicted sides. The model was constructed with SWISS-MODEL (https://swissmodel.expasy.org/templates/1qjb.1) [96].

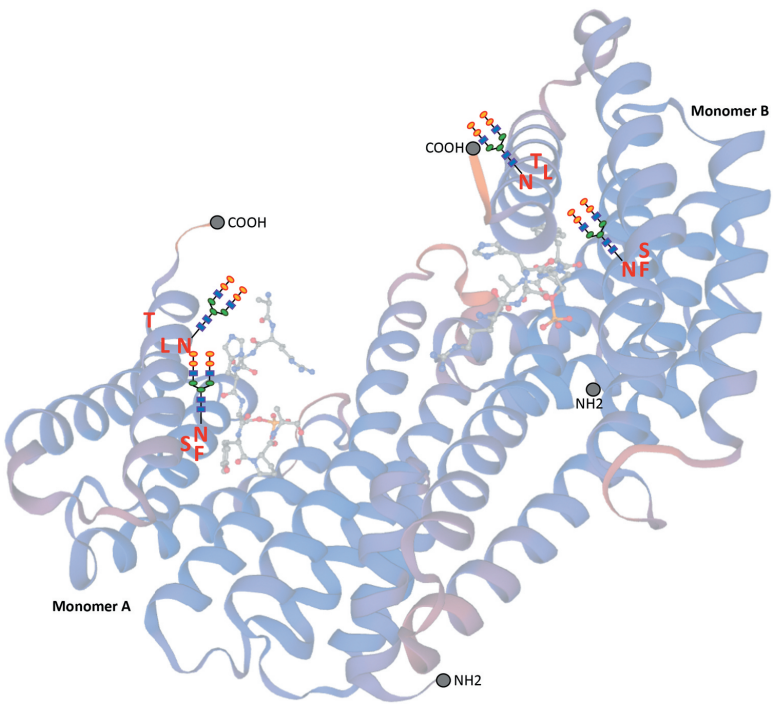

The likely explanation for this finding is that peptides with α-Gal modifications were not detected due to changes in peptide masses [92]. Although both proteins were identified in tick sialome SG, sialome SA and alphagalactome SG, only Aam-56,458 was found in alphagalactome SA and identified by AGS Patient 1 (Table 2), suggesting that this protein is modified with α-Gal to a grater extend than Aam-55,458. Consequently, peptides with glycan signature but without α-Gal were detected in Aam-55,458.

However, in Aam-56,458 peptides with glycan signature were modified with α-Gal and thus not identified by the proteomics analysis performed in this study.

Taken together, these results support the presence of α-Gal modifications in peptides of the C-terminus of Aam-56,458 and reinforce the possible role of this protein in AGS and the potential to be used as diagnostic biomarker.

Acknowledgments

We thank Sara Artigas-Jerónimo, Sara Baz, Francisco Ruiz-Fons (SaBio, IREC, Ciudad Real, Spain), Gabriela de la Fuente (Sabiotec, Ciudad Real, Spain), Agustín Estrada-Peña (Department of Animal Pathology, Faculty of Veterinary Medicine, Zaragoza, Spain), Sandra Antunes, Joana Couto, Ana Domingos (GHMT - Global Health and Tropical Medicine, Instituto de Higiene e Medicina Tropical - IHMT, Universidade Nova de Lisboa - UNL, Lisbon, Portugal) and the following veterinary clinics in Australia, Manly Road Veterinary Hospital (Manly West, Qld), The Cat Clinic (Mt Gravatt East, Qld), SuperVets (Manly West, Qld), Wynnum Bayside Vet Surgery (Wynnum West, Qld), Sinnamon Park Vet and Pet Emporium (Darra, Qld), and the Royal Society for the Prevention of Cruelty to Animals: RSPCA Wildlife Hospital (Wacol, Qld) for tick and host sampling and for tick morphological classification. The authors thank Dr. Thomas P. Karbanowicz, Ms. Greta Busch (QAAFI, UQ, Australia), and Dr. Diane Vankan (School of Veterinary Science, UQ, Australia), for their contribution in the collection of ticks (D. Vankan) including coordination of posted ticks from veterinary surgeries in southeast Queensland and northern NSW (G. Busch), the collection of tick saliva (G. Busch), and the preparation of salivary gland extracts (G. Busch, T.P. Karbanowicz).

Author contributions

M. Villar: Investigation, Conceptualization, Methodology, Supervision, Writing-Reviewing and Editing, Project administration, Funding acquisition.

I. Pacheco: Investigation, Visualization, Data curation.

L. Mateos-Hernández: Investigation, Visualization, Data curation.

A. Cabezas-Cruz: Conceptualization, Investigation.

A.E. Tabor: Investigation.

A. Mulenga: Methodology.

K.M. Kocan: Investigation.

E.F. Blouin: Investigation. José de la Fuente: Conceptualization, Methodology, Supervision, Writing-Reviewing and Editing, Project administration, Funding acquisition.

Funding

This work was supported by the State Research Agency, Spain, project BIOGAL [PID2020-116761GB-I00], the Spanish Research Council Grant [2020AEP123] and Consejería de Educación, Cultura y Deportes, JCCM, Spain, project CCM17-PIC-036 (SBPLY/17/180501/000185). *Ixodes holocyclus* saliva and salivary gland collections was supported by the Australian Research Council Linkage Grant [LP120200836 (2013-2018)]. MV was supported by the University of Castilla La Mancha, UCLM, Spain, and the Fondo Europeo de Desarrollo Regional, FEDER, EU.

Declaration of interest

The authors have no relevant financial involvement with any organization or entity with a financial interest in or financial conflict with the subject matter or materials discussed in the manuscript.

Reviewer disclosures

Peer reviewers on this manuscript have no relevant financial or other relationships to disclose.

ORCID

Margarita Villar http://orcid.org/0000-0003-4172-9079
José de La Fuente http://orcid.org/0000-0001-7383-9649

References

1. de La Fuente J, Estrada-Peña A, Venzal JM, et al. Overview: ticks as vectors of pathogens that cause disease in humans and animals. Front Biosci. 2008;13:6938–6946.
2. de La Fuente J, Contreras M, Estrada-Peña A, et al. Targeting a global health problem: vaccine design and challenges for the control of tick-borne diseases. Vaccine. 2017;35:5089–5094.
3. Estrada-Peña A, Ostfeld RS, Peterson AT, et al. Effects of environmental change on zoonotic disease risk: an ecological primer. Trends Parasitol. 2014;30:205–214.
4. de La Fuente J. Controlling ticks and tick-borne diseases … looking forward. Ticks Tick Borne Dis. 2018;9:1354–1357.
5. de La Fuente J, Estrada-Peña A. Why new vaccines for the control of ectoparasite vectors have not been registered and commercialized? Vaccines (Basel). 2019;7(3):75.
6. Semenza JC, Paz S. Climate change and infectious disease in Europe: impact, projection and adaptation. Lancet Reg Health Eur. 2021;9:100230. DOI:10.1016/j.lanepe.2021.100230.
7. Valenzuela JG. Exploring tick saliva: from biochemistry to 'sialomes' and functional genomics. Parasitology. 2004;129(Suppl):S83–S94.
8. Ayllón N, Villar V, Galindo RC, et al. Systems biology of tissue-specific response to *Anaplasma phagocytophilum* reveals differentiated apoptosis in the tick vector *Ixodes scapularis*. PLoS Genet. 2015;11:e1005120.
9. Villar M, Ayllón N, Alberdi P, et al. Integrated metabolomics, transcriptomics and proteomics identifies metabolic pathways affected by *Anaplasma phagocytophilum* infection in tick cells. Mol Cell Proteomics. 2015;14(12):3154–3172.
10. Villar M, Pacheco I, Merino O, et al. Tick and host derived compounds modulate the biochemical properties of the cement complex substance. Biomolecules. 2020;10:555.
11. de La Fuente J, Villar M, Cabezas-Cruz A, et al. Tick-host-pathogen Interactions: conflict and Cooperation. PLoS Pathog. 2016;12(4):e1005488. DOI:10.1371/journal.ppat.1005488.
12. de La Fuente J, Pacheco I, Villar M, et al. The alpha-Gal syndrome: new insights into the tick-host conflict and cooperation. Parasit Vectors. 2019;12:154.
13. Nuttall PA. Wonders of tick saliva. Ticks Tick Borne Dis. 2019;10:470–481.
14. Černý J, Lynn G, DePonte K, et al. Fractionation of tick saliva reveals proteins associated with the development of acquired resistance to *Ixodes scapularis*. Vaccine. 2020;38(51):8121–8129.
15. Pham M, Underwood J, Oliva Chávez AS. Changing the recipe: pathogen Directed Changes in Tick Saliva Components. Int J Environ Res Public Health. 2021;18(4):1806.
16. Valenzuela JG, Francischetti IM, Pham VM, et al. Exploring the sialome of the tick Ixodes scapularis. J Exp Biol. 2002;205(Pt 18):2843–2864. DOI:10.1242/jeb.205.18.2843.
17. Mans BJ, Andersen JF, Francischetti IM, et al. Comparative sialomics between hard and soft ticks:implications for the evolution of blood-feeding behavior. Insect Biochem Mol Biol. 2008;38(1):42–58. DOI:10.1016/j.ibmb.2007.09.003.
18. Hughes AL, Friedman R. Distinctive amino acid composition profiles in salivary proteins of the tick *Ixodes scapularis*. Ticks Tick Borne Dis. 2011;2(4):219–224.

19. Chmelař J, Kotál J, Karim S, et al. Sialomes and mialomes: a systems-biology view of tick tissues and tick-host interactions. Trends Parasitol. 2016;32(3):242–254. DOI:10.1016/j.pt.2015.10.002.
20. Perner J, Kropáčková S, Kopáček P, et al. Sialome diversity of ticks revealed by RNAseq of single tick salivary glands. PLoS Negl Trop Dis. 2018;12(4):e0006410. DOI:10.1371/journal.pntd.0006410.
21. Hart CE, Ribeiro JM, Kazimirova M, et al. Tick-borne encephalitis virus infection alters the sialome of *Ixodes ricinus* ticks during the earliest stages of feeding. Front Cell Infect Microbiol. 2020;10:41.
22. Ribeiro JM, Francischetti IM. Role of arthropod saliva in blood feeding: sialome and post-sialome perspectives. Annu Rev Entomol. 2003;48:73–88.
23. Francischetti IM, Meng Z, Mans BJ, et al. An insight into the salivary transcriptome and proteome of the soft tick and vector of epizootic bovine abortion, *Ornithodoros coriaceus*. J Proteomics. 2008;71(5):493–512. DOI:10.1016/j.jprot.2008.07.006.
24. Díaz-Martín V, Manzano-Román R, Valero L, et al. An insight into the proteome of the saliva of the argasid tick *Ornithodoros moubata* reveals important differences in saliva protein composition between the sexes. J Proteomics. 2013;80:216–235.
25. Karim S, Ribeiro JM. An insight into the sialome of the lone star tick, *Amblyomma americanum*, with a glimpse on its time dependent gene expression. PloS One. 2015;10(7):e0131292.
26. Kim TK, Tirloni L, Pinto AF, et al. *Ixodes scapularis* tick saliva proteins sequentially secreted every 24 h during blood feeding. PLoS Negl Trop Dis. 2016;10(1):e0004323. DOI:10.1371/journal.pntd.0004323.
27. Kim TK, Tirloni L, Pinto A, et al. Time-resolved proteomic profile of *Amblyomma americanum* tick saliva during feeding. PLoS Negl Trop Dis. 2020;14(2):e0007758. DOI:10.1371/journal.pntd.0007758.
28. Kim TK, Tirloni L, Bencosme-Cuevas E, et al. *Borrelia burgdorferi* infection modifies protein content in saliva of *Ixodes scapularis* nymphs. BMC Genomics. 2021;22(1):152. DOI:10.1186/s12864-021-07429-0.
29. Villar M, López V, Ayllón N, et al. The intracellular bacterium *Anaplasma phagocytophilum* selectively manipulates the levels of vertebrate host proteins in the tick vector *Ixodes scapularis*. Parasit Vectors. 2016;9:467.
30. Tirloni L, Lu S, Calvo E, et al. Integrated analysis of sialotranscriptome and sialoproteome of the brown dog tick *Rhipicephalus sanguineus* (s.l.): insights into gene expression during blood feeding. J Proteomics. 2020;229:103899.
31. Ribeiro J, Mans BJ. TickSialoFam (TSFam): a database that helps to classify tick salivary proteins, a review on tick salivary protein function and evolution, with considerations on the tick sialome switching phenomenon. Front Cell Infect Microbiol. 2020;10:374.
32. Mans BJ. Quantitative visions of reality at the tick-host interface: biochemistry, genomics, proteomics, and transcriptomics as measures of complete inventories of the tick sialoverse. Front Cell Infect Microbiol. 2020;10:574405.
33. Apostolovic D, Mihailovic J, Commins SP, et al. Allergenomics of the tick *Ixodes ricinus* reveals important α-Gal-carrying IgE-binding proteins in red meat allergy. Allergy. 2020;75(1):217–220. DOI:10.1111/all.13978.
34. Martins LA, Bensaoud C, Kotál J, et al. Tick salivary gland transcriptomics and proteomics. Parasite Immunol. 2021;43(5):e12807. DOI:10.1111/pim.12807.
35. Sanches GS, Villar M, Couto J, et al. Comparative proteomic analysis of *Rhipicephalus sanguineus* sensu lato (Acari: ixodidae) tropical and temperate lineages: uncovering differences during *Ehrlichia canis* infection. Front Cell Infect Microbiol. 2021;10:611113.
36. Oleaga A, Carnero-Morán A, Valero ML, et al. Proteomics informed by transcriptomics for a qualitative and quantitative analysis of the sialoproteome of adult *Ornithodoros moubata* ticks. Parasit Vectors. 2021;14(1):396. DOI:10.1186/s13071-021-04892-2.
37. van Nunen S, O'Connor KS, Clarke LR, et al. The association between *Ixodes holocyclus* tick bite reactions and red meat allergy. Intern Med J. 2007;39:A132.
38. Commins SP, Satinover SM, Hosen J, et al. Delayed anaphylaxis, angioedema, or urticaria after consumption of red meat in patients with IgE antibodies specific for galactose-alpha-1,3-galactose. J Allergy Clin Immunol. 2009;123:426–433.
39. Saleh H, Embry S, Nauli A, et al. Anaphylactic reactions to oligosaccharides in red meat: a syndrome in evolution. Clin Mol Allergy. 2012;10:5.
40. Steinke JW, Platts-Mills TA, Commins SP. The alpha-gal story: lessons learned from connecting the dots. J Allergy Clin Immunol. 2015;135:589–596.
41. Platts-Mills TAE, Schuyler AJ, Tripathi A, et al. Anaphylaxis to the carbohydrate side chain alpha-gal. Immunol Allergy Clin North Am. 2015;35:247–260.
42. Platts-Mills TAE, Commins SP, Biedermann T, et al. On the cause and consequences of IgE to galactose-α-1,3-galactose: a report from the national institute of allergy and infectious disease workshop on understanding IgE-Mediated Mammalian Meat Allergy. J Allergy Clin Immunol. 2020;145:1061–1071.
43. Mateos-Hernández L, Villar M, Moral A, et al. Tick-host conflict: immunoglobulin E antibodies to tick proteins in patients with anaphylaxis to tick bite. Oncotarget. 2017;8:20630–20644.
44. Galili U. Evolution in primates by "catastrophic-selection" interplay between enveloped virus epidemics, mutated genes of enzymes synthesizing carbohydrate antigens, and natural anti-carbohydrate antibodies. Am J Phys Anthropol. 2018;168:352–363.
45. Hilger C, Fischer J, Wölbing F, et al. Role and mechanism of galactose-alpha-1,3-galactose in the elicitation of delayed anaphylactic reactions to red meat. Curr Allergy Asthma Rep. 2019;19:3.
46. Cabezas-Cruz A, Valdés J, de La Fuente J. Cancer research meets tick vectors for infectious diseases. Lancet Infect Dis. 2014;10:916–917.
47. Cabezas-Cruz A, Mateos Hernández L, Alberdi P, et al. Effect of blood type on anti-α-Gal immunity and the incidence of infectious diseases. Exp Mol Med. 2017;49:e301.
48. Cabezas-Cruz A, Hodžić A, Román-Carrasco P, et al. Environmental and molecular drivers of the α-Gal syndrome. Front Immunol. 2019;10:1210.
49. de La Fuente J, Cabezas-Cruz A, Pacheco I. Alpha-gal syndrome: challenges to understanding sensitization and clinical reactions to alpha-gal. Expert Rev Mol Diagn. 2020;20(9):905–911.
50. de La Fuente J, Urra JM, Contreras M, et al. A dataset for the analysis of antibody response to glycan alpha-Gal in individuals with immune-mediated disorders. F1000Res. 2020;9:1366.
51. Sosa JP, Ferreira Caceres MM, Agadi K, et al. Diseases transmitted by the black-legged ticks in the United States: a comprehensive review of the literature. Cureus. 2021;13(8):e17526. DOI:10.7759/cureus.17526.
52. Young I, Prematunge C, Pussegoda K, et al. Tick exposures and alpha-gal syndrome: a systematic review of the evidence. Ticks Tick Borne Dis. 2021;12(3):101674. DOI:10.1016/j.ttbdis.2021.101674.
53. Contreras M, Pacheco I, Alberdi P, et al. Allergic reactions and immunity in response to tick salivary biogenic substances and red meat consumption in the zebrafish model. Front Cell Infect Microbiol. 2020;10:78.
54. Sharma SR, Karim S. Tick saliva and the alpha-gal syndrome: finding a needle in a haystack. Front Cell Infect Microbiol. 2021;11:680264.
55. Cabezas-Cruz A, Hodžić A, Mateos-Hernández L, et al. Tick-human interactions: from allergic klendusity to the α-Gal syndrome. Biochem J. 2021;478(9):1783–1794. DOI:10.1042/BCJ20200915.
56. AGI (alpha-gal information). Ticks and alpha-gal syndrome. 2021. [cited 2021 Sep 15].Available from: https://alphagalinformation.org/ticks-and-ags/
57. Mateos-Hernández L, Obregón D, Maye J, et al. Anti-tick microbiota vaccine impacts *Ixodes ricinus* performance during feeding. Vaccines (Basel). 2020;8(4):702. DOI:10.3390/vaccines8040702.
58. Hodžić A, Mateos-Hernández L, Leschnik M, et al. Tick bites induce anti-α-Gal antibodies in dogs. Vaccines (Basel). 2019;7:114.
59. Stone BF, Doube BM, Binnington KC, et al. Toxins of the Australian paralysis tick *Ixodes holocyclus*. in: Rodriguez JG, (Ed.) Recent Advances in Acarology Vol. 1. Proceedings of the V International Congress of Acarology East Lansing, Michigan, ISA. Academic Press Inc; 1979. 347–356.

60. Hall-Mendelin S. An immunological investigation of salivary gland antigens of the Australian paralysis tick *Ixodes holocyclus* for the development of toxin-specific immunoassays.PhD Thesis. University of Queensland; 2009.
61. Pacheco I, Fernández de Mera IG, Feo Brito F, et al. Characterization of the anti-α-Gal antibody profile in association with Guillain-Barré syndrome, implications for tick-related allergic reactions. Ticks Tick Borne Dis. 2021;12(3):101651. DOI:10.1016/j.ttbdis.2021.101651.
62. Dantas-Torres F. The brown dog tick, *Rhipicephalus sanguineus* (Latreille, 1806) (Acari: ixodidae): from taxonomy to control. Vet Parasitol. 2008;152:173–185.
63. Dantas-Torres F, Latrofa MS, Annoscia G, et al. Morphological and genetic diversity of *Rhipicephalus sanguineus sensu lato* from the new and old Worlds. Parasit Vectors. 2013;6:213.
64. Estrada-Peña A, Mihalca AD, Petney TN. Ticks of Europe and North Africa: a guide to species identification. Switzerland AG: Springer; 2018.
65. Pacheco I, Prado E, Artigas-Jerónimo S, et al. Comparative analysis of *Rhipicephalus* tick salivary gland and cement elementome. Heliyon. 2021;7:e06721.
66. Couto J, Villar V, Mateos-Hernández L, et al. Quantitative proteomics identifies metabolic pathways affected by *Babesia* infection and blood feeding in the sialoproteome of the vector *Rhipicephalus bursa*. Vaccines (Basel). 2020;8:91.
67. Cabezas-Cruz A, Espinosa PJ, Alberdi P, et al. Tick galactosyltransferases are involved in α-Gal synthesis and play a role during *Anaplasma phagocytophilum* infection and *Ixodes scapularis* tick vector development. Sci Rep. 2018;8:14224.
68. Varki A. Biological roles of glycans. Glycobiology. 2016;27:3–49.
69. Wolaver W, Thakrar S, Thomas K, et al. Demystifying α-gal syndrome: identification and risk management in the perioperative setting. Curr Opin Anaesthesiol. 2021;34:761–765. Epub ahead of print DOI:10.1097/ACO.0000000000001066.
70. Hodžić A, Mateos-Hernández L, de La Fuente J, et al. α-Gal-based vaccines: advances, opportunities, and perspectives. Trends Parasitol. 2020;36(12):992–1001. DOI:10.1016/j.pt.2020.08.001.
71. de La Fuente J, Gortázar C, Cabezas-Cruz A. Immunity to glycan α-Gal and possibilities for the control of COVID-19. Immunotherapy. 2021;13(3):185–188.
72. Hundahl CA, Kelsen J, Hay-Schmidt A. Neuroglobin and cytoglobin expression in the human brain. Brain Struct Funct. 2013;218 (2):603–609.
73. Yoshizato K, Thuy L, Shiota G, et al. Discovery of cytoglobin and its roles in physiology and pathology of hepatic stellate cells. Proc Jpn Acad Ser B Phys Biol Sci. 2016;92(3):77–97. DOI:10.2183/pjab.92.77.
74. De Backer J, Maric D, Bosman M, et al. A reliable set of reference genes to normalize oxygen-dependent cytoglobin gene expression levels in melanoma. Sci Rep. 2021;11(1):10879. DOI:10.1038/s41598-021-90284-6.
75. Keller T, Lechauve C, Keller AS, et al. The role of globins in cardiovascular physiology. Physiol Rev. 2021. DOI:10.1152/physrev.00037.2020.
76. Liu X, El-Mahdy MA, Boslett J, et al. Cytoglobin regulates blood pressure and vascular tone through nitric oxide metabolism in the vascular wall. Nat Commun. 2017;8:14807.
77. Arlian LG, Morgan MS, Rider SD. *Sarcoptes scabiei*: genomics to proteomics to biology. Parasit Vectors. 2016;9(1):380.
78. Foote M, Zhou Y. 14-3-3 proteins in neurological disorders. Int J Biochem Mol Biol. 2012;3(2):152–164.
79. Xu Z, Graham K, Foote M, et al. 14-3-3 protein targets misfolded chaperone-associated proteins to aggresomes. J Cell Sci. 2013;126 (Pt18):4173–4186. DOI:10.1242/jcs.126102.
80. Pennington KL, Chan TY, Torres MP, et al. The dynamic and stress-adaptive signaling hub of 14-3-3: emerging mechanisms of regulation and context-dependent protein-protein interactions. Oncogene. 2018;37(42):5587–5604. DOI:10.1038/s41388-018-0348-3.
81. Tabunoki H, Shimada T, Banno Y, et al. Identification of *Bombyx mori* 14-3-3 orthologs and the interactor Hsp60. Neurosci Res. 2008;61(3):271–280. DOI:10.1016/j.neures.2008.03.007.
82. Zhang T, Cui X, Zhang J, et al. Screening and identification of antigenic proteins from the hard tick *Dermacentor silvarum* (Acari: ixodidae). Korean J Parasitol. 2015;53(6):789–793. DOI:10.3347/kjp.2015.53.6.789.
83. Biscotti MA, Barucca M, Carducci F, et al. New perspectives on the evolutionary history of vitellogenin gene family in vertebrates. Genome Biol Evol. 2018;10(10):2709–2715. DOI:10.1093/gbe/evy206.
84. Donohue KV, Khalil SM, Sonenshine DE, et al. Heme-binding storage proteins in the Chelicerata. J Insect Physiol. 2009;55 (4):287–296. DOI:10.1016/j.jinsphys.2009.01.002.
85. Tarling EJ, de Aguiar Vallim TQ, Edwards PA. Role of ABC transporters in lipid transport and human disease. Trends Endocrinol Metab. 2013;24(7):342–350.
86. Kotlyarov S, Kotlyarova A. The role of ABC transporters in lipid metabolism and the comorbid course of chronic obstructive pulmonary disease and atherosclerosis. Int J Mol Sci. 2021;22 (13):6711.
87. Ben Aissa M, Lewandowski CT, Ratia KM, et al. Discovery of non-lipogenic ABCA1 inducing compounds with potential in Alzheimer's disease and type 2 diabetes. ACS Pharmacol Transl Sci. 2021;4(1):143–154. DOI:10.1021/acsptsci.0c00149.
88. de La Fuente J, Contreras M. Vaccinomics: a future avenue for vaccine development against emerging pathogens. Expert Rev Vaccines. 2021;1–9. Epub ahead of print. DOI:10.1080/14760584.2021.1987222.
89. Román-Carrasco P, Lieder B, Somoza V, et al. Only α-Gal bound to lipids, but not to proteins, is transported across enterocytes as an IgE-reactive molecule that can induce effector cell activation. Allergy. 2019;74(10):1956–1968. DOI:10.1111/all.13873.
90. Araujo RN, Franco PF, Rodrigues H, et al. *Amblyomma sculptum* tick saliva: α-Gal identification, antibody response and possible association with red meat allergy in Brazil. Int J Parasitol. 2016;46 (3):213–220. DOI:10.1016/j.ijpara.2015.12.005.
91. Choudhary SK, Karim S, Iweala OI, et al. Tick salivary gland extract induces alpha-gal syndrome in alpha-gal deficient mice. Immun Inflamm Dis. 2021;9(3):984–990. DOI:10.1002/iid3.457.
92. Kim MS, Zhong J, Pandey A. Common errors in mass spectrometry-based analysis of post-translational modifications. Proteomics. 2016;16(5):700–714.
93. Lammerts van Bueren JJ, Rispens T, Verploegen S, et al. Anti-galactose-α-1,3-galactose IgE from allergic patients does not bind α-galactosylated glycans on intact therapeutic antibody Fc domains. Nat Biotechnol. 2011;29(7):574–576. DOI:10.1038/nbt.1912.
94. Lee CS, Kim IS, Park JB, et al. The phox homology domain of phospholipase D activates dynamin GTPase activity and accelerates EGFR endocytosis. Nat Cell Biol. 2006;8(5):477–484. DOI:10.1038/ncb1401.
95. Apostolovic D, Krstic M, Mihailovic J, et al. Peptidomics of an in vitro digested α-Gal carrying protein revealed IgE-reactive peptides. Sci Rep. 2017;7(1):5201. DOI:10.1038/s41598-017-05355-4.
96. Waterhouse A, Bertoni M, Bienert S, et al. Swiss-MODEL: homology modelling of protein structures and complexes. Nucleic Acids Res. 2018;46(W1):W296–W303. DOI:10.1093/nar/gky427.

Supplementary material. Chapter 1a

Supplementary material not included from Villar, M., **Pacheco, I.,** Mateos-Hernández, L., Cabezas-Cruz, A., Tabor, A.E., Rodríguez-Valle, M., Mulenga, A., Kocan, K.M., Blouin, E.F., de la Fuente, J. (2021). Characterization of tick salivary gland and saliva alphagalactome reveals candidate alpha-gal syndrome disease biomarkers. Expert Review of Proteomics. 18 (12), 1099-1116.

https://www.tandfonline.com/doi/abs/10.1080/14789450.2021.2018305?-journalCode=ieru20

- Supplementary Data 1. Amblyomma americanum sialome and alphagalactome SG and SA.
- Supplementary Data 2. Ixodes holocyclus sialome and alphagalactome SG and SA.
- Supplementary Data 3. Proteomics results of A. Americanum SG protein identification and characterization after 2-D gel separation, Western blot using patient and control sera and anti-α-Gal antibodies and MS analysis.

Chapter 1b. Tick and host derived compounds modulate the biochemical properties of the cement complex substance

Villar, M., **Pacheco, I.,** Merino, O., Contreras, M., Mateos-Hernández, L., Prado, E., Barros-Picanco, D.K., Francisco Lima-Barbero, J., Artigas-Jerónimo, S., Alberdi, P., Fernández de Mera, I.G., Estrada-Peña, A., Cabezas-Cruz, A., de la Fuente, J. (2020). Tick and host derived compounds modulate the biochemical properties of the cement complex substance. Biomolecules 10, 555. https://doi.org/10.3390/biom10040555

biomolecules

MDPI

Article

Tick and Host Derived Compounds Detected in the Cement Complex Substance

Margarita Villar [1,2,†], Iván Pacheco [1,†], Octavio Merino [3,†], Marinela Contreras [1], Lourdes Mateos-Hernández [1,4], Eduardo Prado [5], Dina Karen Barros-Picanço [1], José Francisco Lima-Barbero [1,6], Sara Artigas-Jerónimo [1], Pilar Alberdi [1], Isabel G. Fernández de Mera [1], Agustín Estrada-Peña [7], Alejandro Cabezas-Cruz [4] and José de la Fuente [1,8,*]

1 SaBio, Instituto de Investigación en Recursos Cinegéticos (IREC-CSIC-UCLM-JCCM), Ronda de Toledo s/n, 13005 Ciudad Real, Spain; MargaritaM.Villar@uclm.es (M.V.); ivan.pacheco@uclm.es (I.P.); marinela.contreras@uclm.es (M.C.); lourdes.mateos@vet-alfort.fr (L.M.-H.); dinakarenbarros@gmail.com (D.K.B.-P.); josefranvet@gmail.com (J.F.L.-B.); sara.artigas@uclm.es (S.A.-J.); maria.alberdi@uclm.es (P.A.); mariaisabel.garcia@uclm.es (I.G.F.d.M.)
2 Biochemistry Section, Faculty of Science and Chemical Technologies, and Regional Centre for Biomedical Research (CRIB), University of Castilla-La Mancha, 13071 Ciudad Real, Spain
3 Facultad de Medicina Veterinaria y Zootecnia, Universidad Autónoma de Tamaulipas, Km 5, Carretera Victoria-Mante, CP 87000 Ciudad Victoria, Tamaulipas, Mexico; mero840125@hotmail.com
4 UMR BIPAR, INRAE, ANSES, Ecole Nationale Vétérinaire d'Alfort, Université Paris-Est, 94700 Maisons-Alfort, France; alejandro.cabezas@vet-alfort.fr
5 Department of Applied Physics, Faculty of Chemical Sciences and Technologies, Universidad de Castilla-La Mancha, Avda. Camilo José Cela 10, 13071 Ciudad Real, Spain; eduardo.prado@uclm.es
6 Sabiotec, Camino de Moledores s/n. 13003, 13071 Ciudad Real, Spain
7 Facultad de Veterinaria, Universidad de Zaragoza, 50013 Zaragoza, Spain; aestrada@unizar.es
8 Department of Veterinary Pathobiology, Center for Veterinary Health Sciences, Oklahoma State University, Stillwater, OK 74078, USA
* Correspondence: jose_delafuente@yahoo.com or josedejesus.fuente@uclm.es
† These authors contributed equally to this work.

Received: 4 March 2020; Accepted: 3 April 2020; Published: 5 April 2020

Abstract: Ticks are obligate hematophagous arthropods and vectors of pathogens affecting human and animal health worldwide. Cement is a complex protein polymerization substance secreted by ticks with antimicrobial properties and a possible role in host attachment, sealing the feeding lesion, facilitating feeding and pathogen transmission, and protection from host immune and inflammatory responses. The biochemical properties of tick cement during feeding have not been fully characterized. In this study, we characterized the proteome of *Rhipicephalus microplus* salivary glands (sialome) and cement (cementome) together with their physicochemical properties at different adult female parasitic stages. The results showed the combination of tick and host derived proteins and other biomolecules such as α-Gal in cement composition, which varied during the feeding process. We propose that these compounds may synergize in cement formation, solidification and maintenance to facilitate attachment, feeding, interference with host immune response and detachment. These results advanced our knowledge of the complex tick cement composition and suggested that tick and host derived compounds modulate cement properties throughout tick feeding.

Keywords: tick; cement; proteomics; dispersive energy X-ray spectroscopy; sialome; cementome; alpha-gal

1. Introduction

Ticks (Arthropoda: Ixodida) are obligate hematophagous arthropods and vectors of pathogens affecting human and animal health as well as animal welfare and production worldwide [1–4]. The spread of ticks at different geographical scales increases the risk of pathogen transmission to humans and animals since new colonization events may happen in areas with low awareness towards the diseases caused by these pathogens [5].

Ixodid ticks feed on blood for a relatively long period and an evolutionary adaptation to overcome host inflammatory and immune responses using molecules produced in tick salivary glands or recycled from the host and inoculated with saliva into the feeding site [6–22]. Cattle tick *Rhipicephalus microplus* (Canestrini, 1888) is an Ixodid one-host tick species (all developmental stages remain on the same host) with an impact on cattle industry in tropical and subtropical regions of the world [3,9,10]. However, despite the growing impact of ticks on humans and animals worldwide, effective and environmentally friendly control methods such as vaccines among other interventions are still required to control tick infestations and tick-borne diseases [23–26].

As recently supported by mechanistic studies [27], feeding of ixodid ticks begins with the secretion through inserted mouthparts of cement salivary proteins [28]. Cement is a complex substance secreted by most ticks of the family Ixodidae including *Rhipicephalus* spp. to anchor their mouthparts to the host skin [29]. The cement has not only adhesive properties but has been proposed to have a possible role in antimicrobial properties, seals the lesion during feeding, facilitates feeding and pathogen transmission, and protects ticks from host immune and inflammatory responses [22,29]. Tick cement has been studied using different methodological approaches to characterize its structure, protein and chemical composition, and functional implications such as decrease in the width of cement cone as it goes deeper into the host skin or after Glycine-rich protein coding gene knockdown in *Amblyomma americanum* [16,20,29,30]. However, the biochemical properties of tick cement during different ectoparasite feeding stages have not been fully characterized.

The objective of this study was to characterize the tick and host derived compounds present in the cement throughout tick feeding. To address this objective, in this study we characterized the proteome of tick *R. microplus* salivary glands (sialome) and cement (cementome) together with physical and chemical properties of the cement collected at different adult female parasitic stages. Our experimental approach using proteomics allowed high throughput identification of tick and host derived proteins in both sialome and cementome. Additionally, the first analysis of the chemical elements using scanning electron microscopy (SEM) combined with dispersive energy X-ray spectroscopy (EDS) allowed the characterization of changes in their composition in tick salivary glands and cement during tick feeding, which correlated with changes in protein profiles. The composition of glycan α-Gal was characterized in tick sialome and cementome with putative functional implications (see Section 3.7). These results advanced our knowledge of the complex tick cement composition and suggested that tick and host derived compounds modulate the biochemical properties of the cement throughout tick feeding.

2. Materials and Methods

2.1. Ticks

The R. microplus (Susceptible Media Joya strain, CENAPA, Mexico) ticks were obtained from a laboratory colony maintained at the University of Tamaulipas (UAT), Mexico [31]. Tick larvae were fed on cross-bred Bos taurus cattle and collected after repletion to allow for oviposition and hatching in humidity chambers at 12 h light:12 h dark photoperiod, 22–25 °C and 95% relative humidity (RH). Larvae were used for infestations at 15 days after hatching from eggs. Female ticks were manually detached at different time points (50 ticks per replicate, n = 2 biological replicates). The study was conducted in accordance with standards specified in the Guide for Care and Use of Laboratory Animals

for the University of Tamaulipas (UAT), Mexico. The protocol was approved by the ethics committee of the UAT (No. CBBA_17_0).

2.2. Collection of Tick Cement Cones and Salivary Glands

Tick cement cones were carefully collected using soft tissue forceps from mouthparts of manually detached adult female ticks after feeding on cattle for 14–17 (T1), 18–20 (T2), and 21–25 (T3) days post-infestation (dpi) and corresponding to parasitic stages immediately after molting to adults (T1), secondary cement production (T2), and just before tick detachment (T3). Special attention was taken to remove all host-derived skin or hairs attached to the cement. Salivary glands were extracted from the same dissected ticks. Collected cement cones were rinsed with PBS with 1% of protease inhibitor cocktail M221 (VWR Life Science AMRESCO, OH, USA) and kept in PBS/M221 or RNAlater (Sigma-Aldrich, St. Louis, MO, USA). Salivary glands were dissected from female ticks and washed in ice-cold PBS containing the protease inhibitor cocktail to remove hemolymphs-related cells as previously described [14,32] and kept in RNAlater (Sigma-Aldrich) until analysis.

2.3. Protein Extraction from Tick Salivary Glands and Cement

Tick salivary glands and cement samples were resuspended in 200 µL 50 mM Tris-HCl pH 7.4 supplemented with 4% sodium dodecyl sulfate (SDS), 1 mM DTT and complete protease inhibitor cocktail (Roche, Basel, Switzerland) using a 1 mL syringe with a 40 mm needle (Terumo Europe España SL, Alcalá de Henares, Spain). Samples were sonicated for 3 min in an ultrasonic cooled bath, followed by vortexing for 10 sec. After five cycles of sonication-vortex, tick salivary glands and cement lysates were centrifuged at 200× *g* for 5 min. Salivary glands were completely solubilized and salivary glands and cement supernatants were collected. Pellet cement samples were homogenized in lysis buffer (8 M urea, 2 M thiourea, and 2% 3-[(3-cholamidopropyl) dimethylammonio]-1-propanesultonate (CHAPS), following the same protocol until cement samples were completely homogenized. Protein concentration in salivary glands and SDS and urea cement extracts was determined using the Bicinchoninic acid (BCA) Protein Assay Kit (Thermo Fisher Scientific, Waltham, MA, USA) following manufacture's recommendations. Proteins extracts were methanol/chloroform precipitated and stored at −20 °C until analysis.

2.4. Proteomics Analysis of Tick Sialome and Cementome

The sialome and cementome of *R. microplus* female ticks collected at different feeding stages were characterized by proteomics analysis using reverse phase liquid chromatography mass spectrometry (RP–LC–MS/MS) using an ekspertTM nanoLC 415 system coupled on line with a 6600 TripleTOF mass spectrometer (Ab Sciex, Framingham, MA, USA) through information-cyclic data independent acquisition (DIA) followed by sequential windowed data independent acquisition of the total high-resolution mass spectra (SWATH)-mass spectrometry (MS). Fifty micrograms of proteins from each sample were on-gel concentrated by SDS–PAGE and trypsin digested as previously described [33]. Resulting peptides were desalted onto OMIX Pipette tips C18 (Agilent Technologies, Santa Clara, CA, USA), dried-down and stored at −20 °C until analysis. The desalted protein digests were resuspended in 2% acetonitrile, 5% acetic acid in water for analysis. Approximately 4 µg of each protein digest of the two biological replicates were pooled together as a mixed sample from tick salivary glands and SDS and urea-extracted cement samples, respectively, collected at three different feeding stages (T1–T3), which were used for the generation of the reference spectral ion library as part of the SWATH-MS analysis. The peptides were concentrated using a 0.1 × 20 mm C18 RP precolumn (Thermo Fisher Scientific), and then separated using a 0.075 × 250 mm C18 RP column (New Objective, Woburn, MA, USA) operating at 0.3 mL/min. Peptides were eluted using a 120 min gradient from 5% to 30% solvent B in solvent A followed by 15 min gradient from 30% to 60% solvent B in solvent A (Solvent A: 0.1% formic acid in water, solvent B: 0.1% formic acid in acetonitrile) and directly injected into the mass spectrometer for analysis. For IDA experiments, the mass spectrometer was set to

scanning full spectra (350–1400 *m*/*z*) using 250 ms accumulation time per spectrum, followed by up to 50 MS/MS scans (100–1500 *m*/*z*). Candidate ions with a charge state between +2 and +5 and counts per second above a minimum threshold of 100 were isolated for fragmentation. One MS/MS spectrum was collected for 100 ms, before adding those precursor ions to the exclusion list for 15 sed (mass spectrometer operated by Analyst TF 1.6, Ab Sciex). Dynamic background subtraction was turned off. MS/MS analyses were recorded in high sensitivity mode with rolling collision energy on and a collision energy spread of 5. For SWATH quantitative analysis, fifty-four independent samples (three technical replicates of each biological replicate from salivary glands, SDS cement and urea cement extracts collected at T1, T2, and T3 dpi) (8 µg each) were subjected to the cyclic data independent acquisition (DIA) of mass spectra using the SWATH variable windows calculator (V 1.0, Ab Sciex) and the SWATH acquisition method editor (Ab Sciex), similar to established methods [34]. A set of 50 overlapping windows was constructed (containing 1 *m*/*z* for the window overlap), covering the precursor mass range of 400–1250 *m*/*z*. For these experiments, a 50 ms survey scan (350–1400 *m*/*z*) was acquired at the beginning of each cycle, and SWATH–MS/MS spectra were collected from 100–1500 *m*/*z* for 70 ms at high sensitivity mode, resulting in a cycle time of 3.6 sec. Collision energy for each window was determined according to the calculation for a charge +2 ion-centered upon the window with a collision energy spread of 15.

2.5. Library Generation, Protein Identification, Data Processing, and Relative Quantitation

To create a spectral library of all the detectable peptides in the samples, the IDA MS raw files were combined and subjected to database searches in unison using ProteinPilot software v. 5.0.1 (Ab Sciex) with the Paragon algorithm. Spectra identification was performed by searching against a compiled database containing all the sequences from Uniprot (https://www.uniprot.org) Ixodidae and *Bos taurus* taxa (148,942 and 32,715 entries, respectively, in April, 2019) with the following parameters: iodoacetamide cysteine alkylation, trypsin digestion, gel-based ID as special factor, identification focus on biological modification and thorough ID as search effort. We used the Ixodidae database to improve protein identification for a more comprehensive proteomics analysis because it contains 148,942 entries while for *Rhipicephalus* only 46,429 are available. The detected protein threshold was set at 0.05. An independent False Discovery Rate (FDR) analysis, using the target-decoy approach provided by Protein Pilot (Ab Sciex; https://sciex.com/products/software/proteinpilot-software), was used to assess the quality of identifications. Positive identifications were considered when identified proteins reached a 1% global FDR. For SWATH processing, up to ten peptides with seven transitions per protein were automatically selected by the SWATH Acquisition MicroApp 2.0 in the PeakView 2.2 software (Ab Sciex; https://sciex.com/products/software/peakview-software) with the following parameters: 15 ppm ion library tolerance, 5 min XIC extraction window, 0.01 Da XIC width, and considering only peptides with at least 99% confidence and excluding those which were shared or contained modifications. However, to ensure reliable quantitation, only proteins that had 3 or more peptides available for quantitation were selected for XIC peak area extraction and exported for analysis in the MarkerView 1.3 software (Ab Sciex; https://sciex.com/products/software/markerview-software). Global normalization was performed according to the Total Area Sums (TAS) of all detected proteins in the samples. The Student's t-test ($p < 0.05$) was used to perform two-sample comparisons between the averaged TASs of all the transitions derived from each protein across the three replicate runs for each sample under comparison in order to identify proteins that were significantly differentially represented between time points (T1–T3). Gene ontology (GO) annotations were obtained using Blast2GO software (http://www.blast2go.org). Host and tick derived proteins identified in the sialome and cementome differentially represented in at least one comparison between the different time points (T1 vs. T2, T2 vs. T3, and T1 vs. T3) were grouped based on the assignment to putative categories of developmentally relevant processes according to their representation profile. Based on representation profiles, proteins were putatively assigned to different categories of developmental processes including secondary cement production I and II, cement maintenance, feeding, feeding and oogenesis, molting, and detachment.

Biomolecules **2020**, *10*, 555

Proteins without significant differences in representation at different time points were assigned to housekeeping functions (Figure 1). The assignments to developmental processes were used for protein profile classification and some proteins may be implicated in different tissue-specific processes. Raw proteomics data were deposited at the PeptideAtlas repository (http://www.peptideatlas.org/) with the dataset identifier PASS01524. Results are included in Data S1–S4 and Tables S1 and S2.

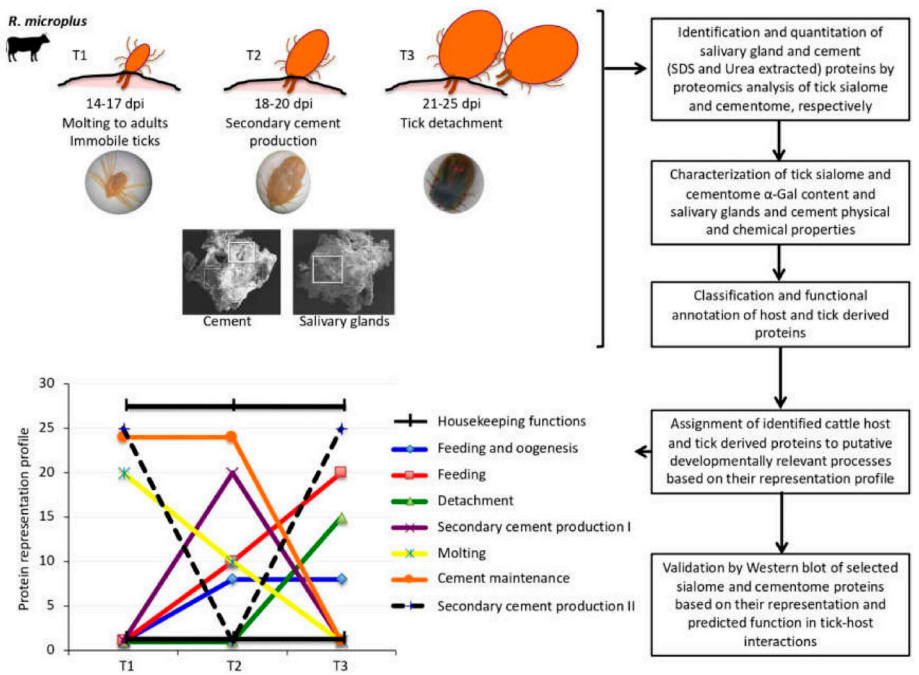

Figure 1. Experimental design. The sialome, cementome, and salivary glands and cement physical and chemical properties were characterized in *R. microplus* adult female ticks during feeding on cattle in samples collected at three time points corresponding to 14–17 dpi (T1; immediately after molting to adults immobile ticks), 18-20 dpi (T2; during secondary cement production), and 21–25 dpi (T3; just prior to tick detachment). After protein extraction, proteomics was used for the identification, quantitation, functional annotation, and assignment to putative developmentally relevant processes based on the representation of sialome and cementome proteins derived from bovine host and tick. Based on representation profiles in arbitrary units, proteins were putatively assigned to different categories of developmental processes including secondary cement production, cement maintenance, feeding, oogenesis, molting, detachment, and housekeeping functions. Cement physical and chemical properties and α-Gal content were also characterized. Finally, selected proteins based on their representation and predicted function in tick-host interactions were analyzed by Western blot.

2.6. Tick salivary Glands and Cement Physical and Chemical Properties

The amino acid composition, theoretical isoelectric point (pI), atomic composition, instability index. and grand average of hydropathicity (GRAVY) of the peptides used to identify all host proteins identified in the cementome but not in the sialome (host), 100 randomly selected tick proteins identified in the sialome but not in the cementome (tick), all host proteins identified in the sialome and cementome (host cement), and all tick proteins identified in the cementome (tick cement) (Data S4) were analyzed using the ProtParam tool (https://web.expasy.org/protparam) [35]. Results are included in Table S3. Individual tick cement and salivary gland samples collected at the same time points (T1–T3) were dehydrated in an incubator at 37 °C for 24 h in preparation for analysis with SEM.

The samples were placed and mounted on standard aluminum SEM sample holders with conductive carbon adhesive tabs. The samples were observed and analyzed with a field emission scanning electron microscope (Zeiss GeminiSEM 500, Oberkochen, Germany) operating in high vacuum mode at an acceleration voltage of 15 kV and without metal coating. For the analysis of chemical elements, 3 area scans per sample were included using an 80 mm^2 EDS detector (Oxford Instruments, Abingdon, United Kingdom). Results are included in Data S5 and S6. The composition of chemical elements in the cement and salivary glands of *R. microplus* were compared at different time points by One-way ANOVA test (https://www.socscistatistics.com/tests/anova/default2.aspx; $p < 0.05$, n = 2–4 biological replicates). The correlation analysis between total protein atomic composition in tick-derived proteins identified in the sialome but not in the cementome (Tick), all tick-derived proteins identified in the cementome (Tick cement) and all host-derived proteins identified in the sialome and cementome (Host cement) (Table S3) and T1–T3 average chemical atomic percentage of relative abundance in tick salivary glands and cement (Data S6) was performed using the elements identified in both sialome/cementome and tick salivary glands/cement chemical composition (C, N, O, and S) with Spearman's Rho test calculator (https://www.socscistatistics.com/tests/spearman/default2.aspx).

2.7. Tick Sialome and Cementome α-Gal Content

The Galα1-3Galβ1-(3)4GlcNAc-R (α-Gal; Figure S1) content was analyzed in tick sialome and cementome at different time points (T1–T3). An ELISA test was used to determine the α-Gal levels in protein extracts. Plates were coated with 100 ng of protein per well in carbonate/bicarbonate buffer and incubated overnight at 4 °C and blocked with 1% human serum albumin (Sigma-Aldrich) in PBS for 1 h at room temperature (RT), following three washes with PBS containing 0.05% Tween 20 (PBST). The anti-α-Gal epitope monoclonal antibody (M86; Farmingdale, NY, USA) was added at 1:50 dilution in PBS and incubated for 1 h at 37 °C followed by three washes with PBST. Then, goat anti-mouse IgM (μ-chain specific) peroxidase-conjugated antibodies (Sigma-Aldrich) were added at 1:20000 dilution in PBS. The reaction was visualized by adding 100 μL of 3,3′,5,5′- Tetramethylbenzidine (Promega, Madison, WI, USA) and incubated for 20 min in the dark at RT. The optical density (OD) was measured at 450 nm with a Multiskan FC ELISA reader (Thermo Fisher Scientific). The average value of the blanks (wells without tick protein coating; n = 3) was subtracted from all reads and the average of 3 replicates for each sample was used for further analysis. Protein extracts from human promyelocytic leukemia HL60 cells (ATCC CCL-240) and pork (*Sus scrofa*) kidney were included as negative and positive controls, respectively. A calibration curve with 0.0 to 1.0 ng bovine serum albumin (BSA)-α-Gal (Dextra, Shinfield, UK) and O.D. values at 450 nm was constructed using Microsoft Excel for Mac (v. 16.26) to convert ELISA reader values to α-Gal content per sample ($R^2 = 0.913$; Figure S2). The results (average + S.D. of α-Gal/1 μg protein) were compared between pork kidney positive control, salivary gland or cement samples and HL60 cells negative control and between salivary gland and cement samples at different time points (T1–T3) by Student's t-test with unequal variance ($p < 0.05$, $n = 3$ biological replicates). Variations in α-Gal levels at different time points (T1–T3) in both sialome and cementome were compared by one-way ANOVA test (https://www.socscistatistics.com/tests/anova/default2.aspx) ($p < 0.05$, $n = 3$ biological replicates).

2.8. Network Analysis of Tick Cementome

A network of interactions was used for the integration of data obtained from *R. microplus* proteins identified by proteomics in the cementome at different feeding stages. The methodology to build the network of interactions has been previously described and validated [36]. This network consists of a set of nodes that are connected by edges where nodes are the interacting items, and links between nodes represent the strength with which they interact. In this development, we used the Sparse Correlation for Compositional Data (SparCC) to obtain the strength of association between proteins [37], which infers associations in compositional data by estimating the linear Pearson's correlations between the log-transformed components. Correlation values from SparCC between co-occurring proteins

were used to populate the weights of the links among nodes and build the network. Centrality is a fundamental property of the network because it refers to nodes that connect high score nodes [36,38]. In this context, "high score" applies to other nodes with high importance in the network. We calculated the importance of a node in the "traffic" between different nodes of the network using Betweenness Centrality (BNC), giving a higher score to a node that sits on many shortest paths of other node pairs [36,39]. In our context, this score is an indicator of the relative importance of a protein co-occurring with two or more proteins.

2.9. Recombinant Proteins and Antibodies

Recombinant tick histone H4 (Q4PM69), aminopeptidase N (A0A131YLU7) and Glycine-rich superfamily member (A0A224YEQ4) proteins (Table S4) were produced in *Escherichia coli*. Genes coding for histone H4 and aminopeptidase N were cloned by RT-PCR using *R. microplus* RNA and gene-specific primers (Table S4). The Glycine-rich superfamily member was amplified from a synthetic gene optimized for codon usage in *E. coli* (Genscript Corporation, Piscataway, NJ, USA) (Table S4). For the production of the membrane-bound histone H4-*Anaplasma marginale* major surface protein 1a (MSP1a) chimera, recombinant *E. coli* BL21 cells transformed with the pMBXAF3 expression vector were used [40]. In this construct, as for others MSP1a chimeras [41], the inserted histone H4 coding region is fused to MSP1a and is under the control of the inducible tac promoter [40]. The amplified DNA fragments from aminopeptidase N and Glycine-rich superfamily member protein coding regions were cloned into the expression vector pET101 and all the proteins were produced in the *E. coli* strain BL21 using the Champion pET101 Directional TOPO Expression kit (Carlsbad, CA, USA). Recombinant histone H4-MSP1a was purified as previously reported [42]. Briefly, recombinant proteins were fused to Histidine tags for purification by affinity to Ni [43,44]. Transformed *E. coli* strains were induced with IPTG for 4.5 h to produce recombinant proteins, which were purified to >85% of total cell proteins by Ni affinity chromatography as previously described [43,44] using 1 mL HisTrap FF columns mounted on an AKTA-FPLC system (GE Healthcare, Piscataway, NJ, USA) in the presence of 7 M urea lysis buffer. The purified antigens were refolded by dialysis against 1,000 volumes of PBS (137 mM NaCl, 2.7 mM KCl, 10 mM Na_2HPO_4, 1.8 mM KH_2PO_4, pH 7.4) for 12 h at 4 °C and stored at −20 °C until used.

For histone H4-MSP1a and aminopeptidase N recombinant proteins, two New Zealand white rabbits (*Oryctulagus cuniculus*) were subcutaneously injected at weeks 0, 4, and 6 with 50 µg protein in 0.4 mL Montanide ISA 50 V adjuvant (Seppic, Paris, France). Blood was collected before injection and 2 weeks after the last immunization to prepare preimmune and immune sera, respectively. Serum aliquots were kept at 4 °C for immediate use or at −20 °C for long-term storage. The IgG were purified from serum samples using the Montage antibody purification kit and spin columns with PROSEP-A media (Millipore, Billerica, MA, USA) following the manufacturer's recommendations. Commercial antibodies against host pan-keratins (ab190625), desmoplakin (ab106342) and alpha-2-HS-glycoprotein (AHSG; ab112528) proteins (Abcam, Cambridge, UK) were used for analysis. In a previously described validation approach [45], these antibodies were used to detect host-derived proteins in fed ticks (Figure S3).

2.10. Western Blot or Dot Blot Analysis of Recombinant Proteins and the Tick Sialome and Cementome

2.10.1. Recombinant Proteins (Histone H4-MSP1a, Aminopeptidase N, and Glycine-Rich Superfamily Member Protein; Figure S4)

For Western blot analysis, 10 µg of purified recombinant proteins were separated by electrophoresis on a sodium dodecyl sulfate (SDS)-12% polyacrylamide gel (Life Science, Hercules, CA, USA) and either stained with Coomassie Brilliant Blue or transferred to a nitrocellulose membrane. The membrane was blocked with 5% BSA (Sigma-Aldrich) for 2 h at RT, washed four times with Tris-buffered saline (TBS; 50 mM Tris-Cl, pH 7.5, 150 mM NaCl, 0.5% Tween 20). Pooled sera collected from histone H4,

Aminopeptidase N vaccinated rabbits and polyclonal rabbit anti-Glycine-rich superfamily member protein antibodies (Abcam) were used as primary antibodies. Primary antibodies were used at a 1:200 dilution in TBS, and the membrane was incubated overnight at 4 °C and washed four times with TBS. The membrane was then incubated with an anti-rabbit IgG-horseradish peroxidase (HRP) conjugate (Sigma-Aldrich) diluted 1:1000 in TBS with 3% BSA (BSA/TBS). The membrane was washed five times with TBS and finally developed with TMB (3,3´, 5,5´-tetramethylbenzidine) stabilized substrate for HRP (Promega, Madrid, Spain) according to the manufacturer recommendations.

2.10.2. Tick Cementome and Sialome

Cement protein lysate (10 μg) and salivary gland protein lysate (20 μg) were methanol/chloroform precipitated, resuspended in Laemmli sample buffer and separated on an SDS-polyacrylamide precast gel (ClearPage Expedeon, VWR, Radnor, PA, USA). Due to the limited amount of cementome and sialome proteins, Western blot analysis was performed for aminopeptidase N only to avoid the limitations posed by the different representation profiles of protein families such as Histones and Glycine-rich superfamily member proteins (Figure S5). After electrophoresis, proteins were transferred to a nitrocellulose blotting membrane (GE Healthcare Dharmacon Inc., Lafayette, CO, USA), blocked with 3% BSA (Sigma-Aldrich) in TBS (3% BSA/TBS) and incubated overnight at 4 °C with antibodies against tick recombinant aminopeptidase N diluted 1:200 in 3% BSA/TBS. To detect the IgG antibodies bound to tick proteins, membranes were incubated with goat anti-rabbit IgG peroxidase antibody (Sigma-Aldrich) diluted 1:1000 in 3% BSA/TBS. Immunoreactive proteins were visualized by chemiluminescence with Pierce ECL Western Blotting Substrate (Thermo Fisher Scientific). Quantitative analysis was performed using the Fiji ImageJ (https://imagej.nih.gov/ij/download.html) to measure the intensity of the protein bands and after substation of the intensity of the PBS control to compare the results at different time points. For the dot blot analysis of the other selected proteins (Figures S6–S8), cement and salivary gland proteins were applied onto each strip in 6 different dots (volume per dot, 25 μL at 5 μg/μL. Then the dots were allowed to dry by gravity flow, immersed in 50 μL of 3% BSA/TBS for 15 min approximately and filtered by gravity. Membranes were washed two times with TBS and incubated with primary antibodies diluted at different concentrations in 1% BSA/TBS against Histone H4 (1:100), Glycine-rich superfamily member proteins (1:200) and host pan-keratins (1:300), desmoplakin (1:300) and alpha-2-HS-glycoprotein (1:300). To detect the IgG antibodies bound to tick proteins, membranes were incubated with goat anti-rabbit IgG peroxidase antibody (Sigma-Aldrich) diluted 1:1000 in 1% BSA/TBS. Membranes were washed two times with TBS and immunoreactive proteins were visualized with chemiluminescence with Pierce ECL Western blotting substrate (Thermo Fisher Scientific). Quantitative analysis was performed as described above for Western blot analysis.

3. Results and Discussion

3.1. Experimental Design and Rationale

Rhipicephalus microplus are one-host ticks that complete parasitic stages of their life cycle while feeding on the same host and with an impact on cattle industry in tropical and subtropical regions of the world [3,46]. The *R. microplus* were selected for analysis because little information is available on cement composition in this tick species. The experimental design (Figure 1) included the characterization of sialome, cementome, and salivary gland and cement physical and chemical properties in *R. microplus* adult female ticks during feeding on cattle in samples collected at three time points corresponding to 14–17 dpi (T1; immediately after molting to adults immobile ticks), 18–20 dpi (T2; during secondary cement production), and 21–25 dpi (T3; just prior to tick detachment). *R. microplus* one-host ticks remain attached to the host throughout all parasitic stages with a continuously functioning feeding apparatus during molting [47]. Sampling times were selected based on the well-known life cycle in cattle of the *R. microplus* susceptible Media Joya strain laboratory colony maintained at the UAT, Mexico [31]. The SDS-based

Biomolecules **2020**, *10*, 555

protein extraction is commonly used for proteomics analysis of tick samples such as salivary glands, saliva, and cultured cells [12,32,33]. However, probably due to cement composition with previously unknown components, it was not fully dissolved in SDS-containing buffer. Therefore, to improve protein extraction for cementome analysis, a urea-containing buffer previously applied to tick cement analysis [16,30] was used in addition to SDS. This approach resulted in a higher protein identification in the tick cementome (654 proteins) when compared to SDS-based (388 proteins) or urea-based (266 proteins) extraction protocols alone (Figure 2A). After protein extraction, proteomics was used for the identification, quantitation, functional annotation, and assignment to putative developmentally relevant processes based on novel methodology based on the representation profile of sialome and cementome proteins derived from bovine host and tick. Based on representation profiles after significant differences in pairwise comparisons between time points, proteins were putatively assigned to different categories of developmental processes including secondary cement production, cement maintenance, feeding, oogenesis, molting, detachment, and housekeeping functions. Salivary glands, cement physical and chemical properties, and α-Gal content were also characterized. The selection of proteins for analysis was focused on the cementome because little information is available for this complex substance playing a key role during tick parasitic stages [16,29,30,48]. Finally, selected proteins based on their representation and predicted function in tick-host interactions were analyzed by Western blot to further validate proteomics results.

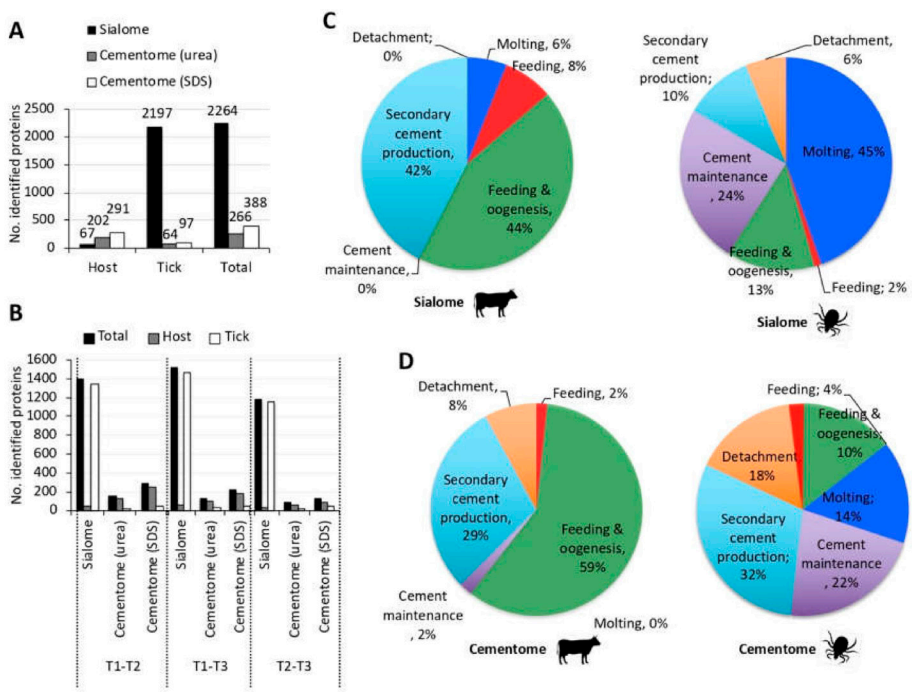

Figure 2. Protein representation profiles in tick sialome and cementome. (**A**) Number of host, tick, and total proteins identified in the sialome and cementome (proteins extracted with urea and sodium dodecyl sulfate (SDS)). (**B**) Host, tick, and total number of differentially represented proteins ($p < 0.05$; Data S4) identified in the sialome and cementome (proteins extracted with urea and SDS). (**C**) Assignment of host and tick derived differentially represented proteins identified in the sialome to putative categories of developmentally relevant processes based on their representation profile. (**D**) Assignment of host and tick derived differentially represented proteins identified in the cementome to putative categories of developmentally relevant processes based on their representation profile. Proteins in the cementome extracted with urea and SDS were grouped together with unique non-redundant entries (Data S4).

3.2. The Representation of R. Microplus Tick and Cattle Host Derived Proteins in the Sialome and Cementome Change during Adult Female Parasitic Stages

Proteins have been identified as the main components of the tick cement [49]. Our experimental approach using proteomics allowed the identification of tick and host derived proteins in the sialome and cementome (2264 and 654 total number of proteins identified in the sialome and cementome, respectively; Figure 2A) (Data S1–S4). These results expand the repertoire of identified cementome tick and host derived proteins, which were previously limited to less than 200 proteins [16,30]. Cattle host-derived proteins were identified in the tick sialome and cementome with higher representation in the later (Figure 2A). As expected, tick-derived proteins were also identified in the sialome and cementome but with over 15-fold representation in the sialome (Figure 2A). Similar results were obtained when only differentially represented proteins ($p < 0.05$ at least between two time points; Data S4) were considered (Figure 2B).

Host and tick derived differentially represented proteins identified in the sialome and cementome were then grouped based on the assignment to putative categories of developmentally relevant processes according to their representation profile (Figure 1, C,D). The sialome host-derived proteins were mostly represented (86%) in feeding and oogenesis and secondary cement production, while 69% of tick-derived proteins were represented in the molting and cement maintenance representation profiles (Figure 2C). Additionally, cement maintenance and detachment profiles appeared only in the tick-derived sialome. In the cementome, host-derived proteins were as in the sialome mostly represented (88%) in feeding and oogenesis and secondary cement production (Figure 2D). However, tick-derived cementome profile was different from the sialome with higher representation of secondary cement production and cement maintenance (Figure 2D).

These results also provided insight into the origin of host and tick derived proteins identified in the sialome and cementome (Figure 3A). Of the 62 proteins found in both sialome and cementome, 13 and 49 were tick and host derived proteins, respectively. In the sialome, 61 host proteins were present of which 49 were secreted into the cement. An additional 250 host-derived proteins were identified in the cement, most of which were likely contaminants from host cells attached to the tick cement cone. Of the 1936 tick proteins identified in the sialome, only 13 appeared as secreted into the cement. However, an additional 68 tick-derived proteins present in the cementome were not identified in the sialome, probably due to the low representation of these proteins in the sialome when compared to the cementome.

Based on their representation profile (Figure 1), proteins present in the sialome and cementome were assigned to secondary cement production, maintenance and/or decomposition for tick detachment, but may also be implicated in tick feeding, molting and/or oogenesis. Proteins in the sialome but not in the cementome may function in different processes such as feeding and oogenesis, and in metabolic pathways involved in the synthesis of metabolite cement components. Proteins in the cementome and/or sialome with similar representation throughout tick feeding and therefore without significant differences in their representation at different time points (Data S1–S4) may be involved in housekeeping functions as well as in other processes. Despite significant differences in protein representation and profiles, some of the tick proteins identified in the cementome may constitute secreted proteins not incorporated into the cement.

Biomolecules **2020**, *10*, 555

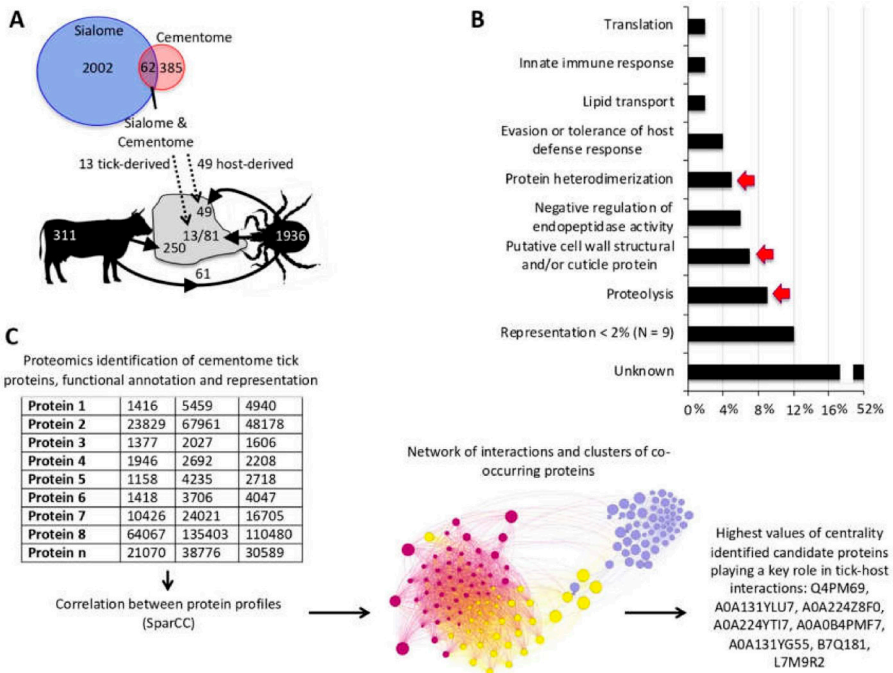

Figure 3. Composition of the tick cementome. (**A**) Of the 62 proteins found in both sialome and cementome, 13 and 49 were tick and host derived proteins, respectively. An additional 68 tick derived proteins present in the cement were not identified in the sialome, resulting in a total of 81 tick-derived proteins in the cementome composition. Other host derived proteins in the cementome were likely contaminants from host cells attached to the tick cement cone. (**B**) Biological processes annotated in tick-derived cementome proteins. Processes containing proteins selected for further analysis are shown with arrows. (**C**) Network analysis of tick-derived cementome proteins. Using co-occurring proteins at different feeding stages, a network was built using correlation values from SparCC. Network centrality was then used to identify the most central proteins in the dataset putatively playing a key role in cement biological processes affecting tick-host interactions.

3.3. Tick-Derived Cementome Proteins Appear to be Involved in Cement Formation, Solidification, Maintenance, Feeding, and Interference with Host Immune Response and Detachment

Tick-derived cementome proteins were selected for consideration in further analyses based on one of the following criteria (Table S1): (a) identified in both sialome and cementome; (b) being among the two proteins with highest representation in feeding, feeding and oogenesis, molting, secondary cement production, cement maintenance or detachment profile categories; and (c) predicted to play a key role in cementome biological processes affecting tick-host interactions due to over 4% representation in biological processes (Figure 3B) or after network analysis (Figure 3C). Network analysis of tick-derived cementome proteins was conducted using interactions and clusters of co-occurring proteins at different feeding stages and correlation values from SparCC. Network centrality index was then used to identify in the dataset the proteins with highest values of centrality and consequently putatively playing a key role in cement biological processes affecting tick-host interactions Figure 3C).

Tick proteins fulfilling these criteria were found in most of the processes previously proposed to be present in the cementome [29] (Figure 4A). Most proteins appeared putatively involved in cement formation, solidification, and maintenance (45%), and tick feeding (26%) (Figure 4B). Other identified proteins had putative functions in detachment and interference with host immune response (Figure 4B). However, acidic chitinase proteins proposed to function in sealing of the feeding lesion [48] or proteins

Biomolecules **2020**, *10*, 555

with antimicrobial activity were not identified while 18% of the proteins had an unknown function with possible implication in cement formation, solidification and maintenance, and tick feeding and oogenesis (Figure 4B). The protein representation profiles of selected tick cementome proteins were mainly assigned to secondary cement production, maintenance, and detachment (Table S1).

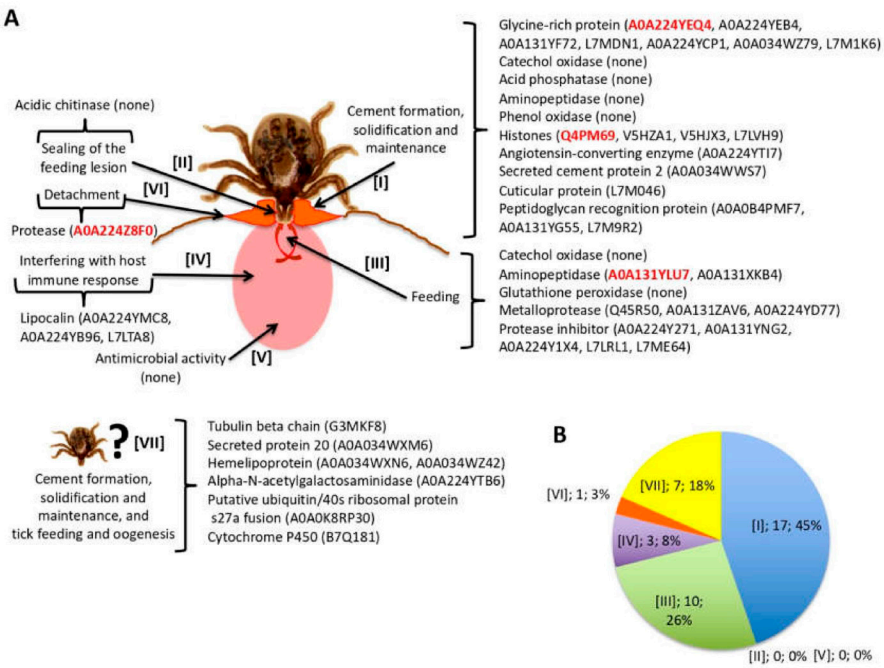

Figure 4. Tick-derived cementome proteins. (**A**) Selected tick-derived cementome proteins (Table S1) were found in most of the processes previously proposed to be present in the tick cementome. Proteins selected for further analyses are highlighted in red. (**B**) Protein representation (process, number of proteins, percentage) in the different processes previously proposed to be present in the tick cementome.

3.4. Host-Derived Cementome Proteins Co-Exist with Tick-Derived Proteins and May Contribute to Cement Structure and Function

As with tick-derived proteins, the analysis was focused on bovine host-derived proteins identified in the cementome. In particular and to reduce the possible contamination with host-derived proteins, the analysis was focused on the 49 host proteins identified in the sialome and secreted into the cementome (Figure 3A, Table S2). Of these 49 proteins, 10 corresponded to keratins of which two were represented in the cementome with more than 1 million TAS at all time points (Table S2). Based on the processes previously proposed to be present in the cementome [29], most host-derived proteins appeared as putatively involved in cement formation, solidification and maintenance (35%), and tick feeding (25%) (Figure 5A,B). Other identified proteins had putative functions in detachment and interference with host immune response (Figure 5B). These results were similar to those found with tick-derived proteins (Figure 4B). However, proteins putatively involved in sealing of the feeding lesion and with antimicrobial activity that were not found in tick-derived proteins (Figure 4B) were present among host-derived proteins (Figure 5B). Additionally, 12% of the host-derived proteins were identified with possible implication in cement formation, solidification and maintenance, and tick feeding and oogenesis (Figure 5B).

Biomolecules **2020**, *10*, 555

These results suggested that in the cementome, host-derived proteins might be involved in the cement structure and function, possibly complementing and synergizing with tick-derived proteins. The cement protein representation profiles of selected host-derived cementome proteins were mainly assigned to feeding and oogenesis, secondary cement production, maintenance, and detachment (Table S2).

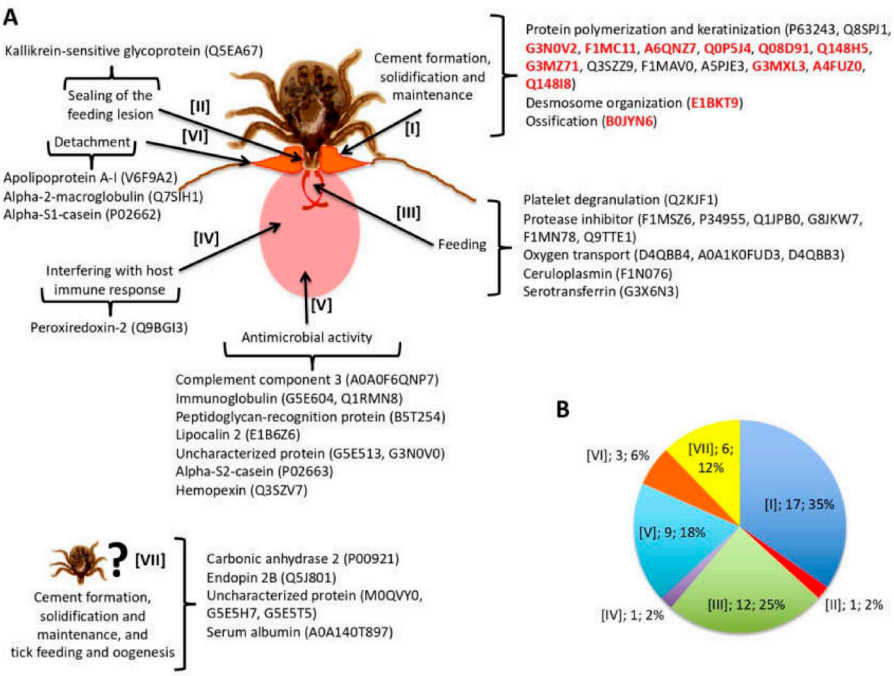

Figure 5. Host-derived cementome proteins. (**A**) Host proteins identified in both sialome and cementome (Table S2) were found in all of the processes previously proposed to be present in the tick cementome. Proteins selected for further analyses are highlighted in red. (**B**) Protein representation (process, number of proteins, and percentage) in the different processes previously proposed to be present in the tick cementome.

3.5. Biological Processes Represented in the Tick and Host Cementome Support Proposed Complementation and Synergy in Cement Formation and Function between Tick and Host Derived Proteins

To further characterize the differences between tick and host sialome and cementome, a summary of the biological processes (P) affected by these proteins was included within the experimental approach used here for the different developmentally relevant processes (Figure 6 and Data S4). The results showed differences in the P affected by tick and host derived proteins, further supporting the possibility of complementation and synergy between these proteins in cement formation and function. In the cementome, the most represented biological processes (P) (>30%) were translation, cytoskeleton organization, proteolysis, immune response, catalytic activity, carbohydrate metabolism, protein processing and transport, and blood circulation and coagulation (Figure 6). As it has been proposed for cement properties and function [22,29], the cementome P support the presence of antimicrobial properties, feeding and metabolism, and protection from host immune and inflammatory responses.

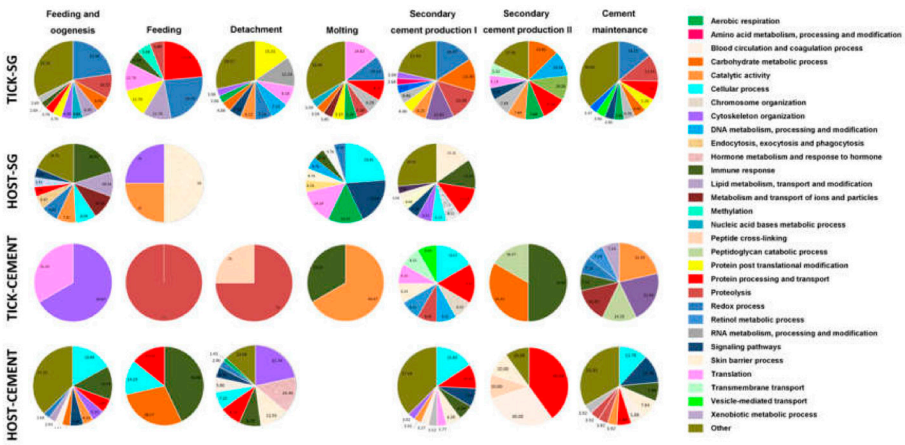

Figure 6. Classification according to biological processes (P) of the host and tick derived proteins identified in the sialome (HOST-SG and TICK-SG) and cementome (HOST-CEMENT and TICK-CEMENT) and putatively assigned to the different categories of developmental processes including secondary cement production I and II, cement maintenance, feeding, feeding and oogenesis, molting, and detachment. All P were considered, but only the ten most abundant (percentage of representation within the total P per sample) are displayed in the figure. The GO P categories were grouped in different P and less abundant categories were grouped as Other (Data S4). A high resolution image was include in Data S4.

3.6. Physical and Chemical Properties of Tick Salivary Glands and Cement Show Tissue-Specific Differences and Vary during Tick Feeding

The *R. microplus* cement physical and chemical properties were analyzed (Figures 7 and 8, Table S3, Data S5 and S6). The analysis of amino acid composition of tick cementome showed that Gly was the amino acid with highest representation in the tick-derived proteins and lowest representation in the host-derived proteins (Figure 7A,B). This finding correlated with previous reports [16,29,30] and the high representation of Glycine-rich superfamily member proteins (three proteins with more than three million TAS) found here in the tick cementome, which are putatively involved in cement formation, solidification, and maintenance (Figure 4A,B, Table S1, Data S4). Additionally, Tyr representation was augmented in both host and tick derived proteins in the cementome when compared to non-cementome host and tick derived proteins, respectively (Figure 7B). Other amino acids such as Phe and Trp were represented at higher levels in host-derived cementome than in non-cementome proteins (Figure 7B).

The amino acid profile of dragline silk in *Argiope trifasciata* has a high Gly content (approximately 40%), which correlates with the Gly content (36.5%–43.9%) of the two major components of the spider dragline silk, MaSp1 and MaSp2 proteins [50]. A family of low-molecular weight Cysteine-rich proteins have been also characterized as involved in dragline silk formation [51]. However, Cys was an amino acid with a relative low representation (1.8%–2.0%) in tick cement (Table S3).

The analysis of peptides used to identify host and tick derived proteins (Data S7) evidenced some distinctive characteristics of the cementome tick-derived proteins (Table S3). These characteristics included a higher pI suggesting a more basic protein composition, lower aliphatic index associated with lower thermostability of globular proteins [52], and a lower GRAVY index suggesting the presence of less hydrophilic proteins [53].

Biomolecules **2020**, *10*, 555

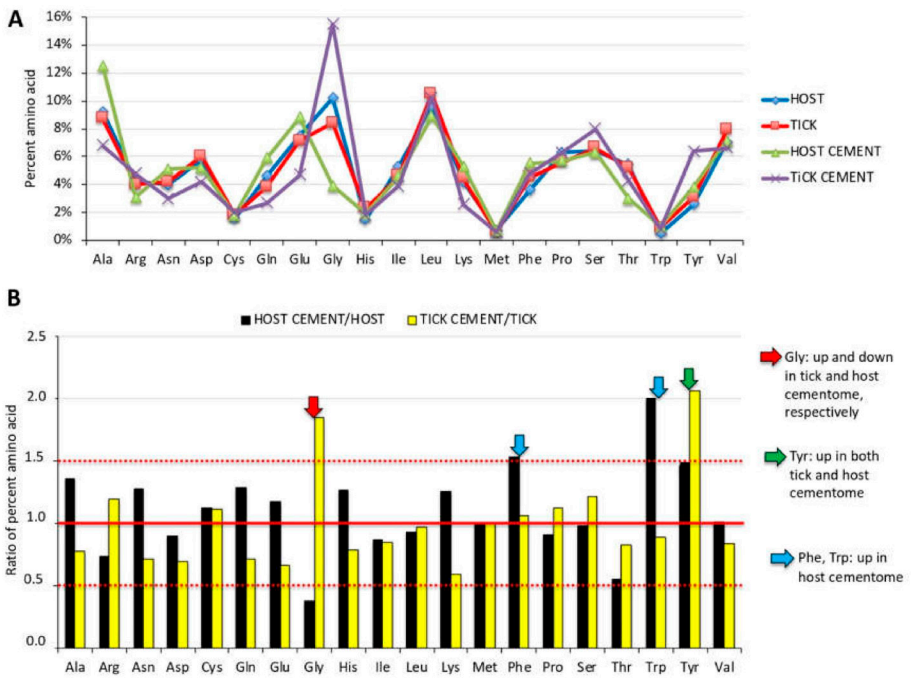

Figure 7. Amino acid composition of tick cementome. (**A**) Amino acid composition of all host proteins identified in the cementome but not in the sialome (HOST), 100 randomly selected tick proteins identified in the sialome but not in the cementome (TICK), all host proteins identified in the sialome and cementome (HOST CEMENT), and all tick proteins identified in the cementome (TICK CEMENT) (Data S6) were analyzed using the ProtParam tool. (**B**) Amino acids with highest changes (0.5 ≥ ratio of percent amino acid ≥ 1.5) in the cementome composition when compared to non-cementome host-derived (host cement/host) or tick-derived (tick cement/tick) proteins.

The SEM combined with EDS was used for the analysis of chemical elements in *R. microplus* salivary glands and cement cones (Figure 8A,B, Data S5 and S6). The results showed the presence with high relative abundance (>10 atomic %) of C, O, and N in all samples and feeding stages (T1–T3) (Figure 8A). Other elements such as S, P, Cl, Na, and K were present with low relative abundance (<1 atomic %) in most samples and feeding stages (Figure 8A). These results were similar to those recently reported in tick exoskeleton using a similar experimental approach [45]. The analysis of the composition of chemical elements in the cement and salivary glands of *R. microplus* at different time points showed significant variations in both samples but with differences in the chemical elements and profiles (Figure 8B). While C and O relative abundance did not change in the salivary glands, it increased and decreased, respectively in the cement. For N and S, relative abundance increased at T2 or T3 in the salivary glands but decreased in the cement. However, Cl relative abundance increased at T3 in both salivary glands and cement. Other elements such as Na, K, and P showed significant variations in the salivary glands only. Elements Br and Zn were only rarely found in some samples and were not included in the analysis (Data S6). As expected considering that proteins are the major source of certain chemical elements in both tick salivary glands and cement, a positive correlation ($r_s = 1$, $p = 0$) was obtained between the relative abundance of C, N, O, and S in the salivary glands and cement and the atomic composition of sialome tick-derived proteins and cementome tick and host derived proteins, respectively (Table S3). Furthermore, the profile of the highly represented Gly ($C_2H_5NO_2$)-rich superfamily member proteins in the cementome that have been implicated in

tick response to oxidative stress [20] showed a decrease in protein representation during tick feeding (e.g., A0A224YEQ4; Data S4), which correlated with changes in the composition of O and N chemical elements (Figure 8B). Glycine-rich proteins are highly represented in the sialome of different tick species and were also shown to decrease in abundance during feeding of adult female *A. americanum* [54]. Changes in the composition of cement chemical elements during tick feeding may be also related to physiological mechanisms such as the increase in the intensity of respiratory patterns in *R. sanguineus* ticks during feeding [55]. Differences in the diversity and representation of chemical elements in *R. microplus* uninfected fed female ticks between previously reported results in the exoskeleton (C, O, and N elements with >5 atomic % and $n = 10$ elements with >0.2 atomic % in at least two samples) [45] and the results reported here in the cement cone (C, O, N, and S elements with >5 atomic % and $n = 7$ elements with >0.2 atomic % in at least two samples; Data S6) using the same methodological approach (SEM–EDS) suggested that these two complex substances are formed by different proteins and/or other components.

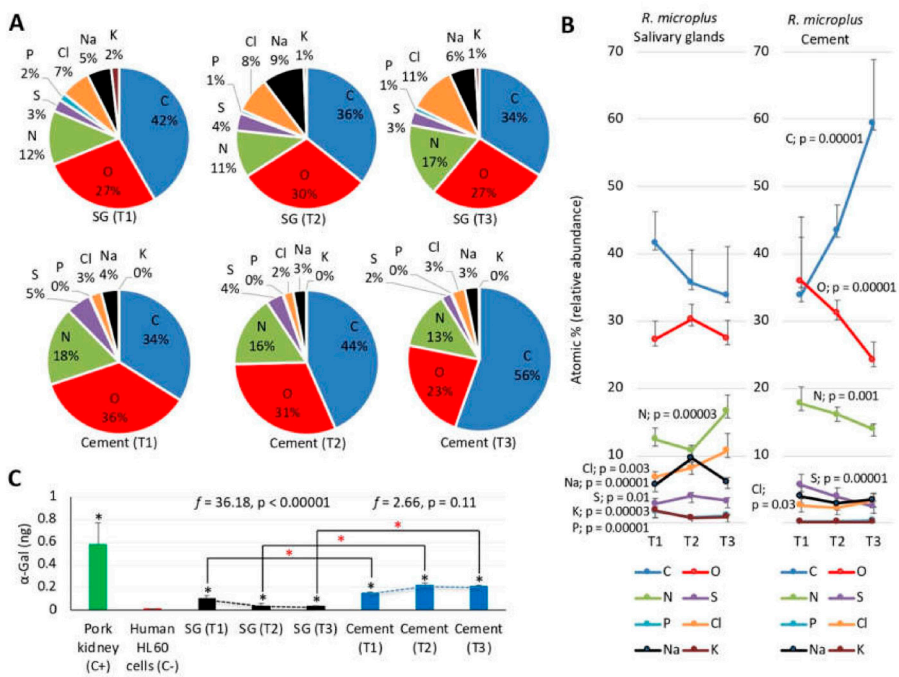

Figure 8. Composition of chemical elements in tick salivary glands and cement. Chemical elements were characterized by SEM combined with EDS analysis in samples from tick salivary glands (SG) and cement. (**A**) Representation (%) of the chemical elements at different feeding stages (T1–T3). (**B**) Changes in the representation (%) of the chemical elements at different feeding stages (T1–T3). The composition of chemical elements was compared at different time points by One-way ANOVA test (https://www.socscistatistics.com/tests/anova/default2.aspx; $p < 0.05$, $n = 2$–4 biological replicates). (**C**) Characterization of α-Gal content in tick SG and cement protein extracts and in comparison with human promyelocytic leukemia HL60 cells (ATCC CCL-240) and pork (*Sus scrofa*) kidney as negative and positive controls, respectively. A calibration curve with 0.0–1.0 ng α-Gal and O.D. values at 450 nm was constructed using Microsoft Excel for Mac (v. 16.26) to convert ELISA reader values to α-Gal content per sample ($R^2 = 0.913$). The results (average + S.D. of α-Gal/1 μg protein) were compared between pork kidney positive control, salivary gland or cement samples and HL60 cells negative

control (black * $p < 0.05$, $n = 3$ biological replicates) and between salivary gland and cement samples at different time points (T1–T3) (red * $p < 0.05$, $n = 3$ biological replicates) by Student's t-test with unequal variance. Variations in α-Gal levels at different time points (T1–T3) in both sialome and cementome were compared by one-way ANOVA test (https://www.socscistatistics.com/tests/anova/default2.aspx) (f and p values are shown, $n = 3$ biological replicates).

Previous analyses of chemical composition identified the presence of N in canine *fascia lata* and hair fiber [56,57], thus suggesting that this tick cement element may have a host origin [58]. Trace elements such as Se, Cu, Mn, Zn, and Co present in mammalian cover hair [59] were not identified in the tick cement, thus suggesting a low contribution of the host to tick cement chemical composition. In addition to tick and host derived proteins, chemical composition may be affected by cofactors such as nicotinamide adenine dinucleotide phosphate (NADPH; $C_{21}H_{26}N_7O_{17}P_3$). Reduced NAPDH is an essential electron donor that provides the reducing power regulating multiple anabolic reactions, including those responsible for the biosynthesis of all major cell components in all organisms including ticks [60–62]. Increased levels of NADPH in ticks have been associated with response to *Anaplasma phagocytophilum* pathogen infection and tolerance to oxidative stress [61,62]. The source of other chemical elements such as Na, K, Cl, and P, which may contribute to cement biomineralization and coating [29,63] probably come from environmental sources (e.g., water, air, and soil).

3.7. The Glycan α-Gal Content is Higher in the Cementome than in the Sialome throughout Tick Feeding

Glycans are constituents of matrix proteins, which are important for maintenance of tissue structure, porosity, integrity, and matrix organization through binding to other glycoproteins [64]. We focused the study on the glycan α-Gal ($C_{12}H_8O_{11}$; Figure S1) that is present in glycoproteins and glycolipids from tick saliva that mediate the alpha-Gal syndrome (AGS) characterized by delayed anaphylaxis to red meat consumption, and immediate anaphylaxis to tick bites, xenotransplantation, and certain drugs such as cetuximab [65–76]. Several tick species including *Rhipicephalus* spp. have been associated with the AGS and the production of tick proteins with α-Gal modifications has been demonstrated in various tick species including *R. microplus* [70,75]. The results showed that the α-Gal content in *R. microplus* tick sialome and cementome was higher than in proteins from α-Gal-negative human HL60 cells (black asterisks in Figure 8C). The comparison between samples showed higher α-Gal content in the cementome than in the sialome at all time points (red asterisks in Figure 8C). Furthermore, the α-Gal content at different tick feeding stages (T1–T3) decreased with tick feeding in the sialome but did not change in the cementome (Figure 8C). The results suggested that although host-derived proteins or lipids may contribute to α-Gal content in both salivary glands and cement, the fact that α-Gal levels decreased with tick feeding in the sialome but remained higher in the cementome support that at least some of these components are not storage but synthesized and secreted from the salivary glands. These results suggested a possible role for α-Gal-containing compounds in cement composition.

3.8. Western Blot Analysis of Selected Tick and Cattle Host Derived Cementome Proteins Support Proteomics Results

Herein, we used a validated label-free relative quantitation by sequential window acquisition of all theoretical mass spectra (SWATH) approach for proteomics analysis [77]. Nevertheless, selected tick and host derived proteins were used for providing additional support to proteomics data using Western blot or dot blot analyses in both cementome and sialome (Figures S5–S8). Tick-derived cementome proteins fulfilling three to four of the selection criteria were selected for analysis (Histones, Glycine-rich superfamily member proteins, and aminopeptidase N; Table S1). These proteins were putatively involved in cement formation, solidification and maintenance, tick feeding, and detachment (Figure 4A), and showed representation profiles assigned to molting, secondary cement production, cement maintenance, feeding, and detachment (Figures S5 and S6). These proteins were also annotated into the biological processes of protein heterodimerization, putative cell wall structural and/or

cuticle protein, and proteolysis (Figure 3B). Host-derived alpha-2-HS-glycoprotein, desmoplakin and pan-keratins identified in the sialome and cementome were selected for analysis because were putatively involved in cement formation, solidification, and maintenance (Figure 5B and Table S2). These proteins showed representation profiles assigned to secondary cement production, detachment, and feeding and oogenesis (Figures S7 and S8).

The quantitative results of Western blot or dot blot analyses of both sialome and cementome at different feeding times showed protein profiles similar to those described by proteomics analysis (Figures S5–S8). Despite the limitations posed by protein families such as Histones, Glycine-rich superfamily member proteins, and pan-keratins with multiple profiles, the results provided additional support for proteomics dataset and the possibility of using these antibodies for additional studies.

4. Conclusions

Our experimental approach using proteomics allowed the high throughput identification of tick and host derived proteins in both sialome (2264 proteins) and cementome (654 proteins) of *R. microplus* female ticks collected at different feeding stages. Innovative experimental approaches may provide new insights to complex biological questions [78]. Based on a novel methodology for proteomics data analysis using the protein representation profiles after significant differences in pairwise comparisons between time points, proteins were putatively assigned to different categories of developmental processes. This methodology provides a functional relevant alternative to other methodologies such as the analyses using QuiXoT [32] or normalized spectral abundance factors (NSAF) and z-score statistics [54]. Additionally, the first analysis of the chemical elements using SEM combined with EDS allowed the characterization of changes in their composition in tick salivary glands and cement during tick feeding, which correlated with changes in protein profiles. The glycan α-Gal content in the tick sialome and cementome also showed differences between samples and time points and suggested a possible role for α-Gal-containing compounds in cement composition. These results advanced our knowledge of the tick cement composition. The dynamics of cement composition throughout adult tick feeding stages suggested that tick and host derived compounds modulate the biochemical properties of the cement complex substance. Future experiments should focus on providing experimental evidence for the role of the different compounds in modulating tick cement biochemical properties and function.

Both cattle host and tick derived proteins were identified in the *R. microplus* sialome and cementome. Some of the tick-derived proteins identified in this study in the *R. microplus* cementome have been previously reported and characterized in the tick sialome/sialotranscriptome (e.g., Table S5). Similarly, host-derived proteins such as immunoglobulins and apolipoprotein A-I identified here in the cementome have been previously described in the sialome [6,12,54,79–85] and in unfed ticks [86,87]. However, the cementome protein content described here supports a highly complex composition of both tick and host derived proteins involved in multiple biological processes such as cement formation, solidification and maintenance, feeding, interference with host immune response, and detachment playing a key role in tick biology. Additionally, pending functional studies, we propose that host-derived cementome proteins may complement and synergize with tick-derived proteins in cement structure and function.

Based on these results, our hypothesis is that ticks evolved to combine tick and host derived proteins and other biomolecules such as α-Gal to synergize in cement formation, solidification and maintenance to facilitate attachment, feeding, interference with host immune response, and detachment (Figure 9). In addition to the role of cementome proteins in the inhibition/interference with host immune response, the recycling of host-derived proteins in cement formation reduces host immune response as these proteins are recognized as self-antigens (Figure 8). In this way, the combination of tick and host derived proteins in the cementome resulted in an evolutionary adaptation to long-lasting ectoparasitic blood feeding.

Future studies using these data could be focused on the characterization of salivary gland proteins in early feeding stages of *R. microplus*. Finally, based on currently available information and the results

obtained in this study, we predict that the characterization of the tick cementome will contribute to developing vaccines targeting tick adhesion and feeding for the control of tick infestations and pathogen transmission (Table S6) [14,20,88–90] and new applications in medicine and industry as a biological glue [21,29,91].

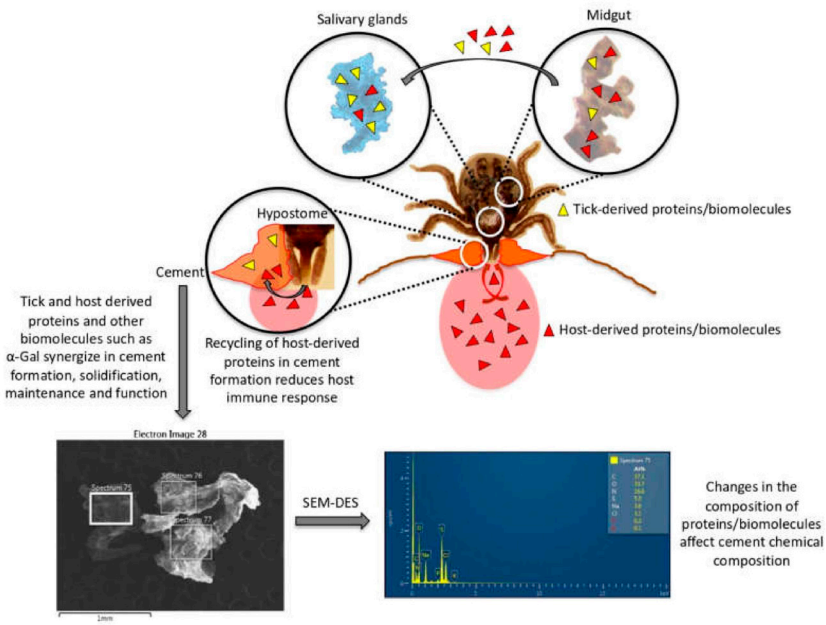

Figure 9. The combination of tick and host derived proteins in the cementome resulted in an evolutionary adaptation to long-lasting ectoparasitic blood feeding. Our hypothesis is that ticks evolved to combine tick and host derived proteins and other biomolecules such as α-Gal to synergize in cement formation, solidification, and maintenance to facilitate attachment, feeding, interference with host immune response, and detachment. Changes in the composition of proteins/biomolecules affect cement chemical composition. In addition to the role of cementome proteins in the inhibition/interference with host immune response, the recycling of host-derived proteins in cement formation reduces host immune response as these proteins are recognized as self-antigens. Representative images of SEM–EDS analysis are shown, and all results are displayed in Data S5.

Supplementary Materials: The following are available online at http://www.mdpi.com/2218-273X/10/4/555/s1, Supporting Information [Table S1: *R. microplus* tick-derived proteins identified in the cementome. Table S2: Cattle host-derived proteins identified in *R. microplus* tick cementome. Table S3: Comparative analysis of amino acid composition of cattle host and tick *R. microplus* derived proteins identified in the cementome. Table S4: Recombinant tick proteins used for validation by Western blot analysis. Table S5: Examples of tick-derived proteins identified in this study in the cementome and previously characterized and reported in the sialome/sialotranscriptome. Table S6: Published results about the potential role of selected tick cementome proteins for novel vaccine development. Figure S1: Chemical structure and atomic composition of Galα1-3Galβ1-(3)4GlcNAc-R (α-Gal). Figure S2: ELISA test for characterizing α-Gal levels. Figure S3: Validation of commercial antibodies against host proteins by immunofluorescence assay. Figure S4: Western blot analysis of recombinant tick proteins. Figure S5: Western blot analysis of tick-derived aminopeptidase N protein in the *R. microplus* cementome (Cement) and sialome (SG). Figure S6: Dot blot analysis of tick-derived histones and Glycine-rich superfamily member proteins in the *R. microplus* cementome (Cement) and sialome (SG). Figure S7: Dot blot analysis of host-derived desmoplakin and alpha-2-HS-glycoprotein in the *R. microplus* cementome (Cement) and sialome (SG). Figure S8: Dot blot analysis of host-derived pan-keratins in the *R. microplus* cementome (Cement) and sialome (SG)]. Data S1: Proteomics analysis of *R. microplus* tick sialome. Data S2: Proteomics analysis of *R. microplus* tick cementome with urea-extracted proteins. Data S3: Proteomics analysis of *R. microplus* tick cementome with SDS-extracted proteins.

Data S4: Protein profile of tick sialome and cementome throughout tick *R. microplus* parasitic stages. Data S5: Composition of chemical elements in *R. microplus* tick cement and salivary glands. Data S6: Statistical analysis of chemical element composition in *R. microplus* tick cement and salivary glands. Data S7: Peptide sequences for tick *R. microplus* and cattle host derived proteins identified in the sialome and cementome. Host-derived proteins in the cementome were included only if identified in both sialome and cementome.

Author Contributions: Conceptualization, J.d.l.F. and M.V.; methodology, J.d.l.F. and M.V.; validation, M.C., P.A., and D.K.B.-P.; investigation, M.V., I.P., O.M., M.C., L.M.-H., E.P., P.A., D.K.B.-P., J.F.L.-B., S.A.-J., I.G.F.d.M., A.E.-P., and A.C.-C.; data curation, M.V., J.d.l.F., and I.P.; writing—original draft preparation, J.d.l.F.; writing—review and editing, J.d.l.F.; supervision, J.d.l.F. and M.V.; project administration, J.d.l.F. and M.V.; funding acquisition, J.d.l.F. and M.V. All authors have read and agreed to the published version of the manuscript.

Funding: This research was funded by the Consejería de Educación, Cultura y Deportes, JCCM, Spain, project CCM17-PIC-036 (SBPLY/17/180501/000185). M.V. was supported by the University of Castilla La Mancha, UCLM, Spain, and the Fondo Europeo de Desarrollo Regional, FEDER, EU. I.G.F.M. was supported by the University of Castilla La Mancha, UCLM, Spain.

Acknowledgments: We thank Katherine M. Kocan (Oklahoma State University, Stillwater, OK, USA) for tick images displayed in Figure 4, Figure 5, and Figure 8.

Conflicts of Interest: The authors declare no conflict of interest.

References

1. Jongejan, F.; Uilenberg, G. The global importance of ticks. *Parasitology* **2004**, *129*, S3–S14. [CrossRef] [PubMed]
2. De la Fuente, J.; Estrada-Peña, A.; Venzal, J.M.; Kocan, K.M.; Sonenshine, D.E. Overview: Ticks as vectors of pathogens that cause disease in humans and animals. *Front. Biosci.* **2008**, *13*, 6938–6946. [CrossRef] [PubMed]
3. Rashid, M.; Rashid, M.I.; Akbar, H.; Ahmad, L.; Hassan, M.A.; Ashraf, K.; Saeed, K.; Gharbi, M. A systematic review on modelling approaches for economic losses studies caused by parasites and their associated diseases in cattle. *Parasitology* **2019**, *146*, 129–141. [CrossRef] [PubMed]
4. Paules, C.I.; Marston, H.D.; Bloom, M.E.; Fauci, A.S. Tickborne diseases - confronting a growing threat. *N. Engl. J. Med.* **2018**, *379*, 701–703. [CrossRef]
5. Molaei, G.; Little, E.A.; Williams, S.C.; Stafford, K.C. Bracing for the worst - range expansion of the lone star tick in the northeastern United States. *N. Engl. J. Med.* **2019**, *381*, 2189–2192. [CrossRef]
6. Wang, H.; Nuttall, P.A. Excretion of host immunoglobulin in tick saliva and detection of IgG-binding proteins in tick haemolymph and salivary glands. *Parasitology* **1994**, *109*, 525–530. [CrossRef]
7. Jasinskas, A.; Jaworski, D.C.; Barbour, A.G. *Amblyomma americanum*: Specific uptake of immunoglobulins into tick hemolymph during feeding. *Exp. Parasitol.* **2000**, *96*, 213–221. [CrossRef]
8. Jasinskas, A.; Barbour, A.G. The Fc fragment mediates the uptake of immunoglobulin C from the midgut to hemolymph in the ixodid tick *Amblyomma americanum* (Acari: Ixodidae). *J. Med. Entomol.* **2005**, *42*, 359–366. [CrossRef]
9. Kazimírová, M.; Štibrániová, I. Tick salivary compounds: Their role in modulation of host defences and pathogen transmission. *Front. Cell. Infect. Microbiol.* **2013**, *3*, 43. [CrossRef]
10. Hajdušek, O.; Šíma, R.; Ayllón, N.; Jalovecká, M.; Perner, J.; de la Fuente, J.; Kopáček, P. Interaction of the tick immune system with transmitted pathogens. *Front. Cell. Infect. Microbiol.* **2013**, *3*, 26. [CrossRef]
11. Kotál, J.; Langhansová, H.; Lieskovská, J.; Andersen, J.F.; Francischetti, I.M.; Chavakis, T.; Kopecký, J.; Pedra, J.H.; Kotsyfakis, M.; Chmelař, J. Modulation of host immunity by tick saliva. *J. Proteomics.* **2015**, *128*, 58–68. [CrossRef]
12. Kim, T.K.; Tirloni, L.; Pinto, A.F.; Moresco, J.; Yates, J.R., 3rd; da Silva Vaz, I., Jr.; Mulenga, A. Ixodes scapularis tick saliva proteins sequentially secreted every 24 h during blood feeding. *PLoS Negl. Trop. Dis.* **2016**, *10*, e0004323. [CrossRef] [PubMed]
13. Anderson, J.M.; Moore, I.N.; Nagata, B.M.; Ribeiro, J.M.C.; Valenzuela, J.G.; Sonenshine, D.E. Ticks, *Ixodes scapularis*, feed repeatedly on white-footed mice despite strong inflammatory response: An expanding paradigm for understanding tick-host interactions. *Front. Immunol.* **2017**, *8*, 1784. [CrossRef] [PubMed]
14. Antunes, S.; Couto, J.; Ferrolho, J.; Rodrigues, F.; Nobre, J.; Santos, A.S.; Santos-Silva, M.M.; de la Fuente, J.; Domingos, A. *Rhipicephalus bursa* sialotranscriptomic response to blood feeding and *Babesia ovis* infection: Identification of candidate protective antigens. *Front. Cell. Infect. Microbiol.* **2018**, *8*, 116. [CrossRef] [PubMed]

15. Perner, J.; Kropáčková, S.; Kopáček, P.; Ribeiro, J.M.C. Sialome diversity of ticks revealed by RNAseq of single tick salivary glands. *PLoS Negl. Trop. Dis.* **2018**, *12*, e0006410. [CrossRef] [PubMed]
16. Hollmann, T.; Kim, T.K.; Tirloni, L.; Radulović, Ž.M.; Pinto, A.F.M.; Diedrich, J.K.; Yates, J.R., 3rd; da Silva Vaz, I., Jr.; Mulenga, A. Identification and characterization of proteins in the *Amblyomma americanum* tick cement cone. *Int. J. Parasitol.* **2018**, *48*, 211–224. [CrossRef] [PubMed]
17. Abreu, M.R.; Pereira, M.C.; Simioni, P.U.; Nodari, E.F.; Paiatto, L.N.; Camargo-Mathias, M.I. Immunomodulatory and morphophysiological effects of *Rhipicephalus sanguineus* s.l. (Acari: Ixodidae) salivary gland extracts. *Vet. Immunol. Immunopathol.* **2019**, *207*, 36–45. [CrossRef] [PubMed]
18. Narasimhan, S.; Booth, C.J.; DePonte, K.; Wu, M.J.; Liang, X.; Mohanty, S.; Kantor, F.; Fikrig, E. Host-specific expression of *Ixodes scapularis* salivary genes. *Ticks Tick-Borne Dis.* **2019**, *10*, 386–397. [CrossRef]
19. Mans, B.J. Chemical equilibrium at the tick-host feeding interface: A critical examination of biological relevance in hematophagous behavior. *Front. Physiol.* **2019**, *10*, 530. [CrossRef]
20. Bullard, R.; Sharma, S.R.; Das, P.K.; Morgan, S.E.; Karim, S. Repurposing of glycine-rich proteins in abiotic and biotic stresses in the Lone-Star tick (*Amblyomma americanum*). *Front. Physiol.* **2019**, *10*, 744. [CrossRef]
21. Chmelař, J.; Kotál, J.; Kovaříková, A.; Kotsyfakis, M. The use of tick salivary proteins as novel therapeutics. *Front. Physiol.* **2019**, *10*, 812. [CrossRef] [PubMed]
22. Nuttall, P.A. Wonders of tick saliva. *Ticks Tick-Borne Dis.* **2019**, *10*, 470–481. [CrossRef] [PubMed]
23. De la Fuente, J.; Contreras, M.; Estrada-Peña, A.; Cabezas-Cruz, A. Targeting a global health problem: Vaccine design and challenges for the control of tick-borne diseases. *Vaccine* **2017**, *35*, 5089–5094. [CrossRef] [PubMed]
24. De la Fuente, J. Controlling ticks and tick-borne diseases...looking forward. *Ticks Tick Borne Dis.* **2018**, *9*, 1354–1357. [CrossRef]
25. Wikel, S.K. Ticks and tick-borne infections: Complex ecology, agents, and host interactions. *Vet. Sci.* **2018**, *5*, 60. [CrossRef]
26. De la Fuente, J.; Estrada-Peña, A. Why new vaccines for the control of ectoparasite vectors have not been registered and commercialized? *Vaccines* **2019**, *7*, 75. [CrossRef]
27. Vancová, M.; Bílý, T.; Šimo, L.; Touš, J.; Horodyský, P.; Růžek, D.; Novobilský, A.; Salát, J.; Strnad, M.; Sonenshine, D.E.; et al. Three-dimensional reconstruction of the feeding apparatus of the tick *Ixodes ricinus* (Acari: Ixodidae): A new insight into the mechanism of blood-feeding. *Sci. Rep.* **2020**, *10*, 165. [CrossRef]
28. Jaworski, D.C.; Rosell, R.; Coons, L.B.; Needham, G.R. Tick (Acari: Ixodidae) attachment cement and salivary gland cells contain similar immunoreactive polypeptides. *J. Med. Entomol.* **1992**, *29*, 305–309. [CrossRef]
29. Suppan, J.; Engel, B.; Marchetti-Deschmann, M.; Nürnberger, S. Tick attachment cement- reviewing the mysteries of a biological skin plug system. *Biol. Rev. Camb. Philos. Soc.* **2018**, *93*, 1056–1076. [CrossRef]
30. Bullard, R.; Allen, P.; Chao, C.C.; Douglas, J.; Das, P.; Morgan, S.E.; Ching, W.M.; Karim, S. Structural characterization of tick cement cones collected from in vivo and artificial membrane blood-fed Lone Star ticks (*Amblyomma americanum*). *Ticks Tick-Borne Dis.* **2016**, *7*, 880–892. [CrossRef]
31. Merino, O.; Almazán, C.; Canales, M.; Villar, M.; Moreno-Cid, J.A.; Estrada-Peña, A.; Kocan, K.M.; de la Fuente, J. Control of *Rhipicephalus (Boophilus) microplus* infestations by the combination of subolesin vaccination and tick autocidal control after subolesin gene knockdown in ticks fed on cattle. *Vaccine* **2011**, *29*, 2248–2254. [CrossRef] [PubMed]
32. Ayllón, N.; Villar, V.; Galindo, R.C.; Kocan, K.M.; Šíma, R.; López, J.A.; Vázquez, J.; Alberdi, P.; Cabezas-Cruz, A.; Kopáček, P.; et al. Systems biology of tissue-specific response to *Anaplasma phagocytophilum* reveals differentiated apoptosis in the tick vector *Ixodes scapularis*. *PLoS Genetics* **2015**, *11*, e1005120. [CrossRef] [PubMed]
33. Villar, M.; Ayllón, N.; Alberdi, P.; Moreno, A.; Moreno, M.; Tobes, R.; Mateos-Hernández, L.; Weisheit, S.; Bell-Sakyi, L.; de la Fuente, J. Integrated metabolomics, transcriptomics and proteomics identifies metabolic pathways affected by *Anaplasma phagocytophilum* infection in tick cells. *Mol. Cell. Proteomics.* **2015**, *14*, 3154–3172. [CrossRef] [PubMed]
34. Gillet, L.C.; Navarro, P.; Tate, S.; Rost, H.; Selevsek, N.; Reiter, L.; Bonner, R.; Aebersold, R. Targeted data extraction of the MS/MS spectra generated by data-independent acquisition: A new concept for consistent and accurate proteome analysis. *Mol. Cell. Proteomics.* **2012**, *11*. [CrossRef]
35. Gasteiger, E.; Hoogland, C.; Gattiker, A.; Duvaud, S.; Wilkins, M.R.; Appel, R.D.; Bairoch, A. Protein identification and analysis tools on the ExPASy Server. *Humana Press* **2005**. [CrossRef]

36. Estrada-Peña, A.; Villar, M.; Artigas-Jerónimo, S.; López, V.; Alberdi, P.; Cabezas-Cruz, A.; de la Fuente, J. Use of graph theory to characterize human and arthropod vector cell protein response to infection. *Front. Cell. Infect. Microbiol.* **2018**, *8*, 265. [CrossRef]
37. Layeghifard, M.; Hwang, D.M.; Guttman, D.S. Disentangling interactions in the microbiome: A network perspective. *Trends Microbiol.* **2017**, *25*, 217–228. [CrossRef]
38. Opsahl, T.; Agneessens, F.; Skvoretz, J. Node centrality in weighted networks: generalizing degree and shortest paths. *Soc. Networks* **2010**, *32*, 245–251. [CrossRef]
39. Barthelemy, M. Betweenness centrality in large complex networks. *Eur. Phys. J. B.* **2004**, *38*, 163–168. [CrossRef]
40. Almazán, C.; Moreno-Cantú, O.; Moreno-Cid, J.A.; Galindo, R.C.; Canales, M.; Villar, M.; de la Fuente, J. Control of tick infestations in cattle vaccinated with bacterial membranes containing surface-exposed tick protective antigens. *Vaccine* **2012**, *30*, 265–272. [CrossRef]
41. Canales, M.; Almazán, C.; Pérez de la Lastra, J.M.; de la Fuente, J. *Anaplasma marginale* major surface protein 1a directs cell surface display of tick BM95 immunogenic peptides on *Escherichia coli*. *J. Biotechnol.* **2008**, *135*, 326–332. [CrossRef] [PubMed]
42. Marinela, C.; Moreno-Cid, J.A.; Domingos, A.; Canales, M.; Díez-Delgado, I.; Pérez de la Lastra, J.M.; Sánchez, E.; Merino, O.; López Zavala, R.; Ayllón, N.; et al. Bacterial membranes enhance the immunogenicity and protective capacity of the surface exposed tick Subolesin-*Anaplasma marginale* MSP1a chimeric antigen. *Ticks Tick-Borne Dis.* **2015**, *6*, 2820–2828.
43. Merino, M.; Antunes, S.; Mosqueda, J.; Moreno-Cid, J.A.; Pérez de la Lastra, J.M.; Rosario-Cruz, R.; Rodríguez, S.; Domingos, A.; de la Fuente, J. Vaccination with proteins involved in tick-pathogen interactions reduces vector infestations and pathogen infection. *Vaccine* **2013**, *31*, 5889–5896. [CrossRef] [PubMed]
44. Moreno-Cid, J.A.; Pérez de la Lastra, J.M.; Villar, M.; Jiménez, M.; Pinal, R.; Estrada- Peña, A.; Molina, R.; Lucientes, J.; Gortázar, C.; de la Fuente, J. Control of multiple arthropod vector infestations with subolesin/akirin vaccines. *Vaccine* **2013**, *31*, 1187–1196. [CrossRef] [PubMed]
45. De la Fuente, J.; Lima-Barbero, J.F.; Prado, E.; Pacheco, I.; Alberdi, P.; Villar, M. *Anaplasma* pathogen infection alters chemical composition of the exoskeleton of hard ticks (Acari: Ixodidae). *Comput. Struct. Biotechnol. J.* **2020**, *18*, 253–257. [CrossRef]
46. Senbill, H.; Kanta Hazarika, L.; Baruah, A.; Kumar Borah, D.; Bhattacharyya, B.; Rahman, S. Life cycle of the southern cattle tick, *Rhipicephalus* (*Boophilus*) *microplus* Canestrini 1888 (Acari: Ixodidae) under laboratory conditions. *Syst. Appl. Acarol.* **2018**, *23*, 1169–1179. [CrossRef]
47. Jorgensen, W.K.; Kemp, D.H. Continued functioning of the feeding apparatus during moulting of *Boophilus microplus* as an adaptation of one-host ticks. *J. Parasitol.* **1986**, *72*, 846–851. [CrossRef]
48. Kim, T.K.; Curran, J.; Mulenga, A. Dual silencing of long and short *Amblyomma americanum* acidic chitinase forms weakens the tick cement cone stability. *J. Exp. Biol.* **2014**, *217*, 3493–3503. [CrossRef]
49. Chinery, W.A. The nature and origin of the "cement" substance at the site of attachment and feeding of adult *Haemaphysalis spinigera* (Ixodidae). *J. Med. Entomol.* **1973**, *10*, 355–362. [CrossRef]
50. Marhabaie, M.; Leeper, T.C.; Blackledge, T.A. Protein composition correlates with the mechanical properties of spider (*Argiope trifasciata*) dragline silk. *Biomacromolecules* **2014**, *15*, 20–29. [CrossRef]
51. Pham, T.; Chuang, T.; Lin, A.; Joo, H.; Tsai, J.; Crawford, T.; Zhao, L.; Williams, C.; Hsia, Y.; Vierra, C. Dragline silk: A fiber assembled with low-molecular-weight cysteine-rich proteins. *Biomacromolecules* **2014**, *15*, 4073–4081. [CrossRef] [PubMed]
52. Ikai, A. Thermostability and aliphatic index of globular proteins. *J. Biochem.* **1980**, *88*, 1895–1898. [PubMed]
53. Huang, H.J.; Chen, W.Y.; Wu, J.H. Total protein extraction for metaproteomics analysis of methane producing biofilm: The effects of detergents. *Int. J. Mol. Sci.* **2014**, *15*, 10169–10184. [CrossRef] [PubMed]
54. Kim, T.K.; Tirloni, L.; Pinto, A.F.M.; Diedrich, J.K.; Moresco, J.J.; Yates, J.R., 3rd; da Silva Vaz, I., Jr.; Mulenga, A. Time-resolved proteomic profile of *Amblyomma americanum* tick saliva during feeding. *PLoS Negl. Trop. Dis.* **2020**, *14*, e0007758. [CrossRef] [PubMed]
55. Landulfo, G.A.; Li, A.Y.; Lima, A.S.; Silva, N.C.S.; Vale, T.L.; Costa-Junior, L.M. Feeding and respiratory gas exchange of *Rhipicephalus sanguineus* sensu lato (Acari: Ixodidae). *Exp. Appl. Acarol.* **2019**, *78*, 173–179. [CrossRef] [PubMed]
56. Maksymowicz, K.; Marycz, K.; Szotek, S.; Kaliński, K.; Serwa, E.; Łukomski, R.; Czogała, J. Chemical composition of human and canine fascia lata. *Acta Biochim. Pol.* **2012**, *59*, 531–535. [CrossRef]

57. Ragaisiene, A.; Rusinavičiūtė, J.; Milašiene, D.; Ivanauskas, R. Comparison of selected chemical properties of fibres from different breeds of dogs and German blackface sheep. *Fibres & textiles in Eastern Europe* **2016**, *24*, 21–28.
58. Heylen, D.; Schmidt, O.; Dautel, H.; Gern, L.; Kampen, H.; Newton, J.; Gray, J. Host identification in unfed ticks from stable isotope compositions (δ_{13} C and δ_{15} N). *Med. Vet. Entomol.* **2019**, *33*, 360–366. [CrossRef]
59. Analysis of Trace Elements in Cattle. BioCheck - Labor fur Veterinardiagnostik und Umwelthygiene GmbH. 2014. Available online: https://www.biocheck-leipzig.de/images/stories/biocheck/pdf/News_2_14_e.pdf (accessed on 26 February 2020).
60. Spaans, S.K.; Weusthuis, R.A.; van der Oost, J.; Kengen, S.W. NADPH-generating systems in bacteria and archaea. *Front. Microbiol.* **2015**, *6*, 742. [CrossRef]
61. Alberdi, P.; Cabezas-Cruz, A.; Espinosa, P.J.; Villar, M.; Artigas-Jerónimo, S.; de la Fuente, J. The redox metabolic pathways function to limit *Anaplasma phagocytophilum* infection and multiplication while preserving fitness in tick vector cells. *Sci. Rep.* **2019**, *9*, 13236. [CrossRef]
62. Della Noce, B.; Carvalho Uhl, M.V.; Machado, J.; Waltero, C.F.; de Abreu, L.A.; da Silva, R.M.; da Fonseca, R.N.; de Barros, C.M.; Sabadin, G.; Konnai, S.; et al. Carbohydrate metabolic compensation coupled to high tolerance to oxidative stress in ticks. *Sci. Rep.* **2019**, *9*, 4753. [CrossRef] [PubMed]
63. Gallant, J.; Hochberg, R. Elemental characterization of the exoskeleton in the whipscorpions *Mastigoproctus giganteus* and *Typopeltis dalyi* (Arachnida: Thelyphonida). *Invertebrate Biol.* **2017**, *136*, 345–359. [CrossRef]
64. Varki, A. Biological roles of glycans. *Glycobiology* **2016**, *27*, 3–49. [CrossRef] [PubMed]
65. Van Nunen, S.; O'Connor, K.S.; Clarke, L.R.; Boyle, R.X.; Fernando, S.L. The association between *Ixodes holocyclus* tick bite reactions and red meat allergy. *Intern. Med. J.* **2007**, *39*, A132.
66. Commins, S.P.; Satinover, S.M.; Hosen, J.; Mozena, J.; Borish, L.; Lewis, B.D.; Woodfolk, J.A.; Platts-Mills, T.A. Delayed anaphylaxis, angioedema, or urticaria after consumption of red meat in patients with IgE antibodies specific for galactose-alpha-1,3-galactose. *J. Allergy Clin. Immunol.* **2009**, *123*, 426–433. [CrossRef]
67. Saleh, H.; Embry, S.; Nauli, A.; Atyia, S.; Krishnaswamy, G. Anaphylactic reactions to oligosaccharides in red meat: A syndrome in evolution. *Clin. Mol. Allergy.* **2012**, *10*, 5. [CrossRef]
68. Steinke, J.W.; Platts-Mills, T.A.; Commins, S.P. The alpha-gal story: Lessons learned from connecting the dots. *J. Allergy Clin. Immunol.* **2015**, *135*, 589–596. [CrossRef]
69. Platts-Mills, T.A.; Schuyler, A.J.; Tripathi, A.; Commins, S.P. Anaphylaxis to the carbohydrate side chain alpha-gal. *Immunol. Allergy Clin. North. Am.* **2015**, *35*, 247–260. [CrossRef]
70. Mateos-Hernández, L.; Villar, M.; Moral, A.; Rodríguez, C.G.; Arias, T.A.; de la Osa, V.; Brito, F.F.; Fernández de Mera, I.G.; Alberdi, P.; Ruiz-Fons, F.; et al. Tick-host conflict: Immunoglobulin E antibodies to tick proteins in patients with anaphylaxis to tick bite. *Oncotarget* **2017**, *8*, 20630–20644. [CrossRef]
71. Galili, U. Evolution in primates by "catastrophic-selection" interplay between enveloped virus epidemics, mutated genes of enzymes synthesizing carbohydrate antigens, and natural anticarbohydrate antibodies. *Am. J. Phys. Anthropol.* **2018**, *168*, 352–363. [CrossRef]
72. Hilger, C.; Fischer, J.; Wölbing, F.; Biedermann, T. Role and mechanism of galactose-alpha-1,3-galactose in the elicitation of delayed anaphylactic reactions to red meat. *Curr. Allergy Asthma Rep.* **2019**, *19*, 3. [CrossRef] [PubMed]
73. Cabezas-Cruz, A.; Valdés, J.; de la Fuente, J. Cancer research meets tick vectors for infectious diseases. *Lancet. Infect. Dis.* **2014**, *10*, 916–917. [CrossRef]
74. Cabezas-Cruz, A.; Mateos-Hernández, L.; Alberdi, P.; Villar, M.; Riveau, G.; Hermann, E.; Schacht, A.; Khalife, J.; Correia-Neves, M.; Gortázar, C.; et al. Effect of blood type on anti-α-Gal immunity and the incidence of infectious diseases. *Exp. Mol. Med.* **2017**, *49*, e301. [CrossRef] [PubMed]
75. Cabezas-Cruz, A.; Hodžić, A.; Román-Carrasco, P.; Mateos-Hernández, L.; Duscher, G.G.; Sinha, D.K.; Hemmer, W.; Swoboda, I.; Estrada-Peña, A.; de la Fuente, J. Environmental and molecular drivers of the α-Gal syndrome. *Front. Immunol.* **2019**, *10*, 1210. [CrossRef] [PubMed]
76. De la Fuente, J.; Pacheco, I.; Villar, M.; Cabezas-Cruz, A. The alpha-Gal syndrome: New insights into the tick-host conflict and cooperation. *Parasit. Vectors* **2019**, *12*, 154. [CrossRef] [PubMed]
77. Huang, Q.; Yang, L.; Luo, J.; Guo, L.; Wang, Z.; Yang, X.; Jin, W.; Fang, Y.; Ye, J.; Shan, B.; et al. SWATH enables precise label-free quantification on proteome scale. *Proteomics* **2015**, *15*, 1215–1223. [CrossRef] [PubMed]

78. Artigas-Jerónimo, S.; Pastor Comín, J.J.; Villar, M.; Contreras, M.; Alberdi, P.; León Viera, I.; Soto, L.; Cordero, R.; Valdés, J.J.; Cabezas-Cruz, A.; et al. A novel combined scientific and artistic approach for advanced characterization of interactomes: The Akiri/Subolesin model. *Vaccines* **2020**, *8*, 77. [CrossRef]
79. Villar, M.; López, V.; Ayllón, N.; Cabezas-Cruz, A.; López, J.A.; Vázquez, J.; Alberdi, P.; de la Fuente, J. The intracellular bacterium *Anaplasma phagocytophilum* selectively manipulates the levels of vertebrate host proteins in the tick vector *Ixodes scapularis*. *Parasit. Vectors* **2016**, *9*, 467. [CrossRef]
80. Valenzuela, J.G.; Francischetti, I.M.; Pham, V.M.; Garfield, M.K.; Mather, T.N.; Ribeiro, J.M. Exploring the sialome of the tick *Ixodes scapularis*. *J. Exp. Biol.* **2002**, *205*, 2843–2864.
81. Madden, R.D.; Sauer, J.R.; Dillwith, J.W. A proteomics approach to characterizing tick salivary secretions. *Exp. Appl. Acarol.* **2002**, *28*, 77–87. [CrossRef]
82. Diaz-Martin, V.; Manzano-Roman, R.; Valero, L.; Oleaga, A.; Encinas-Grandes, A.; Perez-Sanchez, R. An insight into the proteome of the saliva of the argasid tick *Ornithodoros moubata* reveals important differences in saliva protein composition between the sexes. *J. Proteomics.* **2013**, *80*, 216–235. [CrossRef] [PubMed]
83. Oliveira, C.J.; Anatriello, E.; de Miranda-Santos, I.K.; Francischetti, I.M.; Sá-Nunes, A.; Ferreira, B.R.; Ribeiro, J.M. Proteome of *Rhipicephalus sanguineus* tick saliva induced by the secretagogues pilocarpine and dopamine. *Ticks Tick-Borne Dis.* **2013**, *4*, 469–477. [CrossRef] [PubMed]
84. Tirloni, L.; Reck, J.; Terra, R.M.; Martins, J.R.; Mulenga, A.; Sherman, N.E.; Fox, J.W.; Yates, J.R., 3rd; Termignoni, C.; Pinto, A.F.; et al. Proteomic analysis of cattle tick *Rhipicephalus* (*Boophilus*) *microplus* saliva: A comparison between partially and fully engorged females. *PLoS ONE* **2014**, *9*, e94831. [CrossRef] [PubMed]
85. Tirloni, L.; Islam, M.S.; Kim, T.K.; Diedrich, J.K.; Yates, J.R., 3rd; Pinto, A.F.; Mulenga, A.; You, M.J.; da Silva Vaz, I., Jr. Saliva from nymph and adult females of *Haemaphysalis longicornis*: A proteomic study. *Parasit. Vectors* **2015**, *8*, 338. [CrossRef] [PubMed]
86. Wickramasekara, S.; Bunikis, J.; Wysocki, V.; Barbour, A.G. Identification of residual blood proteins in ticks by mass spectrometry proteomics. *Emerg. Infect. Dis.* **2008**, *14*, 1273–1275. [CrossRef] [PubMed]
87. Villar, M.; Torina, A.; Nuñez, Y.; Zivkovic, Z.; Marina, A.; Alongi, A.; Scimeca, S.; La Barbera, G.; Caracappa, S.; Vázquez, J.; et al. Application of highly sensitive saturation labelling to the analysis of differential protein expression in infected ticks from limited samples. *Proteome Sci.* **2010**, *8*, 43. [CrossRef]
88. Willadsen, P.; Smith, D.; Cobon, G.; McKenna, R.V. Comparative vaccination of cattle against *Boophilus microplus* with recombinant antigen Bm86 alone or in combination with recombinant Bm91. *Parasite Immunol.* **1996**, *18*, 241–246. [CrossRef]
89. Masina, S.; Broady, K.W. Tick paralysis: Development of a vaccine. *Int. J. Parasitol.* **1999**, *29*, 535–541. [CrossRef]
90. Contreras, M.; Alberdi, P.; Fernández de Mera, I.G.; Krull, C.; Nijhof, A.; Villar, M.; de la Fuente, J. Vaccinomics approach to the identification of candidate protective antigens for the control of tick vector infestations and *Anaplasma phagocytophilum* infection. *Front. Cell. Infect. Microbiol.* **2017**, *7*, 360. [CrossRef]
91. Stewart, R.J.; Ransom, T.C.; Hlady, V. Natural underwater adhesives. *Journal of Polymer Science Part. B: Polymer Physics* **2011**, *49*, 757–771. [CrossRef]

Supplementary material. Chapter 1b

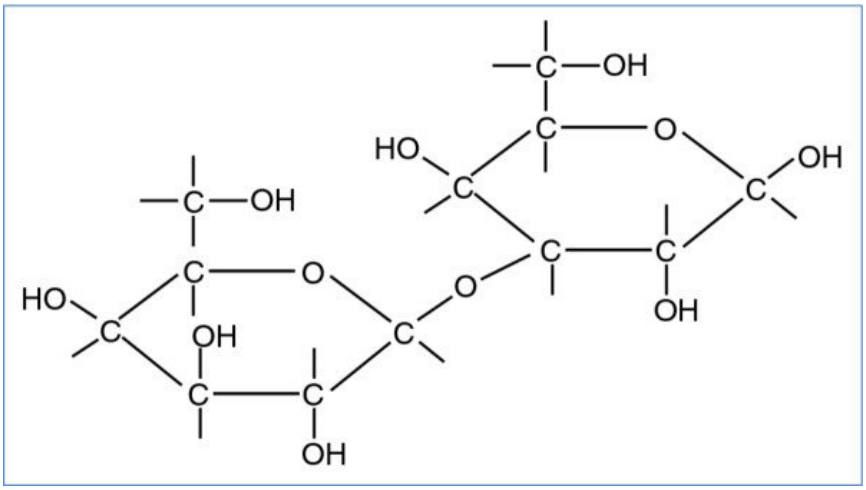

Atomic composition	
Carbon C	38.7%
Oxygen O	35.5%
Hydrogen H	25.8%

Figure S1. Chemical structure and atomic composition of Galα1-3Galβ1-(3)4GlcNAc-R (α-Gal; $C_{12}H_8O_{11}$).

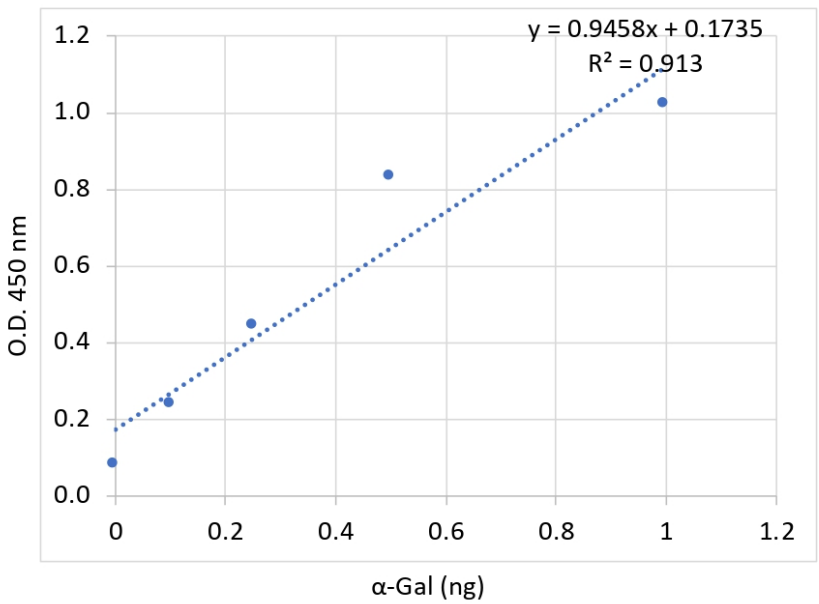

Figure S2. ELISA test for characterizing α-Gal levels. The α-Gal levels were determined by ELISA using BSA-α-Gal and *R. microplus* sialome and cementome proteins. The average value of the blanks (wells without sample proteins; N = 5) was subtracted from all reads and the average of 9 replicates for each sample was used for analysis. A calibration curve with 0.0 to 1.0 ng α-Gal and O.D. values at 450 nm was constructed using Microsoft Excel for Mac (v. 16.26) to convert ELISA reader values to α-Gal content per sample.

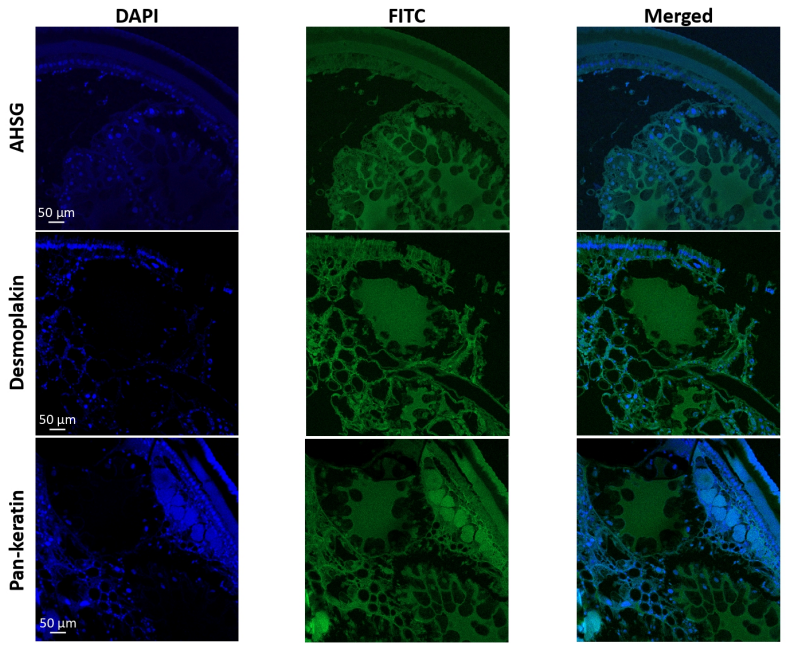

Figure S3. Validation of commercial antibodies against host proteins by immunofluorescence assay. Female *Ixodes scapularis* ticks fed on uninfected sheep and fixed with 4% paraformaldehyde in 0.2 M sodium cacodylate buffer were embedded in paraffin and used to prepare sections on glass slides as previously described (Ayllón et al., PLoS Genetics 2015;11: e1005120 and de la Fuente et al., Computational and Structural Biotechnology Journal 2020;18: 253-257). The paraffin was removed from the sections with xylene and then hydrated by successive 2 min washes with a graded series of 100, 95, 80, 75, and 50% ethanol. The slides were treated with Proteinase K (Dako, Barcelona, Spain) for 7 min, washed with PBS and incubated with 3% BSA (Sigma-Aldrich) in PBS for 1 h at RT. Then the slides were incubated with antibodies against desmoplakin (ab106342) and pan-keratin (ab190625) (Abcam, Cambridge, UK) diluted 1:100 in 3% BSA/PBS for 14 h at 4 °C. After additional washes in PBS, the sections were incubated with FITC conjugated goat anti-rabbit IgG secondary antibodies (Sigma-Aldrich), diluted 1:80 in 3% BSA/PBS, for 1 h at RT. Finally, the slides were mounted using Prolong Gold antifade reagent with DAPI reagent (Molecular Probes, Eugene, OR, USA). The slides were examined using a Zeiss LSM 800 laser scanning confocal microscope (Carl Zeiss, Oberkochen, Germany) with a 10x objective.

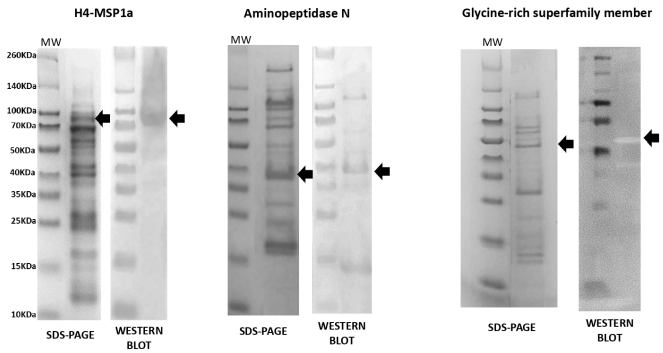

Figure S4. Western blot analysis of recombinant tick proteins. The recombinant histone H4-MSP1a, aminopeptidase N, and Glycine-rich superfamily member proteins were produced in *E. coli*. Samples were taken after purification. Ten µg proteins were loaded per well in an SDS-12% polyacrylamide gel. The gel was stained with Coomassie Brilliant Blue. The position of the recombinant proteins is indicated with arrows. For Western blot analysis, recombinant proteins were separated by electrophoresis and transferred to a nitrocellulose membrane. The membrane was incubated with pooled sera collected from histone H4, aminopeptidase N vaccinated rabbits and commercial rabbit anti-Glycine-rich superfamily member protein antibodies (Abcam). The position of the recombinant proteins in the Western blot is indicated with arrows. Abbreviation: MW, molecular weight markers (Spectra multicolor broad range protein ladder; Thermo Fisher Scientific).

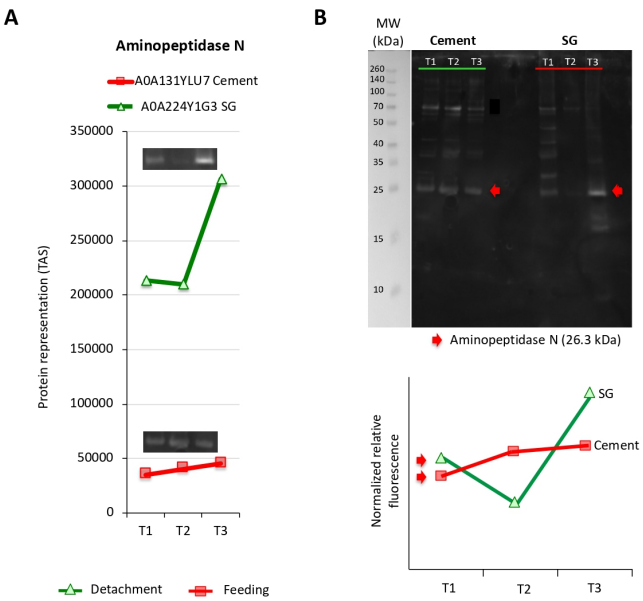

Figure S5. Western blot analysis of tick-derived aminopeptidase N protein in the *R. microplus* cementome (Cement) and sialome (SG). (A) Based on proteomics representation profiles, proteins were putatively assigned to different categories of developmental processes (Figure 1). (B) Cement protein lysate (10 µg) and salivary gland protein lysate (20 µg) were methanol/chloroform precipitated, resuspended in Laemmli sample buffer and separated on an SDS-polyacrylamide precast gel (ClearPage Expedeon, VWR, Radnor, PA, USA). After electrophoresis, proteins were transferred to a nitrocellulose blotting membrane (GE Healthcare Dharmacon Inc., Lafayette, CO, USA), blocked with 3% BSA (Sigma-Aldrich) in TBS and incubated overnight at 4 °C with antibodies against tick recombinant aminopeptidase N, diluted 1:200 in 3% BSA/TBS. To detect the IgG antibodies bound to tick proteins, membranes were incubated with goat anti-rabbit IgG peroxidase antibody (Sigma-Aldrich) diluted 1:1000 in 3% BSA/TBS. Immunoreactive proteins were visualized with chemiluminescence with Pierce ECL Western Blotting Substrate (Thermo Fisher Scientific). Quantitative analysis was performed using the Fiji ImageJ (https://imagej.nih.gov/ij/download.html) to measure the intensity of the protein bands and after substation of the intensity of the PBS control to compare the results at different time points. The results of the Western blot reproduced those obtained with proteomics analysis.

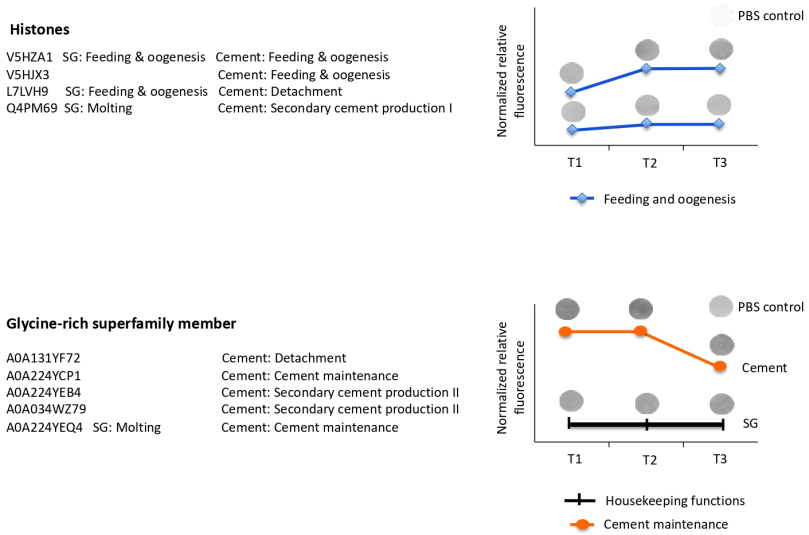

Figure S6. Dot blot analysis of tick-derived histones and Glycine-rich superfamily member proteins in the *R. microplus* cementome (Cement) and sialome (SG). Cement and salivary gland proteins were applied onto each strip in 6 different dots (volume per dot, 25 µl at 5 µg/µl. Then the dots were allowed to dry by gravity flow, immersed in 50 µl of 3% BSA/TBS for 15 min approximately and filtered by gravity. Membranes were washed two times with TBS and incubated with primary antibodies diluted at different concentrations in 1% BSA/TBS against Histone H4 (1:100) and Glycine-rich superfamily member proteins (1:200) To detect the IgG antibodies bound to tick proteins, membranes were incubated with goat anti-rabbit IgG peroxidase antibody (Sigma-Aldrich) diluted 1:1000 in 1% BSA/TBS. Membranes were washed two times with TBS and immunoreactive proteins were visualized with chemiluminescence with Pierce ECL Western Blotting Substrate (Thermo Fisher Scientific). Quantitative analysis was performed using the Fiji ImageJ (https://imagej.nih.gov/ij/download.html) to measure the intensity of the protein bands and after substation of the intensity of the PBS control to compare the results at different time points. Based on proteomics representation profiles, proteins were putatively assigned to different categories of developmental processes (Figure 1). Because these proteins constitute a protein family they were assigned to multiple developmental processes. Accordingly, the results of the dot blot reproduced some of the profiles obtained with proteomics analysis.

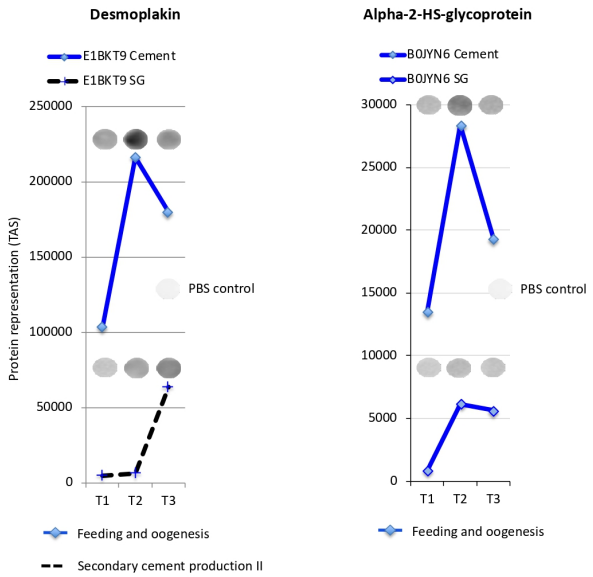

Figure S7. Dot blot analysis of host-derived desmoplakin and alpha-2-HS-glycoprotein in the *R. microplus* cementome (Cement) and sialome (SG). Cement and salivary gland proteins were applied onto each strip in 6 different dots (volume per dot, 25 µl at 5 µg/µl. Then the dots were allowed to dry by gravity flow, immersed in 50 µl of 3% BSA/TBS for 15 min approximately and filtered by gravity. Membranes were washed two times with TBS and incubated with primary antibodies diluted at different concentrations in 1% BSA/TBS against desmoplakin (1:300) and alpha-2-HS-glycoprotein (1:300). To detect the IgG antibodies bound to tick proteins, membranes were incubated with goat anti-rabbit IgG peroxidase antibody (Sigma-Aldrich) diluted 1:1000 in 1% BSA/TBS. Membranes were washed two times with TBS and immunoreactive proteins were visualized with chemiluminescence with Pierce ECL Western Blotting Substrate (Thermo Fisher Scientific). Quantitative analysis was performed using the Fiji ImageJ (https://imagej.nih.gov/ij/download.html) to measure the intensity of the protein bands and after substation of the intensity of the PBS control to compare the results at different time points. Based on proteomics representation profiles, proteins were putatively assigned to different categories of developmental processes (Figure 1). Because these proteins constitute a protein family they were assigned to multiple developmental processes. The results of the dot blot reproduced those obtained with proteomics analysis.

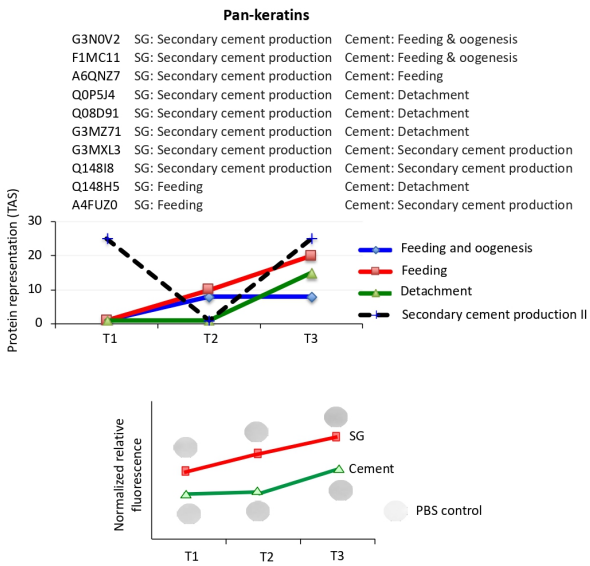

Figure S8. Dot blot analysis of host-derived pan-keratins in the *R. microplus* cementome (Cement) and sialome (SG). Cement and salivary gland proteins were applied onto each strip in 6 different dots (volume per dot, 25 µl at 5 µg/µl. Then the dots were allowed to dry by gravity flow, immersed in 50 µl of 3% BSA/TBS for 15 min approximately and filtered by gravity. Membranes were washed two times with TBS and incubated with primary antibodies diluted 1:300 in 1% BSA/TBS against pan-keratins. To detect the IgG antibodies bound to tick proteins, membranes were incubated with goat anti-rabbit IgG peroxidase antibody (Sigma-Aldrich) diluted 1:1000 in 1% BSA/TBS. Membranes were washed two times with TBS and immunoreactive proteins were visualized with chemiluminescence with Pierce ECL Western Blotting Substrate (Thermo Fisher Scientific). Quantitative analysis was performed using the Fiji ImageJ (https://imagej.nih.gov/ij/download.html) to measure the intensity of the protein bands and after substation of the intensity of the PBS control to compare the results at different time points. Based on proteomics representation profiles, proteins were putatively assigned to different categories of developmental processes (Figure 1). Because these proteins constitute a protein family they were assigned to multiple developmental processes. Accordingly, the results of the dot blot reproduced some of the profiles obtained with proteomics analysis.

Supplementary material not included from Villar, M., **Pacheco, I.,** Merino, O., Contreras, M., Mateos-Hernández, L., Prado, E., Barros-Picanco, D.K., Francisco Lima-Barbero, J., Artigas-Jerónimo, S., Alberdi, P., Fernández de Mera, I.G., Estrada-Peña, A., Cabezas-Cruz, A., de la Fuente, J. (2020). Tick and host derived compounds modulate the biochemical properties of the cement complex substance. Biomolecules 10, 555.

https://www.mdpi.com/2218-273X/10/4/555

- Table S1: *R. microplus* tick-derived proteins identified in the cementome.
- Table S2: Cattle host-derived proteins identified in *R. microplus* tick cementome.
- Table S3: Comparative analysis of amino acid composition of cattle host and tick *R. microplus* derived proteins identified in the cementome.
- Table S4: Recombinant tick proteins used for validation by Western blot analysis.
- Table S5: Examples of tick-derived proteins identified in this study in the cementome and previously characterized and reported in the sialome/sialotranscriptome.
- Table S6: Published results about the potential role of selected tick cementome proteins for novel vaccine development.
- Data S1: Proteomics analysis of *R. microplus* tick sialome.
- Data S2: Proteomics analysis of *R. microplus* tick cementome with urea-extracted proteins.
- Data S3: Proteomics analysis of *R. microplus* tick cementome with SDS-extracted proteins.
- Data S4: Protein profile of tick sialome and cementome throughout tick *R. microplus* parasitic stages.

- Data S5: Composition of chemical elements in *R. microplus* tick cement and salivary glands.
- Data S6: Statistical analysis of chemical element composition in *R. microplus* tick cement and salivary glands.
- Data S7: Peptide sequences for tick *R. microplus* and cattle host derived proteins identified in the sialome and cementome. Host-derived proteins in the cementome were included only if identified in both sialome and cementome.

CHAPTER 2.
Inmune response to alpha-Gal for the Alpha Gal Syndrome

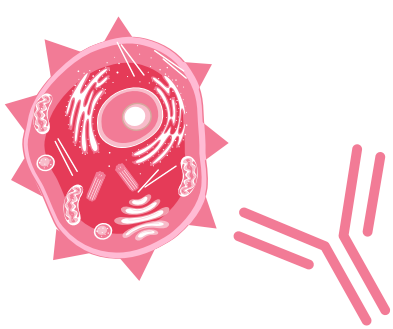

Chapter 2. Immune response to alpha-Gal and implications for the Alpha Gal Syndrome

(a) de la Fuente, J., Cabezas-Cruz, A., **Pacheco, I.** (2020). Alpha-Gal Syndrome: challenges to understanding sensitization and clinical reactions to alpha-gal. Expert Review of Molecular Diagnostics 20, 905-911. https://doi.org/10.1080/14737159.2020.1792781

(b) de la Fuente, J., Urra, J.M., Contreras, M., **Pacheco, I.,** Ferreras-Colino, E., Doncel-Pérez, E., Fernández de Mera, I.G., Villar, M., Cabrera, C.M., Gómez Hernando, C., Vargas Baquero, E., Blanco García, J., Rodríguez Gómez, J., Velayos Galán, A., Feo Brito, F., Gómez Torrijos, E., Cabezas-Cruz, A., Gortázar, C. (2021). A dataset for the analysis of antibody response to glycan alpha-Gal in individuals with immune-mediated disorders. F1000Research 9,1366. https://doi.org/10.12688/f1000research.27495.2

(c) **Pacheco, I.,** Fernández de Mera, I.G., Feo Brito, F., Gómez Torrijos, E., Villar, M., Contreras, M., Lima-Barbero, J.F., Doncel-Pérez, E., Cabezas-Cruz, A., Gortázar, C., de la Fuente, J. (2021). Characterization of the anti-alpha-Gal antibody profile in association with Guillain-Barré syndrome, implications for tick-related allergic reactions. Ticks and Tick-Borne Diseases 12, 101651. https://doi.org/10.1016/j.ttbdis.2021.101651

(d) Contreras, M., **Pacheco, I.,** Alberdi, P., Díaz-Sánchez, S., Artigas-Jerónimo, S., Mateos-Hernández, L., Villar, M., Cabezas-Cruz, A., de la Fuente, J. (2020). Allergic reactions and immunity in response to tick salivary biogenic substances and red meat consumption in the zebrafish model. Frontiers in Cellular and Infection Microbiology 10, 78. https://doi.org/10.3389/fcimb.2020.00078

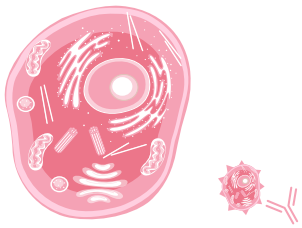

Chapter 2a. Alpha-Gal Syndrome: challenges to understanding sensitization and clinical reactions to alpha-gal

de la Fuente, J., Cabezas-Cruz, A., **Pacheco, I.** (2020). Alpha-Gal Syndrome: challenges to understanding sensitization and clinical reactions to alpha-gal. Expert Review of Molecular Diagnostics 20, 905-911. https://doi.org/10.1080/14737159.2020.1792781

EXPERT REVIEW OF MOLECULAR DIAGNOSTICS
2020, VOL. 20, NO. 9, 905–911
https://doi.org/10.1080/14737159.2020.1792781

Taylor & Francis
Taylor & Francis Group

SPECIAL REPORT

Alpha-gal syndrome: challenges to understanding sensitization and clinical reactions to alpha-gal

José de la Fuente [a,b], Alejandro Cabezas-Cruz[c] and Iván Pacheco[a]

[a]SaBio. Instituto De Investigación En Recursos Cinegéticos IREC-CSIC-UCLM-JCCM, , Ciudad Real, Spain; [b]Department of Veterinary Pathobiology, Center for Veterinary Health Sciences, Oklahoma State University, Stillwater OK, USA; [c]UMR BIPAR, INRAE, ANSES, Ecole Nationale Vétérinaire d'Alfort, Université Paris-Est, Maisons-Alfort, France

ABSTRACT

Introduction: The α-Gal syndrome (AGS) is a type of allergy characterized by an IgE antibody response against the carbohydrate Galα1-3Galβ1-4GlcNAc-R (α-Gal). Tick bites are recognized as the most important cause of anti-α-Gal IgE antibody increase in humans. Several risk factors have been associated with the development of AGS, but their integration into a standardized disease diagnosis has proven challenging.

Areas covered: Herein we discuss the current AGS diagnosis based on anti-α-Gal IgE titers and propose an algorithm that considers all co-factors in the clinical history of α-Gal-sensitized patients to be incorporated into the AGS diagnosis. The need for identification of host-derived gene markers and tick-derived proteins for the diagnosis of the AGS is also discussed.

Expert opinion: The current AGS diagnosis based on anti-α-Gal IgE titers has limitations because not all patients sensitized to α-Gal and with anti-α-Gal IgE antibodies higher than the cutoff (0.35 IU/ml) develop anaphylaxis to mammalian meat and AGS. The basophil activation test proposed to differentiate between patients with AGS and asymptomatic α-Gal sensitization cannot be easily implemented as a generalized clinical test. In coming years, the algorithm proposed here could be used in a mobile application for easier AGS diagnosis in the clinical practice.

ARTICLE HISTORY
Received 27 April 2020
Accepted 3 July 2020

KEYWORDS
Alpha-gal; antibody; allergy; interleukin; tick; mammalian meat

1. Introduction

Recent investigations have focused on the α-Gal Syndrome (AGS), a disease that is associated with tick bites with a growing incidence worldwide [1–6]. Tick saliva contains glycoproteins with Galα1-3Galβ1-(3)4GlcNAc-R (α-Gal) modifications that can induce in some individuals the production of high levels of anti-α-Gal IgE antibodies that mediate delayed anaphylaxis to mammalian meat consumption and immediate anaphylaxis to tick bites, xenotransplantation and certain drugs such as cetuximab [1,3–13].

Humans and crown catarrhines evolved with the inability to synthesize the α-Gal [10]. In turn, they produce high quantities of anti-α-Gal IgM/IgG, which can be protective against pathogens with this modification on their surface [14,15]. However, the capacity to produce anti-α-Gal antibodies increases the risk to develop anti-α-Gal IgE-mediated allergies associated with the AGS [4,10]. Natural anti-α-Gal antibodies, primarily of the IgM/IgG subtypes, occur in humans in response to bacteria of the microbiota containing this modification [14].

Currently, the main method of AGS diagnosis is the measurement of anti-α-Gal IgE antibody levels [6]. However, this test has some limitations and should be considered as a tool to complement other approaches for the effective diagnosis of the AGS.

2. Classical diagnosis of the AGS based on anti-α-Gal IgE titers

The measurement of the anti-α-Gal IgE antibody levels is the approach used for classical diagnosis of the AGS in patients with a clinical history of typical allergies associated with the disease [4,7,16,17]. This analysis is performed using ImmunoCAP, a solid-phase antibody detection test with different α-Gal-containing glycoproteins, mainly bovine thyroglobulin and cetuximab [6,7,16,17]. However, not all subjects who are sensitized to α-Gal and thus showing positive anti-α-Gal IgE antibody levels (cutoff 0.35 IU/ml) report allergic reactions to the consumption of mammalian meat or innards (Table 1), one of the main manifestations of the AGS. One study in South Africa showed that both anti-α-Gal IgE levels and anti-α-Gal IgE to total IgE ratio strongly correlated with the occurrence of mammalian meat allergy [18], while other studies conducted in different countries (Germany, Spain, Australia, Sweden, U.S.A., Denmark), reported a 39.1–1.8% prevalence of anti-α-Gal IgE (cutoff 0.35 IU/ml), but in most cases without allergy to mammalian meat consumption (Table 1). These facts support that the classical diagnosis of the AGS based on anti-α-Gal IgE titers is necessary but not sufficient.

Skin prick test with commercial whole-meat extracts has also been used for the diagnosis of AGS, but this test was found to be unreliable as it generally yields poor or false negative results and

CONTACT José de la Fuente jose_delafuente@yahoo.com; josedejesus.fuente@uclm.es Instituto De Investigación En Recursos Cinegéticos IREC-CSIC-UCLM-JCCM, , 13005 Ciudad Real, Spain

Article highlights

- The Alpha-Gal Syndrome (AGS) is a disease associated with tick bites and anti-α-Gal IgE-mediated allergic reactions to mammalian meat consumption.
- The classical diagnosis of the AGS based on anti-α-Gal IgE titers is necessary but not sufficient.
- Several co-factors may affect the outcome of disease symptoms and the clinical history of the AGS is important for effective diagnosis of the syndrome.
- Exposure to these co-factors may enhance absorption of the α-Gal-containing antigens, decrease the threshold of response, and/or contribute to the severity of the allergic reactions to α-Gal.
- The quantitation of tick sialome immunoreactive proteins and immune response markers serum and/or mRNA levels may be developed as a complementary approach for the diagnosis of the AGS.

Future studies should be focused on the molecular mechanisms triggering the AGS, the biological processes involved in α-Gal processing after mammalian meat consumption, co-factors that may affect disease symptoms, and the identification of host and tick-derived targets for the development of new diagnostic tools.

consequently leads to incorrect guidance for patients [7,25]. The prick-to-prick test usually yields false-negative or just weak skin reactions [4,26]. The basophil activation test (BAT) is very accurate and differentiate between patients with AGS and asymptomatic α-Gal sensitization. However, BAT is currently employed only in an experimental setting [25,27]. In-patient oral food challenge using, for example, cooked pork or porcine kidney is the gold standard in food allergy diagnosis [28]. However, using this method in diagnosis of the AGS is not recommended because of the delayed nature of the reaction and also because it may cause a severe and potentially fatal anaphylactic reaction [28]. These facts demonstrate the current challenges of AGS diagnosis, and the pitfalls of the current methods used to diagnose this disease. As occurs with other allergies, co-factors related to the clinical history may affect the results and thus are important to consider for the diagnosis of the AGS [6].

3. Co-factors in the clinical history that play an important role in diagnosis of the AGS

Patients with AGS report different symptoms of the α-Gal food allergy (i.e. urticaria, pruritus, recurrent angioedema, systemic anaphylaxis), which vary between mild or no reaction to anaphylaxis [25]. Several co-factors related to the clinical history of the disease may affect the outcome of these symptoms. The proposed co-factors include but are not limited to (a) age, (b) repeat exposure to the same food, (c) exposure to meats of different origin, (d) exposure to meat or innards with higher α-Gal content, (e) exposure to tick bites, (f) alcohol consumption, (g) exercise, (h) exposure to non-steroidal anti-inflammatory medications, (i) atopic allergy, (j) ABO blood group, (k) exposure to cats and other pets, (l) helminths infection, and (m) systemic mastocytosis [4,26,29–37].

Among the co-factors associated to the AGS, several evidence show that exposure to tick bites is an essential risk factor for the development of this syndrome [6]: (i) tick bites elicit an increase in the levels of IgE to α-Gal of 20-fold or greater [2], (ii) most AGS patients have a history of tick bites [26,34,38], (iii) AGS patients have antibodies reactive to tick antigens [2], and (iv) a strong positive correlation between anti-α-Gal IgE and anti-tick IgE levels was reported [2,3]. However, some patients that develop strong allergic reactions to tick bites and have high levels of IgE to α-Gal are mammalian meat tolerant [9]. This finding suggests that mammalian meat allergy is a special type of allergy within a wide spectrum of allergies related to tick bites. AGS has been associated with several tick species including *Amblyomma americanum* (USA), *Amblyomma sculptum* (Brazil), *Amblyomma testudinarium,* and *Haemaphysalis longicornis* (Japan), *Ixodes holocyclus* (Australia) and the principal vector of Lyme disease in Europe, *Ixodes ricinus* [8,39]. Surprisingly, *Ixodes scapularis*, the main vector of Lyme disease in the USA, which produces α-Gal [40,41] and is closely related to *I. ricinus*, is almost certainly not a major cause of AGS in the USA [6].

The occurrence of AGS has no obvious connection with age and gender and the role of atopy in the development of syndrome is still debated. There are studies that described an impact of age and atopy on the development of AGS [38,42,43]. For example, a recent study of a European cohort found that the majority of AGS patients (n = 128) were middle aged and atopic, with equal gender distribution [38]. Despite atopy increased the risk of anaphylaxis with pulmonary manifestations in the European cohort [38], another study reported no association between anti-α-Gal IgE antibodies and asthma [44]. The National Institute of Allergy and Infectious Diseases Workshop on understanding the AGS concluded that the AGS does not appear to be overrepresented among subjects with atopic dermatitis [6].

A co-factor showing strong association with the AGS is the ABO blood group. Several studies reported that individuals with blood groups AB and B are significantly underrepresented among AGS patients [38,45–48]. Brestoff et al. [45] showed that the blood group B protects individuals from developing AGS. The presence of blood type B reduces the capacity of the immune system to produce anti-α-Gal antibodies, due to tolerance to α-Gal, which is very similar in structure to the blood group B antigen [47]. In consequence, it was proposed that the analysis of ABO blood groups should be included in studies assessing the epidemiology of AGS [49].

The α-Gal epitope is present on pet dander and ownership of pets, especially cats, was associated with the presence of anti-α-Gal IgE antibodies in cat owners [42,44,50]. However, despite a very strong positive correlation between IgE antibodies to cat and to α-Gal [44,50], an airborne-triggered α-Gal sensitization due to cat dander was ruled out as the cause and anti-α-Gal IgE positivity was not linked to cat allergy analyzed by skin prick test [42]. Pet-associated endoparasites have been also proposed to potentially induce sensitization to α-Gal in humans [50]. Particularly, strong correlation was found between IgE antibodies to α-Gal and *Echinococcus* spp., but no *Ascaris* spp., antigens which suggested that the tapeworm could be responsible for α-Gal sensitization in Africa [50]. However, recent research provided evidence on the potential role of the nematode *Toxocara canis* infection in decreasing anti-α-Gal IgE levels and suppressing the allergic response to α-Gal [34]. Systemic mastocytosis, a form of clonal mast cell disorder in which mast cells accumulate

Table 1. Population diversity in the antibody response to α-Gal.

Study population	Findings	Conclusions	References
Southwest Germany: 300 hunters and forest workers.	19.3% prevalence of anti-α-Gal IgE (cutoff 0.35 IU/ml), but only 5 individuals had allergic symptoms to mammalian meat or innards.	Not all individuals who are sensitized to α-Gal report allergic reactions to mammalian meat or tick bites.	[19]
Spain: 126 cases with urticaria or anaphylaxis and 126 healthy controls.	15.7% prevalence (26.3% in cases and 2.4% in controls) of anti-α-Gal IgE (cutoff 0.35 IU/ml). Prevalence varied between Northern (46.3%), central (0.7%) and Mediterranean (0%) regions. Association with tick bites, outdoor activities, pet ownership, consumption of mammalian meat and alcohol.	The anti-α-Gal IgE response is associated with tick bites and varies geographically.	[20]
Spain: 169 foresters and forest workers and 100 individuals without record of tick bites.	15% and 4% prevalence of anti-α-Gal IgE (cutoff 0.35 IU/ml) in foresters and controls, respectively.	Anti-α-Gal IgE prevalence is associated with the number of tick bites/year. None of the individuals sensitized to mammalian meat developed AGS.	[21]
Spain: 444 randomly selected adults.	8.1% (cutoff 0.1 IU/ml) and 2.2% (cutoff 0.35 IU/ml) prevalence of anti-α-Gal IgE in randomly selected adults.	α-Gal sIgE positivity was associated with a history of tick bites, atopy, and cat ownership.	[42]
Australia: 118 individuals (26 with AGS).	84.6% and 39.1% prevalence of anti-α-Gal IgE (cutoff 0.35 IU/ml) in patients with and without AGS, respectively. Association with AGS and tick bites.	Anti-α-Gal IgE is a good indicator of AGS and history of tick bite but is of limited diagnostic utility for AGS in tick-endemic populations.	[22]
Various patient populations.	Risk factors for AGS include exposure to ticks of certain species. Common symptoms include urticaria and isolated abdominal reactions.	Age and gender differences likely reflect exposure to ticks that vary according to setting.	[23]
Sweden: 51 patients with AGS and 102 healthy blood donors.	100% and 14.7% prevalence of anti-α-Gal IgE (cutoff 0.35 IU/ml) in patients with and without AGS, respectively with higher levels in AGS patients.	Patients with AGS show higher anti-α-Gal IgE and IgG levels when compared to healthy controls. Blood group B donors have significantly reduced antibody responses to α-Gal, due to similarities with the B-antigen.	[24]
Various patient populations. USA: 121 patients with AGS, 56 with Asthma, 49 with cancer and 341 controls. Kenya: 254 individuals exposed to tick bites.	USA: 97%, 11%, 6% and <1% prevalence of anti-α-Gal IgE (cutoff 0.35 IU/ml) in patients with AGS, Asthma, cancer and controls, respectively. Kenya: 53% prevalence of anti-α-Gal IgE (cutoff 0.35 IU/ml)	Tick bites are a cause of IgE specific for α-Gal.	[2]
South Africa: 131 individuals with symptoms of adverse reaction to mammalian meat and 26 healthy controls.	64.1% prevalence of anti-α-Gal IgE (cutoff 0.1 IU/ml) in patients with adverse reaction to mammalian meat.	Strong correlation between anti-α-Gal IgE levels and AGS in a population with high prevalence of mammalian meat allergy.	[18]
USA: 118 subjects at cardiovascular risk.	26% correlation between prevalence of anti-α-Gal IgE and amounts of athero-sclerotic plaque.	Association between coronary artery disease and anti-α-Gal IgE.	[28]
Japan: 115 patients with tick bites and 21 healthy controls.	0%, 4.4%, 34.6%, 66.7% and 65% prevalence of anti-α-Gal IgE in healthy individuals and patients with record of one, two, three and more than 4 tick bites, respectively.	Patients with more than 2 tick bites have anti-α-Gal IgE antibody levels than those with one tick bite or healthy individuals.	[39]
Denmark: 2297 randomly selected adults.	5.5% (cutoff 0.1 IU/ml) and 1.8% (cutoff 0.35 IU/ml) prevalence of anti-α-Gal IgE in randomly selected adults.	α-Gal sIgE positivity was associated with a history of tick bites, atopy, and cat ownership.	[42]
Various patient populations. 92 with AGS and 188 controls.	Patients with blood type B were approximately 5 times less likely to have AGS than those with blood type O.	Blood group B protect from develop allergic sensitization to α-Gal.	[45]

in internal tissues and organs, has also been identified as a major risk factor for developing AGS [35–37]. Mastocytosis is associated with sensitivity to venom in patients and, although not as common, severe reactions to foods and α-Gal sensitivity are also reported in patients suffering this disease [35–37].

Nevertheless, these co-factors in the clinical history of the AGS could be used for disease risk assessment using a similar experimental approach previously proposed for tick-borne diseases [51]. For example, to estimate the risk (probability) that a patient with anti-α-Gal IgE antibody levels higher than 0.35 IU/ml develop allergic reactions to the consumption of mammalian meat or innards, we propose to consider these co-factors (CF) as Risk (R) = CF(a) X CF(b) X CF(c) X CF(d) X … CF(n). It is necessary to collect the information about these co-factors from individuals who are sensitized to α-Gal and/or showing signs of allergy to the consumption of mammalian meat or innards, tick bites, xenotransplantation or certain α-Gal-containing drugs. Furthermore, when enough data becomes available it may be possible to use machine learning algorithms by assigning different risk values to each co-factor as input variables to estimate R as the response variable for high or low risk of AGS [52] (Table 2).

The mechanisms triggering the AGS have not been fully characterized, but the biological processes involved in α-Gal-containing biomolecules absorption, digestion, and subsequent presentation to the host immune system after mammalian meat consumption appear to be very important [4,28,53]. Therefore, although still to be demonstrated, exposure to these co-factors related to the clinical history of the AGS may enhance absorption of the α-Gal-containing antigens, decrease the threshold of response, and/or contribute to the severity of the allergic reactions to α-Gal [6,17]. Finally, the natural history of α-Gal IgE sensitization is important to determine whether early symptomatology would develop over time into more severe, anaphylactic reactions.

Table 2. Proposed machine learning algorithm. Example data are for illustrative purposes only.

	Input co-factor variables (putative observed predictors as described in section 3)									Response risk variables (R)	
Individuals (I)	CF (a)	CF(b)	CF(c)	CF(d)	CF(e)	CF(f)	CF(g)	CF (h)	CF (n)	R	High (H) Low (L) risk
Known information	Average importance of each co-factor (learned from known information)										
I3	24	9	8	14	25	79	3	4	–	–	–
I1	100	20	12	10	11	13	90	50	0	34%	H
I2	22	31	50	20	33	82	75	30	25	41%	H
I3	0	44	21	0	3	0	100	0	2	19%	L
In	21	0	2	0	7	6	50	2	10	11%	L
New individuals	New information (collected from new individuals)										Predictions
New I1	25	24	19	10	61	20	90	18	1	30%	H
New I2	1	3	1	35	12	2	20	1	1	8%	L
New In	17	2	10	22	70	9	100	100	15	38%	H

4. Identification of host-derived immune response markers for the diagnosis of the AGS

The C57BL/6 α1,3-Galactosyltransferase-knockout (α1,3-GalT-KO) mice and zebrafish that like humans do not synthesize α-Gal have been used as a model to characterize the molecular mechanisms in response to percutaneous sensitization to α-Gal [54,55] and the IgE-mediated immune response to *Amblyomma* spp. tick saliva or proteins [54,56].

The results from experiments in these animal models together with the evidence obtained from studies in humans suggest that the mechanisms triggering the AGS involve Toll-like receptor (TLR)-mediated responses in both Th1 and Th2 cells that are involved in macrophage cell-mediated innate immune response and B cell/antibody-mediated adaptive immune response [4,55–57-60]. Basophils have been also proposed to play a role in this process [4,57]. Based on these predicted regulatory pathways, cytokines such as interleukins (IL) IL-1 and IL-4 were suggested to play a key role in the response to α-Gal-containing biomolecules resulting in the development of the AGS (recently summarized by [55]). These results suggested the possibility of exploring the quantitation of immune response markers such as IL-1 and IL-4 serum and/or mRNA levels as a complementary approach for the diagnosis of the AGS. However, this possibility requires additional studies in animal models and analyses in human samples to evaluate its efficacy.

5. Identification of tick-derived proteins for the diagnosis of the AGS

It has been shown that tick saliva contains glycoproteins with α-Gal modifications that after tick bite can induce in some individuals the production of high anti-α-Gal IgE antibody levels that may result in the AGS (recently reviewed by [4]). The presence of α-Gal in tick glycolipids has not been demonstrated. Furthermore, studies in tick salivary glands and saliva have shown the presence of α-Gal that may be synthesized by ticks and/or come from host biomolecules present in the bloodmeal [4,9,40,41,55,58].

Recently, an experimental approach was proposed using one-dimensional and two-dimensional Western blot combined with proteomics to identify *Rhipicephalus bursa* and *Hyalomma marginatum* proteins that contain α-Gal and react with sera from individuals with and without AGS [9]. Another study used a similar approach and identified α-Gal-carrying IgE-binding proteins in adults and larvae *I. ricinus* [59]. The results showed the presence of proteins with α-Gal and reactive only to patient-specific antibodies. However, tick salivary gland proteins differentially recognized by IgE in patient's sera were not positive for α-Gal, thus suggesting that tick proteins without this modification could be also used to evaluate exposure to tick bites and risk for AGS [9,15]. Some of these proteins could be potentially used to develop ELISA tests to quantify the antibody response as a complementary approach for the diagnosis of the AGS.

6. Conclusions

The incidence of the AGS is growing worldwide and requires effective diagnosis approaches to implement interventions limiting disease impact on human health. The classical diagnosis of the AGS based on anti-α-Gal IgE titers is necessary but not sufficient for an effective diagnosis of the syndrome. Several co-factors may affect disease symptoms and thus are important to consider for the diagnosis of the AGS. Some of these co-factors have been identified but additional studies are required to develop more effective diagnosis tools. These studies should be focused on the molecular mechanisms triggering the AGS, the biological processes involved in α-Gal absorption, digestion, and subsequent presentation to the host immune system after mammalian meat consumption, the identification of early symptomatology factors that develop over time into more severe anaphylactic reactions, and the identification of host-derived immune response markers and tick-derived proteins for the development of new diagnostic tools.

7. Expert opinion

Conclusive diagnosis of AGS cannot be achieved using anti-α-Gal IgE titers information alone. BAT was proposed to differentiate between patients with AGS and asymptomatic α-Gal sensitization [27]. However, BAT requires highly specialized expertise and laboratory equipment and reagents not

available in Primary Healthcare Centers, and therefore this methodology is currently only employed in an experimental setting [25]. In 2018, the National Institute of Allergy and Infectious Diseases Workshop on understanding the AGS agreed that future research should focus in incorporating the natural history of α-Gal IgE sensitization in the diagnosis of the AGS and to determine whether early symptomatology can be used to predict the development of more severe anaphylactic reactions to α-Gal [6]. The list of risk factors that have been associated with the development of AGS is long and complex and therefore difficult to incorporate into a procedure of standardized diagnostics for AGS [4].

In this expert opinion, we propose an integrative diagnostic methodology in which several co-factors associated with the clinical history of the AGS are combined in a machine learning algorithm to improve AGS diagnosis. Such an algorithm can be coded in a programming language to create a software that could be the basis for a mobile application (app) to be implemented in the clinical practice for the diagnosis of AGS. One of the limitations of current AGS diagnosis is the lack of standardization in the co-factors considered by physicians when assessing the risk of developing AGS. A mobile app using the algorithm proposed here can include a standardized questionnaire filled by physicians in which, in addition to anti-α-Gal IgE levels, co-factors information can be included to calculate the risk of developing AGS as low, moderate, and high for each patient. Standardization in diagnostic methodologies decreases the rate of false positive and false negative results (e.g. [61]).

Funding

This paper was partially funded by the Consejería de Educación, Cultura y Deportes, JCCM, Spain, project CCM17-PIC-036 (SBPLY/17/180501/000185).

Declaration of interest

The authors have no relevant affiliations or financial involvement with any organization or entity with a financial interest in or financial conflict with the subject matter or materials discussed in the manuscript. This includes employment, consultancies, honoraria, stock ownership or options, expert testimony, grants or patents received or pending, or royalties.

Reviewer disclosures

One peer reviewer is in a research group that has received unrestricted research support from Thermo-Fisher/Phadia. Peer reviewers on this manuscript have no other relevant financial relationships or otherwise to disclose.

ORCID

José de la Fuente http://orcid.org/0000-0001-7383-9649

References

Papers of special note have been highlighted as either of interest (•) or of considerable interest (••) to readers.

1. van Nunen S, O'Connor KS, Clarke LR, et al. The association between *Ixodes holocyclus* tick bite reactions and red meat allergy. Intern Med J. 2007;39:A132.

•• **First description that tick bites were associated with allergy to mammalian meat.**

2. Commins SP, James HR, Kelly LA, et al. The relevance of tick bites to the production of IgE antibodies to the mammalian oligosaccharide galactose-α-1,3-galactose. J Allergy Clin Immunol. 2011;127(5):1286–1293.e6.

•• **First description that tick bites were associated with an increase in anti-α-Gal IgE antibodies and allergy to mammalian meat.**

3. Steinke JW, Platts-Mills TA, Commins SP. The alpha-gal story: lessons learned from connecting the dots. J Allergy Clin Immunol. 2015;135:589–596.
4. Cabezas-Cruz A, Hodžić A, Román-Carrasco P, et al. Environmental and molecular drivers of the α-Gal syndrome. Front Immunol. 2019;10:1210.
5. de la Fuente J, Pacheco I, Villar M, et al. The alpha-Gal syndrome: new insights into the tick-host conflict and cooperation. Parasit Vectors. 2019;12:154.
6. TAE P-M, Commins SP, Biedermann T, et al. On the cause and consequences of IgE to galactose-α-1,3-galactose: A report from the National Institute of Allergy and Infectious Diseases Workshop on understanding IgE-mediated mammalian meat allergy. J Allergy Clin Immunol. 2020;145(4):1061–1071.
7. Commins SP, Satinover SM, Hosen J, et al. Delayed anaphylaxis, angioedema, or urticaria after consumption of red meat in patients with IgE antibodies specific for galactose-alpha-1,3-galactose. J Allergy Clin Immunol. 2009;123:426–433.
8. Platts-Mills TA, Schuyler AJ, Tripathi A, et al. Anaphylaxis to the carbohydrate side chain alpha-gal. Immunol Allergy Clin North Am. 2015;35:247–260.
9. Mateos-Hernández L, Villar M, Moral A, et al. Tick-host conflict: immunoglobulin E antibodies to tick proteins in patients with anaphylaxis to tick bite. Oncotarget. 2017;8:20630–20644.

• **Describes proteins carrying α-Gal and reactive to anti-α-Gal IgE antibodies in ticks.**

10. Galili U. Evolution in primates by "Catastrophic-selection" interplay between enveloped virus epidemics, mutated genes of enzymes synthesizing carbohydrate antigens, and natural anticarbohydrate antibodies. Am J Phys Anthropol. 2019;168:352–363.
11. Hilger C, Fischer J, Wölbing F, et al. Role and mechanism of galactose-alpha-1,3-galactose in the elicitation of delayed anaphylactic reactions to red meat. Curr Allergy Asthma Rep. 2019;19:3.
12. Cabezas-Cruz A, Valdés J, de la Fuente J. Cancer research meets tick vectors for infectious diseases. Lancet Infect Dis. 2014;14:916–917.
13. Iweala OI, Choudhary SK, Addison CT, et al. Glycolipid-mediated basophil activation in alpha-gal allergy. J Allergy Clin Immunol. 2020;S0091-6749(20)30258-X. [published online ahead of print, 2020 Feb 20].
14. Yilmaz B, Portugal S, TM T, et al. Gut microbiota elicits a protective immune response against malaria transmission. Cell. 2014;159:1277–1289.

• **Provides evidence that gut microbiota induces protective anti-α-Gal IgM antibodies.**

15. Cabezas-Cruz A, Mateos-Hernández L, Pérez-Cruz M, et al. Regulation of the immune response to a-Gal and vector-borne diseases. Trends Parasitol. 2015;31:470–476.
16. Jappe U, Minge S, Kreft B, et al. Meat allergy associated with galactosyl-alpha-(1,3)-galactose (alpha-Gal)-Closing diagnostic gaps by anti-alpha-Gal IgE immune profiling. Allergy. 2018;73(1):93–105.
17. Wilson JM, Platts-Mills TAE. The oligosaccharide galactose-α-1,3-galactose and the α -Gal syndrome: insights from an epitope that is causal in IgE-mediated immediate and delayed anaphylaxis. EMJ Allergy Immunol. 2018;3(1):89–98.
18. Mabelane T, Basera W, Botha M, et al. Predictive values of alpha-gal IgE levels and alpha-gal IgE: total IgE ratio and oral food challenge-proven meat allergy in a population with a high prevalence of reported red meat allergy. Pediatr Allergy Immunol. 2018;29(8):841–849.

19. Fischer J, Lupberger E, Hebsaker J, et al. Prevalence of type I sensitization to alpha-gal in forest service employees and hunters. Allergy. 2017;72(10):1540–1547.
20. Mateo Borrega MB, Garcia B, Larramendi CH, et al. IgE-mediated sensitization to Galactose-α-1,3- Galactose (α-Gal) in urticaria and anaphylaxis in Spain: geographical variations and risk factors. J Investig Allergol Clin Immunol. 2019;29(6):436–443.
21. Venturini M, Lobera T, Sebastián A, et al. IgE to α-Gal in foresters and forest workers from La Rioja, North of Spain. J Investig Allergol Clin Immunol. 2018;28(2):106–112.
22. Li J, Fulton RB, O'Connell R, et al. Specific-IgE to galactose-α-1,3-galactose (alpha-gal) has limited utility in diagnosing meat allergy in a tick-endemic population. Ann Allergy Asthma Immunol. 2018;121(4):509–511.
23. Levin M, Apostolovic D, Biedermann T, et al. Galactose α-1,3-galactose phenotypes: lessons from various patient populations. Ann Allergy Asthma Immunol. 2019;122(6):598–602.
24. Apostolovic D, Rodrigues R, Thomas P, et al. Immunoprofile of α-Gal- and B-antigen-specific responses differentiates red meat-allergic patients from healthy individuals. Allergy. 2018;73(7):1525–1531.
25. Weins AB, Eberlein B, Biedermann T. Diagnostik des α-Gal-syndroms: aktuelle standards, fallstricke und perspektiven [Diagnostics of alpha-gal syndrome: current standards, pitfalls and perspectives]. Hautarzt. 2019;70(1):36–43.
26. Fischer J, Yazdi AS, Biedermann T. Clinical spectrum of alpha-Gal syndrome: from immediate-type to delayed immediate-type reactions to mammalian innards and meat. Allergo J Int. 2016;25:55–62.
27. Mehlich J, Fischer J, Hilger C, et al. The basophil activation test differentiates between patients with alpha-gal syndrome and asymptomatic alpha-gal sensitization. J Allergy Clin Immunol. 2019;143(1):182–189.
28. Wilson JM, Schuyler AJ, Schroeder N, et al. Galactose-α-1,3-Galactose: atypical food allergen or model IgE hypersensitivity? Curr Allergy Asthma Rep. 2017;17:8.
29. Commins SP. Invited commentary: alpha-Gal allergy: tip of the iceberg to a pivotal immune 507 response. Curr Allergy Asthma Rep. 2016;16(9):61.
30. Wolbing F, Fischer J, Koberle M, et al. About the role and underlying mechanisms of cofactors in anaphylaxis. Allergy. 2013;68(9):1085–1092.
31. Commins SP, James HR, Stevens W, et al. Delayed clinical and ex vivo response to mammalian meat in patients with IgE to galactose-alpha-1,3-galactose. J Allergy Clin Immunol. 2014;134(1):108–115.
32. Fischer J, Hebsaker J, Caponetto P, et al. Galactose-alpha-1,3-galactose sensitization is a prerequisite for pork-kidney allergy and cofactor-related mammalian meat anaphylaxis. J Allergy Clin Immunol. 2014;134(3):755–759e1.
33. Morisset M, Richard C, Astier C, et al. Anaphylaxis to pork kidney is related to IgE antibodies specific for galactose-alpha-1,3-galactose. Allergy. 2012;67(5):699–704.
34. Hodžić A, Mateos-Hernández L, Fréalle E, et al. Infection with *Toxocara canis* inhibits the production of IgE antibodies to α-Gal in humans: towards a conceptual framework of the hygiene hypothesis? Vaccines (Basel). 2020;8(2):E167.
• **First description that helminths infection decreases the levels of anti-α-Gal IgE antibodies.**
35. Diaz JH. Red meat allergies after lone star tick (*Amblyomma americanum*) bites. South Med J. 2020;113(6):267–274.
36. Carter MC, Ruiz-Esteves KN, Workman L, et al. Identification of alpha-gal sensitivity in patients with a diagnosis of idiopathic anaphylaxis. Allergy. 2018;73(5):1131–1134.
37. Roenneberg S, Böhner A, Brockow K, et al. α-Gal-a new clue for anaphylaxis in mastocytosis. J Allergy Clin Immunol Pract. 2016;4(3):531–532.
38. Kiewiet MBG, Apostolovic D, Starkhammar M, et al. Clinical and serological characterization of the α-Gal syndrome-importance of atopy for symptom severity in a European Cohort. J Allergy Clin Immunol Pract. 2020;8(6):2027–2034.e2. [published online ahead of print, 2020 Mar 3].
39. Hashizume H, Fujiyama T, Umayahara T, et al. Repeated Amblyomma testudinarium tick bites are associated with increased galactose-α-1,3-galactose carbohydrate IgE antibody levels: A retrospective cohort study in a single institution. J Am Acad Dermatol. 2018;78(6):1135–1141.e3.
40. Cabezas-Cruz A, Espinosa PJ, Alberdi P, et al. Tick galactosyltransferases are involved in α-Gal synthesis and play a role during *Anaplasma phagocytophilum* infection and *Ixodes scapularis* tick vector development. Sci Rep. 2018;8:14224.
• **Describes the molecular basis of α-Gal synthesis by ticks.**
41. Crispell G, Commins SP, Archer-Hartman SA, et al. Discovery of alpha-gal-containing antigens in North American tick species believed to induce red meat allergy. Front Immunol. 2019;10:1056.
42. Gonzalez-Quintela A, Dam Laursen AS, Vidal C, et al. IgE antibodies to alpha-gal in the general adult population: relationship with tick bites, atopy, and cat ownership. Clin Exp Allergy. 2014;44(8):1061–1068.
43. Villalta D, Pantarotto L, Da Re M, et al. High prevalence of sIgE to Galactose-α-1,3-galactose in rural pre-Alps area: a cross-sectional study. Clin Exp Allergy. 2016;46(2):377–380.
44. Commins SP, Kelly LA, Rönmark E, et al. Galactose-α-1,3-galactose-specific IgE is associated with anaphylaxis but not asthma. Am J Respir Crit Care Med. 2012;185(7):723–730.
45. Brestoff JR, Tesfazghi MT, Zaydman MA, et al. The B antigen protects against the development of red meat allergy. J Allergy Clin Immunol Pract. 2018;6(5):1790–1791.e3.
46. Apostolovic D, Tran TA, Starkhammar M, et al. The red meat allergy syndrome in Sweden. Allergo J Int. 2016;25(2):49–54.
47. Rispens T, Derksen NI, Commins SP, et al. IgE production to α-gal is accompanied by elevated levels of specific IgG1 antibodies and low amounts of IgE to blood group B. PLoS One. 2013;8(2):e55566.
48. Wilson JM, Schuyler AJ, Workman L, et al. Investigation into the α-Gal syndrome: characteristics of 261 children and adults reporting red meat allergy. J Allergy Clin Immunol Pract. 2019;7(7):2348–2358.e4.
49. Cabezas-Cruz A, de la Fuente J, Fischer J, et al. Prevalence of type I sensitization to alpha-gal in forest service employees and hunters: is the blood type an overlooked risk factor in epidemiological studies of the α-Gal syndrome? Allergy. 2017;72(12):2044–2047.
50. Hosen J, Perzanowski M, Carter MC, et al. IgE antibodies to helminths and the cross-reactive oligosaccharide galactose-alpha-1,3-galactose (alphaGal) among children in a village in Africa. J Allergy Clin Immunol. 2008;121(2, Suppl 1):S140.
51. de la Fuent J, Contreras M, Estrada-Peña A, et al. Targeting a global health problem: vaccine design and challenges for the control of tick-borne diseases. Vaccine. 2017;35:5089–5094.
52. de la Fuente J, Villar M, Estrada-Peña A, et al. High throughput discovery and characterization of tick and pathogen vaccine protective antigens using vaccinomics with intelligent Big Data analytic techniques. Expert Rev Vaccines. 2018;17:569–576.
53. Steinke JW, Pochan SL, James HR, et al. Altered metabolic profile in patients with IgE to galactose-alpha-1,3-galactose following in vivo food challenge. J Allergy Clin Immunol. 2016; 138:1465–1467.e8
• **Shows metabolic alterations potentially associated with the AGS.**
54. Araujo RN, Franco PF, Rodrigues H, et al. Amblyomma sculptum tick saliva: α-Gal identification, antibody response and possible association with red meat allergy in Brazil. Int J Parasitol. 2016;46:213–220.
55. Contreras M, Pacheco I, Alberdi P, et al. Allergic reactions and immunity in response to tick salivary biogenic substances and red meat consumption in the zebrafish model. Front Cell Infect Microbiol. 2020;10:78.
56. Chandrasekhar JL, Cox KM, Loo WM, et al. Cutaneous exposure to clinically relevant Lone Star ticks promotes IgE production and hypersensitivity through CD4+ T Cell- and MyD88-dependent pathways in mice. J Immunol. 2019;203:813–824.

57. Kageyama R, Fujiyama T, Satoh T, et al. The contribution made by skin-infiltrating basophils to the development of alpha gal syndrome. Allergy. 2019;74(9):1805–1807.
58. Villar M, Pacheco I, Merino O, et al. Tick and host derived compounds detected in the cement complex substance. Biomolecules. 2020;10(4):E555P.
• **First characterization of the α-Gal content in tick cement.**
59. Apostolovic D, Mihailovic J, Commins SP, et al. Allergenomics of the tick Ixodes ricinus reveals important α-Gal-carrying IgE-binding proteins in red meat allergy. Allergy. 2020;75(1):217–220.
60. Lee B, Lee JS, Lee YW, et al. Effect of the standardization of diagnostic tests on the prevalence of diabetes mellitus and impaired fasting glucose. J Korean Med Sci. 2018;33(10):e81.

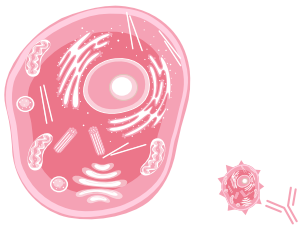

Chapter 2b. A dataset for the analysis of antibody response to glycan alpha-Gal in individuals with immune-mediated disorders

de la Fuente, J., Urra, J.M., Contreras, M., **Pacheco, I.,** Ferreras-Colino, E., Doncel-Pérez, E., Fernández de Mera, I.G., Villar, M., Cabrera, C.M., Gómez Hernando, C., Vargas Baquero, E., Blanco García, J., Rodríguez Gómez, J., Velayos Galán, A., Feo Brito, F., Gómez Torrijos, E., Cabezas-Cruz, A., Gortázar, C. (2021). A dataset for the analysis of antibody response to glycan alpha-Gal in individuals with immune-mediated disorders. F1000Research 9,1366. https://doi.org/10.12688/f1000research.27495.2

F1000Research F1000Research 2020, 9:1366 Last updated: 11 DEC 2020

DATA NOTE

A dataset for the analysis of antibody response to glycan alpha-Gal in individuals with immune-mediated disorders [version 1; peer review: 1 approved]

José de la Fuente[1,2], José Miguel Urra[3,4], Marinela Contreras[5], Iván Pacheco[1], Elisa Ferreras-Colino[1], Ernesto Doncel-Pérez[6], Isabel G. Fernández de Mera[1], Margarita Villar[1,7], Carmen M. Cabrera[3,4], Cesar Gómez Hernando[8], Eduardo Vargas Baquero[6], Javier Blanco García[6], Javier Rodríguez Gómez[6], Alberto Velayos Galán[9], Francisco Feo Brito[10], Elisa Gómez Torrijos[10], Alejandro Cabezas-Cruz[11], Christian Gortázar[1]

[1]SaBio, Instituto de Investigación en Recursos Cinegéticos IREC, Ciudad Real, 13005, Spain
[2]Department of Veterinary Pathobiology, Center for Veterinary Health Sciences, Oklahoma State University, Stillwater, OK, 74078, USA
[3]Immunology Department, Hospital General Universitario de Ciudad Real, Ciudad Real, 13005, Spain
[4]School of Medicine, Universidad de Castilla la Mancha (UCLM), Ciudad Real, 13005, Spain
[5]Interdisciplinary Laboratory of Clinical Analysis, Interlab-UMU, Regional Campus of International Excellence Campus Mare Nostrum, University of Murcia, Murcia, 30100, Spain
[6]Hospital Nacional de Parapléjicos, Servicio de Salud de Castilla La Mancha, Toledo, 45071, Spain
[7]Biochemistry Section, Faculty of Science and Chemical Technologies, and Regional Centre for Biomedical Research (CRIB), University of Castilla-La Mancha, Ciudad Real, 13071, Spain
[8]Hospital Virgen de la Salud, Toeldo, 45001, Spain
[9]Servicio de Neurología, Hospital General La Mancha Centro, Alcázar de San Juan, 13600, Spain
[10]Allergy Section, General University Hospital of Ciudad Real, Ciudad Real, 13005, Spain
[11]UMR BIPAR, INRAE, ANSES, Ecole Nationale Vétérinaire d'Alfort, Université Paris-Est, Maisons-Alfort, 94700, France

v1 **First published:** 24 Nov 2020, **9**:1366
https://doi.org/10.12688/f1000research.27495.1
Latest published: 24 Nov 2020, **9**:1366
https://doi.org/10.12688/f1000research.27495.1

Abstract

Humans evolved by losing the capacity to synthesize the glycan Galα1-3Galβ1-(3)4GlcNAc-R (α-Gal), which resulted in the development of a protective response mediated by anti-α-Gal IgM/IgG/IgA antibodies against pathogens containing this modification on membrane proteins. As an evolutionary trade-off, humans can develop the alpha-Gal syndrome (AGS), a recently diagnosed disease mediated by anti-α-Gal IgE antibodies and associated with allergic reactions to mammalian meat consumption and tick bites. However, the anti-α-Gal antibody response may be associated with other immune-mediated disorders such as those occurring in patients with COVID-19 and Guillain-Barré syndrome (GBS). Here, we provide a dataset (209 entries) on the IgE/IgM/IgG/IgA anti-α-Gal antibody response in healthy individuals and patients diagnosed with AGS, tick-borne

Open Peer Review

Reviewer Status ✓

	Invited Reviewers
	1
version 1 24 Nov 2020	✓ report

1. **Jacques Le Pendu**, Université de Nantes, Inserm, Nantes, France

Any reports and responses or comments on the article can be found at the end of the article.

allergies, GBS and COVID-19. The data allows correlative analyses of the anti-α-Gal antibody response with factors such as patient and clinical characteristics, record of tick bites, blood group, age and sex. These analyses could provide insights into the role of anti-α-Gal antibody response in disease symptomatology and possible protective mechanisms.

Keywords
alpha Gal, immune response, antibody, allergy, tick, coronavirus, COVID-19, Guillain-Barré syndrome, alpha-Gal syndrome

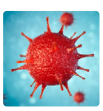

This article is included in the Disease Outbreaks gateway.

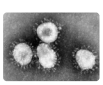

This article is included in the Coronavirus collection.

Corresponding author: José de la Fuente (jose_delafuente@yahoo.com)

Author roles: de la Fuente J: Conceptualization, Data Curation, Funding Acquisition, Investigation, Methodology, Project Administration, Supervision, Visualization, Writing – Original Draft Preparation, Writing – Review & Editing; **Urra JM**: Data Curation, Investigation, Resources, Writing – Review & Editing; **Contreras M**: Investigation, Methodology, Writing – Review & Editing; **Pacheco I**: Investigation, Methodology, Writing – Review & Editing; **Ferreras-Colino E**: Investigation, Methodology, Writing – Review & Editing; **Doncel-Pérez E**: Investigation, Methodology, Resources, Writing – Review & Editing; **Fernández de Mera IG**: Funding Acquisition, Investigation, Methodology, Resources, Writing – Review & Editing; **Villar M**: Conceptualization, Funding Acquisition, Investigation, Methodology, Project Administration, Resources, Writing – Review & Editing; **Cabrera CM**: Investigation, Methodology, Resources; **Gómez Hernando C**: Methodology, Resources; **Vargas Baquero E**: Methodology, Resources; **Blanco García J**: Methodology, Resources; **Rodríguez Gómez J**: Methodology, Resources; **Velayos Galán A**: Methodology, Resources; **Feo Brito F**: Conceptualization, Investigation, Methodology, Writing – Review & Editing; **Gómez Torrijos E**: Investigation, Methodology, Resources, Writing – Review & Editing; **Cabezas-Cruz A**: Conceptualization, Investigation, Methodology, Writing – Review & Editing; **Gortázar C**: Conceptualization, Funding Acquisition, Investigation, Methodology, Project Administration, Resources, Writing – Review & Editing

Competing interests: No competing interests were disclosed.

Grant information: This work was partially supported by the Consejería de Educación, Cultura y Deportes, JCCM, Spain, project CCM17-PIC-036 (SBPLY/17/180501/000185).
The funders had no role in study design, data collection and analysis, decision to publish, or preparation of the manuscript.

How to cite this article: de la Fuente J, Urra JM, Contreras M *et al.* **A dataset for the analysis of antibody response to glycan alpha-Gal in individuals with immune-mediated disorders [version 1; peer review: 1 approved]** F1000Research 2020, **9**:1366 https://doi.org/10.12688/f1000research.27495.1

First published: 24 Nov 2020, **9**:1366 https://doi.org/10.12688/f1000research.27495.1

F1000Research 2020, 9:1366 Last updated: 11 DEC 2020

Introduction

The gene coding for α-1,3-galactosyltransferase (*α1,3GT*) was inactivated in old-world monkeys, an evolutionary adaptation that resulted in the production of high antibody titers against glycan Galα1-3Galβ1-(3)4GlcNAc-R (α-Gal) (Galili, 2015). Previous results showed that up to 1–5% of the circulating IgM/IgG found in healthy individuals are directed against α-Gal (Macher & Galili, 2008). Bacteria in the human gut microbiome express *α1,3GT* genes to produce α-Gal epitopes (Montassier *et al*., 2020), suggesting that natural anti-α-Gal antibodies are produced in response to gut microbiota (Bello-Gil *et al*., 2019; Galili *et al*., 1988; Mañez *et al*., 2001; Yilmaz *et al*., 2014). This evolutionary adaptation has been associated with the protective response of anti-α-Gal IgM/IgG antibodies against pathogens containing this modification on membrane proteins (Galili, 2018; Hodžić *et al*., 2020). In contrast, the presence of α-Gal in tick salivary glycoproteins and glycolipids (Araujo *et al*., 2016; Cabezas-Cruz *et al*., 2018; Chinuki *et al*., 2016; Crispell *et al*., 2019) and tick cement (Villar *et al*., 2020) induces anti-α-Gal IgE antibodies that mediate delayed anaphylaxis to mammalian meat consumption and immediate anaphylaxis to tick bites, xenotransplantation and certain drugs such as cetuximab (Cabezas-Cruz *et al*., 2019; Commins *et al*., 2009; Contreras *et al*., 2020; de la Fuente *et al*., 2019a; de la Fuente *et al*., 2020; Fischer *et al*., 2016; Levin *et al*., 2019; Mateos-Hernández *et al*., 2017; Platts-Mills *et al*., 2020; Steinke *et al*., 2015; van Nunen *et al*., 2007).

Factors that may affect the antibody response to α-Gal include but are not limited to age, repeat consumption of certain food and meats of different origin or innards with higher α-Gal content, exposure to tick bites, ABO blood group, co-occurring disorders and exposure to cats and other pets (Cabezas-Cruz *et al*., 2017; Cabezas-Cruz *et al*., 2019; Commins, 2016; Commins *et al*., 2014; de la Fuente *et al*., 2020a; Fischer *et al*., 2014; Fischer *et al*., 2016; Morisset *et al*., 2012; Platts-Mills *et al*., 2020; Wölbing *et al*., 2013). Additionally, the anti-α-Gal-specific IgE response has been associated with other diseases such as atopy, coronary artery disease and atherosclerosis (Gonzalez-Quintela *et al*., 2014; Wilson *et al*., 2017; Wilson *et al*., 2019). Furthermore, α-Gal-mediated innate and adaptive immune response mechanisms have been associated with protection against pathogen infection in various animal models (Hodžić *et al*., 2020). However, little is known about the influence of anti-α-Gal immune response on immune-mediated disorders such as those occurring in patients with COVID-19 and Guillain-Barré syndrome (GBS).

These results raise questions and hypothesis regarding the role of α-Gal-mediated immune responses in disease symptomatology and possible protective mechanisms (de la Fuente *et al*., 2019b; de la Fuente *et al*., 2020b; Pacheco *et al*., 2020; Urra *et al*., 2020). Consequently, to advance in addressing these questions and hypothesis, here we provide data on the IgE/IgM/IgG/IgA anti-α-Gal antibody response in healthy individuals and patients diagnosed with AGS, tick-borne allergies, GBS and COVID-19. These data contribute to correlative analyses of the anti-α-Gal antibody response with factors such as patient and clinical characteristics, record of tick bites, blood group, age and sex. These analyses could provide insights into the role of anti-α-Gal antibody response in disease symptomatology and protection against immune-mediated disorders.

Materials and methods

Essential methods used for the generation of the dataset (de la Fuente *et al*., 2020) were described in Urra *et al*. (2020) with additional information in Pacheco *et al*. (2020) and Doncel-Pérez *et al*. (2020).

Patients and healthy individuals

A retrospective case-control study was conducted in patients suffering from COVID-19 admitted to the University General Hospital of Ciudad Real (HGUCR), Spain from March 1 to April 15, 2020. The infection by SARS-CoV-2 was confirmed in all patients included in the study by the real-time reverse transcriptase-polymerase chain reaction (RT-PCR) assay from Abbott Laboratories (Abbott RealTime SARS-COV-2 assay, Abbott Park, Illinois, USA) from upper respiratory tract samples after hospital admission. Clinical features, as well as laboratory determinations were obtained from patient's medical records. The patients were grouped as hospital discharge, hospitalized and intensive care unit (Urra *et al*., 2020). Patients were hospitalized for developing a moderate-severe clinical condition with radiologically demonstrated pneumonia and failure in blood oxygen saturation. Patients with acute respiratory failure who needed mechanical ventilation support were admitted to a hospital ICU. The patients were discharged from the hospital due to the clinical and radiological improvement of pneumonia caused by the SARS-CoV-2, along with the normalization of analytical parameters indicative of inflammation, such as C-reactive protein (CRP), D-Dimer and blood cell count (Urra *et al*., 2020). Samples from asymptomatic COVID-19 cases with positive anti-SARS-CoV-2 IgG antibody titers but negative by RT-PCR were collected in May 22–29, 2020 and included in the dataset (Urra *et al*., 2020). Samples from healthy individuals (individuals without record of tick bites and allergic reactions) and patients diagnosed with tick-borne allergic reactions (AGS, anaphylaxis or urticaria) were collected prior to COVID-19 pandemic in April 2019 (Pacheco *et al*., 2020). The use of human peripheral blood serum samples from healthy individuals and patients diagnosed with tick-borne allergic reactions was done with their written informed consent in compliance with the Helsinki Declaration. Nursing personnel at the General University Hospital of Ciudad Real, Spain, extracted blood samples. Samples and data from patients with GBS included in this dataset were provided by the BioB-HVS, integrated into the Spanish National Biobanks Network. All samples were processed following standard operating procedures with the appropriate approval of the Ethical and Scientific Committees (Toledo Hospitable Complex 29012014-No17, University Hospital of Ciudad Real C-352 and SESCAM C-73).

Preparation of serum samples

For the preparation of serum samples, a sterile tube without anticoagulant was used to collect blood samples. The blood from each patient and the healthy individual was maintained in standing position at room temperature (RT) for clotting (20–30 min) and centrifuged at 1,500 × g for 20 min at RT.

F1000Research 2020, 9:1366 Last updated: 11 DEC 2020

Serum was collected and conserved at -20°C until used for analysis.

Determination of antibody titers against α-Gal

For ELISA, high absorption capacity polystyrene microtiter plates were coated with 50 ng of BSA coated with α-Gal (BSA-α-Gal, thereafter named α-Gal; Dextra, Shinfield, UK) per well in carbonate-bicarbonate buffer (Sigma-Aldrich, St. Louis, MO, USA). After an overnight incubation at 4°C, coated plates were washed one time with 100 µl/well PBS with 0.05% Tween 20 (PBST) (Sigma-Aldrich), blocked with 100 µl/well of 1% human serum albumin (HAS) in PBST (Sigma-Aldrich) for 1 h at RT and then washed four times with 100 µl/well of PBST. Human serum samples were diluted 1:100 in PBST with 1% HAS and 100 µl/well were added into the wells of the antigen-coated plates and incubated for 1 h at 37°C. Plates were washed four times with PBST and 100 µl/well of goat anti-human immunoglobulins-peroxidase IgG (FC specific) (Cat. No. I2136), IgM (µ-chain specific) (Cat. No. I1636), and IgE (ε-chain specific) (Cat. No. I6284) secondary antibodies (Sigma-Aldrich) diluted 1:1000, v/v in blocking solution were added and incubated for 1 h at RT. Plates were washed four times with 100 µl/well of PBST and 100 µl/well of 3,3´,5,5-tetramethylbenzidine TMB (Promega, Madison, WI, USA) were added and incubated for 20 min at RT. Finally, the reaction was stopped with 50 µl/well of 2 N H_2SO_4 and the O.D. was measured in a spectrophotometer at 450 nm. The average of two technical replicates per sample was used for analysis after background (coated wells incubated with PBS and secondary antibodies) subtraction.

Statistical analysis

Anti-α-Gal IgE, IgM and IgG antibody titers (O.D. at 450 nm values) were compared for each Ig by one-way ANOVA test ($p < 0.05$) (https://www.socscistatistics.com/tests/anova/default2.aspx) (Figure 1A and 1C). A Spearman Rho correlation analysis ($p < 0.01$; https://www.socscistatistics.com/tests/spearman/default2.aspx) was conducted between anti-α-Gal IgE, IgM and IgG antibody titers and age (Figure 1B).

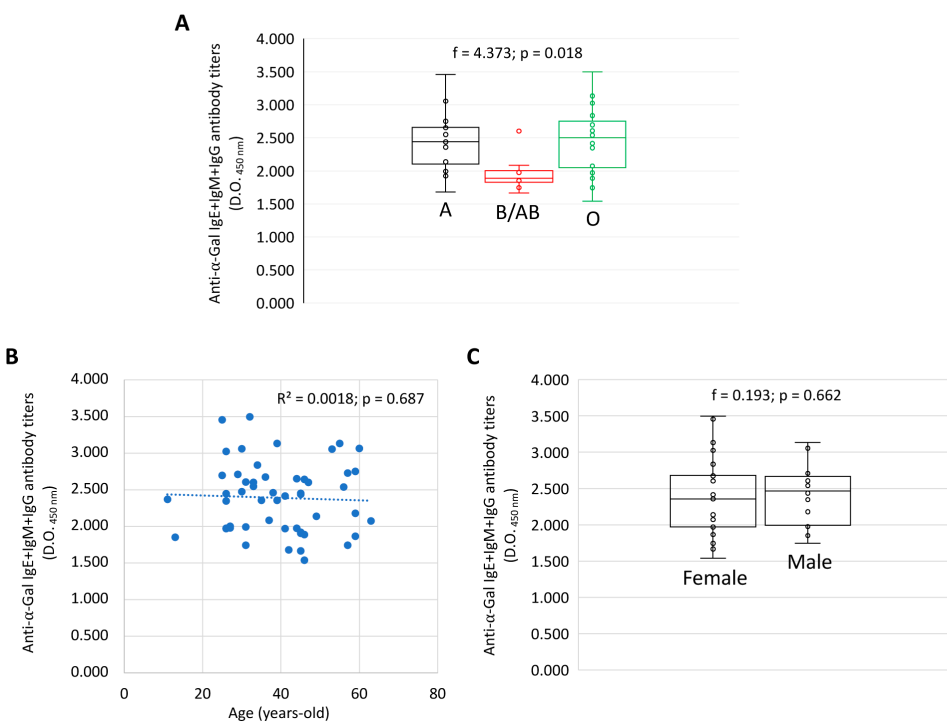

Figure 1. An example of the effect of certain factors such as (**A**) blood group, (**B**) age and (**C**) sex on the antibody response to α-Gal in healthy individuals. Anti-α-Gal IgE, IgM and IgG antibody titers were determined by ELISA. (**A, C**) The ELISA O.D. at 450 nm values were compared for each Ig by one-way ANOVA test ($p < 0.05$). (**B**) A Spearman Rho correlation analysis ($p < 0.01$) was conducted between anti-α-Gal IgE, IgM and IgG antibody titers and age. Correlation coefficient (R^2) is shown.

Dataset validation

The dataset (de la Fuente *et al*., 2020) was validated in studies reported by Urra *et al*. (2020), Pacheco *et al*. (2020) and Doncel-Pérez *et al*. (2020). Additionally, a comparative analysis was conducted between the IgE+IgM+IgG antibody response to α-Gal and blood groups (Figure 1A), age (Figure 1B) and sex (Figure 1C) in healthy individuals (n = 75) to illustrate lower antibody titers in blood group B/AB individuals as previously reported (Cabezas-Cruz *et al*., 2017) but no differences regarding age and sex, which have been reported before as factors affecting the antibody response to α-Gal, infection and vaccination (Buonomano *et al*., 1999; Giefing-Kröll *et al*., 2015; Wang *et al*., 1995).

The main limitation of the dataset is sample size for some factors (i.e. age, sex or blood group), which were not disclosed by all individuals, and anti-α-Gal IgA antibody titers that could be considered in the analysis (Mateos-Hernández *et al*., 2020; Urra *et al*., 2020).

Data availability

Underlying data

Harvard Dataverse: A dataset for the analysis of antibody response to glycan alpha-Gal in individuals with immune-mediated disorders. https://doi.org/10.7910/DVN/RBU2VR (de la Fuente *et al*., 2020).

This dataset contains characteristics and serum antibody levels of the individuals included in the study and was used in analyses reported in publications by Urra *et al*. (2020), Pacheco *et al*. (2020) and Doncel-Pérez *et al*. (2020).

Acknowledgments

We want to particularly acknowledge the patients, healthy volunteers and the Guillain-Barré Syndrome Collection (TOSGB) from BioB-HVS integrated into the Spanish National Biobanks Network for their collaboration in this study. We thank members of our laboratories for fruitful discussions and Almudena González García (IREC, Spain) for technical assistance. We acknowledge UCLM, Spain support to Group SaBio.

References

Araujo RN, Franco PF, Rodrigues H, *et al.*: ***Amblyomma sculptum* tick saliva: α-Gal identification, antibody response and possible association with red meat allergy in Brazil.** *Int J Parasitol.* 2016; **46**(3): 213–220.
PubMed Abstract | Publisher Full Text | Free Full Text

Bello-Gil D, Audebert C, Olivera-Ardid S, *et al.*: **The Formation of Glycan-Specific Natural Antibodies Repertoire in GalT-KO Mice Is Determined by Gut Microbiota.** *Front Immunol.* 2019; **10**: 342.
PubMed Abstract | Publisher Full Text | Free Full Text

Buonomano R, Tinguely C, Rieben R, *et al.*: **Quantitation and characterization of anti-Galalpha1-3Gal antibodies in sera of 200 healthy persons.** *Xenotransplantation.* 1999; **6**(3): 173–180.
PubMed Abstract | Publisher Full Text

Cabezas-Cruz A, Mateos-Hernández L, Alberdi P, *et al.*: **Effect of blood type on anti-α-Gal immunity and the incidence of infectious diseases.** *Exp Mol Med.* 2017; **49**(3): e301.
PubMed Abstract | Publisher Full Text | Free Full Text

Cabezas-Cruz A, Espinosa PJ, Alberdi P, *et al.*: **Tick galactosyltransferases are involved in α-Gal synthesis and play a role during *Anaplasma phagocytophilum* infection and *Ixodes scapularis* tick vector development.** *Sci Rep.* 2018; **8**(1): 14224.
PubMed Abstract | Publisher Full Text | Free Full Text

Cabezas-Cruz A, Hodžić A, Román-Carrasco P, *et al.*: **Environmental and Molecular Drivers of the α-Gal Syndrome.** *Front Immunol.* 2019; **10**: 1210.
PubMed Abstract | Publisher Full Text | Free Full Text

Chinuki Y, Ishiwata K, Yamaji K, *et al.*: ***Haemaphysalis longicornis* tick bites are a possible cause of red meat allergy in Japan.** *Allergy.* 2016; **71**(3): 421–425.
PubMed Abstract | Publisher Full Text

Commins SP: **Invited Commentary: Alpha-Gal Allergy: Tip of the Iceberg to a Pivotal Immune Response.** *Curr Allergy Asthma Rep.* 2016; **16**(9): 61.
PubMed Abstract | Publisher Full Text

Commins SP, Satinover SM, Hosen J, *et al.*: **Delayed anaphylaxis, angioedema, or urticaria after consumption of red meat in patients with IgE antibodies specific for galactose-alpha-1,3-galactose.** *J Allergy Clin Immunol.* 2009; **123**(2): 426–433.
PubMed Abstract | Publisher Full Text | Free Full Text

Commins SP, James HR, Stevens W, *et al.*: **Delayed clinical and *ex vivo* response to mammalian meat in patients with IgE to galactose-alpha-1,3-galactose.** *J Allergy Clin Immunol.* 2014; **134**(1): 108–115.
PubMed Abstract | Publisher Full Text | Free Full Text

Contreras M, Pacheco I, Alberdi P, *et al.*: **Allergic Reactions and Immunity in Response to Tick Salivary Biogenic Substances and Red Meat Consumption in the Zebrafish Model.** *Front Cell Infect Microbiol.* 2020; **10**: 78.
PubMed Abstract | Publisher Full Text | Free Full Text

Crispell G, Commins SP, Archer-Hartman SA, *et al.*: **Discovery of Alpha-Gal-Containing Antigens in North American Tick Species Believed to Induce Red Meat Allergy.** *Front Immunol.* 2019; **10**: 1056.
PubMed Abstract | Publisher Full Text | Free Full Text

de la Fuente J, Pacheco I, Villar M, *et al.*: **The alpha-Gal syndrome: new insights into the tick-host conflict and cooperation.** *Parasit Vectors.* 2019a; **12**(1): 154.
PubMed Abstract | Publisher Full Text | Free Full Text

de la Fuente J, Pacheco I, Contreras M, *et al.*: **Guillain-Barré and Alpha-Gal syndromes: Saccharides-induced immune responses.** *Explor Res Hypothesis Med.* 2019b; **4**(4): 87–89.
Publisher Full Text

de la Fuente J, Urra JM, Contreras M, *et al.*: **A dataset for the analysis of antibody response to glycan alpha-Gal in individuals with immune-mediated disorders**. Harvard Dataverse, V1. 2020.
http://www.doi.org/10.7910/DVN/RBU2VR

de la Fuente J, Cabezas-Cruz A, Pacheco I: **Alpha-gal syndrome: challenges to understanding sensitization and clinical reactions to alpha-gal.** *Expert Rev Mol Diagn.* 2020a; **20**(9): 905–911.
PubMed Abstract | Publisher Full Text

de la Fuente J, Gortázar C, Cabezas-Cruz A, *et al.*: **Boosting anti-alpha-Gal immune response to control COVID-19.** *Royal Society Open Science Stage1 Registered Report, date of in-principle acceptance.* 2020b.
http://www.doi.org/10.17605/OSF.IO/XHDPU

Doncel-Pérez E, Contreras M, Gómez Hernando C, *et al.*: **What is the impact of the antibody response to glycan alpha-Gal in Guillain-Barré syndrome associated with SARS-CoV-2 infection?** *Merit Research Journal of Medicine and Medical Sciences (MRJMMS).* submitted. 2020.

Fischer J, Hebsaker J, Caponetto P, *et al.*: **Galactose-alpha-1,3-galactose**

sensitization is a prerequisite for pork-kidney allergy and cofactor-related mammalian meat anaphylaxis. *J Allergy Clin Immunol.* 2014; **134**(3): 755–759e1.
PubMed Abstract | Publisher Full Text

Fischer J, Yazdi AS, Biedermann T: **Clinical spectrum of α-Gal syndrome: from immediate-type to delayed immediate-type reactions to mammalian innards and meat.** *Allergo J Int.* 2016; **25**: 55–62.
PubMed Abstract | Publisher Full Text | Free Full Text

Galili U: **Significance of the evolutionary α1,3-galactosyltransferase (*GGTA1*) gene inactivation in preventing extinction of apes and old world monkeys.** *J Mol Evol.* 2015; **80**(1): 1–9.
PubMed Abstract | Publisher Full Text

Galili U: **Evolution in primates by "Catastrophic-selection" interplay between enveloped virus epidemics, mutated genes of enzymes synthesizing carbohydrate antigens, and natural anti-carbohydrate antibodies.** *Am J Phys Anthropol.* 2018; **168**(2): 352–363.
PubMed Abstract | Publisher Full Text

Galili U, Mandrell RE, Hamadeh RM, *et al.*: **Interaction between human natural anti-alpha-galactosyl immunoglobulin G and bacteria of the human flora.** *Infect Immun.* 1988; **56**(7): 1730–1737.
PubMed Abstract | Publisher Full Text | Free Full Text

Gonzalez-Quintela A, Dam Laursen AS, Vidal C, *et al.*: **IgE antibodies to alpha-gal in the general adult population: relationship with tick bites, atopy, and cat ownership.** *Clin Exp Allergy.* 2014; **44**(8): 1061–1068.
PubMed Abstract | Publisher Full Text

Giefing-Kröll C, Berger P, Lepperdinger G, *et al.*: **How sex and age affect immune responses, susceptibility to infections, and response to vaccination.** *Aging Cell.* 2015; **14**(3): 309–321.
PubMed Abstract | Publisher Full Text | Free Full Text

Hodžić A, Mateos-Hernández L, de la Fuente J, *et al.*: **α-Gal-Based Vaccines: Advances, Opportunities, and Perspectives.** *Trends Parasitol.* 2020; **36**(12): 992–1001.
PubMed Abstract | Publisher Full Text

Levin M, Apostolovic D, Biedermann T, *et al.*: **Galactose α-1,3-galactose phenotypes: Lessons from various patient populations.** *Ann Allergy Asthma Immunol.* 2019; **122**(6): 598–602.
PubMed Abstract | Publisher Full Text | Free Full Text

Macher BA, Galili U: **The Galalpha1,3Galbeta1,4GlcNAc-R (alpha-Gal) epitope: a carbohydrate of unique evolution and clinical relevance.** *Biochim Biophys Acta.* 2008; **1780**(2): 75–88.
PubMed Abstract | Publisher Full Text | Free Full Text

Mañez R, Blanco FJ, Díaz I, *et al.*: **Removal of bowel aerobic gram-negative bacteria is more effective than immunosuppression with cyclophosphamide and steroids to decrease natural alpha-galactosyl IgG antibodies.** *Xenotransplantation.* 2001; **8**(1): 15–23.
PubMed Abstract | Publisher Full Text

Mateos-Hernández L, Villar M, Moral A, *et al.*: **Tick-host conflict: immunoglobulin E antibodies to tick proteins in patients with anaphylaxis to tick bite.** *Oncotarget.* 2017; **8**(13): 20630–20644.
PubMed Abstract | Publisher Full Text | Free Full Text

Mateos-Hernández L, Risco-Castillo V, Torres-Maravilla E, *et al.*: **Gut Microbiota Abrogates Anti-α-Gal IgA Response in Lungs and Protects against Experimental *Aspergillus* Infection in Poultry.** *Vaccines (Basel).* 2020; **8**(2): 285.
PubMed Abstract | Publisher Full Text | Free Full Text

Montassier E, Al-Ghalith GA, Mathé C, *et al.*: **Distribution of Bacterial α1,3-Galactosyltransferase Genes in the Human Gut Microbiome.** *Front Immunol.* 2020; **10**: 3000.
PubMed Abstract | Publisher Full Text | Free Full Text

Morisset M, Richard C, Astier C, *et al.*: **Anaphylaxis to pork kidney is related to IgE antibodies specific for galactose-alpha-1,3-galactose.** *Allergy.* 2012; **67**(5): 699–704.
PubMed Abstract | Publisher Full Text

Pacheco I, Fernández de Mera IG, Feo Brito F, *et al.*: **Characterization of the anti-α-Gal antibody profile in association with Guillain-Barré syndrome, implications for tick-related allergic reactions.**. Ticks and Tick-Borne Diseases, submitted. 2020.

Platts-Mills TAE, Commins SP, Biedermann T, *et al.*: **On the cause and consequences of IgE to galactose-α-1,3-galactose: A report from the National Institute of Allergy and Infectious Diseases Workshop on Understanding IgE-Mediated Mammalian Meat Allergy.** *J Allergy Clin Immunol.* 2020; **145**(4): 1061–1071.
PubMed Abstract | Publisher Full Text | Free Full Text

Steinke JW, Platts-Mills TAE, Commins SP: **The alpha-gal story: lessons learned from connecting the dots.** *J Allergy Clin Immunol.* 2015; **135**(3): 589–596; quiz 597.
PubMed Abstract | Publisher Full Text | Free Full Text

Urra JM, Ferreras-Colino E, Contreras M, *et al.*: **The antibody response to the glycan α-Gal correlates with COVID-19 disease symptoms.** *J Med Virol.* 2020.
PubMed Abstract | Publisher Full Text | Free Full Text

van Nunen S, O'Connor KS, Clarke LR, *et al.*: **The association between Ixodes holocyclus tick bite reactions and red meat allergy.** *Intern Med J.* 2007; **39**: A132.
Reference Source

Villar M, Pacheco I, Merino O, *et al.*: **Tick and Host Derived Compounds Detected in the Cement Complex Substance.** *Biomolecules.* 2020; **10**(4): 555.
PubMed Abstract | Publisher Full Text | Free Full Text

Wang L, Anaraki F, Henion TR, *et al.*: **Variations in activity of the human natural anti-Gal antibody in young and elderly populations.** *J Gerontol A Biol Sci Med Sci.* 1995; **50**(4): M227–M233.
PubMed Abstract | Publisher Full Text

Wilson JM, Schuyler AJ, Schroeder N, *et al.*: **Galactose-α-1,3-Galactose: Atypical Food Allergen or Model IgE Hypersensitivity?** *Curr Allergy Asthma Rep.* 2017; **17**(1): 8.
PubMed Abstract | Publisher Full Text | Free Full Text

Wilson JM, McNamara CA, Platts-Mills TAE: **IgE, α-Gal and atherosclerosis.** *Aging (Albany NY).* 2019; **11**(7): 1900–1902.
PubMed Abstract | Publisher Full Text | Free Full Text

Wölbing F, Fischer J, Koberle M, *et al.*: **About the role and underlying mechanisms of cofactors in anaphylaxis.** *Allergy.* 2013; **68**(9): 1085–1092.
PubMed Abstract | Publisher Full Text

Yilmaz B, Portugal S, Tran TM, *et al.*: **Gut microbiota elicits a protective immune response against malaria transmission.** *Cell.* 2014; **159**(6): 1277–1289.
PubMed Abstract | Publisher Full Text | Free Full Text

Supplementary material. Chapter 2b

Supplementary material not included from de la Fuente, J., Urra, J.M., Contreras, M., **Pacheco, I.,** Ferreras-Colino, E., Doncel-Pérez, E., Fernández de Mera, I.G., Villar, M., Cabrera, C.M., Gómez Hernando, C., Vargas Baquero, E., Blanco García, J., Rodríguez Gómez, J., Velayos Galán, A., Feo Brito, F., Gómez Torrijos, E., Cabezas-Cruz, A., Gortázar, C. (2021). A dataset for the analysis of antibody response to glycan alpha-Gal in individuals with immune-mediated disorders. F1000Research 9,1366.

https://f1000research.com/articles/9-1366/v2

- Data. Characteristics and serum antibody levels of the individuals included in the study.

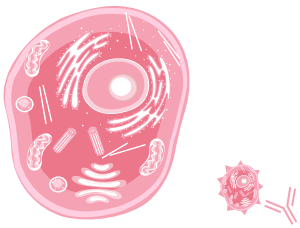

Chapter 2c. Characterization of the anti-alpha-Gal antibody profile in association with Guillain-Barré syndrome, implications for tick-related allergic reactions

Pacheco, I., Fernández de Mera, I.G., Feo Brito, F., Gómez Torrijos, E., Villar, M., Contreras, M., Lima-Barbero, J.F., Doncel-Pérez, E., Cabezas-Cruz, A., Gortázar, C., de la Fuente, J. (2021). Characterization of the anti-alpha-Gal antibody profile in association with Guillain-Barré syndrome, implications for tick-related allergic reactions. Ticks and Tick-Borne Diseases 12, 101651. https://doi.org/10.1016/j.ttbdis.2021.101651

Ticks and Tick-borne Diseases 12 (2021) 101651

Contents lists available at ScienceDirect

Ticks and Tick-borne Diseases

journal homepage: www.elsevier.com/locate/ttbdis

Characterization of the anti-α-Gal antibody profile in association with Guillain-Barré syndrome, implications for tick-related allergic reactions

Iván Pacheco [a], Isabel G. Fernández de Mera [a], Francisco Feo Brito [b], Elisa Gómez Torrijos [b], Margarita Villar [a,c], Marinela Contreras [d], José Francisco Lima-Barbero [a], Ernesto Doncel-Pérez [e], Alejandro Cabezas-Cruz [f], Christian Gortázar [a], José de la Fuente [a,g,*]

[a] SaBio, Instituto de Investigación en Recursos Cinegéticos IREC-CSIC-UCLM-JCCM, Ronda de Toledo s/n, 13005, Ciudad Real, Spain
[b] Allergy Section, General University Hospital of Ciudad Real, Calle Obispo Rafael Torija s/n, 13005, Ciudad Real, Spain
[c] Biochemistry Section, Faculty of Science and Chemical Technologies, and Regional Centre for Biomedical Research (CRIB), University of Castilla-La Mancha, 13071, Ciudad Real, Spain
[d] Interdisciplinary Laboratory of Clinical Analysis, Interlab-UMU, Regional Campus of International Excellence Campus Mare Nostrum, University of Murcia, Espinardo, 30100, Murcia, Spain
[e] Laboratorio de Química Neuro-Regenerativa, Hospital Nacional de Parapléjicos, Servicio de Salud de Castilla La Mancha (SESCAM), Finca La Peraleda s/n, 45071, Toledo, Spain
[f] UMR BIPAR, INRAE, ANSES, Ecole Nationale Vétérinaire d'Alfort, Université Paris-Est, Maisons-Alfort, 94700, France
[g] Department of Veterinary Pathobiology, Center for Veterinary Health Sciences, Oklahoma State University, Stillwater, OK, 74078, USA

ARTICLE INFO

Keywords:
Tick
Alpha-Gal
Allergy
Guillain-Barré syndrome
Immunology
Antibody
Alpha-Gal syndrome

ABSTRACT

Humans evolved by losing the capacity to synthesize the glycan Galα1-3Galβ1-(3)4GlcNAc-R (α-Gal), which resulted in the capacity to develop a protective response mediated by anti-α-Gal IgM/IgG antibodies against pathogens containing this modification on membrane proteins. As an evolutionary trade-off, humans can develop the alpha-Gal syndrome (AGS), a recently diagnosed disease mainly associated with allergic reactions to mammalian meat consumption. The etiology of the AGS is the exposure to tick bites and the IgE antibody response against α-Gal-containing glycoproteins and glycolipids. The objective of this study was to characterize the anti-α-Gal antibody response in association with the immune-mediated peripheral neuropathy, Guillain-Barré syndrome (GBS), and compare it with different factors known to modulate the antibody response to α-Gal such as exposure to tick bites and development of allergic reactions in response to tick bites. The results showed a significant decrease in the IgM/IgG response to α-Gal in GBS patients when compared to healthy individuals. In contrast, the IgM/IgG levels to α-Gal did not change in patients with allergic reactions to tick bites. The IgE response was not affected in GBS patients, but as expected, the IgE levels significantly increased in individuals exposed to tick bites and patients with tick-associated allergies. These results suggest that the immune pathways of anti-α-Gal IgM/IgG and IgE production are independent. Further studies should consider the susceptibility to allergic reactions to tick bites in GBS patients.

1. Introduction

Inactivation of the α-1,3-galactosyltransferase (α1,3 G T) gene in old world monkeys, apes and humans resulted in an almost unique ability of this group of primates to produce high antibody titres against Galα1-3Galβ1-(3)4GlcNAc-R (α-Gal) (Galili, 2015). Previous results showed that up to 1 %–5 % of the circulating IgM/IgG found in healthy individuals are directed against α-Gal (Macher and Galili, 2008). Bacteria in the human gut microbiome produce α1,3 G T genes (Montassier et al., 2020) and experimental enrichment of gut milieu with *Escherichia coli* O86:B7 with high levels of α-Gal on its surface, elicited an anti-α-Gal IgM/IgG response that protected α1,3 G T-deficient mice against malaria transmission (Yilmaz et al., 2014). These results strongly suggest that natural anti-α-Gal antibodies are produced in response to gut microbiota (Galili et al., 1988; Mañez et al., 2001; Bello-Gil et al., 2019). This evolutionary adaptation has been associated with the protective response of anti-α-Gal IgM/IgG antibodies against pathogens containing this modification on membrane proteins (Galili, 2018; Hodžić et al.,

* Corresponding author at: SaBio, Instituto de Investigación en Recursos Cinegéticos, Ronda de Toledo s/n, 13005 Ciudad Real, Spain.
E-mail address: josedejesus.fuente@uclm.es (J. de la Fuente).

https://doi.org/10.1016/j.ttbdis.2021.101651
Received 24 May 2020; Received in revised form 1 October 2020; Accepted 5 January 2021
Available online 11 January 2021

2020a). In contrast, the presence of α-Gal in tick salivary glycoproteins and glycolipids (Araujo et al., 2016; Chinuki et al., 2016; Cabezas-Cruz et al., 2018; Crispell et al., 2019) and possibly tick cement (Villar et al., 2020), induces anti-α-Gal IgE antibodies that mediate delayed anaphylaxis to mammalian meat consumption and immediate anaphylaxis to tick bites, xenotransplantation and certain drugs such as cetuximab (van Nunen et al., 2007; Commins et al., 2009; Steinke et al., 2015; Fischer et al., 2016; Mateos-Hernández et al., 2017; Cabezas-Cruz et al., 2019; Levin et al., 2019; Platts-Mills et al., 2020; de la Fuente et al., 2019a, 2020; Contreras et al., 2020).

Factors that may affect the antibody response to α-Gal include but are not limited to age, repeat consumption of certain food and meats of different origin or innards with higher α-Gal content, exposure to tick bites, alcohol consumption, exercise, use of non-steroidal anti-inflammatory medications, ABO blood group, co-occurring disorders and exposure to cats and other pets (Commins, 2016; Wölbing et al., 2013; Commins et al., 2014; Fischer et al., 2014; Morisset et al., 2012; Fischer et al., 2016; Cabezas-Cruz et al., 2017, 2019; Platts-Mills et al., 2020; de la Fuente et al., 2020). Additionally, the anti-α-Gal-specific IgE response has been associated with other diseases such as atopy, coronary artery disease and atherosclerosis (Gonzalez-Quintela et al., 2014; Wilson et al., 2017, 2019). However, little is known about the influence of immune-mediated peripheral neuropathies on the antibody response to α-Gal. In this regard, a particularly interesting question is whether immune-mediated disorders such as Guillain-Barré syndrome (GBS) that are associated with deregulation of the response to self-antigens also produce deregulation of the immune response to α-Gal. GBS is an autoimmune disease associated with recent bacterial or viral infection and with the involvement of both cellular and humoral immune responses (Van den Berg et al., 2014; Doncel-Pérez et al., 2016). The objective of this study was to evaluate the anti-α-Gal response in GBS patients. A cohort of patients from the same geographical origin and suffering tick-related allergies was used for comparative purposes. This study is of clinical relevance because factors affecting the levels of anti-α-Gal may influence the risk of patients to develop tick-induced allergies or their susceptibility to infectious diseases.

2. Materials and methods

2.1. Experimental design

The study focused on the characterization of the effect of GBS on the IgE, IgM and IgG antibody response to α-Gal. Tick bites and allergic reactions to tick bites in healthy individuals and cases of AGS, anaphylaxis and urticaria were included for comparative purposes (Table 1). A correlation analysis between the anti-α-Gal-specific IgE antibody response, which has been associated with the AGS, was conducted with respect to the different cases of GBS and allergy-type reactions to tick bites to provide new insights into the immune-mediated mechanisms associated with GBS.

2.2. Patients and healthy individuals

The use of human peripheral blood serum samples from patients and healthy individuals was done with their written informed consent in compliance with the Helsinki Declaration. Nursing personnel at the General University Hospital of Ciudad Real, Spain, extracted blood samples. Samples and data from patients with GBS included in this study were provided by the BioB-HVS, integrated into the Spanish National Biobanks Network. Both groups of samples were processed following standard operating procedures with the appropriate approval of the Ethical and Scientific Committees (Toledo Hospitable Complex 29012014-No17 and SESCAM C-73).

Table 1
Patients and healthy individuals.

Group	Description	Data of individuals*
Factor: GBS (Fig. 1)	Patients diagnosed with GBS and hospitalized	n = 22 51 ± 21 (12–83) years-old F/M = 0.6 Spain
	No record of tick bites and no allergic reaction	n = 37 40 ± 11 (21–60) years-old F/M = 1.5 Spain
Healthy (Figs. 1, 2A and B, A1B, A1C)	No allergic reactions to tick bites or no record of tick bites	n = 75 49 ± 9 (21–60) years-old F/M = 1.2 Spain
Factor: Tick bites (Fig. 2A)	Record of tick bites	n = 52 42 ± 14 (13–74) years-old F/M = 0.6 *A. americanum* *Ixodes scapularis* *Ixodes ricinus* *Rhipicephalus bursa* *Rhipicephalus sanguineus* *Hyalomma lusitanicum* *Hyalomma marginatum* *Dermacentor marginatus* *Rhipicephalus* spp. Unknown Spain, USA, Brazil, Portugal, France, Morocco
	No record of tick bites	n = 37 40 ± 11 (21–60) years-old F/M = 1.5 Spain
Factor: Tick bites and allergy (Fig. 2B)	Record of tick bites and allergic reaction	n = 12 45 ± 16 (26–74) years-old F/M = 0.7 *A. americanum* *Rhipicephalus bursa*, *Rhipicephalus sanguineus* *Rhipicephalus* spp. *Hyalomma marginatum* Unknown Spain, Brazil, France, USA, Morocco
	Record or not of tick bites and no allergic reaction	n = 78 40 ± 12 (13–60) years-old F/M = 0.9 *A. americanum* *Ixodes scapularis* *Ixodes ricinus* *Rhipicephalus bursa* *Hyalomma lusitanicum* *Dermacentor marginatus* *Rhipicephalus* spp. Unknown Spain, USA, Brazil, Portugal
	Record of tick bites and no allergic reaction	n = 41 40 ± 12 (13–57) years-old F/M = 0.6 *A. americanum* *Ixodes scapularis*

(continued on next page)

Table 1 (*continued*)

Group	Description	Data of individuals*
		Ixodes ricinus *Rhipicephalus bursa* *Hyalomma lusitanicum* *Dermacentor marginatus* *Rhipicephalus* spp. Unknown Spain, USA, Brazil, Portugal
AGS (Fig. A1B and A1C)	Patients with diagnosed AGS with history of tick bites, delayed anaphylaxis to mammalian meat consumption and positive anti-α-Gal IgE response (> 6 kU/l)	n = 2 70 ± 6 (65–74) years-old F/M = 1.0 *Amblyomma americanum* USA n = 6 54 ± 16 (26–74) years-old F/M = 1.0
Anaphylaxis (Fig. A1B and A1C)	Patients with immediate anaphylaxis to tick bites	*A. americanum* *Rhipicephalus bursa* *Rhipicephalus* spp. *Hyalomma marginatum* Unknown USA, Spain, Morocco n = 6 35 ± 9 (27–52) years-old F/M = 0.5
Skin local reactions (urticaria) (Fig. A1A-A1C)	Individuals with reported skin local reactions to tick bite	*Rhipicephalus sanguineus* Unknown Spain, Brazil, France

* Data for each group includes number of individuals (n), age (years-old), female to male ratio (FM), tick species and countries where tick bites were recorded.

2.3. Preparation of serum samples

For the preparation of serum samples, a sterile tube without anti-coagulant was used to collect blood samples. The blood from each patient and the healthy individual was maintained in standing position at room temperature (RT) for clotting (20–30 min), and centrifuged at 1,500×*g* for 20 min at RT. Serum was collected and conserved at -20 °C until used for analysis.

2.4. Determination of antibody titers against α-Gal

For ELISA, high absorption capacity polystyrene microtiter plates were coated with 50 ng of BSA coated with α-Gal (BSA-α-Gal, thereafter named α-Gal; Dextra, Shinfield, UK) per well in carbonate-bicarbonate buffer (Sigma-Aldrich, St. Louis, MO, USA). After an overnight incubation at 4 °C, coated plates were washed one time with 100 μL/well PBS with 0.05 % Tween 20 (PBST) (Sigma-Aldrich), blocked with 100 μL/well of 1% human serum albumin (HAS) in PBST (Sigma-Aldrich) for 1 h at RT and then washed 4 times with 100 μL/well of PBST. Human serum samples were diluted 1:50 in PBST with 1% HAS and 100 μL/well were added into the wells of the antigen-coated plates and incubated for 1 h at 37 °C. Plates were washed four times with PBST and 100 μL/well of goat anti-human immunoglobulins-peroxidase IgG (FC specific), IgM (μ-chain specific), and IgE (ε-chain specific) secondary antibodies (Sigma-Aldrich) diluted 1:1000, v/v in blocking solution were added and incubated for 1 h at RT. Plates were washed four times with 100 μL/well of PBST and 100 μL/well of 3,3′5,5-tetramethylbenzidine TMB (Promega, Madison, WI, USA) were added and incubated for 20 min at RT. Finally, the reaction was stopped with 50 μL/well of 2 N H_2SO_4 and the O.D. was measured in a spectrophotometer at 450 nm. The average of two technical replicates per sample was used for analysis after background (coated wells incubated with PBS and secondary antibodies) subtraction. The anti-α-Gal IgE antibody titers were determined in sera from selected individuals (n = 2 from each AGS, anaphylaxis, skin local reaction and no allergic reactions group) using the ImmunoCAP Phadia 250 automated platform (Thermo Fisher Scientific, Uppsala, Sweden) with the commercial ImmunoCap α-Gal bovine Thyroglobulin kit according to the manufacturer's instructions (Mateos-Hernández et al., 2017). These values were used to draw a trendline (R^2 = 0.83) to calculate the corresponding kU/l values for the ELISA O.D. at 450 nm values using the formula IgE titers (kU/l) = EXP ((O.D.450 nm – 2.9)/0.2). Positive anti-α-Gal IgE levels were considered at cut-off value of 0.35 kU/l (Platts-Mills et al., 2020). The ELISA O.D. at 450 nm values were compared between different groups by pairwise comparisons using the nonparametric Mann-Whitney *U* test (p = 0.05, https://www.socscistatistics.com/tests/mannwhitney/default2.aspx). A Spearman Rho (rs) correlation analysis (p = 0.01; https://www.socscistatistics.com/tests/spearman/default2.aspx) was conducted between anti-α-Gal IgE antibody titers and allergy-type reactions.

3. Results and discussion

3.1. Differential regulation of the antibody response to α-Gal in individuals with GBS or tick allergies associated with α-Gal

A new factor that may affect the antibody response to α-Gal was considered in this study. In patients with GBS we found that the anti-α-Gal IgM and IgG antibody levels were significantly lower (p ≤ 0.01) than in healthy control individuals (Fig. 1). These results suggested that the reduction in anti-α-Gal IgM and IgG antibody levels may increase the susceptibility to infectious diseases or contribute to the neuropathy in GBS patients. Considering the recognized pathogen-mediated ethology of GBS (Townson et al., 2007; Van den Berg et al., 2014), it would be interesting to test whether pre-existing low levels of anti-gal antibodies predispose to infection by pathogens triggering autoimmunity associated with anti-GM1 antibodies and GBS. It has been proposed that the GBS may be associated with infection by bacterial or viral pathogens such as *Campylobacter jejuni*, *Haemophilus* bacteria, cytomegalovirus (CMV), hepatitis C virus (HCV), human immunodeficiency virus (HIV) Zika virus (Rosinska et al., 2012; Van den Berg et al., 2014; Nugent et al., 2017; de la Fuente et al., 2019b), and recently SARS-CoV-2 (Zhao et al., 2020; Toscano et al., 2020). Although still controversial (Koga et al., 2005), *Haemophilus influenzae*, a bacterium expressing α1,3 G T-coding genes (Bello-Gil et al., 2019) and recognized by galactose-specific agglutinins from *Ricinus communis* (Kalograiaki et al., 2018), is considered a causative agent of GBS (Mori et al., 2000; Ju et al., 2004). Furthermore, as recently suggested for SARS-CoV-2, enveloped viruses carrying blood type B antigen or virus-like particles (VLPs) with α-Gal modifications can be targeted by anti-α-Gal IgM and IgG (Breiman et al., 2020; Galili, 2020; Chen, 2020; Urra et al., 2020; Bogani et al., 2020). Based on the proposed protective mechanisms in response to α-Gal in the zebrafish animal model (Pacheco et al., 2020), it may be also considered that pathogen infection reduces anti-α-Gal antibody levels through interference with B-cell maturation while anti-GM1 antibodies mediate demyelination and nerve conduction failure. Additionally, it may be possible that targeting of the macrophage FcR by anti-GM1 antibodies may decreases FcR-mediated phagocytosis and macrophage response to facilitate pathogen infection. Another mechanism by which pathogen infection may decrease the levels of anti-α-Gal IgM and IgG is by inducing a dysbiosis in which the abundance of α-Gal-producing bacteria is reduced. Removal of aerobic gram-negative bacteria is more effective than immunosuppression to decrease natural alpha-galactosyl IgG antibodies (Mañez et al., 2001). Microbiota composition influences infection by *C. jejuni*, the major pathogen associated with GBS, and also gut colonization by the pathogen is associated with dysbiosis in different animal models and humans (Indikova et al., 2015; O'Loughlin et al., 2015; Kampmann et al., 2016). If proven right, these results

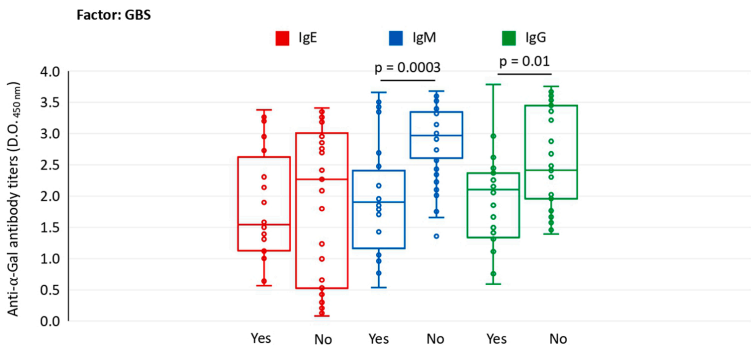

Fig. 1. Effect of GBS on the antibody response to α-Gal. Anti-α-Gal IgE, IgM and IgG antibody titers were determined by ELISA in patients with GBS and healthy individuals (Table 1). The ELISA O.D. at 450 nm values were compared between different groups by pairwise comparisons using the nonparametric Mann-Whitney *U* test ($p < 0.05$). Only significant differences ($p < 0.05$) are shown.

suggest the possibility of boosting the antibody response to α-Gal to prevent infections that may lead to GBS.

In contrast to GBS, the IgM and IgG antibody levels against α-Gal were not affected by tick bites or allergy factors (Fig. 2A and B). In contrast to humans, tick bites increase anti-α-Gal IgM levels but do not affect anti-α-Gal IgE levels in dogs, an animal that produces α-Gal as a self-antigen (Hodžić et al., 2019). These findings suggest that the production of anti-α-Gal IgE autoantibodies is tightly regulated, a hypothesis supported by growing evidence showing that IgE plays an important role in autoimmunity (Sanjuan et al., 2016).

The antibody response to α-Gal has been used to study the AGS but different factors may affect the anti-α-Gal IgE, IgM and IgG antibody levels (Commins, 2016; Wölbing et al., 2013; Commins et al., 2014; Fischer et al., 2014; Morisset et al., 2012; Fischer et al., 2016; Cabezas-Cruz et al., 2017, 2019; Platts-Mills et al., 2020; de la Fuente et al., 2020). To further expand the knowledge of the factors affecting the IgE response to α-Gal and potentially the AGS, we studied the IgE response in GBS. Patients exposed to factors unequivocally known to increase the IgE response (i.e. exposure to tick bites, development of allergic reactions in response to tick bites) were used as controls. As previously reported (recently reviewed by de la Fuente et al., 2020), the results showed a significant increase ($p < 0.05$) in anti-α-Gal IgE antibody levels in response to tick bites (1.3-fold) and allergic reactions to tick bites (1.4−1.5-fold) (Fig. 2A and B). These results support the use of the anti-α-Gal-specific IgE response for the diagnosis of the AGS in patients with an appropriate clinical history (Platts-Mills et al., 2020). Symptomatic individuals included in the study showed different allergic reactions in response to tick bites (Table 1). Allergy-type reactions were rated from severe AGS and anaphylaxis to mild skin local reactions or urticaria to no reactions (Table 1). Patients with anaphylactic reactions to tick bite had different manifestations including generalized itching and erythema, difficult breathing, nausea and somnolence (Mateos-Hernández et al., 2017). Skin reactions to tick bite were manifested as urticaria (Case 1, Fig. A1A) or hives or disseminated rash (Case 2, Fig. A1A). The correlation analysis between anti-α-Gal IgE antibody levels and allergy-type reactions showed a significant positive correlation ($p < 0.0001$) with the severity of allergic manifestations (Fig. A1B). Using the quantitative analysis of anti-α-Gal IgE antibody titers at cut-off value of 0.35 kU/l (Platts-Mills et al., 2020), the results showed that 87.5 % (7/8) of the cases with AGS and anaphylaxis were positive while only 15 % (3/20) of the individuals with urticaria or asymptomatic showed antibody levels higher than 0.35 kU/l (Fig. A1C). In sharp contrast, GBS patients showed no significant changes in the IgE response (Fig. 1). These results are expected considering that switch to IgE is dependent on Th2 associated cytokines (e.g. interleukins IL-4, IL-13) (Aalberse et al., 2009) and that the anti-α-Gal IgE response has been associated to tick bites and parasite infection (Arkestål et al., 2011). In contrast, some parasites were found to inhibits the production of IgE antibodies to α-Gal in humans (Hodžić et al., 2020b). Several biomolecules in tick saliva such as prostaglandin E2 (PGE_2) were proposed to participate in

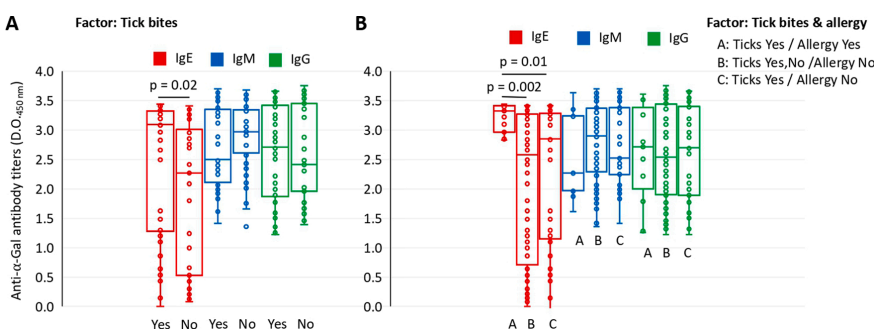

Fig. 2. Effect of different factors on the antibody response to α-Gal. The factors considered in this study included (A) exposure to tick bites (Tick bites) and (B) development of allergic reactions in response to tick bites (Tick bites & allergy) (Table 1). Anti-α-Gal IgE, IgM and IgG antibody titers were determined by ELISA. The ELISA O.D. at 450 nm values were compared between different groups by pairwise comparisons using the nonparametric Mann-Whitney *U* test ($p < 0.05$). Only significant differences ($p < 0.05$) are shown.

inhibition of the Th1 immune response and skew toward Th2 (Cabezas-Cruz et al., 2019).

4. Conclusions

The main conclusions of our study could be summarized as (1) the regulation of anti-α-Gal IgE is not directly linked to that of anti-α-Gal IgM/IgG response, (2) the decrease in the IgM/IgG antibody response to α-Gal observed in GBS patients may reflect gut microbiota dysbiosis associated to infection by pathogens that trigger the neuropathy disorder, and (3) GBS should not be considered as a factor increasing the levels of anti-α-Gal IgE and thus the risk for tick bite-related allergies.

Funding

This work was supported by the Consejería de Educación, Cultura y Deportes, JCCM, Spain, project CCM17-PIC-036 (SBPLY/17/180501/000185). MV was supported by the University of Castilla La Mancha (UCLM, Spain) and the Fondo Europeo de Desarrollo Regional, FEDER, EU. IGFM was supported by the UCLM. MC was funded by the Ministerio de Ciencia, Innovación y Universidades, Spain (grant FJC-2018-038277-I).

CRediT authorship contribution statement

Iván Pacheco: Investigation, Data curation. **Isabel G. Fernández de Mera:** Investigation, Methodology, Data curation. **Francisco Feo Brito:** Investigation, Methodology. **Elisa Gómez Torrijos:** Investigation. **Margarita Villar:** Investigation, Methodology, Project administration, Funding acquisition. **Marinela Contreras:** Investigation. **José Francisco Lima-Barbero:** Investigation. **Ernesto Doncel-Pérez:** Investigation, Data curation. **Alejandro Cabezas-Cruz:** Investigation, Methodology, Writing - review & editing. **Christian Gortázar:** Investigation, Writing - review & editing. **José de la Fuente:** Conceptualization, Methodology, Investigation, Data curation, Supervision, Writing - review & editing, Project administration, Funding acquisition.

Declaration of Competing Interest

No competing interests declared.

Acknowledgments

We want to particularly acknowledge the patients, healthy volunteers and the the Guillain-Barré Syndrome Collection (TOSGB) fromBioB-HVS integrated into the Spanish National Biobanks Network for their collaboration in this study. We thank Almudena González García (IREC, Spain) for technical assistance.

Appendix A. Supplementary data

Supplementary material related to this article can be found, in the online version, at doi:https://doi.org/10.1016/j.ttbdis.2021.101651.

References

Aalberse, R.C., Stapel, S.O., Schuurman, J., Rispens, T., 2009. Immunoglobulin G4: an odd antibody. Clin. Exp. Allergy 39, 469–477. https://doi.org/10.1111/j.1365-2222.2009.03207.x.

Araujo, R.N., Franco, P.F., Rodrigues, H., Santos, L., McKay, C.S., Sanhueza, C.A., Brito, C., Azevedo, M.A., Venuto, A.P., Cowan, P.J., Almeida, I.C., Finn, M.G., Marques, A.F., 2016. *Amblyomma sculptum* tick saliva: α-Gal identification, antibody response and possible association with red meat allergy in Brazil. Int. J. Parasitol. 46, 213–220. https://doi.org/10.1016/j.ijpara.2015.12.005.

Arkestål, K., Sibanda, E., Thors, C., Troye-Blomberg, M., Mduluza, T., Valenta, R., Grönlund, H., van Hage, M., 2011. Impaired allergy diagnostics among parasite-infected patients caused by IgE antibodies to the carbohydrate epitope galactose-α 1,3-galactose. J. Allergy Clin. Immunol. 127, 1024–1028. https://doi.org/10.1016/j.jaci.2011.01.033.

Bello-Gil, D., Audebert, C., Olivera-Ardid, S., Pérez-Cruz, M., Even, G., Khasbiullina, N., Gantois, N., Shilova, N., Merlin, S., Costa, C., Bovin, N., Mañez, R., 2019. The Formation of glycan-specific natural antibodies repertoire in GalT-KO mice is determined by gut microbiota. Front. Immunol. 10, 342. https://doi.org/10.3389/fimmu.2019.00342.

Bogani, G., Raspagliesi, F., Ditto, A., de la Fuente, J., 2020. The adoption of viral capsid-derived virus-like particles (VLPs) for disease prevention and treatments. Vaccines 8, E432. https://doi.org/10.3390/vaccines8030432.

Breiman, A., Ruvën-Clouet, N., Le Pendu, J., 2020. Harnessing the natural anti-glycan immune response to limit the transmission of enveloped viruses such as SARS-CoV-2. PLoS Pathog. 16, e1008556 https://doi.org/10.1371/journal.ppat.1008556.

Cabezas-Cruz, A., Mateos-Hernández, L., Alberdi, P., Villar, M., Riveau, G., Hermann, E., Schacht, A., Khalife, J., Correia-Neves, M., Gortázar, C., de la Fuente, J., 2017. Effect of blood type on anti-α-Gal immunity and the incidence of infectious diseases. Exp. Mol. Med. 49, e301. https://doi.org/10.1038/emm.2016.164.

Cabezas-Cruz, A., Espinosa, P.J., Alberdi, P., Šimo, L., Valdés, J.J., Mateos-Hernández, L., Contreras, M., Rayo, M.V., de la Fuente, J., 2018. Tick galactosyltransferases are involved in α-Gal synthesis and play a role during *Anaplasma phagocytophilum* infection and *Ixodes scapularis* tick vector development. Sci. Rep. 8, 14224. https://doi.org/10.1038/s41598-018-32664-z.

Cabezas-Cruz, A., Hodžić, A., Román-Carrasco, P., Mateos-Hernández, L., Duscher, G.G., Sinha, D.K., Hemmer, W., Swoboda, I., Estrada-Peña, A., de la Fuente, J., 2019. Environmental and molecular drivers of the α-Gal syndrome. Front. Immunol. 10, 1210. https://doi.org/10.3389/fimmu.2019.01210.

Chen, J.M., 2020. SARS-CoV-2 replicating in nonprimate mammalian cells probably have critical advantages for COVID-19 vaccines due to anti-Gal antibodies: a minireview and proposals. J. Med. Virol. https://doi.org/10.1002/jmv.26312.

Chinuki, Y., Ishiwata, K., Yamaji, K., Takahashi, H., Morita, E., 2016. *Haemaphysalis longicornis* tick bites are a possible cause of red meat allergy in Japan. Allergy 71, 421–425. https://doi.org/10.1111/all.12804.

Commins, S.P., 2016. Invited commentary: alpha-Gal allergy: tip of the iceberg to a pivotal immune response. Curr. Allergy Asthma Rep. 16, 61. https://doi.org/10.1007/s11882-016-0641-6.

Commins, S.P., Satinover, S.M., Hosen, J., Mozena, J., Borish, L., Lewis, B.D., Woodfolk, J.A., Platts-Mills, T.A., 2009. Delayed anaphylaxis, angioedema, or urticaria after consumption of red meat in patients with IgE antibodies specific for galactose-alpha-1,3-galactose. J. Allergy Clin. Immunol. 123, 426–433. https://doi.org/10.1016/j.jaci.2008.10.052.

Commins, S.P., James, H.R., Stevens, W., Pochan, S.L., Land, M.H., King, C., Mozzicato, S., Platts-Mills, T.A., 2014. Delayed clinical and ex vivo response to mammalian meat in patients with IgE to galactose-alpha-1,3-galactose. J. Allergy Clin. Immunol. 134, 108–115. https://doi.org/10.1016/j.jaci.2014.01.024.

Contreras, M., Pacheco, I., Alberdi, P., Díaz-Sánchez, S., Artigas-Jerónimo, S., Mateos-Hernández, L., Villar, M., Cabezas-Cruz, A., de la Fuente, J., 2020. Allergic reactions and immunity in response to tick salivary biogenic substances and red meat consumption in the zebrafish model. Front. Cell. Infect. Microbiol. 10, 78. https://doi.org/10.3389/fcimb.2020.00078.

Crispell, G., Commins, S.P., Archer-Hartman, S.A., Choudhary, S., Dharmarajan, G., Azadi, P., Karim, S., 2019. Discovery of alpha-Gal-containing antigens in North American tick species believed to induce red meat allergy. Front. Immunol. 10, 1056. https://doi.org/10.3389/fimmu.2019.01056.

de la Fuente, J., Pacheco, I., Villar, M., Cabezas-Cruz, A., 2019a. The alpha-Gal syndrome: new insights into the tick-host conflict and cooperation. Parasit. Vectors 12, 154. https://doi.org/10.1186/s13071-019-3413-z.

de la Fuente, J., Pacheco, I., Contreras, M., Mateos-Hernández, L., Villar, M., Cabezas-Cruz, A., 2019b. Guillain-Barré and Alpha-Gal syndromes: saccharides-induced immune responses. Explor. Res. Hypothesis Med. 4, 87–89. https://doi.org/10.14218/ERHM.2019.00027.

de la Fuente, J., Cabezas-Cruz, A., Pacheco, I., 2020. Alpha-gal syndrome: challenges to understanding sensitization and clinical reactions to alpha-gal. Expert Rev. Mol. Diagn. Jul 14, 1–7. https://doi.org/10.1080/14737159.2020.1792781.

Doncel-Pérez, E., Mateos-Hernández, L., Pareja, E., García-Forcada, Á., Villar, M., Tobes, R., Romero Ganuza, F., Vila Del Sol, V., Ramos, R., Fernández de Mera, I.G., de la Fuente, J., 2016. Expression of Early Growth Response Gene-2 and regulated cytokines correlates with recovery from Guillain-Barré Syndrome. J. Immunol. 196, 1102–1107. https://doi.org/10.4049/jimmunol.1502100.

Fischer, J., Hebsaker, J., Caponetto, P., Platts-Mills, T.A., Biedermann, T., 2014. Galactose-alpha-1,3-galactose sensitization is a prerequisite for pork-kidney allergy and cofactor-related mammalian meat anaphylaxis. J. Allergy Clin. Immunol. 134 https://doi.org/10.1016/j.jaci.2014.05.051, 755-759e1.

Fischer, J., Yazdi, A.S., Biedermann, T., 2016. Clinical spectrum of alpha-Gal syndrome: from immediate-type to delayed immediate-type reactions to mammalian innards and meat. Allergo J. Int. 25, 55–62. https://doi.org/10.1007/s40629-016-0099-z.

Galili, U., 2015. Significance of the evolutionary α1,3-galactosyltransferase (GGTA1) gene inactivation in preventing extinction of apes and old world monkeys. J. Mol. Evol. 80, 1–9. https://doi.org/10.1007/s00239-014-9652-x.

Galili, U., 2018. Evolution in primates by "catastrophic-selection" interplay between enveloped virus epidemics, mutated genes of enzymes synthesizing carbohydrate antigens, and natural anti-carbohydrate antibodies. Am. J. Phys. Anthropol. 168, 352–363. https://doi.org/10.1002/ajpa.23745.

Galili, U., 2020. Amplifying immunogenicity of prospective Covid-19 vaccines by glycoengineering the coronavirus glycan-shield to present α-gal epitopes. Vaccine 38, 6487–6499. https://doi.org/10.1016/j.vaccine.2020.08.032.

Galili, U., Mandrell, R.E., Hamadeh, R.M., Shohet, S.B., Griffiss, J.M., 1988. Interaction between human natural anti-alpha-galactosyl immunoglobulin G and bacteria of the

human flora. Infect. Immun. 56, 1730–1737. https://doi.org/10.1128/IAI.56.7.1730-1737.1988.
Gonzalez-Quintela, A., Dam Laursen, A.S., Vidal, C., Skaaby, T., Gude, F., Linneberg, A., 2014. IgE antibodies to alpha-gal in the general adult population: relationship with tick bites, atopy, and cat ownership. Clin. Exp. Allergy 44, 1061–1068. https://doi.org/10.1111/cea.12326.
Hodžić, A., Mateos-Hernández, L., Leschnik, M., Alberdi, P., Rego, R.O.M., Contreras, M., Villar, M., de la Fuente, J., Cabezas-Cruz, A., Duscher, G.G., 2019. Tick bites induce anti-α-Gal antibodies in dogs. Vaccines 7, 114. https://doi.org/10.3390/vaccines7030114.
Hodžić, A., Mateos-Hernández, L., de la Fuente, J., Cabezas-Cruz, A., 2020a. α-Gal-based vaccines: advances, opportunities, and perspectives. Trends Parasitol. https://doi.org/10.1016/j.pt.2020.08.001. S1471-4922(20)30215-4.
Hodžić, A., Mateos-Hernández, L., Fréalle, E., Román-Carrasco, P., Alberdi, P., Pichavant, M., Risco-Castillo, V., Le Roux, D., Vicogne, J., Hemmer, W., Auer, H., Swoboda, I., Duscher, G.G., de la Fuente, J., Cabezas-Cruz, A., 2020b. Infection with *Toxocara canis*inhibits the production of IgE antibodies to α-Gal in humans: towards a conceptual framework of the hygiene hypothesis? Vaccines 8, 167. https://doi.org/10.3390/vaccines8020167.
Indikova, I., Humphrey, T.J., Hilbert, F., 2015. Survival with a helping hand: *campylobacter* and microbiota. Front. Microbiol. 6, 1266. https://doi.org/10.3389/fmicb.2015.01266.
Ju, Y.Y., Womersley, H., Pritchard, J., Gray, I., Hughes, R.A., Gregson, N.A., 2004. *Haemophilus influenzae* as a possible cause of Guillain-Barré syndrome. J. Neuroimmunol. 149, 160–166. https://doi.org/10.1016/j.jneuroim.2003.12.011.
Kalograiaki, I., Euba, B., Fernández-Alonso, M., Proverbio, D., St Geme 3rd, J.W., Aastrup, T., Garmendia, J., Cañada, F.J., Solís, D., 2018. Differential recognition of *Haemophilus influenzae* whole bacterial cells and isolated lipooligosaccharides by galactose-specific lectins. Sci. Rep. 8, 16292. https://doi.org/10.1038/s41598-018-34383-x.
Kampmann, C., Dicksved, J., Engstrand, L., Rautelin, H., 2016. Composition of human faecal microbiota in resistance to *Campylobacter* infection. Clin. Microbiol. Infect. 22, 61. https://doi.org/10.1016/j.cmi.2015.09.004 e1-61.e8.
Koga, M., Koike, S., Hirata, K., Yuki, N., 2005. Ambiguous value of *Haemophilus influenzae* isolation in Guillain-Barre and Fisher syndromes. J. Neurol. Neurosurg. Psychiatry. 76, 1736–1738. https://doi.org/10.1136/jnnp.2005.065359.
Levin, M., Apostolovic, D., Biedermann, T., Commins, S.P., Iweala, O.I., Platts-Mills, T.A. E., Savi, E., van Hage, M., Wilson, J.M., 2019. Galactose α-1,3-galactose phenotypes: lessons from various patient populations. Ann. Allergy Asthma Immunol. 122, 598–602. https://doi.org/10.1016/j.anai.2019.03.021.
Macher, B.A., Galili, U., 2008. The Galalpha1,3Galbeta1,4GlcNAc-R (alpha-Gal) epitope: a carbohydrate of unique evolution and clinical relevance. Biochim. Biophys. Acta 1780, 75–88. https://doi.org/10.1016/j.bbagen.2007.11.003.
Mañez, R., Blanco, F.J., Díaz, I., Centeno, A., Lopez-Pelaez, E., Hermida, M., Davies, H.F., Katopodis, A., 2001. Removal of bowel aerobic gram-negative bacteria is more effective than immunosuppression with cyclophosphamide and steroids to decrease natural alpha-galactosyl IgG antibodies. Xenotransplantation 8, 15–23. https://doi.org/10.1034/j.1399-3089.2001.00082.x.
Mateos-Hernández, L., Villar, M., Moral, A., Rodríguez, C.G., Arias, T.A., de la Osa, V., Brito, F.F., Fernández de Mera, I.G., Alberdi, P., Ruiz-Fons, F., Cabezas-Cruz, A., Estrada-Peña, A., de la Fuente, J., 2017. Tick-host conflict: immunoglobulin E antibodies to tick proteins in patients with anaphylaxis to tick bite. Oncotarget 8, 20630–20644. https://doi.org/10.18632/oncotarget.15243.
Montassier, E., Al-Ghalith, G.A., Mathé, C., Le Bastard, Q., Douillard, V., Garnier, A., Guimon, R., Raimondeau, B., Touchefeu, Y., Duchalais, E., Vince, N., Limou, S., Gourraud, P.A., Laplaud, D.A., Nicot, A.B., Soulillou, J.P., Berthelot, L., 2020. Distribution of bacterial α1,3-Galactosyltransferase genes in the human gut microbiome. Front. Immunol. 10, 3000. https://doi.org/10.3389/fimmu.2019.03000.
Mori, M., Kuwabara, S., Miyake, M., Noda, M., Kuroki, H., Kanno, H., Ogawara, K., Hattori, T., 2000. *Haemophilus influenzae* infection and Guillain-Barré syndrome. Brain 123 (Pt 10), 2171–2178. https://doi.org/10.1093/brain/123.10.2171.
Morisset, M., Richard, C., Astier, C., Jacquenet, S., Croizier, A., Beaudouin, E., Cordebar, V., Morel-Codreanu, F., Petit, N., Moneret-Vautrin, D.A., Kanny, G., 2012. Anaphylaxis to pork kidney is related to IgE antibodies specific for galactose-alpha-1,3-galactose. Allergy 67, 699–704. https://doi.org/10.1111/j.1398-9995.2012.02799.x.
Nugent, E.K., Nugent, A.K., Nugent, R., Nugent, K., 2017. Zika virus: epidemiology, pathogenesis and human disease. Am. J. Med. Sci. 353, 466–473. https://doi.org/10.1016/j.amjms.2016.12.018.
O'Loughlin, J.L., Samuelson, D.R., Braundmeier-Fleming, A.G., White, B.A., Haldorson, G.J., Stone, J.B., Lessmann, J.J., Eucker, T.P., Konkel, M.E., 2015. The intestinal microbiota influences *Campylobacter jejuni* colonization and extraintestinal dissemination in mice. Appl. Environ. Microbiol. 81, 4642–4650. https://doi.org/10.1128/AEM.00281-15.
Pacheco, I., Contreras, M., Villar, M., Risalde, M.A., Alberdi, P., Cabezas-Cruz, A., Gortazar, C., de la Fuente, J., 2020. Vaccination with alpha-Gal protects against mycobacterial infection in the zebrafish model of tuberculosis. Vaccines 8, 195. https://doi.org/10.3390/vaccines8020195.
Platts-Mills, T.A.E., Commins, S.P., Biedermann, T., van Hage, M., Levin, M., Beck, L.A., Diuk-Wasser, M., Jappe, U., Apostolovic, D., Minnicozzi, M., Plaut, M., Wilson, J.M., 2020. On the cause and consequences of IgE to galactose-α-1,3-galactose: a report from the national institute of allergy and infectious disease workshop on understanding IgE-Mediated mammalian meat allergy. J. Allergy Clin. Immunol. 145, 1061–1071. https://doi.org/10.1016/j.jaci.2020.01.047.
Rosinska, J., Lukasik, M., Kozubski, W., 2012. Neuropathies in the course of primary hepatotropic virus infections. Neurol. Neurochir. Pol. 46, 263–270. https://doi.org/10.5114/ninp.2012.28916.
Sanjuan, M.A., Sagar, D., Kolbeck, R., 2016. Role of IgE in autoimmunity. J. Allergy Clin. Immunol. 137, 1651–1661. https://doi.org/10.1016/j.jaci.2016.04.007.
Steinke, J.W., Platts-Mills, T.A., Commins, S.P., 2015. The alpha-gal story: lessons learned from connecting the dots. J. Allergy Clin. Immunol. 135, 589–596. https://doi.org/10.1016/j.jaci.2014.12.1947.
Toscano, G., Palmerini, F., Ravaglia, S., Ruiz, L., Invernizzi, P., Cuzzoni, M.G., Franciotta, D., Baldanti, F., Daturi, R., Postorino, P., Cavallini, A., Micieli, G., 2020. Guillain-barré syndrome associated with SARS-CoV-2. 2020. N. Engl. J. Med. 382, 2574–2576. https://doi.org/10.1056/NEJMc2009191.
Townson, K., Boffey, J., Nicholl, D., Veitch, J., Bundle, D., Zhang, P., Samain, E., Antoine, T., Bernardi, A., Arosio, D., Sonnino, S., Isaacs, N., Willison, H.J., 2007. Solid phase immunoadsorption for therapeutic and analytical studies on neuropathy-associated anti-GM1 antibodies. Glycobiology 17, 294–303. https://doi.org/10.1093/glycob/cwl074.
Urra, J.M., Ferreras-Colino, E., Contreras, M., Cabrera, C.M., Fernández de Mera, I.G., Villar, M., Cabezas-Cruz, A., Gortázar, C., de la Fuente, J., 2020. The antibody response to the glycan α-Gal correlates with COVID-19 disease symptoms. J. Med. Virol. 07 (14), 201954. https://doi.org/10.1101/2020.07.14.201954 in press. bioRxiv 2020.
Van den Berg, B., Walgaard, C., Drenthen, J., Fokke, C., Jacobs, B.C., van Doorn, P.A., 2014. Guillain-Barré syndrome: pathogenesis, diagnosis, treatment and prognosis. Nat. Rev. Neurol. 10, 469–482. https://doi.org/10.1038/nrneurol.2014.121.
van Nunen, S., O'Connor, K.S., Clarke, L.R., Boyle, R.X., Fernando, S.L., 2007. The association between *Ixodes holocyclus* tick bite reactions and red meat allergy. Intern. Med. J. 39, A132.
Villar, M., Pacheco, I., Merino, O., Contreras, M., Mateos-Hernández, L., Prado, E., Barros-Picanco, D.K., Francisco Lima-Barbero, J., Artigas-Jerónimo, S., Alberdi, P., Fernández de Mera, I.G., Estrada-Peña, A., Cabezas-Cruz, A., de la Fuente, J., 2020. Tick and host derived compounds modulate the biochemical properties of the cement complex substance. Biomolecules 10, 555. https://doi.org/10.3390/biom10040555.
Wilson, J.M., Schuyler, A.J., Schroeder, N., Platts-Mills, T.A., 2017. Galactose-α-1,3-Galactose: atypical food allergen or model IgE hypersensitivity? Curr. Allergy Asthma Rep. 17, 8. https://doi.org/10.1007/s11882-017-0672-7.
Wilson, J.M., McNamara, C.A., Platts-Mills, T.A.E., 2019. IgE, α-Gal and atherosclerosis. Aging (Albany N. Y.) 11, 1900–1902. https://doi.org/10.18632/aging.101894.
Wölbing, F., Fischer, J., Koberle, M., Kaesler, S., Biedermann, T., 2013. About the role and underlying mechanisms of cofactors in anaphylaxis. Allergy 68, 1085–1092. https://doi.org/10.1111/all.12193.
Yilmaz, B., Portugal, S., Tran, T.M., Gozzelino, R., Ramos, S., Gomes, J., Regalado, A., Cowan, P.J., d'Apice, A.J., Chong, A.S., Doumbo, O.K., Traore, B., Crompton, P.D., Silveira, H., Soares, M.P., 2014. Gut microbiota elicits a protective immune response against malaria transmission. Cell 159, 1277–1289. https://doi.org/10.1016/j.cell.2014.10.053.
Zhao, H., Shen, D., Zhou, H., Liu, J., Chen, S., 2020. Guillain-Barré syndrome associated with SARS-CoV-2 infection: causality or coincidence? Lancet Neurol. 19, 383–384. https://doi.org/10.1016/S1474-4422(20)30109-5.

Supplementary material. Chapter 2c

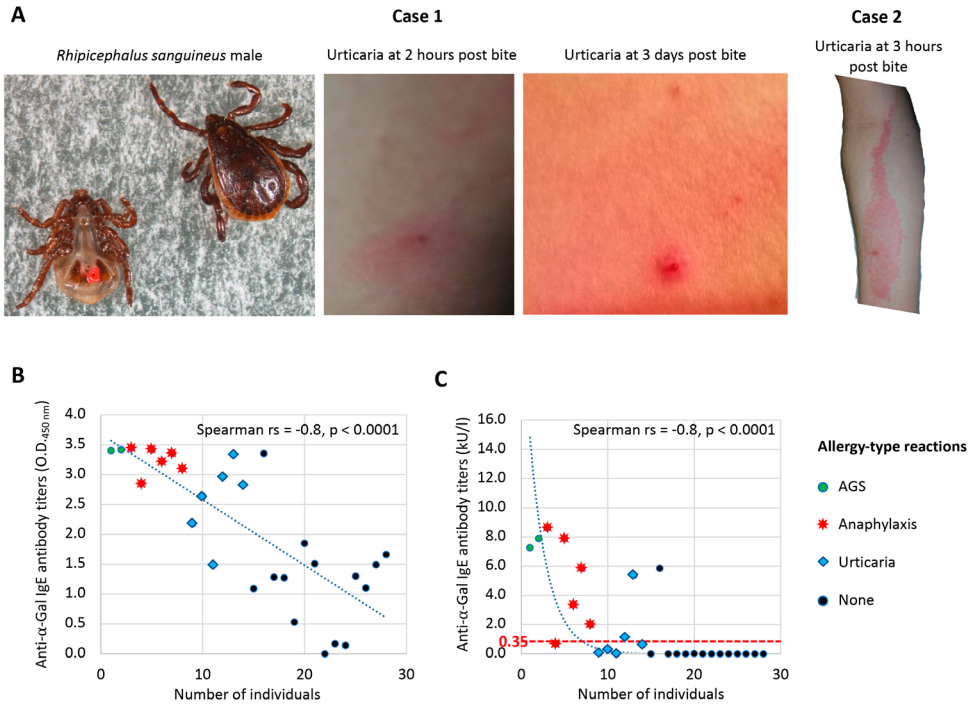

Figure A1. Allergic reactions in response to tick bites. (A) Representative cases of patients with skin urticarial type reactions after tick bite. Case 1, local urticaria after R. sanguineus bite. Case 2, hives or disseminated rash after tick bite of unknown species. (B, C) Correlation analysis between different allergy-type reactions to tick bites and anti-α-Gal IgE antibody response (Table 1). A Spearman Rho (rs) correlation analysis ($p < 0.01$) was conducted between allergy-type reactions and (B) anti-α-Gal IgE antibody titers determined by ELISA (O.D. at 450 nm) and (C) converted to kU/l. Positive anti-α-Gal IgE levels were considered at cut-off value of 0.35 kU/l (red dashed line).

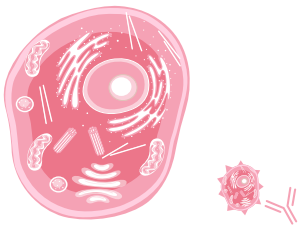

Chapter 2d. Allergic reactions and immunity in response to tick salivary biogenic substances and red meat consumption in the zebrafish model

Contreras, M., **Pacheco, I.,** Alberdi, P., Díaz-Sánchez, S., Artigas-Jerónimo, S., Mateos-Hernández, L., Villar, M., Cabezas-Cruz, A., de la Fuente, J. (2020). Allergic reactions and immunity in response to tick salivary biogenic substances and red meat consumption in the zebrafish model. Frontiers in Cellular and Infection Microbiology 10, 78. https://doi.org/10.3389/fcimb.2020.00078

frontiers in Cellular and Infection Microbiology

ORIGINAL RESEARCH
published: 10 March 2020
doi: 10.3389/fcimb.2020.00078

Allergic Reactions and Immunity in Response to Tick Salivary Biogenic Substances and Red Meat Consumption in the Zebrafish Model

Marinela Contreras[1†], Iván Pacheco[1†], Pilar Alberdi[1], Sandra Díaz-Sánchez[1], Sara Artigas-Jerónimo[1], Lourdes Mateos-Hernández[1,2], Margarita Villar[1], Alejandro Cabezas-Cruz[2] and José de la Fuente[1,3]*

[1] SaBio, Instituto de Investigación en Recursos Cinegéticos IREC-CSIC-UCLM-JCCM, Ciudad Real, Spain, [2] UMR BIPAR, INRA, ANSES, Ecole Nationale Vétérinaire d'Alfort, Université Paris-Est, Maisons-Alfort, France, [3] Department of Veterinary Pathobiology, Center for Veterinary Health Sciences, Oklahoma State University, Stillwater, OK, United States

OPEN ACCESS

Edited by:
Itabajara Silva Vaz Jr., Federal University of Rio Grande Do Sul, Brazil

Reviewed by:
Alexandre F. Marques, Federal University of Minas Gerais, Brazil
Sheryl Anne Van Nunen, Royal North Shore Hospital, Australia

***Correspondence:**
José de la Fuente
jose_delafuente@yahoo.com

[†] These authors have contributed equally to this work

Specialty section:
This article was submitted to Parasite and Host, a section of the journal Frontiers in Cellular and Infection Microbiology

Received: *13 January 2020*
Accepted: *17 February 2020*
Published: *10 March 2020*

Citation:
Contreras M, Pacheco I, Alberdi P, Díaz-Sánchez S, Artigas-Jerónimo S, Mateos-Hernández L, Villar M, Cabezas-Cruz A and de la Fuente J (2020) Allergic Reactions and Immunity in Response to Tick Salivary Biogenic Substances and Red Meat Consumption in the Zebrafish Model. Front. Cell. Infect. Microbiol. 10:78. doi: 10.3389/fcimb.2020.00078

Ticks are arthropod ectoparasite vectors of pathogens and the cause of allergic reactions affecting human health worldwide. In humans, tick bites can induce high levels of immunoglobulin E antibodies against the carbohydrate Galα1-3Galβ1-(3)4GlcNAc-R (α-Gal) present in glycoproteins and glycolipids from tick saliva that mediate anaphylactic reactions known as the alpha-Gal syndrome (AGS) or red meat allergy. In this study, a new animal model was developed using zebrafish for the study of allergic reactions and the immune mechanisms in response to tick salivary biogenic substances and red meat consumption. The results showed allergic hemorrhagic anaphylactic-type reactions and abnormal behavior patterns likely in response to tick salivary toxic and anticoagulant biogenic compounds different from α-Gal. However, the results showed that only zebrafish previously exposed to tick saliva developed allergic reactions to red meat consumption with rapid desensitization and tolerance. These allergic reactions were associated with tissue-specific Toll-like receptor-mediated responses in types 1 and 2 T helper cells (T_H1 and T_H2) with a possible role for basophils in response to tick saliva. These results support previously proposed immune mechanisms triggering the AGS and provided evidence for new mechanisms also potentially involved in the AGS. These results support the use of the zebrafish animal model for the study of the AGS and other tick-borne allergies.

Keywords: alpha gal, alpha gal syndrome, tick, zebrafish, allergy

INTRODUCTION

Arthropod ectoparasites are a growing burden worldwide (Stutzer et al., 2018). Local allergic reactions to the bite of arthropod ectoparasites such as mosquitoes, ticks, fleas, mites, and lice are common, but in some cases large local and anaphylactic reactions are possible (Lee et al., 2016; Mihara, 2017; Stringer et al., 2017; Haddad et al., 2018; Ha et al., 2019).

Ticks are vectors of pathogens affecting human and animal health worldwide (de la Fuente et al., 2008, 2017). Tick saliva contains multiple biomolecules such as proteins and lipids that facilitate feeding while counteracting host defense responses, properties that also lead to possible

application of these molecules in therapeutic interventions (Chmelar et al., 2019). However, tick bites themselves can induce a spectrum of inflammatory reactions in response to toxic and anticoagulant biogenic substances present in tick saliva and/or mouthpart penetration such as coagulative necrosis producing firm papules, tick paralysis, intense pruritus, tick bite alopecia, cutaneous lymphoid hyperplasia, and cell histiocytosis (Mihara, 2017; Stringer et al., 2017; Haddad et al., 2018; Ha et al., 2019). Additionally, tick bites can induce in humans high levels of immunoglobulin E (IgE) antibodies against the carbohydrate Galα1-3Galβ1-(3)4GlcNAc-R (α-Gal) present in glycoproteins and glycolipids from tick saliva that mediate delayed anaphylaxis to red meat consumption, and immediate anaphylaxis to tick bites, xenotransplantation, and certain drugs such as cetuximab (Mateos-Hernández et al., 2017; Hilger et al., 2019). These anaphylactic reactions are known as the alpha-Gal syndrome (AGS) or red meat allergy and are now the focus of recent investigations (Commins et al., 2009; Van Nunen et al., 2009; Platts-Mills et al., 2015; Steinke et al., 2015; Galili, 2018; Cabezas-Cruz et al., 2019; de la Fuente et al., 2019; Hilger et al., 2019).

Recently, C57BL/6 α1,3-galactosyltransferase-knockout (α1,3-GalT-KO) mice that like humans do not synthesize α-Gal have been used as a model to characterize the percutaneous sensitization to α-Gal and *Amblyomma sculptum* tick saliva (Araujo et al., 2016) and the IgE-mediated immune response to cutaneous exposure to *Amblyomma americanum* tick proteins (Chandrasekhar et al., 2019). Additionally, this animal model has been used to study the antibody response to the carbohydrate α-Gal and its potential for the control of infectious diseases caused by pathogens with this modification on their surface (Yilmaz et al., 2014; Cabezas-Cruz et al., 2016; Iniguez et al., 2017; Moura et al., 2017; Portillo et al., 2019). In this context, various fish species constitute models for investigating human diseases (Schartl, 2014), and zebrafish (*Danio rerio* Hamilton 1822) is a relevant animal model for research in genetics, developmental biology, toxicology, oncology, immunology, and allergy (Huang et al., 2018).

In this study, we have developed a new zebrafish animal model for the study of tick-borne allergies caused by biogenic substances present in tick saliva. First, we showed that as occurs in humans, zebrafish do not have α-Gal in their tissues and produce anti–α-Gal IgM antibodies likely in response to bacteria with this modification present in the gut microbiota. Then, an experiment was conducted to evaluate the effect of tick saliva and the salivary components α-Gal and prostaglandin E_2 (PGE_2) alone and in combination with red meat consumption on zebrafish allergic response and survival. The results showed that some zebrafish develop hemorrhagic anaphylactic-type reactions provoking deaths in response to tick saliva, but only fish previously exposed to tick saliva develop allergic reactions to red meat consumption with rapid desensitization and tolerance. The immunity in response to tick saliva and red meat consumption showed tissue-specific differences and suggested immune mechanisms triggering the AGS. Taken together, these results identified allergic reactions and immune mechanisms in response to tick saliva and red meat consumption and provided a new animal model for the study of the AGS and other tick-borne allergies.

MATERIALS AND METHODS

Ethics Statement

Animal experiments were conducted in strict accordance with the recommendations of the European Guide for the Care and Use of Laboratory Animals. Animals were housed and experiments conducted at experimental facility (IREC, Ciudad Real, Spain) with the approval and supervision of the Ethics Committee on Animal Experimentation of the University of Castilla La Mancha (PR-2018-06-13) and the Counseling of Agriculture, Environment and Rural Development of Castilla La Mancha (ES130340000218).

Zebrafish

Wild-type adult (6–8 months old) AB male and female zebrafish were kindly provided by Dr. Juan Galcerán Sáez from the Instituto de Neurociencias (IN-CSIC-UMH, Sant Joan d'Alacant, Alicante, Spain). These zebrafish were certified by Biosait Europe S.L. (Barcelona, Spain; https://biosait.com) as free of major fish pathogens such as *Mycobacterium* spp., *Pseudoloma neurophilia*, *Pseudocapillaria tomentosa*, and zebrafish retroviruses. The zebrafish were maintained in a flow-through water system at 27°C with a light–dark cycle of 14/10 h and fed twice daily with dry fish feed. For bacterial microbiota studies, 15 freshwater zebrafish adults were also included purchased from a pet store in Ciudad Real, Spain, and used immediately for analysis in the laboratory.

Zebrafish Feeds and Feeding

Zebrafish were fed before and throughout the experiment twice daily at 9:30 a.m. and 1:30 p.m. Before the beginning of the experiment and up to day 2, all fish were fed with fish feed (Premium food tropical fish, DAPC, Valladolid, Spain; 50–70 μg/fish). On day 2, each experimental group was divided into two subgroups. One subgroup continued to be fed with fish feed at the same regimen, and the second subgroup was fed with dog food (Classic red, ACANA; Champion Petfoods LP, Edmonton, Alberta, Canada; 150–200 μg/fish). The fish feed contains cereals, fish and fish byproducts, soya, yeast, crustaceans, and algae. The dog food is composed of lamb meat meal (23%), steel-cut oats (22%), fresh ranch-raised beef (5%), fresh Yorkshire pork (5%), lamb fat (5%), whole red lentils, whole green peas, whole green lentils, raw grass-fed lamb (4%), whole oats, fresh beef liver (2%), pork meat meal (2%), herring oil (2%), fresh pork liver (2%), whole garbanzo beans, whole yellow peas, sun-cured alfalfa, lentil fiber, fresh beef tripe (1%), dried brown kelp, fresh pumpkin, fresh butternut squash, fresh parsnips, fresh green kale, fresh spinach, fresh carrots, fresh Red Delicious apples, fresh Bartlett pears, freeze-dried beef liver (0.1%), fresh cranberries, fresh blueberries, chicory root, turmeric root, milk thistle, burdock root, lavender, marshmallow root, and rosehips.

Tick Saliva and Salivary Biogenic Components

Rhipicephalus sanguineus (Latreille 1806) female ticks were collected in an animal shelter at Ciudad Real, Spain, while feeding on naturally infested dogs. Ticks were collected at different

feeding times for saliva collection as previously described but using pilocarpine hydrochloride (Poole et al., 2013). Partially fed ticks were inoculated with 5 μL of a 2% (wt/vol) solution of pilocarpine hydrochloride in phosphate-buffered saline (PBS), pH 7.4 (Sigma-Aldrich, St. Louis, MO, USA), into the hemocoel using a 50-μL syringe with a 0.33-mm needle (Hamilton Bonaduz AG, Bonaduz, Switzerland). Saliva was harvested using a micropipette, kept on ice, pooled, and stored at −80°C. Saliva protein concentration (1.96 μg/mL) was determined using a BCA Protein Assay Kit (Thermo Fisher Scientific, Waltham, MA, USA) following manufacturer's recommendations. Prostaglandin E_2 was obtained from Sigma-Aldrich. The bovine serum albumin (BSA) coated with α-Gal (thereafter named α-Gal) was obtained from Dextra (NGP0203 Gala1-3Gal-BSA 3 atom spacer; Shinfield, UK).

Protein Extracts From Zebrafish Tissues and Feeds, Human HL60 Cells, Pork Kidney, and Tick Salivary Glands

Zebrafish, HL60 Cells, and Pork Kidney

Wild-type adult AB zebrafish ($N = 5$; three females and two males) were dissected and muscle, liver/kidney, and gut collected for protein extraction. Human promyelocytic leukemia HL60 cells (ATCC CCL-240; α-Gal negative) were cultured in RPMI 1640 medium supplemented with 10% heat-inactivated fetal calf serum, 2 mM L-glutamine, and 25 mM HEPES buffer as previously described (de la Fuente et al., 2005). Pork (*Sus scrofa*) kidney (1 g; α-Gal positive) was obtained from a slaughterhouse at Ciudad Real, Spain. All samples were homogenized in lysis buffer (7 M urea, 2 M thiourea, 2% 3-[(3-cholamidopropyl)dimethylammonio]-1-propanesulfonate, CHAPS) supplemented with complete mini protease inhibitor cocktail (Roche, Basel, Switzerland). Samples were boiled for 2 min, mixed in a thermocycler for 1 h, and sonicated for 1 min in an ultrasonic cooled bath followed by 10-s vortex. After three cycles of sonication vortex, the homogenate was centrifuged at 200 g for 5 min at 4°C, and the supernatant was quantified using an RC DC protein assay (BioRad, Hercules, CA, USA) with BSA as standard. This methodology has been previously shown to preserve the presence of the α-Gal epitope in extracted proteins (Lima-Barbero et al., 2019).

Tick Salivary Glands, Dog Food, and Fish Feed

Salivary glands were dissected from unfed and partially fed *R. sanguineus* female ticks and pooled for analysis ($N = 10$ per pool). Dog food and fish feed were pooled (1 μg per sample) for analysis. Samples were pooled in 500 μL lysis buffer (PBS, 1% Triton X-100) supplemented with complete protease inhibitor mixture (Roche) and homogenized by passing through a needle (27-gauge). Samples were sonicated for 1 min in an ultrasonic cooled bath, followed by vortexing for 10 s. After three cycles of sonication vortex, total protein extracts were centrifuged at 200 g for 5 min to remove debris. The supernatants were collected, and protein concentration was determined using the BCA Protein Assay (Life Technologies, Carlsbad, CA) with BSA as standard following the manufacturer's recommendations.

Determination of α-Gal Content by Enzyme-Linked Immunosorbent Assay

The α-Gal levels were determined by enzyme-linked immunosorbent assay (ELISA) in zebrafish proteins from different organs, *R. sanguineus* saliva and salivary gland proteins, fish feed, and dog food in comparison with pork kidney (α-Gal–positive control) and human HL60 cells (α-Gal–negative control). Plates were coated with 100 ng proteins per well from different samples in carbonate/bicarbonate buffer incubated overnight at 4°C, following five washes with PBS containing 0.05% Tween 20 (PBST). Unspecific unions were blocked with 1% human serum albumin (HSA; Sigma-Aldrich) and the α-Gal epitope monoclonal antibodies (M86; Enzo Life Sciences, Farmingdale, NY, USA) were added at 1:50 dilution in PBS and incubated for 1 h at 37°C followed by five washes with PBST. Finally, anti–mouse IgM (μ-chain specific)–peroxidase antibody produced in goat (Sigma-Aldrich) was added at 1:2,000 dilution in PBS. Reactions were visualized by adding 100 μL of 3,3′,5,5-tetramethylbenzidine (TMB; Promega, Madison, WI, USA) and incubated for 20 min in the dark at room temperature (RT). The optical density (OD) was measured at 450 nm with an ELISA reader. The average value of the blanks (wells without sample proteins; $N = 5$) was subtracted from all reads, and the average of nine replicates for each sample was used for analysis. A calibration curve with 0.0 to 1.0 ng α-Gal and OD values at 450 nm was constructed using Microsoft Excel for Mac (v. 16.26) to convert ELISA reader values to α-Gal content per sample ($R^2 = 0.992$; **Supplementary Figure 5A**). To further validate the calibration curve, a correlation was constructed between 0.0 to 3.5 ng α-Gal and 0.0 to 1.0 μg tick salivary gland proteins using Microsoft Excel for Mac (v. 16.26) ($R^2 = 0.992$; **Supplementary Figure 5B**). The results (average ± SD of α-Gal/1 μg protein) were compared between samples and negative or positive controls by Student *t*-test with unequal variance ($p < 0.05$, $N = 3$–5 biological replicates).

Characterization of α-Gal–Positive Bacteria Zebrafish Gut Microbiota

The study was performed using wild-type adult AB and pet store adult female and male zebrafish ($N = 5$ for each fish group; three females and two males). The microbiota was sampled as previously described (Cantas et al., 2012). Briefly, the ventral belly surface of freshly euthanized fish was opened with sterilized micro–surgical blade and forceps under a light source. The intestinal system was transferred to 1.5-mL tubes containing 200 μL sterile PBS. The intestines were homogenized with a motorized pestle, and disposable plastic loops were used to streak on 5% chicken (α-Gal negative) (Parmentier et al., 2008) blood agar (Rockland Immunochemicals Inc., Pottstown, PA, USA) and tryptic soy agar (Sigma-Aldrich) bacteriological plates for isolation of aerobic and anaerobic bacteria, respectively, following four serial dilutions. The plates were incubated at 28°C and followed by inspections every day for up to 1 week. Bacterial colonies were morphologically classified as aerobic types I (circular, pink, raised punctiform colonies), II (circular, diameter ≤5 mm, creamy white, raised colonies),

III (irregular, dry white, flat colonies), and anaerobic types Ib (circular, diameter ≤5 mm, creamy white, raised colonies) and IIb (circular, white, raised, punctiform colonies). Bacteria isolated from the zebrafish gut microbiota were washed in PBS, fixed, and permeabilized with the Intracell fixation and permeabilization kit (Immunostep, Salamanca, Spain) following manufacturer recommendations. The cells were incubated with 3% HSA (Sigma-Aldrich) in PBS for 1 h at RT. Then, cells were incubated for 14 h at 4°C with the anti–α-Gal monoclonal antibody (M86; Enzo Life Sciences) diluted 1:50 in 3% HSA/PBS. Fluorescein isothiocyanate (FITC) goat anti–mouse IgM (Abcam, Cambridge, UK)–labeled antibody diluted 1:200 in 3% HSA/PBS was used as a secondary antibody and incubated for 1 h at RT. The *Escherichia coli* O86:B7 (ATCC 12701) and BL21 (DE3) cells were included as positive and negative α-Gal controls, respectively (Cabezas-Cruz et al., 2017c). Samples were analyzed on a FACScalibur flow cytometer equipped with CellQuest Pro software (BD BioSciences, Madrid, Spain). The viable cell population was gated according to forward-scatter and side-scatter parameters. The mean fluorescence intensity (MFI) was determined by flow cytometry, and the geometric mean compared between aerobic and anaerobic bacteria by Student *t*-test with unequal variance ($p = 0.05$, $N = 5$ biological replicates).

Zebrafish Treatment With Tick Saliva and Salivary Biogenic Components

The first trial (Experiment 1) was designed and performed to evaluate the allergic reactions and immune response in zebrafish treated with tick saliva and salivary components and in response to red meat consumption (**Figure 3A**). Adult zebrafish were randomly distributed into five gender-balanced groups (tick saliva, α-Gal, PGE_2, α-Gal + PGE_2, PBS) (**Figure 3A**, **Table 1**). Fish were intramuscularly injected at days 1, 3, and 8 with a Monoject insulin syringe fitted with a 1-cm, 29-gauge needle at the muscle close to the caudal fin with 2.5 μL *R. sanguineus* saliva in 10 μL PBS (tick saliva), 5 μg α-Gal in 10 μL PBS (α-Gal), 350 pg PGE_2 in 10 μL PBS (PGE_2), 5 μg α-Gal and 350 pg PGE_2 in 10 μL PBS (α-Gal + PGE_2), and 10 μL PBS (PBS). On day 2, each experimental group was randomly divided into two subgroups allocated in two separate water tanks and continued to be fed with fish feed or changed to dog food until the end of the experiment at day 14 when all surviving fish were euthanized (**Figure 3A**, **Table 1**). Zebrafish local allergic reactions and behavior were examined immediately after treatment or feed change and followed daily until the end of the experiment at day 14. After fish death or euthanize, serum was collected from each animal to determine anti–α-Gal and antitick salivary gland protein IgM antibody titers. Fish were then divided into two longitudinal halves. One-half was used to dissect intestine and kidney for RNA extraction to characterize the mRNA levels for selected immune response markers–correlates of allergy. The second half was used for histochemical characterization of local basophils. Accumulated zebrafish survival was analyzed by a Cox proportional survival regression test (http://statpages.info/prophaz.html) ($p = 0.05$; N = 7–9 biological replicates). Accumulated zebrafish allergy was analyzed by a one-way analysis of variance (ANOVA) test (https://www.socscistatistics.com/tests/anova/default2.aspx) ($p = 0.05$; N = 7–9 biological replicates). The risk of allergic reactions was analyzed in female and male zebrafish by McNemar test (https://www.graphpad.com/quickcalcs/McNemar1.cfm) ($p = 0.05$; $N = 7–9$).

A second trial (Experiment 2) was conducted with 10 zebrafish per group and treated with tick saliva and PBS control (**Figure 3B**). Experiment 2 was conducted to inject fish with less amount of tick saliva than in Experiment 1 (1 μL instead of 2.5 μL *R. sanguineus* saliva) to reduce response to toxic and anticoagulant biogenic compounds different from α-Gal and PGE_2 present in tick saliva and to better monitor the incidence of allergic reactions, abnormal behavior patterns, and feeding during the experiment. As in Experiment 1, adult zebrafish were randomly distributed into two gender-balanced groups (tick saliva PBS) (**Figure 3B**). Fish were intramuscularly injected at days 1, 3, and 8 as in Experiment 1 with 1 μL *R. sanguineus* saliva in 10 μL PBS (tick saliva) and 10 μL PBS (PBS) as control. On day 2, each experimental group was randomly divided into two subgroups ($N = 5$ each) allocated in two separate water tanks and continued to be fed with fish feed or changed to dog food until the end of the experiment at day 10 when all surviving fish were euthanized (**Figure 3B**). Zebrafish local allergic reactions and behavior were examined immediately after treatment or feed change and followed daily until the end of the experiment at day 10. After fish were euthanized, serum was collected from each animal to determine anti–α-Gal IgM antibody titers. The percent of zebrafish affected by allergic reactions and abnormal behavior and feeding on each group fed with fish feed or dog food was compare between saliva-treated and PBS-treated control fish by a one-way ANOVA test (https://www.socscistatistics.com/tests/anova/default2.aspx) ($p = 0.05$; $N = 4–5$ biological replicates).

Anti–α-Gal IgM Antibody Titers in Zebrafish

For ELISA, high-absorption-capacity polystyrene microtiter plates were coated with 100 ng of α-Gal per well in carbonate–bicarbonate buffer (Sigma-Aldrich). After an overnight incubation at 4°C, coated plates were washed one time with 100 μL/well PBST (Sigma-Aldrich) and then blocked with 100 μL/well of 1% HSA (Sigma-Aldrich) for 1 h at RT. Serum peritoneal fluid samples were diluted (1:100, vol/vol) in blocking solution, and 100 μL/well was added into the wells of the antigen-coated plates and incubated for 1.5 h at 37°C. Plates were washed three times with PBST, and 100 μL/well of species-specific rabbit anti–zebrafish IgM antibodies diluted (1:1,000, vol/vol) in blocking solution was added and incubated for 1 h at RT. Plates were washed three times with 300 μL/well of PBST. A goat anti–rabbit IgG-peroxidase conjugate (Sigma-Aldrich) was added, diluted 1:3,000 in blocking solution, and incubated for 1 h at RT. After four washes with 100 μL/well of PBST, 100 μL/well of TMB (Promega) was added and incubated for 15 min at RT. Finally, the reaction was stopped with 50 μL/well of 2 N H_2SO_4, and the OD was measured in a spectrophotometer at 450 nm. The OD at 450 nm was compared between fish treated with saliva, α-Gal, PGE_2, or α-Gal + PGE_2, and the PBS-treated control group by Student *t* test with unequal variance ($p = 0.005$; $N = 7–9$). A Spearman ρ correlation analysis (https://

TABLE 1 | Experiment 1 design and records of zebrafish allergies and deaths.

Group	Fish No.	Gender	Feed	Day													
				1[a]	2[b]	3[a]	4	5	6	7	8[a]	9	10	11	12	13	14
Saliva	26-1	Female	Fish	A	D							Dead					
	26-2	Female	Fish	A	D							Dead					
	26-3	Female	Fish	A	D							Dead					
	26-4	Female	Fish	—	—	—	—	—	—	—	—	—	—	—	—	—	E
	26-5	Male	Fish	—	—	—	—	—	—	—	—	—	—	—	—	—	E
	26-6	Male	Fish	—	—	—	—	—	—	—	—	—	—	—	—	—	E
	14-7	Female	Dog	—	—	A	A	—	—	—	—	—	—	—	—	—	E
	14-8	Male	Dog	—	—	A	A	—	—	—	—	—	—	—	—	—	E
	14-9	Female	Dog	—	—	A	A	—	—	—	—	—	—	—	—	—	E
α-Gal	27-1	Male	Fish	—	—	—	—	—	—	—	—	—	—	—	—	—	E
	27-2	Female	Fish	—	—	—	—	—	—	—	—	—	—	—	—	—	E
	27-3	Female	Fish	—	—	—	—	—	—	—	—	—	—	—	—	—	E
	27-4	Male	Fish	—	—	—	—	—	—	—	—	—	—	—	—	—	E
	15-5	Male	Dog	—	—	—	—	—	—	—	—	—	—	—	—	—	E
	15-5	Male	Dog	—	—	—	—	—	—	—	—	—	—	—	—	—	E
	15-7	Female	Dog	—	—	—	—	—	—	—	—	—	—	—	—	—	E
PGE_2	28-1	Female	Fish	—	—	—	—	—	—	D				Dead			
	28-2	Female	Fish	—	—	—	—	—	—	—	—	—	—	—	—	—	E
	28-3	Male	Fish	—	—	—	—	—	—	—	—	—	—	—	—	—	E
	28-4	Male	Fish	—	—	—	—	—	—	—	—	—	—	—	—	—	E
	16-5	Female	Dog	—	—	—	—	—	—	—	—	—	—	—	—	—	E
	16-6	Male	Dog	—	—	—	—	—	—	—	—	—	—	—	—	—	E
	16-7	Male	Dog	—	—	—	—	—	—	—	—	—	—	—	—	—	E
α-Gal + PGE_2	29-1	Female	Fish	AD							Dead						
	29-2	Male	Fish	—	—	—	—	—	—	—	—	—	—	—	—	—	E
	29-3	Male	Fish	—	—	—	—	—	—	—	—	—	—	—	—	—	E
	29-4	Female	Fish	—	—	—	—	—	—	—	—	—	—	—	—	—	E
	29-5	Male	Fish	—	—	—	—	—	—	—	—	—	—	—	—	—	E
	17-6	Male	Dog	—	—	—	—	—	—	—	—	—	—	—	—	—	E
	17-7	Male	Dog	—	—	—	—	—	—	—	—	—	—	—	—	—	E
	17-8	Female	Dog							Disappeared from the tank							
PBS	30-1	Female	Fish	—	—						Died from injection						
	30-2	Female	Fish	—	—	—	—	—	—	—	—	—	—	—	—	—	E
	30-3	Male	Fish	—	—	—	—	—	—	—	—	—	—	—	—	—	E
	30-4	Male	Fish	—	—	—	—	—	—	—	—	—	—	—	—	—	E
	18-5	Female	Dog	—	—	—	—	—	—	—	—	—	—	—	—	—	E
	18-6	Male	Dog	—	—	—	—	—	—	—	—	—	—	—	—	—	E
	18-7	Male	Dog	—	—	—	—	—	—	—	—	—	—	—	—	—	E

[a]*Treatments according to the experimental group were done at days 1, 3, and 8.*

[b]*Feed change (fish feed to dog food for some animals) occurred at day 2. The appearance of allergic reactions (A) and death due to allergic reactions (D) were recorded. The absence of allergic reactions and deaths are represented with a dash (—). All surviving fish were euthanized (E) at the end of the experiment.*

www.socscistatistics.com/tests/spearman/Default2.aspx) was performed between anti–α-Gal IgM antibody levels and allergic reactions to tick saliva rated as 10 for fish with allergic reactions and death (AD), 8 for fish with allergic reactions only (A), and 0 for fish without reactions (NR), $\rho = 0.179$, two-tailed $p = 0.283$.

Anti-tick Salivary Gland Proteins IgM Antibody Titers in Zebrafish

Proteins were extracted from *R. sanguineus* salivary glands as described above. For ELISA, high-absorption-capacity polystyrene microtiter plates were coated with 100 ng of protein extracts of salivary glands per well in carbonate–bicarbonate buffer (Sigma-Aldrich). After an overnight incubation at 4°C, coated plates were washed one time with 100 μL/well PBST (Sigma-Aldrich) and then blocked with 100 μL /well of 2% BSA (Sigma-Aldrich) for 1 h at RT. Serum peritoneal fluid samples were diluted (1:100, vol/vol) in blocking solution, and 100 μL/well was added into the wells of the antigen-coated plates and incubated for 1.5 h at 37°C. Plates were washed three times with PBST and 100 μL/well of species-specific rabbit anti–zebrafish IgM antibodies diluted (1:2,000, vol/vol) in blocking solution were added and incubated for 1 h at RT. Plates were washed three times with 100 μL/well of PBST. A goat anti–rabbit IgG–horseradish peroxidase conjugate (Sigma-Aldrich) was added diluted 1:3,000 in blocking solution and incubated for 1 h at RT. After four washes with 100 μL/well of PBST, 100 μL/well of TMB solution (Promega) was added and incubated for 10 min at RT. Finally, the reaction was stopped with 50 μL/well of 2 N H_2SO_4 and the OD measured in a spectrophotometer at 450 nm. A Student *t*-test with unequal variance was used to compare the OD at 450 nm of IgM antibody titers against tick salivary gland proteins between fish treated with saliva, α-Gal, PGE_2, or α-Gal + PGE_2, and the PBS-treated control group ($p = 0.05$; $N = 7$–9) and between zebrafish fed with fish feed or dog food ($p = 0.05$; $N = 3$–6).

Expression of Selected Immune Response Markers by Quantitative Reverse Transcription–Polymerase Chain Reaction

Total RNA was extracted from zebrafish intestine and kidney samples using the AllPrep DNA/RNA/Protein (Qiagen, Hilden, Germany). The expression of selected zebrafish immune response and food allergy markers (Lu et al., 2008; Huang et al., 2018) *akirin 2* (*akr2*), *complement component c3a* (*c3a*), *interleukin 1-beta* (*il1b*), *interleukin* 4 (*il4*), *nuclear factor interleukin 3 regulated* (*nfil3*), *Toll-like receptor 4b* (*tlr4b*), *interferon-induced GTP-binding protein MxA* (*mxa*), *interferon* (*ifn*), and *MYD88 innate immune signal transduction adaptor* (*myd88*) was analyzed by quantitative reverse transcription–polymerase chain reaction (qRT-PCR) with gene-specific primers (**Supplementary Table 1**) using the KAPA SYBR FAST one-step universal kit (Sigma-Aldrich) in the Rotor-Gene Q (Qiagen) thermocycler following manufacturer's recommendations. A dissociation curve was run at the end of the reactions to ensure that only one amplicon was formed and that the amplicon denatured consistently in the same temperature range for every sample (Ririe et al., 1997). The mRNA Ct values were normalized against *D. rerio glyceraldehyde-3-phosphate dehydrogenase* (*gapdh*) using the genNormddCT method (Livak and Schmittgen, 2001). The normalized Ct values were compared between fish treated with saliva, α-Gal, PGE_2, or α-Gal + PGE_2, and the PBS-treated control group and between fish treated with saliva presenting anaphylactic-type reactions and dead on day 2 and fish without reactions by Student *t*-test with unequal variance ($p = 0.005$; $N = 3$–6).

Histochemistry of Local Granulocytes in Zebrafish

Euthanized fish at day 14 were sagittal sectioned and then immediately fixed in 10% neutral buffered formalin for 24 h at 21°C, dehydrated in a graded series of ethanol, immersed in xylol, and embedded in paraffin wax using an automatic processor. Sections were cut at 4 mm and stained with hematoxylin and eosin (Sigma-Aldrich) following manufacturer's instructions and standard procedures (Bennett et al., 2001). Stained tissue sections were examined by light microscopy to count granulocytes (three sections of 40 mm^2 each per fish) and photographed at 40× and 100× magnifications. The average counts of granulocytes were compared between fish treated with tick saliva, α-Gal, or PGE_2 α-Gal + PGE_2, and PBS-treated controls and between fish fed on dog food or fish feed for each treatment by Student *t*-test with unequal variance ($p = 0.05$; $N = 3$–6).

RESULTS

Zebrafish Do Not Produce α-Gal and Have Natural Anti–α-Gal Antibodies in Response to Bacteria in the Gut Microbiota

This study was designed to evaluate the allergic reactions and immunity in response to tick saliva and salivary biogenic substances such as α-Gal and PEG_2 and red meat consumption in the zebrafish model.

Herein we first characterized the α-Gal content in fish tissues (**Figure 1A**). The results showed that only zebrafish gut had α-Gal levels higher than the human HL60 α-Gal–negative control cells, and all zebrafish tissues had significantly lower α-Gal levels than the pork kidney α-Gal–positive control (**Figure 1A**). Then, the presence of α-Gal was characterized in bacteria from the gut microbiota of laboratory wild-type AB and pet store zebrafish (**Figures 1B–D**). Identified anaerobic and aerobic gut bacteria had α-Gal levels higher than the *E. coli*—negative and—positive controls (**Figure 1B**), with higher levels in aerobic than in anaerobic bacteria (**Figure 1C**). A total of five morphologically different bacterial colonies were isolated in both fish groups with α-Gal content higher than the *E. coli*-negative control (**Figure 1D**). These results were similar to those described in humans (Galili, 2018) and suggested that natural anti–α-Gal IgM antibody levels in untreated zebrafish are produced in response to gut bacterial microbiota (PBS-treated group; **Figure 2A**).

Additionally, zebrafish treated with tick saliva, α-Gal, and α-Gal+PGE_2 developed IgM antibodies against α-Gal that showed higher levels than in fish treated with PGE_2 or PBS (**Figure 2A**). Zebrafish treated with tick saliva, α-Gal, PGE_2, and

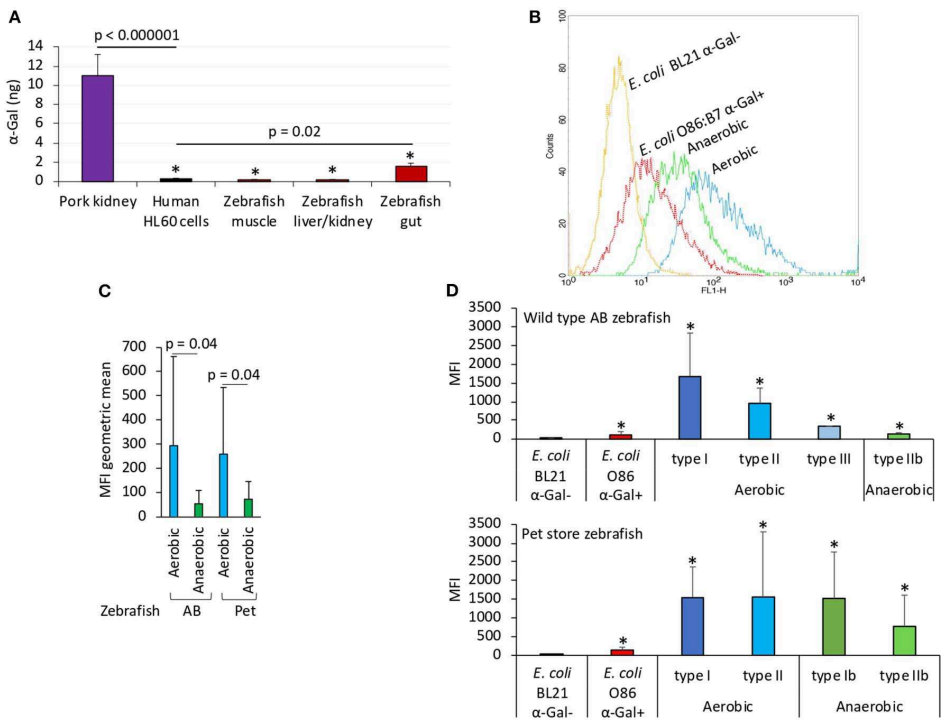

FIGURE 1 | The α-Gal content is similar in humans and zebrafish. The α-Gal content was determined in zebrafish tissues and gut bacterial microbiota and in *R. sanguineus* salivary glands. **(A)** The α-Gal levels were determined by ELISA in zebrafish muscle, liver/kidney, and gut and in comparison with pork kidney (α-Gal positive) and human HL60 cells (α-Gal negative) as positive and negative controls, respectively. The results were converted to α-Gal content per sample using a calibration curve ($R^2 = 0.992$; **Supplementary Figure 5A**) and compared between all samples and negative (lines) or positive (*$p <$ 1E-8) controls by Student *t*-test with unequal variance ($p < 0.05$, $N = 5$ biological replicates). **(B)** Flow cytometry showing the presence of α-Gal on the surface of aerobic and anaerobic bacteria isolated from zebrafish gut microbiota. *Escherichia coli* O86:B7 and BL21 (DE3) strains were included as positive and negative controls for α-Gal, respectively. For flow cytometry, cells were stained with *Bandeiraea simplicifolia* I-isolectin B4–FITC to visualize α-Gal, and the viable cell population was gated according to forward-scatter and side-scatter parameters. **(C)** The MFI was determined by flow cytometry, and the geometric mean ± SD compared between aerobic and anaerobic bacteria by Student *t*-test with unequal variance ($p = 0.05$, $N = 5$ biological replicates). **(D)** Distribution of the MFI among aerobic and anaerobic type bacteria in wild-type AB and pet store zebrafish and in comparison with *E. coli* O86:B7 and BL21 (DE3)–positive and –negative controls for α-Gal, respectively. The results (average ± SD) were compared between all samples and negative control by Student *t*-test with unequal variance (*$p < 0.05$, $N = 5$ biological replicates).

α-Gal+PGE_2 but not PBS also developed IgM antibodies against proteins present in tick salivary glands (**Figure 2B**). Salivary gland proteins in both unfed and partially fed ticks and in tick saliva showed the presence of α-Gal (**Figure 2C**), thus suggesting that *R. sanguineus* synthesize α-Gal and explaining the anti–α-Gal IgM antibody titers in zebrafish treated with tick saliva (**Figure 2A**). As expected, because of the presence of PGE_2 in tick saliva and salivary glands, zebrafish treated with PGE_2 developed antibodies against salivary gland proteins (**Figure 2B**) but not against α-Gal (**Figure 2A**). Finally, a tendency was observed toward higher IgM titers against tick salivary gland proteins in fish fed with dog food when compared to those fed with fish feed (**Supplementary Figure 1**).

Taken together, these results evidenced similarities in α-Gal content and anti–α-Gal antibody response in zebrafish and humans, suggesting that zebrafish may be evaluated like an animal model for the study of tick-borne allergies produced by salivary biogenic components.

Zebrafish Develop Hemorrhagic Anaphylactic-Type Reactions and Abnormal Behavior Patterns in Response to Tick Saliva

The study was designed with two experiments to characterize the allergic response in zebrafish exposed to tick saliva and salivary biogenic components such as α-Gal and PGE_2 (**Figures 3A,B**). In Experiment 1 (**Figure 3A**), zebrafish were injected with 2.5 μL tick saliva and biogenic substances α-Gal and PGE_2 to evaluate the allergic reactions and immune response in fish feeding on fish feed or dog food. Experiment 2 (**Figure 3B**) was then conducted to inject fish with less

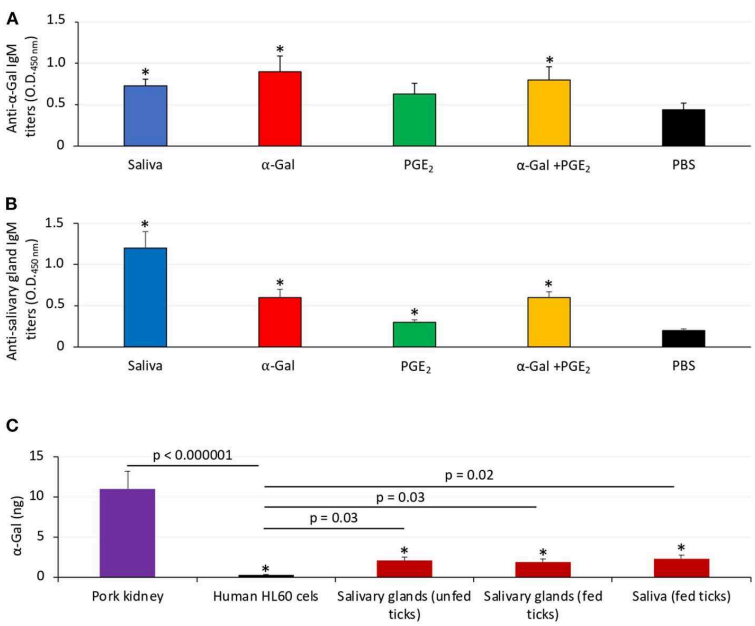

FIGURE 2 | Zebrafish develop antibodies against tick α-Gal and proteins. **(A)** The IgM antibody titers against α-Gal were determined by ELISA, represented as the average ± SD OD at 450 nm and compared between fish treated with saliva, α-Gal, PGE_2, or α-Gal + PGE_2, and the PBS-treated control group by Student *t*-test with unequal variance (*$p < 0.005$; $N = 7–9$). **(B)** The IgM antibody titers against tick salivary gland proteins were determined by ELISA, represented as the average ± SD OD at 450 nm and compared between fish treated with saliva, α-Gal, PGE_2, or α-Gal + PGE_2 and the PBS-treated control group by Student *t*-test with unequal variance (*$p < 0.001$; $N = 7–9$). **(C)** The α-Gal levels were determined by ELISA in salivary glands from unfed and partially fed ticks and saliva from fed ticks in comparison with pork kidney (α-Gal positive) and human HL60 cells (α-Gal negative) as positive and negative controls, respectively. The results were converted to α-Gal content per sample using a calibration curve ($R^2 = 0.992$; **Supplementary Figure 5A**) and compared between all samples and negative (lines) or positive (*$p <$ 1E-8) controls by Student *t*-test with unequal variance ($p < 0.05$, $N = 3$ biological replicates).

tick saliva than in Experiment 1 (1 μL instead of 2.5 μL *R. sanguineus* saliva) to reduce responses to toxic and anticoagulant biogenic compounds different from α-Gal and PGE_2 present in tick saliva and to better monitor the incidence of allergic reactions, abnormal behavior patterns, and feeding during the experiment.

In Experiment 1, the results showed that the incidence of allergic reactions was statistically significant in zebrafish treated with tick saliva (six animals; 66%) but not in fish treated with α-Gal, PGE_2, α-Gal + PGE_2, and PBS (**Figure 4A**, **Table 1**). In three animals treated with tick saliva (33%) and before food change, these reactions resulted in death that significantly affected fish survival rate (**Figure 4B**, **Table 1**). Although not statistically significant, one fish treated with α-Gal + PGE_2 also developed allergy and died at day 1 (**Figures 4A–C**, **Table 1**). The results showed that zebrafish response to tick saliva was characterized by hemorrhagic anaphylactic-type reactions appearing 3 to 5 h posttreatment (hpt) with hemorrhage affecting various organs (**Figure 4D**). Although allergy was more prevalent in female than male zebrafish, the analysis by McNemar test of the risk of developing allergic reactions in response to tick saliva did not show a significant association in female ($p = 0.07$) and male ($p = 1.00$) zebrafish.

Abnormal behavior patterns in Experiment 1 consisted of low mobility, permanence at the bottom of the water tank, and zigzag-type swimming (**Supplementary Figures 2A–F**). Low mobility and permanence at the bottom of the water tank were shown in three zebrafish injected with tick saliva (**Supplementary Figure 2A**), one zebrafish injected with α-Gal (**Supplementary Figure 2C**), and one zebrafish injected with α-Gal + PGE_2 (**Supplementary Figure 2E**). Normal behavior patterns were seen in all zebrafish injected with PGE_2 and PBS (**Supplementary Figures 2D,F**).

These results provided evidence to support that zebrafish develop delayed hemorrhagic anaphylactic-type reactions affecting survival and behavior in response to tick saliva.

Zebrafish Develop Allergic Reactions and Abnormal Behavior Patterns in Response to Red Meat Consumption After Exposure to Tick Saliva

The results of the Experiment 1 (**Figure 3A**) showed that zebrafish develop delayed hemorrhagic anaphylactic-type reactions and abnormal behavior patterns primarily in response to tick saliva resulting in deaths for 33% of the animals

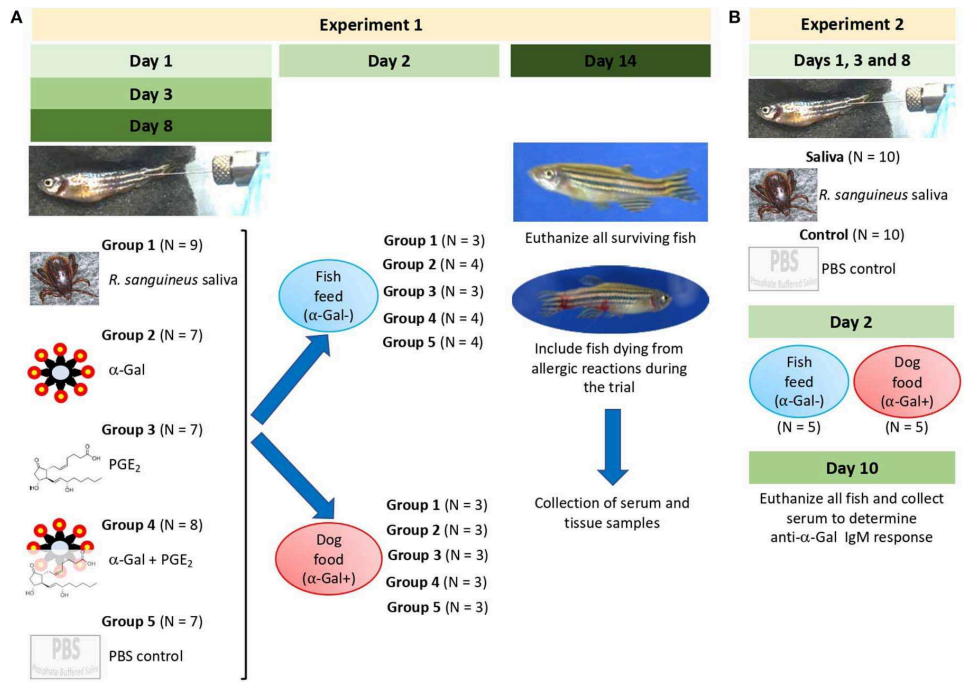

FIGURE 3 | Experimental design. Experiments were designed and performed to evaluate the allergic reactions and immune response in zebrafish treated with tick saliva and salivary components and in response to red meat consumption. **(A)** In Experiment 1, zebrafish were injected with 2.5 μL tick saliva and biogenic substances α-Gal and PGE_2 to evaluate the allergic reactions and immune response in fish feeding on fish feed or dog food. Serum and tissue samples were collected to determine anti–α-Gal IgM response, intestine and kidney for qRT-PCR analysis of immune response markers, and half fish for histochemical characterization of local granulocytes. **(B)** Experiment 2 was conducted to inject fish with less amount of tick saliva than in Experiment 1 (1 μL instead of 2.5 μL *R. sanguineus* saliva) to reduce response to toxic and anticoagulant biogenic compounds different from α-Gal and PGE_2 present in tick saliva and to better monitor the incidence of allergic reactions, abnormal behavior patterns, and feeding during the experiment. Zebrafish local allergic reactions and behavior were examined immediately after treatment or feed change and followed daily until the end of the experiment at day 14 (Experiment 1) or day 10 (Experiment 2). Fish and tick representative images are shown.

(**Figures 5A,B**). However, anaphylaxis to consumption of red meat with high α-Gal content is one of the symptoms of the AGS.

To address this sign of the AGS, zebrafish on each treatment group in Experiment 1 and without reactions in response to first treatment with tick saliva on day 1 were split into two subgroups on day 2 (**Figures 3A**, **5A**, **Table 1**). One subgroup continued to feed on fish feed without α-Gal, whereas the other was fed with dog food containing α-Gal (**Figure 6A**), and both were treated again with tick saliva on day 3 (**Figures 3A**, **5A**, **Table 1**). All zebrafish feeding on fish feed did not develop any visible reaction to tick saliva injected on day 3 (**Figure 5A**, **Table 1**). However, zebrafish fed with dog food and treated with tick saliva on day 3 did develop delayed (3–5 hpt) hemorrhagic anaphylactic-type reactions that lasted for 48 h (**Figures 5A,B**, **Table 1**). An abnormal zig-zag type swimming was also observed at day 3 in fish No. 14-8 injected with tick saliva and fed with dog food (**Supplementary Figures 2B, 3**). These fish recovered from allergic reactions after 48 h and as animals fed on fish feed did not develop any reactions when treated again with tick saliva on day 8 (**Figure 5A**). Although a tendency was observed toward a positive correlation between allergic reactions to tick saliva and anti–α-Gal IgM antibody levels, the correlation was not significant (**Figure 6B**). However, all fish developing anaphylactic-type reactions had IgM antibody levels higher than 0.6 OD at 450 nm (**Figure 5C**).

To gain additional information on the zebrafish allergic reactions and abnormal behavior patterns in response to red meat consumption after exposure to tick saliva, Experiment 2 was conducted (**Figure 3B**). One fish died on each group on day 5 but for reasons not related to the treatments. Although fish were injected with less tick saliva than in Experiment 1, the anti–α-Gal IgM antibody levels were higher than in PBS-treated controls (**Figure 7A**). Furthermore, in fish treated with tick saliva but not in controls, the anti–α-Gal IgM antibody levels were higher in fish fed on dog food than in those fed with fish feed (**Figure 7A**). The analysis of the fish affected by hemorrhagic-type allergic reactions and abnormal behavior and feeding showed that the percentage of affected fish with allergic reactions was higher

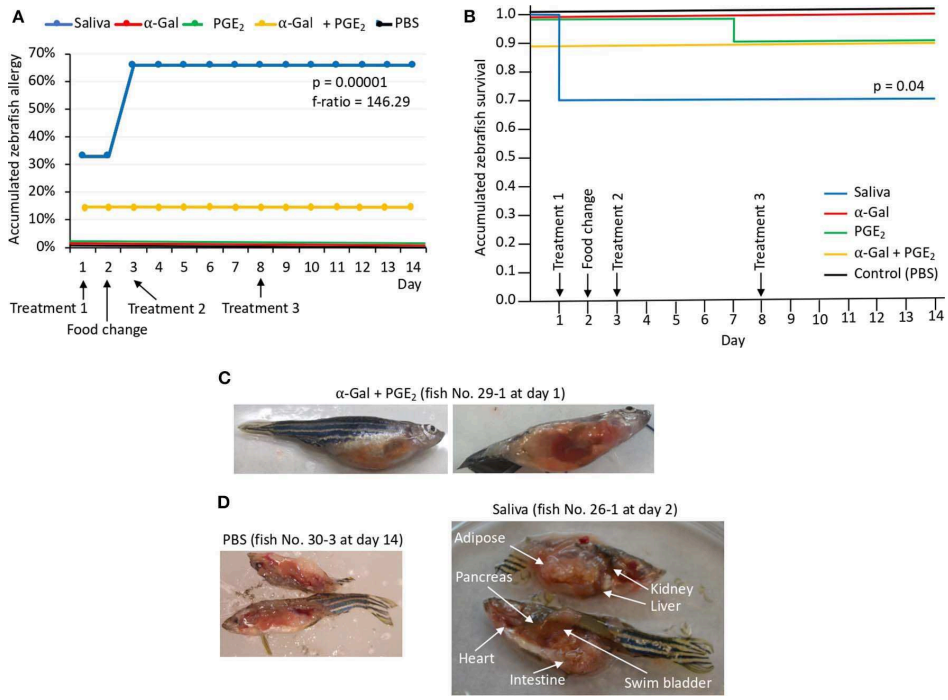

FIGURE 4 | Zebrafish injected with tick saliva develop hemorrhagic anaphylactic-type reactions (Experiment 1). **(A)** Accumulated zebrafish allergy was compared between different groups by a one-way ANOVA test ($p < 0.05$; $N = 7$–9 biological replicates). **(B)** Accumulated zebrafish survival in the different groups was compared by a Cox proportional survival regression test ($p < 0.05$; $N = 7$–9 biological replicates). **(C)** Signs of hemorrhagic anaphylactic-type reactions in zebrafish 29-1 injected with α-Gal + PGE_2. Fish No. 29-1 died on day 1. **(D)** Representative comparison between necropsied control fish No. 30-1 injected with PBS and fish No. 26-1 injected with tick saliva. Evidence of hemorrhage is shown in organs of a saliva-injected fish.

in saliva-treated than in PBS-treated controls fed with either fish or dog food (**Figure 7B**). However, these reactions appeared after third treatment with tick saliva only in fish fed on dog food (**Figure 7B**). Abnormal behavior patterns and feeding were higher in saliva-treated fish than in controls only when feeding on dog food (**Figure 7B**).

These results showed that zebrafish treated with tick saliva develop hemorrhagic-type allergic reactions with abnormal behavior patterns with higher incidence in fish fed with α-Gal–positive dog food than with α-Gal–negative fish feed. Once recovered from allergic reactions, fish continuing feeding on dog food became tolerant to tick saliva. A risk factor associated with anti–α-Gal IgM antibody levels was also identified.

Allergic Reactions to Tick Saliva and Red Meat Consumption in Zebrafish Are Associated With Different Tissue-Specific Immune Response Mechanisms

The expressions of selected immune response and food allergy markers were characterized in Experiment 1 using the kidney and intestine involved in both innate and adaptive fish immunity. Different immune responses were observed in zebrafish kidney and intestine and between fish fed on dog food and fish feed (**Figures 8A,B**). In the kidney of zebrafish fed on dog food but not on fish feed, except for *c3a*, all genes were downregulated in response to tick saliva when compared to PBS-treated controls (**Figures 8A,B**). However, in the intestine of fish fed on dog food all genes except for *myd88*, *akr2*, and *il1b* were upregulated in response to tick saliva but not to other treatments (**Figures 8A,B**). In response to α-Gal or PGE_2 but not to the combined α-Gal + PGE_2, various genes were downregulated in the kidney of zebrafish fed on dog food (**Figures 8A,B**). Minor or no changes in gene expression were observed in the kidney and intestine of fish fed on fish feed and treated with tick saliva, α-Gal, PGE_2, or α-Gal + PGE_2 when compared to PBS controls (**Figures 8A,B**).

The analysis of granulocytes in zebrafish tissue sections collected in Experiment 1 identified the presence of these cells mainly in the skeletal muscle (**Figure 9A** and **Supplementary Figure 4**). The results showed a higher number ($p = 0.00000002$) of granulocytes and granulocyte agglomerations in zebrafish treated with tick saliva (8.8 ± 0.8) when compared to fish treated with α-Gal (2.7 ± 0.8),

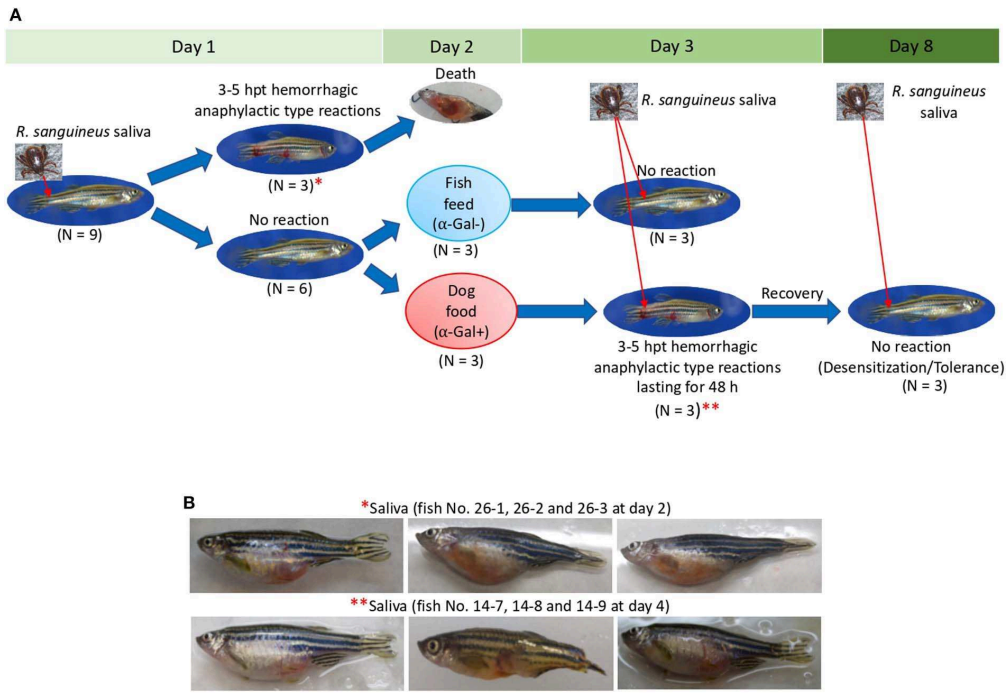

FIGURE 5 | Zebrafish injected with tick saliva and fed with red meat develop hemorrhagic anaphylactic-type reactions and desensitization (Experiment 1). **(A)** In the zebrafish model, 33% of animals treated with tick saliva on day 1 developed hemorrhagic anaphylactic-type allergic reactions 3–5 hpt and died. Furthermore, 100% of fish fed with dog food, but none of the fish that continued feeding on fish feed at day 2, developed allergy to tick saliva injected on day 3. Once recovered from anaphylactic-type reactions, all fish were desensitized and became tolerant to tick saliva injected on day 8. **(B)** Signs of hemorrhagic anaphylactic-type reactions in zebrafish No. 26-1, 26-2, and 26-3 injected with tick saliva and dying at day 2 before food change. After food change, only fish No. 14-7, 14-8, and 14-9 feeding on dog food developed anaphylactic-type reactions. Asterisks in red connect representative fish images in **(A)** with results in **(B)**.

PGE_2 (3.2 ± 0.8), α-Gal + PGE_2 (3.2 ± 1.0), or PBS (2.3 ± 0.6) (**Figures 9A,B**, **Supplementary Figure 4**). No differences were observed between fish fed on fish feed or dog food for each treatment (**Supplementary Figure 4**). At a higher magnification, the structure of the granulocytes showed characteristics of fish basophils/eosinophils such as a highly granular cytoplasm with large and spherical granules (**Figure 9C**).

Finally, of the selected zebrafish immune response and food allergy markers, only the expression of *il1b* was significantly higher in the intestine of zebrafish treated with tick saliva and presenting anaphylactic-type reactions and death when compared to fish without reactions on day 2 (**Figure 9D**).

These results suggested that tick salivary biogenic components different from or in combination with α-Gal and PGE_2 are essential for the modulation of zebrafish immune response to tick saliva and red meat consumption in both kidney and intestine but affecting different tissue-specific mechanisms. The results also suggested a role for basophils/eosinophils in zebrafish response to tick saliva.

DISCUSSION

Tick saliva contains biogenic substances including proteins, lipids, and other biomolecules such as PGE_2 and α-Gal that modulate multiple biological processes affecting ectoparasite feeding and pathogen infection and transmission (Oliveira et al., 2011; Poole et al., 2013; Chmelar et al., 2019). These molecules may also affect host immune response leading to allergic diseases such as the AGS (Araujo et al., 2016; Cabezas-Cruz et al., 2017c, 2019; Chandrasekhar et al., 2019; Hilger et al., 2019). In this study, we focused on the brown dog tick *R. sanguineus* based on the worldwide distribution of this tick species as a major dog ectoparasite, the risk it poses for urban populations, its role in the transmission of pathogens such as *Rickettsia rickettsii* causing Rocky Mountain spotted fever and the cause of anaphylactic reactions to tick bite, and its phylogenetically close relationship with tick species such as *Rhipicephalus bursa* and *Rhipicephalus microplus* previously shown to contain α-Gal–modified proteins (Valls et al., 2007; Uspensky, 2014; de la Fuente et al., 2017; Mateos-Hernández et al., 2017).

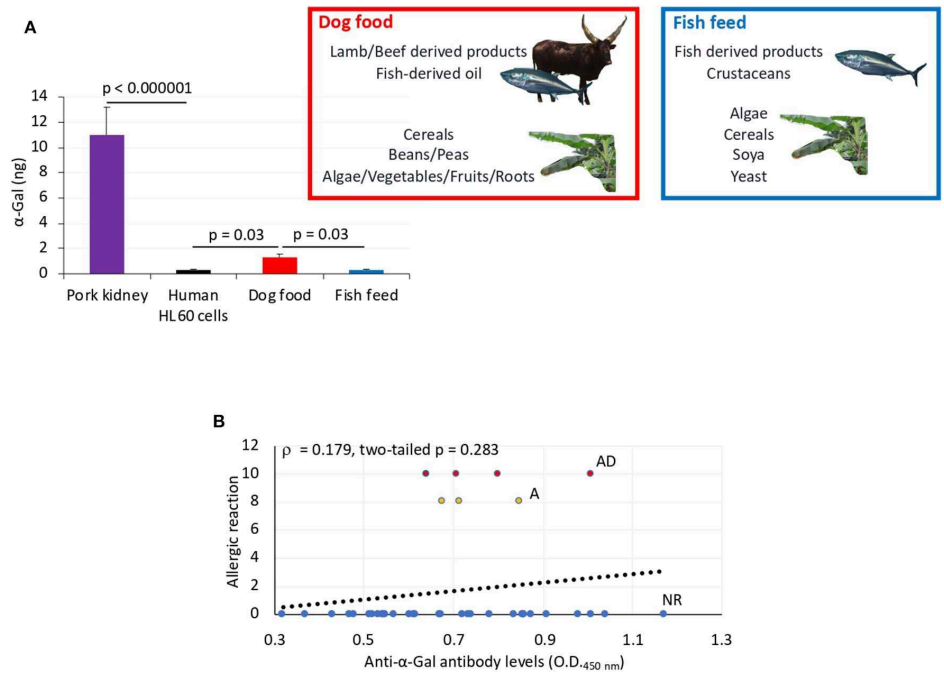

FIGURE 6 | α-Gal levels in dog food and fish feed and correlation analysis between anti–α-Gal IgM antibody levels and allergic reactions to tick saliva. **(A)** The α-Gal levels were determined by ELISA in fish feed and dog food and in comparison with pork kidney (α-Gal positive) and human HL60 cells (α-Gal negative) as positive and negative controls, respectively. The results were converted to α-Gal content per sample using a calibration curve ($R^2 = 0.992$; **Supplementary Figure 5A**) and compared between samples and negative control and between dog food and fish feed by Student *t*-test with unequal variance ($p < 0.05$, $N = 3$ biological replicates). The main components of dog food and fish feed are shown. Only dog food contains α-Gal–positive animal-derived products. **(B)** Spearman ρ correlation analysis between anti–α-Gal IgM antibody levels and allergic reactions to tick saliva in Experiment 1 rated as 10 for fish with allergic reactions and death (AD), 8 for fish with allergic reactions only (A), and 0 for fish without reactions (NR). Correlation rank coefficient (ρ) and *p*-value are shown.

Humans evolved with the inactivation of the α1,3-GalT gene, which resulted in the recognition of the carbohydrate α-Gal as a non–self-antigen, thus inducing the production of high antibody titers against this molecule (Galili, 2018). This evolutionary trait benefits humans by providing immunity to pathogens containing α-Gal in the surface while increasing the risks of developing the AGS triggered by the IgE antibody response against α-Gal present in glycoproteins and glycolipids from tick saliva and tissues of non-catarrhine mammals (Commins et al., 2009; Van Nunen et al., 2009; Platts-Mills et al., 2015; Steinke et al., 2015; Galili, 2018; Cabezas-Cruz et al., 2019; de la Fuente et al., 2019; Hilger et al., 2019; Román-Carrasco et al., 2019; Park et al., 2020). The AGS is characterized by delayed anaphylaxis to red meat consumption and immediate anaphylaxis to tick bites, xenotransplantation, and certain drugs such as cetuximab (Mateos-Hernández et al., 2017; Hilger et al., 2019). Despite recent advances in the study of the AGS (Commins et al., 2009; Van Nunen et al., 2009; Platts-Mills et al., 2015; Steinke et al., 2015; Mateos-Hernández et al., 2017; Galili, 2018; Cabezas-Cruz et al., 2019; de la Fuente et al., 2019; Hilger et al., 2019), the immune-mediated mechanisms induced by tick bites and leading to the AGS have been only partially characterized in α1,3-GalT-KO mice (Araujo et al., 2016; Chandrasekhar et al., 2019). The development of new animal models for tick-borne allergies such as the AGS would contribute to these studies.

Considering that zebrafish are evolutionarily naive to tick saliva as they are not naturally exposed to ticks, the observed allergic hemorrhagic anaphylactic-type reactions and abnormal behavior patterns may occur in response to toxic and anticoagulant biogenic compounds different from α-Gal and PGE_2 present in tick saliva (Francischetti et al., 2009; Aleman and Wolberg, 2013; Mihara, 2017; Stringer et al., 2017; Haddad et al., 2018). For example, although uncommon, episodic hemorrhage has been described in humans during honeybee venom anaphylaxis (Mingomataj and Bakiri, 2012). This episodic hemorrhage has been associated with honeybee venom components that interfere with complement cleavage and bradykinin release, thus affecting coagulation, thrombolysis, hemolysis, and smooth muscle tone. Additionally, infestations by sea lice of the family Caligidae such as *Lepeophtheirus* and *Caligus*

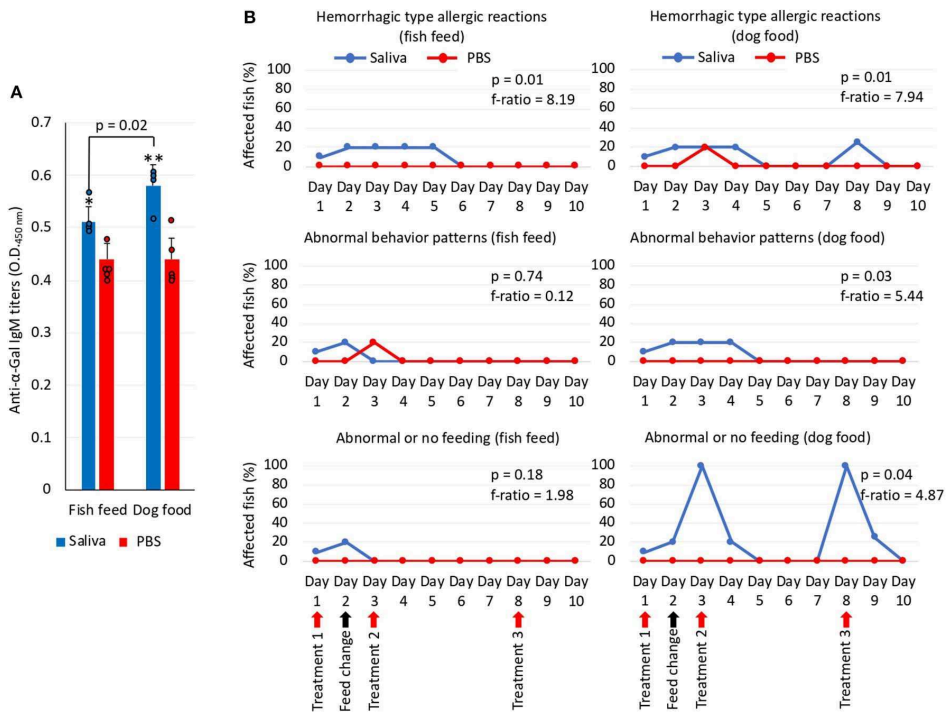

FIGURE 7 | Zebrafish injected with tick saliva and fed with red meat develop allergic reactions and abnormal behavior and feeding patterns (Experiment 2). **(A)** The IgM antibody titers against α-Gal were determined by ELISA, represented as the average ± SD OD at 450 nm and compared between fish treated with tick saliva and the PBS-treated control group and between fish fed on fish feed or dog food Student *t*-test ($^{*}p = 0.003$, $^{**}p = 0.0008$; $N = 4$–5 biological replicates with individual values shown). **(B)** Zebrafish local allergic reactions and behavior were examined immediately after treatment or feed change and followed daily until the end of the experiment at day 10. The percent of zebrafish affected by allergic reactions and abnormal behavior and feeding on each group fed with fish feed or dog food was compared between saliva-treated and PBS-treated control fish by a one-way ANOVA test (https://www.socscistatistics.com/tests/anova/default2.aspx) ($p = 0.05$; $N = 4$–5 biological replicates).

species affect fish behavior and cause abrasion-like lesions at their attachment and feeding sites by changing mucus consistency and damaging the epithelium, which results in loss of blood and fluids and cortisol release (Fast, 2014; Øverli et al., 2014). Some species of fish will spend more time lying on the bottom of the tank when they become stressed, which will also reduce eating (Kalueff et al., 2013). Zigzagging is also a behavior associated with fish stress (Kalueff et al., 2013).

Anaphylactic-type reactions have been previously described in channel catfish (*Ictalurus punctatus* Refinesque) and goldfish (*Carassius auratus* L.) following immunization and challenge with solubilized protozoa (*Tetrahymena pyriformis*) and human serum proteins, respectively, but not when challenged with the heterologous BSA antigen (Goven et al., 1980). The fishes sensitized and challenged with homologous antigens showed abnormal behavior patterns consisting of disorientation, breading problems, and increased defecation. Severe respiratory distress resulted in 33% death of treated catfish. The authors concluded that type I hypersensitivity reactions were the cause of observed anaphylaxis, a mechanism currently defined as type 2 T helper (T_H2) immunity that has been proposed to be associated with the AGS (Wilson et al., 2017; Cabezas-Cruz et al., 2019; Chandrasekhar et al., 2019). In our study, the potential role of BSA present in in the α-Gal–coated particles in the observed allergic reactions when administered to zebrafish was discarded because as previously described (Goven et al., 1980), fish were not previously exposed to BSA, and BSA was likely not present in the tick saliva. Although fish were intramuscularly injected with tick salivary biogenic substances, part of the injected liquid remained subcutaneous, which would better resemble tick bites.

The effect of red meat consumption in the form of dog food containing α-Gal in zebrafish previously treated with tick saliva and normally fed with fish feed free of α-Gal is relevant for the study of the AGS. Dog feed was used because it contains fish- and plant-derived components also present in fish food, and it is registered for animal use. Both fish feed and dog food contained plant-derived compounds together for either fish or animal (red meat) products, thus making it difficult to assign the observed

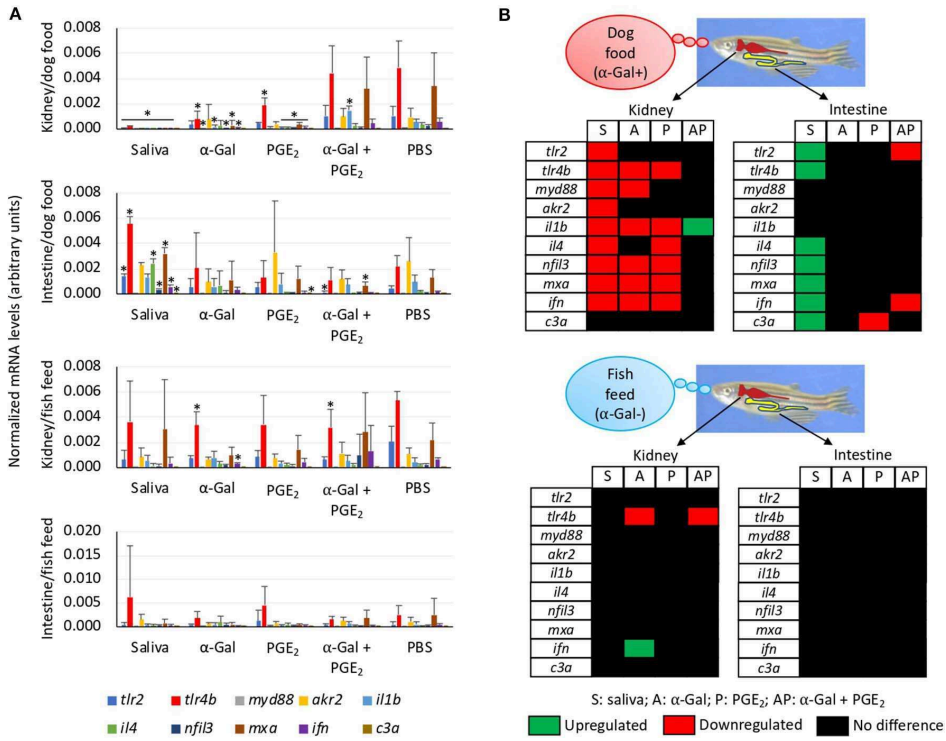

FIGURE 8 | Tissue-specific differences in the immune response of zebrafish injected with tick saliva and fed with red meat (Experiment 1). **(A)** The expression of selected immune response and food allergy markers was analyzed by qRT-PCR in the kidney and intestine of zebrafish fed on dog food or fish feed. The mRNA Ct values were normalized against *D. rerio gapdh*, presented as average ± SD, and compared between fish treated with saliva, α-Gal, PGE_2, or α-Gal + PGE_2, and the PBS-treated control group by Student *t*-test with unequal variance (*$p < 0.05$; $N = 3$–6). **(B)** Representation of differential gene expression with respect to PBS-treated controls in the kidney and intestine of zebrafish fed on dog food or fish feed. Data were obtained from the analysis described in **(A)**.

reactions to other compounds present in dog food. We did not add α-Gal to fish feed because it is possible that the immune response to α-Gal depends on the way this molecule is presented on proteins or lipids and not only the carbohydrate by itself. For still unknown reasons and despite identified risk factors such as gender, pollen allergy, bronchial asthma, pet keeping, age, blood group, and lifestyle (Cabezas-Cruz et al., 2017a,b, 2019), only a fraction of the humans exposed to tick bites develop the AGS, and cases of mammalian meat desensitization have been recently reported (Yucel et al., 2019). Despite the limitations associated with the low number of fish included on each treatment, in the zebrafish model 33% (Experiment 1) and 20% (Experiment 2) of the animals treated with tick saliva developed allergic reactions with no reactions in control fish. However, when fed with dog food, 100% of the animals in both experiments presented allergic reactions including abnormal behavior or feeding after treatment with tick saliva. Furthermore, once recovered from anaphylactic-type reactions, fish became tolerant to tick saliva by still unknown mechanisms. Differences in the presentations of allergic reactions between Experiments 1 and 2 may be due to the amount of tick saliva injected in fish (2.5 μL in Experiment 1 vs. 1 μL in Experiment 2). These results suggested a role for red meat consumption in the allergic reactions to tick saliva in zebrafish and in a rapid desensitization process to become tolerant to tick saliva.

In humans, anti–α-Gal IgE antibody levels (≥0.35 kU/L) have been identified like a risk factor for the development of the AGS (Commins et al., 2009; Van Nunen et al., 2009; Platts-Mills et al., 2015; Steinke et al., 2015; Galili, 2018; Cabezas-Cruz et al., 2019; de la Fuente et al., 2019; Hilger et al., 2019). Recently and albeit that cofactors are influential in the expression of mammalian meat allergy (Platts-Mills et al., 2020), Mabelane et al. (2018) reported that anti–α-Gal IgE antibody levels higher than 5.5 kU/L are an indicator of AGS with 95% confidence. Herein we showed that zebrafish as humans do not synthesize α-Gal and produce natural anti–α-Gal IgM antibodies in response to gut bacterial microbiota. However, in zebrafish, a significant correlation was not observed between anti–α-Gal IgM antibody

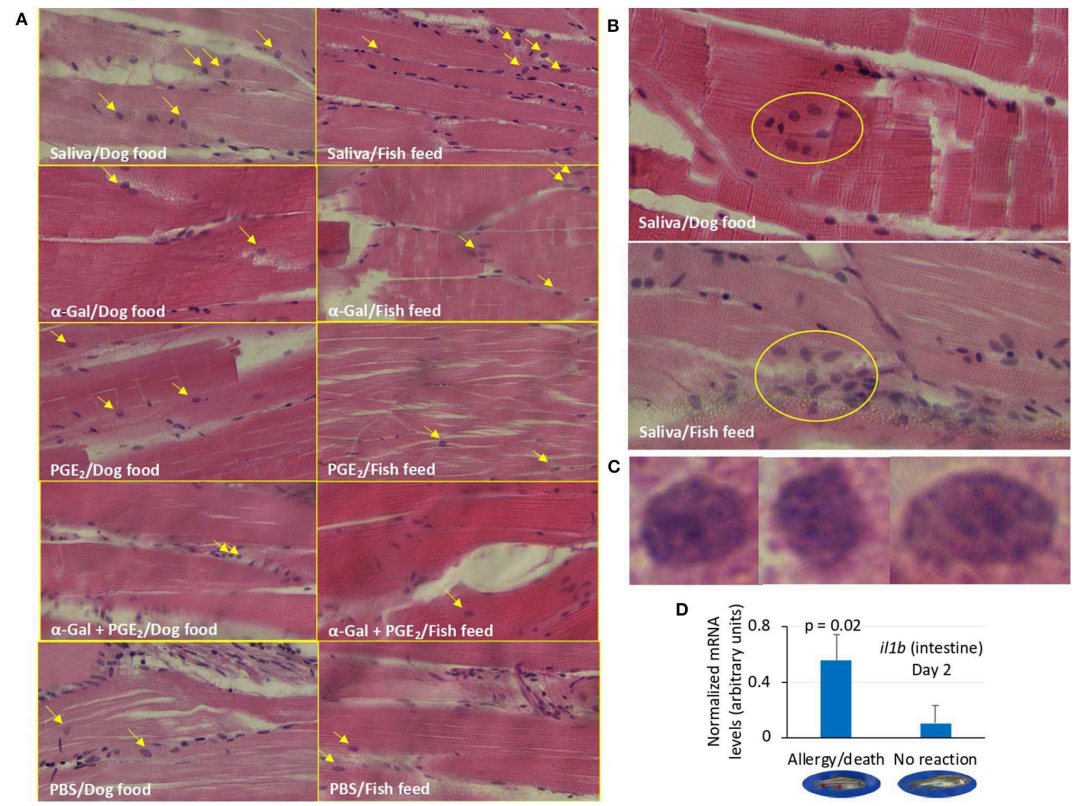

FIGURE 9 | Granulocyte profile in zebrafish (Experiment 1). **(A)** Representative images of granulocytes detected in tissue sections stained with hematoxylin and eosin of zebrafish treated with saliva, α-Gal, PGE_2, or α-Gal + PGE_2, or the PBS control and fed with dog food or fish feed. The fields were randomly chosen, and granulocytes are indicated with arrows. The average counts of granulocytes were compared between fish treated with tick saliva, α-Gal, or PGE_2 α-Gal + PGE_2, and PBS-treated controls and between fish fed on dog food or fish feed for each treatment by Student *t*-test with unequal variance ($p < 0.05$; $N = 3$–6; **Supplementary Figure 4**). Most granulocytes were observed in the skeletal muscle. Magnification ×40. **(B)** Representative images of granulocytes agglomerations only detected in zebrafish treated with tick saliva. Magnification ×40. **(C)** Selected images for identified granulocytes showing characteristics of basophils/eosinophils. Magnification ×100. **(D)** The expression of selected immune response and food allergy markers was analyzed by qRT-PCR in the kidney and intestine of zebrafish treated with saliva and presenting anaphylactic-type reactions and death on day 2, and fish without reactions and normalized mRNA Ct values (average ± SD) were compared by Student *t*-test with unequal variance ($p < 0.05$; $N = 3$–6). Only *il1b* gene in the intestine showed significant differences.

levels and allergic reactions to tick saliva, but IgM antibody levels higher than 0.6 OD at 450 nm were identified as a risk factor for developing anaphylactic-type reactions to tick saliva and red meat consumption. Nevertheless, these results may be affected by the fact that the antibody levels in zebrafish dying from anaphylactic-type reactions were determined on day 2 after a single treatment with tick saliva, whereas most fish were treated three times and sera collected on day 14 for analysis.

To identify the possible immune mechanisms associated with allergic reactions observed in zebrafish in response to tick saliva and red meat consumption, selected immune response and food allergy markers involved in T_H1 and T_H2 cell–mediated responses (Lu et al., 2008; Huang et al., 2018) were characterized in the kidney and intestine involved in both innate and adaptive fish immunity (Liu et al., 2015; Brugman, 2016; Martins et al., 2019). The $CD4^+$ T cells or T helper cells develop into T_H1 and T_H2 cells (**Figure 10A**). While type 1 T helper (T_H1) cells produce interferon (IFN), interelukin 1 (IL-1), and Mxa, among other proteins, for cell-mediated immunity and macrophage-dependent protective responses, T_H2 cells produce IL-1, IL-4, and other cytokines to induce antibody-mediated adaptive immune response and inhibition of several macrophage functions (Romagnani, 1999). Other cytokines such as IL-3 and regulated factors (NFIL-3) are produced by both T_H1 and T_H2 cells (Romagnani, 1999). Additionally, T_H1 cells are involved in the pathogenesis of organ-specific autoimmune disorders, whereas T_H2 mediates allergen-specific responses (Romagnani, 1999).

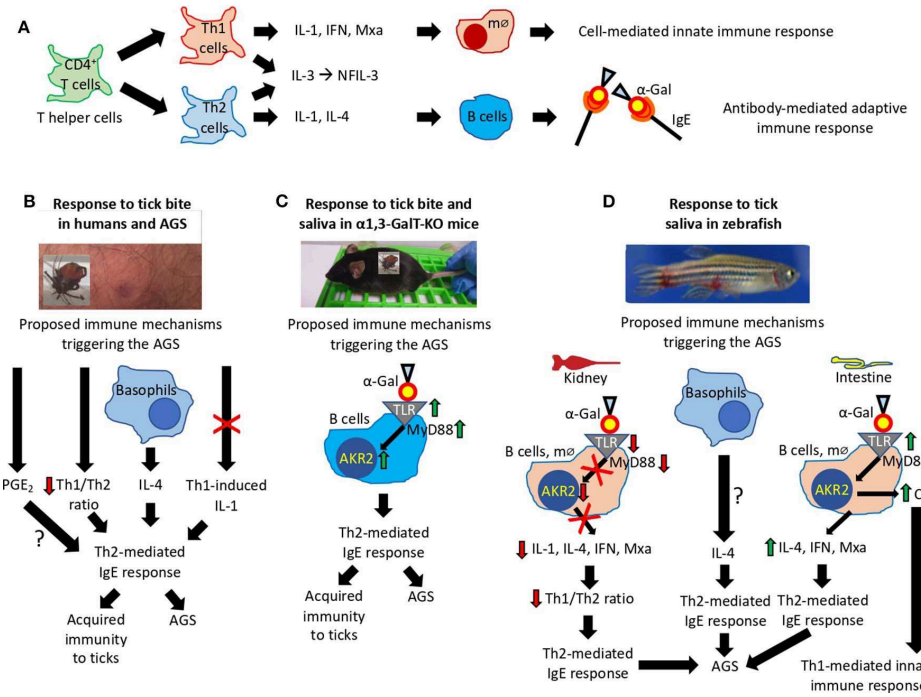

FIGURE 10 | Proposed mechanisms triggering the AGS. **(A)** Mechanisms mediated by $CD4^+$ T cells or T helper (T_H) cells that develop into T_H1 and T_H2 cells regulating cell-mediated and antibody-mediated innate and adaptive immune responses, respectively. **(B–D)** Immune mechanisms triggering the AGS that have been proposed based on existing evidence in **(B)** humans, **(C)** α1,3-GalT-KO mice, and **(D)** our zebrafish animal model. The interrogation marks (?) represent mechanisms that need additional evidence to be sustained.

In humans, the AGS has been proposed to be associated with tick saliva–induced inhibition of T_H1-induced production of IL-1, basophil-mediated production of IL-4, decrease in T_H1/T_H2 ratio, and PGE_2-induced antibody class switching, all resulting in the induction of T_H2-mediated IgE response against α-Gal (Cabezas-Cruz et al., 2019; Kageyama et al., 2019) (**Figure 10B**). As recently concluded by Kageyama et al. (2019), repeated tick bites promote basophil recruitment and attract T_H2 cells to the skin, which results in a proper cytokine milieu to enhance IgE antibody levels against tick proteins and α-Gal to facilitate acquired immunity to ticks and the AGS.

In the α1,3-GalT-KO mouse model, the induction of α-Gal–specific IgE antibodies following tick feeding and in response to subcutaneous injection of tick saliva was proposed to be associated with the salivary proteins modified with α-Gal–like antigens that might modulate host immune response toward anti–α-Gal IgE antibodies (Araujo et al., 2016). However, recently Román-Carrasco et al. (2019) provided evidence supporting that glycolipids but not glycoproteins containing α-Gal were able to cross the intestinal monolayer and trigger an allergic reaction such as the AGS. To characterize the immune mechanisms leading to production of IgE antibodies and allergic reactions in response to tick bites and red meat consumption, Chandrasekhar et al. (2019) showed in the α1,3-GalT-KO mouse model that the induction of IgE responses was dependent on $CD4^+$ T cells and the expression of the B cell-intrinsic MyD88 adaptor for inflammatory Toll-like receptor (TLR) and IL-1 signaling pathways leading, among others, to the activation of the Akr2/nuclear factor κB (NF-κB) (Deguine and Barton, 2014) (**Figure 10C**).

The results reported here in the zebrafish model support some of the previously proposed immune mechanisms triggering the AGS and provided evidence for different tissue-specific mechanisms also potentially involved in the AGS (**Figure 10D**). While in zebrafish kidney α-Gal–containing glycolipids and glycoproteins may antagonize TLR-mediated response to promote T_H2-mediated IgE response to α-Gal, in the intestine a mechanism similar to that proposed in humans and mouse model may trigger AGS through activation of TLR by α-Gal leading to production of proinflammatory cytokines and anti–α-Gal IgE response. As proposed for humans in response to tick saliva, basophils in zebrafish may be also recruited to attract T_H2 cells producing IL-4 to the muscle inducing T_H2-mediated IgE response to α-Gal. Basophils/eosinophils have been described in zebrafish and other fish species, but the functional role of these cells in immune response and allergy has not been previously

characterized (Ainsworth, 1992; Bennett et al., 2001). The fact that *il1b* was the only gene upregulated in zebrafish suffering and dying of hemorrhagic anaphylactic-type reactions in response to tick saliva on day 2 and the regulation of this gene after red meat consumption suggesting a key role for this cytokine, which has been previously shown to promote adhesion of basophils, eosinophils, and neutrophils to human vascular endothelial cells (Bochner et al., 1991). Although a role for PGE_2 during AGS has been proposed in humans (Cabezas-Cruz et al., 2017c), in the zebrafish model we did not find a correlation between this prostaglandin and the allergic response to tick saliva.

Based on the evidence obtained from studies in humans and the mouse and zebrafish animal models, the proposed mechanisms triggering the AGS involve TLR-mediated responses in both T_H1 and T_H2 cells with a role for basophils in this process (**Figures 10B–D**). The TLRs play a role in immune response by initiating signaling cascades that result in the recruitment of signaling adaptors such as MyD88 to trigger the formation of supramolecular organizing centers that coordinate various cellular responses such as translocation of Akr2/NF-κB and the activation of immune cells leading to the expression of proinflammatory cytokines and IFNs (Rosadini and Kagan, 2015). Pathogen-derived glycoproteins and glycolipids interact with TLRs with different outcomes. The TLR4 sensors bacterial lipopolysaccharides that activate the MyD88-dependent pathway resulting in Akr2/NF-κB activation leading to the production of IFN and proinflammatory cytokines (Perrin-Cocon et al., 2017). However, pathogen-derived glycolipids and glycoproteins can antagonize TLR-mediated response to interfere with cellular immune response (Hajishengallis and Lambris, 2011; Cochet et al., 2019). Basophil levels increase and infiltrate lesions after tick infestations contributing to acquired immunity and secretion of the histamine-repellent factor in tick-resistant animals (Karasuyama et al., 2018b; Tabakawa et al., 2018). Basophils have been also shown to activate T_H2 IL-4–mediated responses (Karasuyama et al., 2018a), which may lead to acquired immunity to ticks and the high anti–α-Gal IgE antibody levels associated with the AGS (Kageyama et al., 2019). Additionally, basophils may attract T_H2 cells to the tick bite site to induce intrinsic T_H2 immunity-promoting adjuvant function of tick salivary components to enhance IgE response to α-Gal–containing tick proteins causing the AGS (Hilger et al., 2019; Kageyama et al., 2019).

CONCLUSIONS

In this study, a new animal model was developed using zebrafish for the study of allergic reactions in response to tick salivary biogenic substances and red meat consumption. The observed allergic hemorrhagic anaphylactic-type reactions and abnormal behavior patterns may occur in response to toxic and anticoagulant biogenic compounds different from α-Gal present in tick saliva. Furthermore, host-derived and not only tick-derived molecules with α-Gal may be involved in the AGS (Platts-Mills et al., 2020). However, the results showed that only zebrafish previously exposed to tick saliva and fed on dog food developed hemorrhagic anaphylactic-type allergic reactions and/or abnormal behavior or feeding patterns with rapid desensitization and tolerance. These allergic reactions were associated with tissue-specific TLR-mediated responses in T_H1 and T_H2 cells with a possible role for basophils in the immune response to tick saliva. The results obtained in this proof-of-concept study support some of the previously proposed immune mechanisms triggering the AGS in humans and the α1,3-GalT-KO mouse model and provided evidence for different tissue-specific mechanisms also potentially involved in the AGS. These results support the use of the zebrafish animal model for the study of the AGS and other tick-borne allergies.

DATA AVAILABILITY STATEMENT

All datasets generated for this study are included in the article/**Supplementary Material**.

ETHICS STATEMENT

The animal study was reviewed and approved by Ethics Committee on Animal Experimentation of the University of Castilla La Mancha (PR-2018-06-13) and the Counseling of Agriculture, Environment and Rural Development of Castilla La Mancha (ES130340000218).

AUTHOR CONTRIBUTIONS

JF and AC-C: conceptualization. JF: methodology, writing-original draft preparation, visualization, supervision, and project administration. MC, IP, and LM-H: validation. MC and JF: formal analysis. MC, IP, PA, SD-S, SA-J, LM-H, and MV: investigation. JF, MC, PA, SA-J, and AC-C: writing-review and editing. JF and MV: funding acquisition.

FUNDING

This study was funded by the Consejería de Educación, Cultura y Deportes, JCCM, Spain, project CCM17-PIC-036 (SBPLY/17/180501/000185). MV was supported by the University of Castilla La Mancha, Spain.

ACKNOWLEDGMENTS

We thank Gabriela de la Fuente (Sabiotec spin-off S.L., Spain) for assistance with collection of *R. sanguineus* ticks, Almudena González García (IREC, Spain) for technical assistance with the fish experimental facility, Francisca Talavera for technical assistance with histochemical analyses and Juan Galcerán Sáez (IN-CSIC-UMH, Spain) for providing zebrafish.

SUPPLEMENTARY MATERIAL

The Supplementary Material for this article can be found online at: https://www.frontiersin.org/articles/10.3389/fcimb.2020.00078/full#supplementary-material

REFERENCES

Ainsworth, A. J. (1992). Fish granulocytes: morphology, distribution, and function. *Annu. Rev. Fish Dis.* 2, 123–148.

Aleman, M. M., and Wolberg, A. S. (2013). Tick spit shines a light on the initiation of coagulation. *Circulation* 128, 203–205. doi: 10.1161/CIRCULATIONAHA.113.003800

Araujo, R. N., Franco, P. F., Rodrigues, H., Santos, L. C. B., McKay, C. S., Sanhueza, C. A., et al. (2016). *Amblyomma sculptum* tick saliva: alpha-Gal identification, antibody response and possible association with red meat allergy in Brazil. *Int. J. Parasitol.* 46, 213–220. doi: 10.1016/j.ijpara.2015.12.005

Bennett, C. M., Kanki, J. P., Rhodes, J., Liu, T. X., Paw, B. H., Kieran, M. W., et al. (2001). Myelopoiesis in the zebrafish, *Danio rerio*. *Blood*. 98, 643–651. doi: 10.1182/blood.v98.3.643

Bochner, B. S., Luscinskas, F. W., Gimbrone, M. A. Jr, Newman, W., Sterbinsky, S. A., Derse-Anthony, C. P., et al. (1991). Adhesion of human basophils, eosinophils, and neutrophils to interleukin 1-activated human vascular endothelial cells: contributions of endothelial cell adhesion molecules. *J. Exp. Med.* 173, 1553–1557. doi: 10.1084/jem.173.6.1553

Brugman, S. (2016). The zebrafish as a model to study intestinal inflammation. *Dev. Comp. Immunol.* 64, 82–92. doi: 10.1016/j.dci.2016.02.020

Cabezas-Cruz, A., de la Fuente, J., Fischer, J., Hebsaker, J., Lupberger, E., Blumenstock, G., et al. (2017a). Prevalence of type I sensitization to alpha-gal in forest service employees and hunters: Is the blood type an overlooked risk factor in epidemiological studies of the α-Gal syndrome? *Allergy* 72, 2044–2047. doi: 10.1111/all.13206

Cabezas-Cruz, A., Hodžić, A., Román-Carrasco, P., Mateos-Hernández, L., Duscher, G. G., Sinha, D. K., et al. (2019). Environmental and molecular drivers of the α-Gal syndrome. *Front. Immunol.* 10:1210. doi: 10.3389/fimmu.2019.01210

Cabezas-Cruz, A., Mateos-Hernández, L., Alberdi, P., Villar, M., Riveau, G., Hermann, E., et al. (2017b). Effect of blood type on anti-α-Gal immunity and the incidence of infectious diseases. *Exp. Mol. Med.* 49:e301. doi: 10.1038/emm.2016.164

Cabezas-Cruz, A., Mateos-Hernández, L., Chmelar, J., Villar, M., and de la Fuente, J. (2017c). Salivary prostaglandin E2: role in tick-induced allergy to red meat. *Trends Parasitol.* 33, 495–498. doi: 10.1016/j.pt.2017.03.004

Cabezas-Cruz, A., Valdés, J. J., and de la Fuente, J. (2016). Control of vector-borne infectious diseases by human immunity against α-Gal. *Expert Rev. Vaccines* 15, 953–955. doi: 10.1080/14760584.2016.1181547

Cantas, L., Sørby, J. R., Aleström, P., and Sørum, H. (2012). Culturable gut microbiota in zebrafish. *Zebrafish* 9, 26–37. doi: 10.1089/zeb.2011.0712

Chandrasekhar, J. L., Cox, K. M., Loo, W. M., Qiao, H., Tung, K. S., and Erickson, L. D. (2019). Cutaneous exposure to clinically relevant Lone Star ticks promotes IgE production and hypersensitivity through CD4+ T Cell- and MyD88-dependent pathways in mice. *J. Immunol.* 203, 813–824. doi: 10.4049/jimmunol.1801156

Chmelar, J., Kotál, J., Kovaríková, A., and Kotsyfakis, M. (2019). The use of tick salivary proteins as novel therapeutics. *Front. Physiol.* 10:812. doi: 10.3389/fphys.2019.00812

Cochet, F., Facchini, F. A., Zaffaroni, L., Billod, J. M., Coelho, H., Holgado, A., et al. (2019). Novel carboxylate-based glycolipids: TLR4 antagonism, MD-2 binding and self-assembly properties. *Sci. Rep.* 9:919. doi: 10.1038/s41598-018-37421-w

Commins, S. P., Satinover, S. M., Hosen, J., Mozena, J., Borish, L., Lewis, B. D., et al. (2009). Delayed anaphylaxis, angioedema, or urticaria after consumption of red meat in patients with IgE antibodies specific for galactose-alpha-1,3-galactose. *J. Allergy Clin. Immunol.* 123, 426–433. doi: 10.1016/j.jaci.2008.10.052

de la Fuente, J., Antunes, S., Bonnet, S., Cabezas-Cruz, A., Domingos, A., Estrada-Peña, A., et al. (2017). Tick-pathogen interactions and vector competence: identification of molecular drivers for tick-borne diseases. *Front. Cell. Infect. Microbiol.* 7:114. doi: 10.3389/fcimb.2017.00114

de la Fuente, J., Ayoubi, P., Blouin, E. F., Almazán, C., Naranjo, V., and Kocan, K. M. (2005). Gene expression profiling of human promyelocytic cells in response to infection with *Anaplasma phagocytophilum*. *Cell. Microbiol.* 7, 549–559. doi: 10.1111/j.1462-5822.2004.00485.x

de la Fuente, J., Estrada-Pena, A., Venzal, J. M., Kocan, K. M., and Sonenshine, D. E. (2008). Overview: ticks as vectors of pathogens that cause disease in humans and animals. *Front. Biosci.* 13, 6938–6946. doi: 10.2741/3200

de la Fuente, J., Pacheco, I., Villar, M., and Cabezas-Cruz, A. (2019). The alpha-Gal syndrome: new insights into the tick-host conflict and cooperation. *Parasit. Vectors* 12:154. doi: 10.1186/s13071-019-3413-z

Deguine, J., and Barton, G. M. (2014). MyD88: a central player in innate immune signaling. *F1000Prime Rep.* 6:97. doi: 10.12703/P6-97

Fast, M. D. (2014). Fish immune responses to parasitic copepod (namely sea lice) infection. *Dev. Comp. Immunol.* 43, 300–312. doi: 10.1016/j.dci.2013.08.019

Francischetti, I. M., Sa-Nunes, A., Mans, B. J., Santos, I. M., and Ribeiro, J. M. (2009). The role of saliva in tick feeding. *Front. Biosci.* 14, 2051–2088. doi: 10.2741/3363

Galili, U. (2018). Evolution in primates by "Catastrophic-selection" interplay between enveloped virus epidemics, mutated genes of enzymes synthesizing carbohydrate antigens, and natural anticarbohydrate antibodies. *Am. J. Phys. Anthropol.* 168, 352–363. doi: 10.1002/ajpa.23745

Goven, B. A., Dawe, D. L., and Gratzek, J. B. (1980). *In vivo* and *in vitro* anaphylactic type reactions in fish. *Dev. Comp. Immunol.* 4, 55–64.

Ha, K., Lewis, K., Patel, V., and Grinceri, J. (2019). A case of tick-borne paralysis in a traveling patient. *Case Rep. Neurol. Med.* 2019:3934696. doi: 10.1155/2019/3934696

Haddad, V. Jr, Haddad, M. R., Santos, M., and Cardoso, J. L. C. (2018). Skin manifestations of tick bites in humans. *An. Bras. Dermatol.* 93, 251–255. doi: 10.1590/abd1806-4841.20186378

Hajishengallis, G., and Lambris, J. D. (2011). Microbial manipulation of receptor crosstalk in innate immunity. *Nat. Rev. Immunol.* 11, 187–200. doi: 10.1038/nri2918

Hilger, C., Fischer, J., Wölbing, F., and Biedermann, T. (2019). Role and mechanism of galactose-alpha-1,3-galactose in the elicitation of delayed anaphylactic reactions to red meat. *Curr. Allergy Asthma Rep.* 19:3. doi: 10.1007/s11882-019-0835-9

Huang, J., Liu, C., Wang, Y., Wang, C., Xie, M., Qian, Y., et al. (2018). Application of *in vitro* and *in vivo* models in the study of food allergy. *Food Sci. Hum. Wellness* 7, 235–243. doi: 10.1016/j.fshw.2018.10.002

Iniguez, E., Schocker, N. S., Subramaniam, K., Portillo, S., Montoya, A. L., Al-Salem, W. S., et al. (2017). An α-Gal-containing neoglycoprotein-based vaccine partially protects against murine cutaneous leishmaniasis caused by *Leishmania major*. *PLoS Negl. Trop. Dis.* 11:e0006039. doi: 10.1371/journal.pntd.0006039

Kageyama, R., Fujiyama, T., Satoh, T., Keneko, Y., Kitano, S., Tokura, Y., et al. (2019). The contribution made by skin-infiltrating basophils to the development of alpha gal syndrome. *Allergy*. 74, 1805–1807. doi: 10.1111/all.13794

Kalueff, A. V., Gebhardt, M., Stewart, A. M., Cachat, J. M., Brimmer, M., Chawla, J. S., et al. (2013). Towards a comprehensive catalog of Zebrafish Behavior 1.0 and Beyond. *Zebrafish* 10, 70–86. doi: 10.1089/zeb.2012.0861

Karasuyama, H., Miyake, K., Yoshikawa, S., Kawano, Y., and Yamanishi, Y. (2018a). How do basophils contribute to Th2 cell differentiation and allergic responses? *Int. Immunol.* 30, 391–396. doi: 10.1093/intimm/dxy026

Karasuyama, H., Tabakawa, Y., Ohta, T., Wada, T., and Yoshikawa, S. (2018b). Crucial role for basophils in acquired protective immunity to tick infestation. *Front. Physiol.* 9:1769. doi: 10.3389/fphys.2018.01769

Lee, H., Halverson, S., and Mackey, R. (2016). Insect allergy. *Prim. Care* 43, 417–431. doi: 10.1016/j.pop.2016.04.010

Lima-Barbero, J. F., Sánchez, M. S., Cabezas-Cruz, A., Mateos-Hernández, L., Contreras, M., Fernández de Mera, I. G. F., et al. (2019). Clinical gamasoidosis and antibody response in two patients infested with *Ornithonyssus bursa* (Acari: Gamasida: Macronyssidae). *Exp. Appl. Acarol.* 78, 555–564. doi: 10.1007/s10493-019-00408-x

Liu, X., Wu, H., Liu, Q., Wang, Q., Xiao, J., Chang, X., et al. (2015). Profiling immune response in zebrafish intestine, skin, spleen and kidney bath-vaccinated with a live attenuated *Vibrio anguillarum* vaccine. *Fish Shellfish Immunol.* 45, 342–345. doi: 10.1016/j.fsi.2015.04.028

Livak, K. J., and Schmittgen, T. D. (2001). Analysis of relative gene expression data using real-time quantitative PCR and the 2(-Delta Delta C(T)) Method. *Methods* 25, 402–408. doi: 10.1006/meth.2001.1262

Lu, M. W., Chao, Y. M., Guo, T. C., Santi, N., Evensen, O., Kasani, S. K., et al. (2008). The interferon response is involved in nervous necrosis virus acute and persistent infection in zebrafish infection model. *Mol. Immunol.* 45, 1146–1152. doi: 10.1016/j.molimm.2007.07.018

Mabelane, T., Basera, W., Botha, M., Thomas, H. F., Ramjith, J., and Levin, M. E. (2018). Predictive values of alpha-gal IgE levels and alpha-gal IgE: total IgE ratio and oral food challenge-proven meat allergy in a population with a high prevalence of reported red meat allergy. *Pediatr. Allergy Immunol.* 29, 841–849. doi: 10.1111/pai.12969

Martins, R. R., Ellis, P. S., MacDonald, R. B., Richardson, R. J., and Henriques, C. M. (2019). Resident immunity in tissue repair and maintenance: the zebrafish model coming of age. *Front. Cell. Dev. Biol.* 7:12. doi: 10.3389/fcell.2019.00012

Mateos-Hernández, L., Villar, M., Moral, A., Rodríguez, C. G., Arias, T. A., de la Osa, V., et al. (2017). Tick-host conflict: immunoglobulin E antibodies to tick proteins in patients with anaphylaxis to tick bite. *Oncotarget* 8, 20630–20644. doi: 10.18632/oncotarget.15243

Mihara, M. (2017). Histopathologic study of the human skin in the early stage after a tick bite: a special reference to cutaneous tissue reaction to the cement substance of tick saliva. *Yonago Acta Med.* 60, 186–199. doi: 10.33160/yam.2017.09.009

Mingomataj, E. C., and Bakiri, A. H. (2012). Episodic hemorrhage during honeybee venom anaphylaxis: potential mechanisms. *J. Investig. Allergol. Clin. Immunol.* 22, 237–244.

Moura, A. P. V., Santos, L. C. B., Brito, C. R. N., Valencia, E., Junqueira, C., Filho, A. A. P., et al. (2017). Virus-like particle display of the α-Gal carbohydrate for vaccination against *Leishmania* infection. *ACS Cent Sci.* 3, 1026–1031. doi: 10.1021/acscentsci.7b00311

Oliveira, C. J., Sá-Nunes, A., Francischetti, I. M., Carregaro, V., Anatriello, E., Silva, J. S., et al. (2011). Deconstructing tick saliva: non-protein molecules with potent immunomodulatory properties. *J. Biol. Chem.* 286, 10960–10969. doi: 10.1074/jbc.M110.205047

Øverli, Ø., Nordgreen, J, Mejdell, C. M., Janczak, A. M., Kittilsen, S., Johansen, I. B., et al. (2014). Ectoparasitic sea lice (*Lepeophtheirus salmonis*) affect behavior and brain serotonergic activity in Atlantic salmon (*Salmo salar* L.): perspectives on animal welfare. *Physiol. Behav.* 132, 44–50. doi: 10.1016/j.physbeh.2014.04.031

Park, Y., Kim, D., Boorgula, G. D., De Schutter, K., Smagghe, G., Šimo, L., et al. (2020). Alpha-gal and cross-reactive carbohydrate determinants in the N-glycans of salivary glands in the lone star tick, *Amblyomma americanum*. *Vaccines* 8:E18. doi: 10.3390/vaccines8010018

Parmentier, H. K., De Vries Reilingh, G., and Lammers, A. (2008). Decreased specific antibody responses to alpha-Gal-conjugated antigen in animals with preexisting high levels of natural antibodies binding alpha-Gal residues. *Poult. Sci.* 87, 918–926. doi: 10.3382/ps.2007-00487

Perrin-Cocon, L., Aublin-Gex, A., Sestito, S. E., Shirey, K. A., Patel, M. C., André, P., et al. (2017). TLR4 antagonist FP7 inhibits LPS-induced cytokine production and glycolytic reprogramming in dendritic cells, and protects mice from lethal influenza infection. *Sci. Rep.* 7:40791. doi: 10.1038/srep40791

Platts-Mills, T. A., Schuyler, A. J., Tripathi, A., and Commins, S. P. (2015). Anaphylaxis to the carbohydrate side chain alpha-gal. *Immunol. Allergy Clin. North Am.* 35, 247–260. doi: 10.1016/j.iac.2015.01.009

Platts-Mills, T. A. E., Commins, S. P., Biedermann, T., et al. (2020). On the cause and consequences of IgE to galactose-α-1,3-galactose: a Report from the National Institute of Allergy and Infectious Disease Workshop on Understanding IgE-Mediated Mammalian Meat Allergy. *J. Allergy Clin. Immunol.* doi: 10.1016/j.jaci.2020.01.047. [Epub ahead of print].

Poole, N. M., Mamidanna, G., Smith, R. A., Coons, L. B., and Cole, J. A. (2013). Prostaglandin E2 in tick saliva regulates macrophage cell migration and cytokine profile. *Parasit. Vectors* 6:261. doi: 10.1186/1756-3305-6-261

Portillo, S., Zepeda, B. G., Iniguez, E., Olivas, J. J., Karimi, N. H., Moreira, O. C., et al. (2019). A prophylactic α-Gal-based glycovaccine effectively protects against murine acute Chagas disease. *NPJ Vaccines* 4:13. doi: 10.1038/s41541-019-0107-7

Ririe, K. M., Rasmussen, R. P., and Wittwer, C. T. (1997). Product differentiation by analysis of DNA melting curves during the polymerase chain reaction. *Anal. Biochem.* 245, 154–160.

Romagnani, S. (1999). Th1/Th2 cells. *Inflamm. Bowel Dis.* 5, 285–294.

Román-Carrasco, P., Lieder, B., Somoza, V., Ponce, M., Szépfalusi, Z., Martin, D., et al. (2019). Only aGal bound to lipids, but not to proteins, is transported across enterocytes as an IgE reactive molecule that can induce effector cell activation. *Allergy* 74, 1956–1968. doi: 10.1111/all.13873

Rosadini, C. V., and Kagan, J. C. (2015). Microbial strategies for antagonizing Toll-like-Receptor signal transduction. *Curr. Opin. Immunol.* 32, 61–70. doi: 10.1016/j.coi.2014.12.011

Schartl, M. (2014). Beyond the zebrafish: diverse fish species for modeling human disease. *Dis. Model. Mech.* 7, 181–192. doi: 10.1242/dmm.012245

Steinke, J. W., Platts-Mills, T. A., and Commins, S. P. (2015). The alpha-gal story: lessons learned from connecting the dots. *J. Allergy Clin. Immunol.* 135, 589–596. doi: 10.1016/j.jaci.2014.12.1947

Stringer, T., Ghazi, E., Alvarez Del Manzano, G., Beasley, J., Brinster, N., and Oza, V. S. (2017). Tick bite mimicking indeterminate cell histiocytosis. *Pediatr. Dermatol.* 34, e347–e348. doi: 10.1111/pde.13291

Stutzer, C., Richards, S. A., Ferreira, M., Baron, S., and Maritz-Olivier, C. (2018). Metazoan parasite vaccines: present status and future prospects. *Front. Cell. Infect. Microbiol.* 8:67. doi: 10.3389/fcimb.2018.00067

Tabakawa, Y., Ohta, T., Yoshikawa, S., Robinson, E. J., Yamaji, K., Ishiwata, K., et al. (2018). Histamine released from skin-infiltrating basophils but not mast cells is crucial for acquired tick resistance in mice. *Front. Immunol.* 9:1540. doi: 10.3389/fimmu.2018.01540

Uspensky, I. (2014). Tick pests and vectors (Acari: Ixodoidea) in European towns: introduction, persistence and management. *Ticks Tick Borne Dis.* 5, 41–47. doi: 10.1016/j.ttbdis.2013.07.011

Valls, A., Pineda, F., Belver, M., Caballero, T., and López Serrano, M. C. (2007). Anaphylactic shock caused by tick (*Rhipicephalus sanguineous*). *J. Investig. Allergol. Clin. Immunol.* 17, 279–280.

Van Nunen, S. A., O'Connor, K. S., Clarke, L. R., Boyle, R. X., and Fernando, S. L. (2009). An association between tick bite reactions and red meat allergy in humans. *Med. J. Aust.* 190:510–511. doi: 10.5694/j.1326-5377.2009.tb02533.x

Wilson, J. M., Schuyler, A. J., Schroeder, N., and Platts-Mills, T. A. (2017). Galactose-α-1,3-Galactose: atypical food allergen or model IgE hypersensitivity? *Curr. Allergy Asthma Rep.* 17:8. doi: 10.1007/s11882-017-0672-7

Yilmaz, B., Portugal, S., Tran, T. M., Gozzelino, R., Ramos, S., Gomes, J., et al. (2014). Gut microbiota elicits a protective immune response against malaria transmission. *Cell* 159, 1277–1289. doi: 10.1016/j.cell.2014.10.053

Yucel, E., Sipahi Cimen, S., Varol, S., Suleyman, A., Ozdemir, C., and Tamay, Z. U. (2019). Red-meat desensitization in a child with delayed anaphylaxis due to alpha-Gal allergy. *Pediatr. Allergy Immunol.* 30, 771–773. doi: 10.1111/pai.13092

Conflict of Interest: The authors declare that the research was conducted in the absence of any commercial or financial relationships that could be construed as a potential conflict of interest.

Supplementary material. Chapter 2d

Allergic reactions and immunity in response to tick salivary biogenic substances and red meat consumption in the zebrafish model

Marinela Contreras, Iván Pacheco, Pilar Alberdi, Sandra Díaz-Sánchez, Sara Artigas-Jerónimo, Lourdes Mateos-Hernández, Margarita Villar, Alejandro Cabezas-Cruz, José de la Fuente

Supplementary Materials:

Supplementary Figures 1-5

Supplementary Table 1

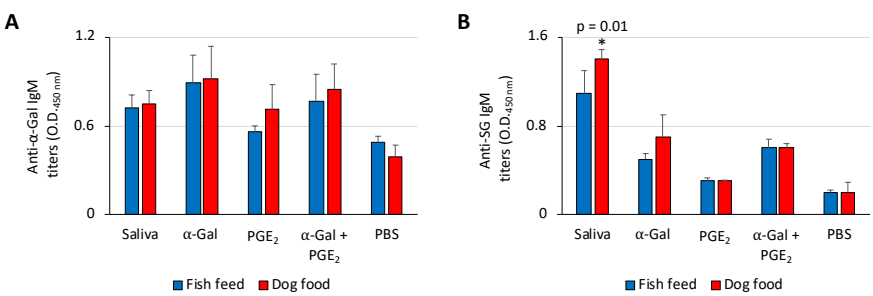

Supplementary Figure 1. Effect of feeding on zebrafish antibody response. The IgM antibody titers against (A) α-Gal and (B) tick salivary gland proteins (SG) were determined by ELISA, represented as the average + S.D. O.D. at 450 nm and compared between zebrafish fed with fish feed or dog food and treated with saliva, α-Gal, PGE_2, α-Gal + PGE_2 and PBS control by Student's t-test with unequal variance (*$p < 0.05$; N = 3-6).

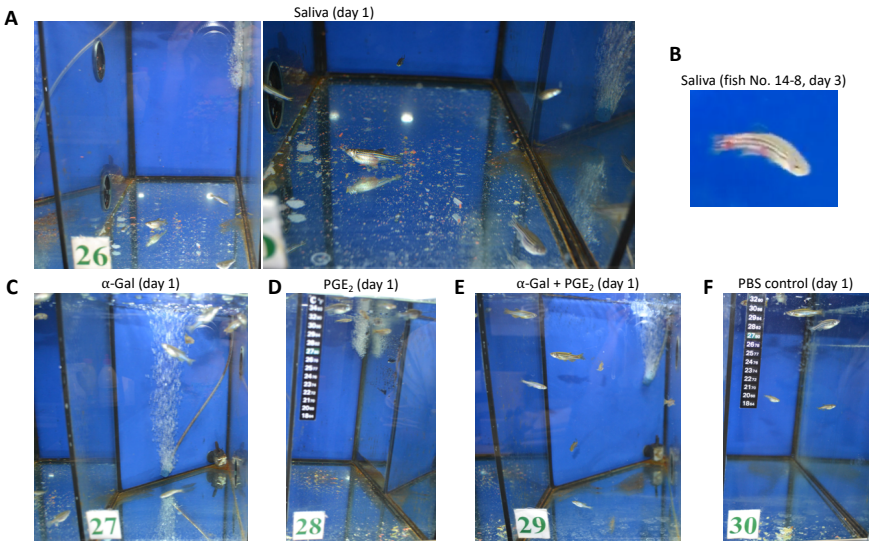

Supplementary Figure 2. Zebrafish injected with tick saliva develop abnormal behavior patterns. (A-F) Zebrafish behavior was recorded at day 1 after treatment. Abnormal behavior patterns consisting of low mobility and permanence at the bottom of the water tank was shown in (A) 3 zebrafish injected with tick saliva, (C) one zebrafish injected with α-Gal and (E) one zebrafish injected with α-Gal + PGE_2. (B) An abnormal zig-zag type swimming was observed at day 3 in fish No. 14-8 injected with tick saliva and fed with dog food (Supplementary Figure 3). Normal behavior patterns were seen in all zebrafish injected with (D) PGE_2 and (F) PBS.

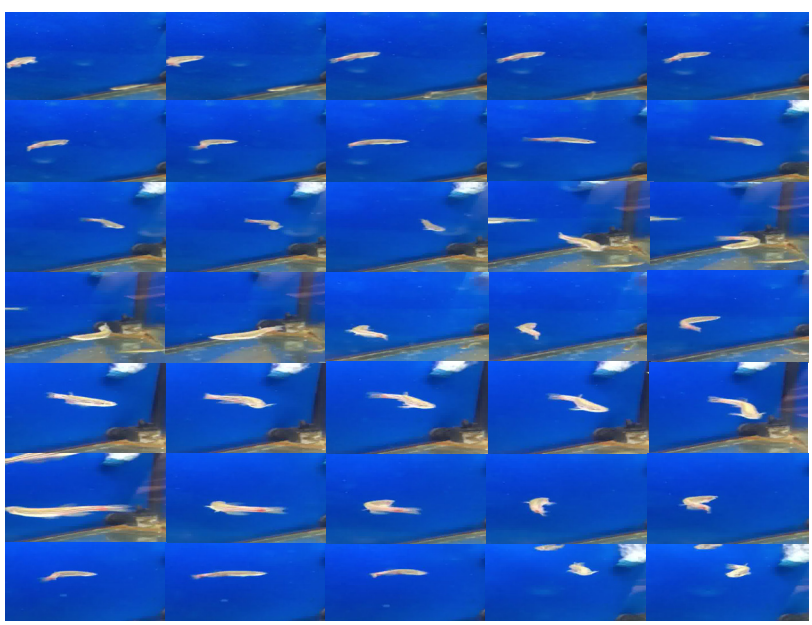

Supplementary Figure 3. Zebrafish injected with tick saliva and fed with dog food develop abnormal behavior patterns. Abnormal zig-zag type swimming at day 3 in zebrafish No. 14-8 injected with tick saliva and fed with dog food. Representative images were extracted from the video (https://youtu.be/ukud2TYN9sQ) using the Filezigzag online file conversion (https://www.filezigzag.com).

Saliva/Dog food

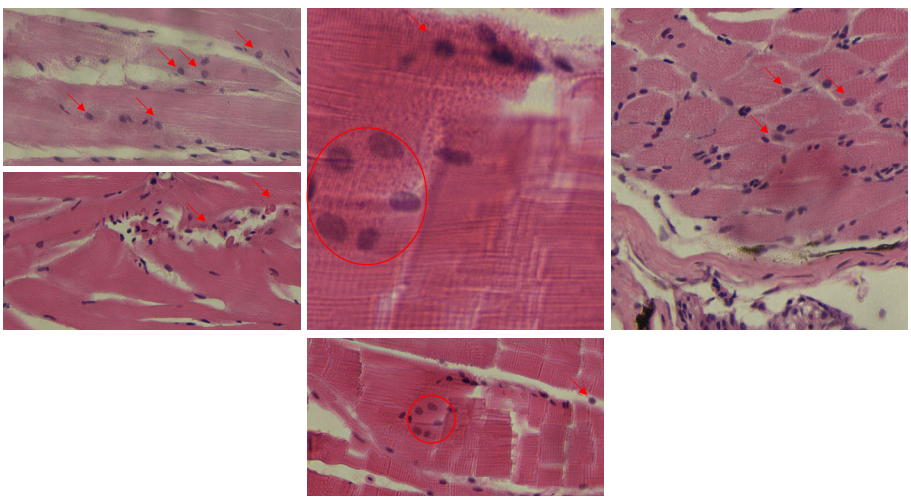

Granulocytes counts Saliva/Dog food	Sample 1	Sample 2	Sample 3	Ave	SD
	9	8	10	9.0	1.0

α-Gal/Dog food

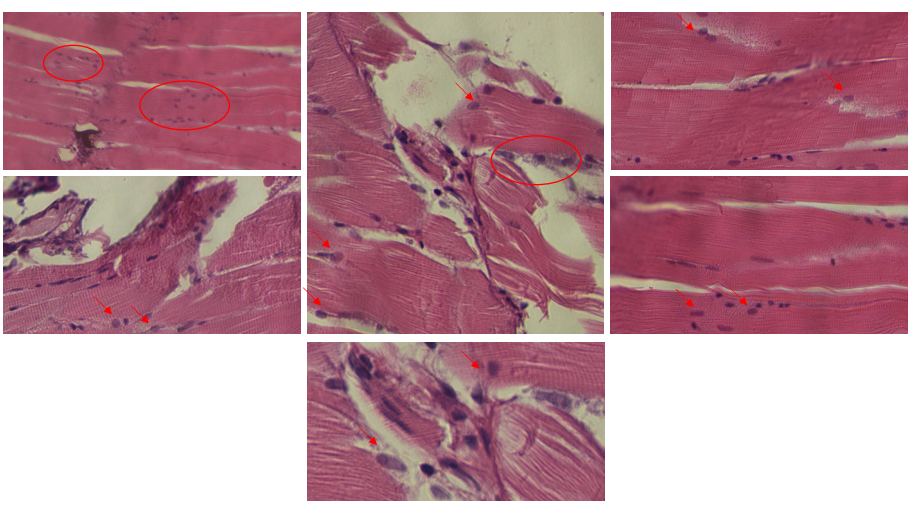

Granulocytes counts α-Gal/Dog food	Sample 1	Sample 2	Sample 3	Ave	SD
	3	2	2	2.3	0.6

PGE_2/Dog food

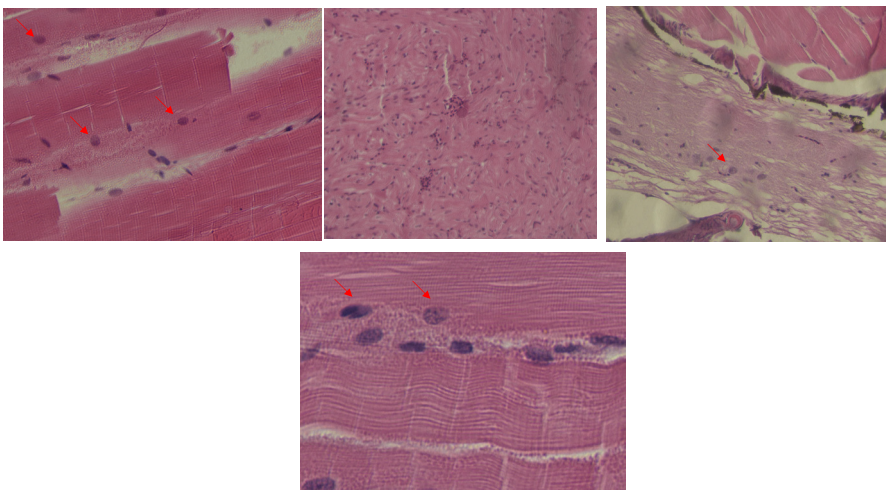

Granulocytes counts	Sample 1	Sample 2	Sample 3	Ave	SD
PEG2/Dog food	4	3	3	3.3	0.6

α-Gal + PGE_2/Dog food

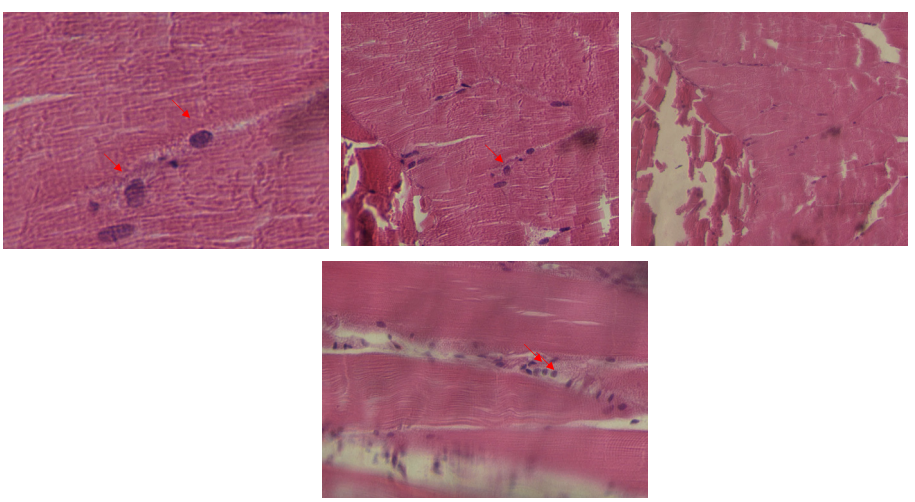

Granulocytes counts	Sample 1	Sample 2	Sample 3	Ave	SD
α-Gal+PGE2/Dog food	2	3	4	3.0	1.0

PBS/Dog food

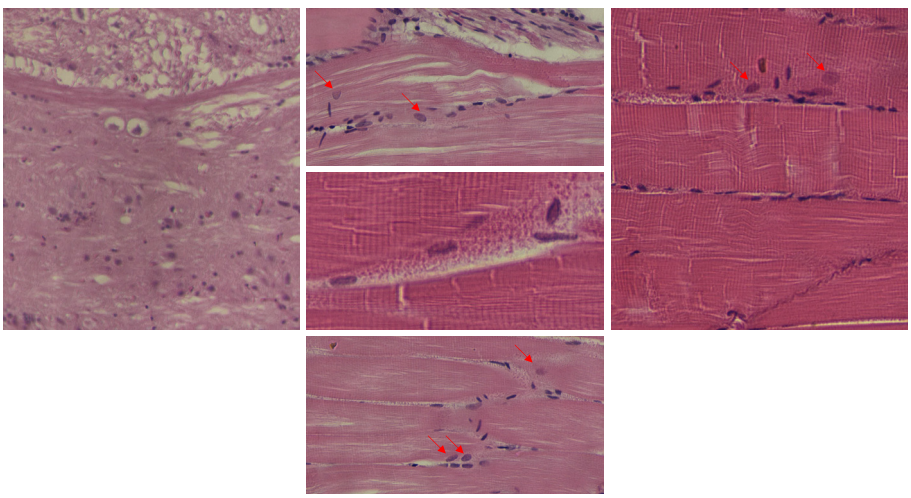

Granulocytes counts	Sample 1	Sample 2	Sample 3	Ave	SD
PBS/Dog food	2	3	3	2.7	0.6

Saliva/Fish feed

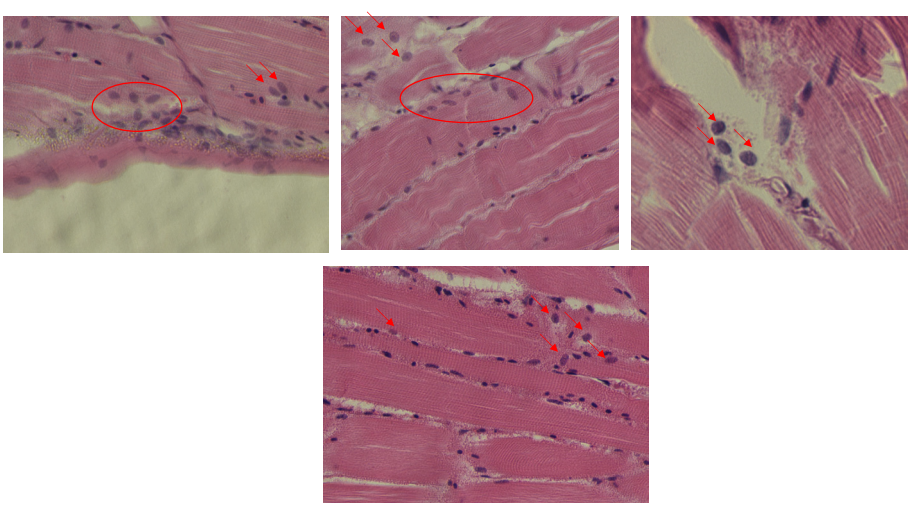

Granulocytes counts	Sample 1	Sample 2	Sample 3	Ave	SD
Saliva/Fish feed	8	9	9	8.7	0.6

α-Gal/Fish feed

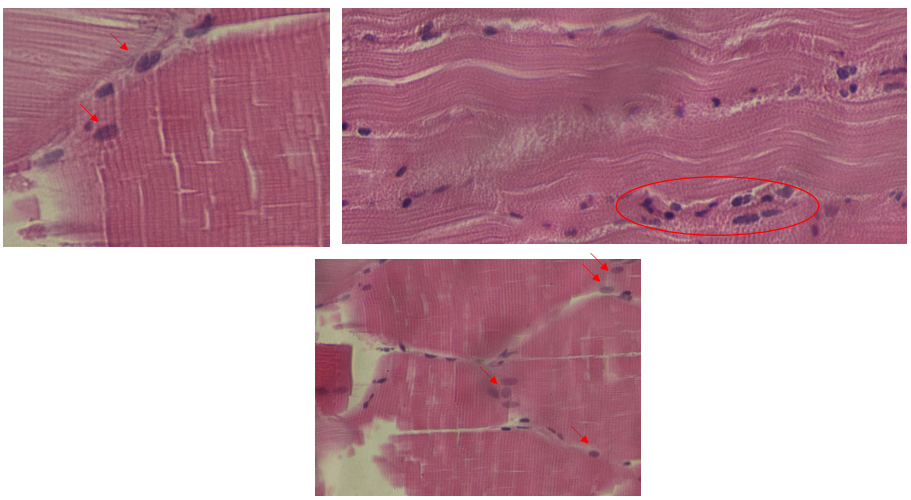

Granulocytes counts	Sample 1	Sample 2	Sample 3	Ave	SD
α-Gal/Fish feed	4	3	2	3.0	1.0

PGE_2/Fish feed

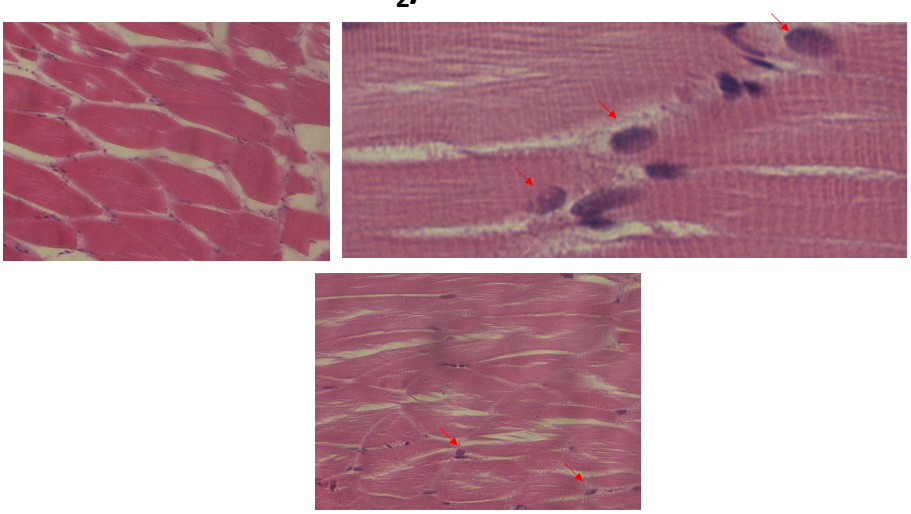

Granulocytes counts	Sample 1	Sample 2	Sample 3	Ave	SD
PGE2/Fish feed	2	3	4	3.0	1.0

α-Gal + PGE_2/Fish feed

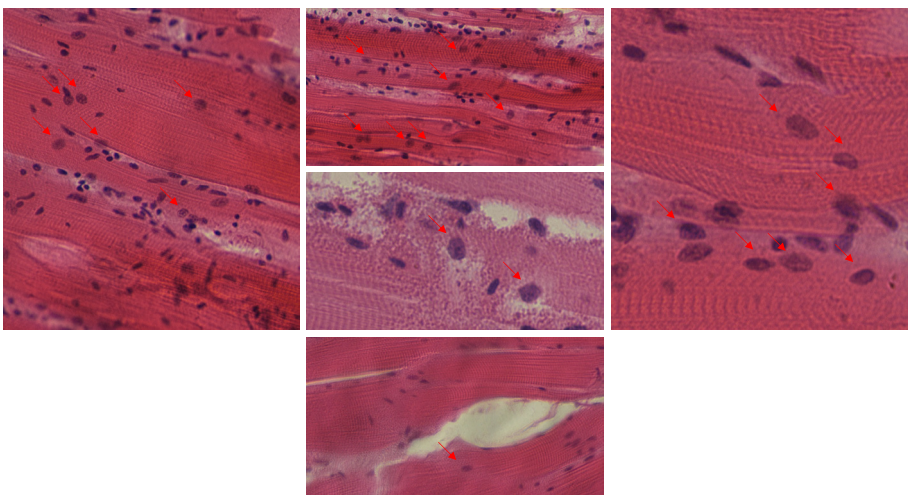

Granulocytes counts α-Gal+PGE2/Fish feed	Sample 1	Sample 2	Sample 3	Ave	SD
	4	2	4	3.3	1.2

PBS/Fish feed

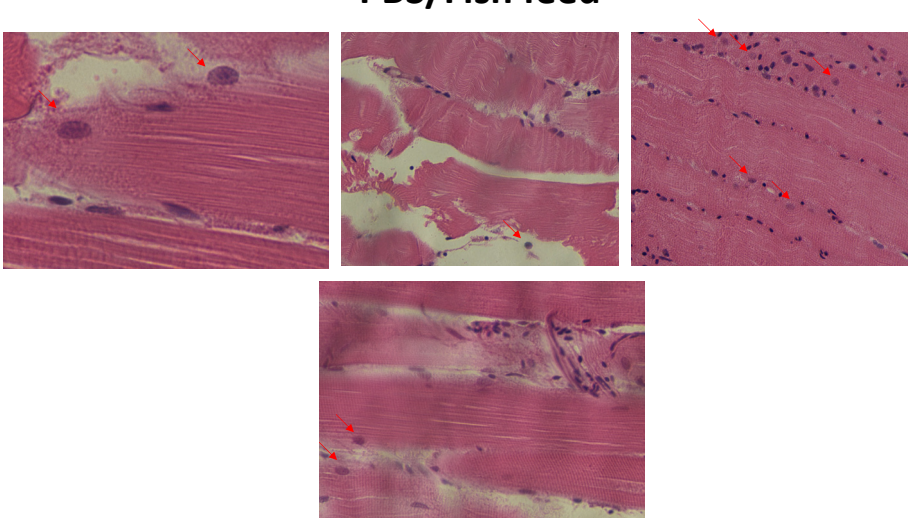

Granulocytes counts PBS/Fish feed	Sample 1	Sample 2	Sample 3	Ave	SD
	2	2	3	2.3	0.6

P (t-Test) Treatment vs. PBS	P (t-Test) Dog vs. Fish feed
Saliva vs. PBS	Saliva
0.00000002	0.32
α-Gal vs. PBS	α-Gal
0.34	0.19
PGE2 vs. PBS	PGE2
0.06	0.32
α-Gal+PGE2 vs. PBS	α-Gal+PGE2
0.09	0.36
	PBS
	0.26

Supplementary Figure 4. Granulocytes in the skeletal muscle of zebrafish. Representative images of granulocytes detected in muscle tissue sections stained with hematoxylin and eosin of zebrafish treated with saliva, α-Gal, PGE_2 or α-Gal + PGE_2 or the PBS control and fed with dog food or fish feed. The fields were randomly chosen, and granulocytes are indicated with arrows. Magnifications, 40X and 100X. The average counts of granulocytes were compared between fish treated with tick saliva, α-Gal or PGE_2 α-Gal + PGE_2 and PBS-treated controls and between fish fed on dog food or fish feed for each treatment by Student's t-test with unequal variance ($p < 0.05$; N = 3-6).

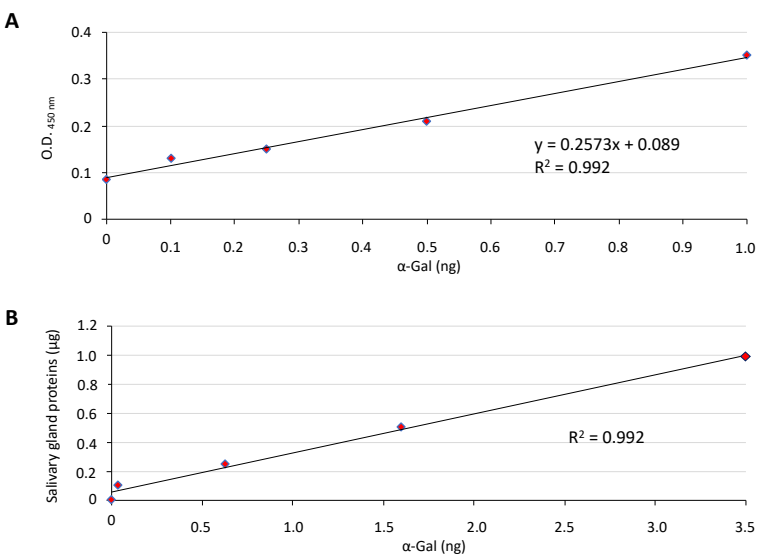

Supplementary Figure 5. ELISA test for characterizing α-Gal levels. The α-Gal levels were determined by ELISA using BSA-α-Gal and *R. sanguineus* salivary gland proteins. The average value of the blanks (wells without sample proteins; N = 5) was subtracted from all reads and the average of 9 replicates for each sample was used for analysis. (A) A calibration curve with 0.0 to 1.0 ng α-Gal and O.D. values at 450 nm was constructed using Microsoft Excel for Mac (v. 16.26) to convert ELISA reader values to α-Gal content per sample. (B) To further validate the calibration curve, a correlation was constructed between 0.0 to 3.5 ng α-Gal and 0.0 to 1.0 µg tick salivary gland proteins using Microsoft Excel for Mac (v. 16.26).

Supplementary Table 1. Oligonucleotide primers and conditions for qRT-PCR.

Gene (Accession No.)	Oligonucleotide primers	Annealing temperature
gapdh NM_001115114.1	Forward: 5′-CGTGGTGCCAGTCAGAACAT-3′ Reverse: 5′-AGTCAGTGGACACAACCTGG-3′	56 ºC
tlr2 NM_212812.1	Forward: 5′-TGAATGGGTCGAGGAGATTC-3′ Reverse: 5′-CACAAAGTGCTCCGACAGAA-3′	56 ºC
tlr4b NM_001131051.1	Forward: 5′-TCACCTGGACAGCAAGAATG-3′ Reverse: 5′-CGATTGACTTCCCTGCTTGA-3′	56 ºC
il1b NM_212844	Forward: 5′-GCATGTCCACATATGCGTCG-3′ Reverse: 5′-GCTGGTCGTATCCGTTTGGA-3′	58 ºC
il4 NM_001170740.1	Forward:5′-GTGAATGGGATCCTGAATGG-3′ Reverse: 5′-TTCCAGTCCCGGTATATGCT-3′	56 ºC
nfil3 NM_001004120.2	Forward: 5′-ATCACCAGGAGGCCCTAACT-3′ Reverse: 5′-CTTTTCAAGCAGGCCACTTC-3′	56 ºC
c3a NM_131243.1	Forward: 5′-ACGCTCTCTGGATTGAAACA-3′ Reverse: 5′-TGCCTTCTTGCATGGCAATC-3′	56 ºC
akr2 NM_213294.2	Forward: 5′-ACTATGGACTTCGATCCGCT-3′ Reverse: 5′-GCTCTGTGGTGAGTGCTGAA-3′	56 ºC
mxa NM_182942.4	Forward: 5′-AGTACCGGGGAAGAGAGCTA-3′ Reverse: 5′-AAGGTGGCATGATTGTCTGT-3′	54 ºC
ifn AJ544822	Forward: 5′-ATGAGAACTCAAATGTGGAC-3′ Reverse: 5′-TTACACTCGAGGATTGAC-3′	50 ºC
myd88 NM_212814.2	Forward: 5′-ATCGCCAGTGAGCTTATCGA-3′ Reverse: 5′-GTCCAGAACCAGACCTGTGT-3′	56 ºC

CHAPTER 3.
Protective capacity and mechanisms in response to alpha-Gal

Chapter 3. Protective capacity and mechanisms in response to alpha-Gal

(a) **Pacheco, I.,** Contreras, M., Villar, M., Risalde, M.A., Alberdi, P., Cabezas-Cruz, A., Gortazar, C., de la Fuente, J. (2020). Vaccination with alpha-Gal protects against mycobacterial infection in the zebrafish model of tuberculosis. Vaccines 8, 195. https://doi.org/10.3390/vaccines8020195

(b) **Pacheco, I.,** Díaz-Sánchez, S., Contreras, M., Villar, M., Cabezas-Cruz, A., Gortázar, C., de la Fuente, J. (2021). Probiotic bacteria with high alpha-Gal content protect zebrafish against mycobacteriosis. Pharmaceuticals 14, 635. https://doi.org/10.3390/ph14070635

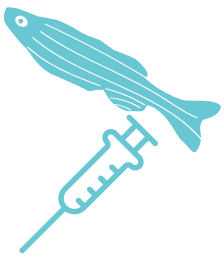

Chapter 3a. Vaccination with alpha-Gal protects against mycobacterial infection in the zebrafish model of tuberculosis

Pacheco, I., Contreras, M., Villar, M., Risalde, M.A., Alberdi, P., Cabezas-Cruz, A., Gortazar, C., de la Fuente, J. (2020). Vaccination with alpha-Gal protects against mycobacterial infection in the zebrafish model of tuberculosis. Vaccines 8, 195. https://doi.org/10.3390/vaccines8020195

vaccines

MDPI

Article

Vaccination with Alpha-Gal Protects Against Mycobacterial Infection in the Zebrafish Model of Tuberculosis

Iván Pacheco [1,†], Marinela Contreras [1,†], Margarita Villar [1,2], María Angeles Risalde [3], Pilar Alberdi [1], Alejandro Cabezas-Cruz [4], Christian Gortázar [1] and José de la Fuente [1,5,*]

1 SaBio Instituto de Investigación en Recursos Cinegéticos IREC-CSIC-UCLM-JCCM, Ronda de Toledo s/n, 13005 Ciudad Real, Spain; ivan.pacheco@uclm.es (I.P.); marinela.contreras@uclm.es (M.C.); MargaritaM.Villar@uclm.es (M.V.); maria.alberdi@uclm.es (P.A.); christian.gortazar@uclm.es (C.G.)
2 Biochemistry Section, Faculty of Science and Chemical Technologies, and Regional Centre for Biomedical Research (CRIB), University of Castilla-La Mancha, 13071 Ciudad Real, Spain
3 Departamento de Anatomía y Anatomía Patológica Comparadas, Facultad de Veterinaria, Universidad de Córdoba (UCO), Agrifood Excellence International Campus (ceiA3), 14071 Córdoba, Spain; mariaa.risalde@uclm.es
4 UMR BIPAR, INRAE, ANSES, Ecole Nationale Vétérinaire d'Alfort, Université Paris-Est, 94700 Maisons-Alfort, France; cabezasalejandrocruz@gmail.com
5 Department of Veterinary Pathobiology, Center for Veterinary Health Sciences, Oklahoma State University, Stillwater, OK 74078, USA
* Correspondence: josedejesus.fuente@uclm.es
† These authors contributed equally.

Received: 24 March 2020; Accepted: 22 April 2020; Published: 24 April 2020

Abstract: The alpha-Gal syndrome (AGS) is associated with tick bites that can induce in humans high levels of IgE antibodies against the carbohydrate Galα1-3Galβ1-(3)4GlcNAc-R (α-Gal) present in glycoproteins and glycolipids from tick saliva that mediate primarily delayed anaphylaxis to mammalian meat consumption. It has been proposed that humans evolved by losing the capacity to synthesize α-Gal to increase the protective immune response against pathogens with this modification on their surface. This evolutionary adaptation suggested the possibility of developing vaccines and other interventions to induce the anti-α-Gal IgM/IgG protective response against pathogen infection and multiplication. However, the protective effect of the anti-α-Gal immune response for the control of tuberculosis caused by *Mycobacterium* spp. has not been explored. To address the possibility of using vaccination with α-Gal for the control of tuberculosis, in this study, we used the zebrafish-*Mycobacterium marinum* model. The results showed that vaccination with α-Gal protected against mycobacteriosis in the zebrafish model of tuberculosis and provided evidence on the protective mechanisms in response to vaccination with α-Gal. These mechanisms included B-cell maturation, antibody-mediated opsonization of mycobacteria, Fc-receptor (FcR)-mediated phagocytosis, macrophage response, interference with the α-Gal antagonistic effect of the toll-like receptor 2 (TLR2)/nuclear factor kappa-light-chain-enhancer of activated B cells (NF-kB)-mediated immune response, and upregulation of pro-inflammatory cytokines. These results provided additional evidence supporting the role of the α-Gal-induced immune response in the control of infections caused by pathogens with this modification on their surface and the possibility of using this approach for the control of multiple infectious diseases.

Keywords: alpha-Gal; vaccine; tuberculosis; vaccine; Mycobacterium; immunology

Vaccines **2020**, *8*, 195

1. Introduction

The alpha-Gal syndrome (AGS), which is now the focus of recent investigations, is associated with tick bites that can induce in humans high levels of IgE antibodies against the carbohydrate Galα1-3Galβ1-(3)4GlcNAc-R (α-Gal) present in glycoproteins and glycolipids from tick saliva that mediate delayed anaphylaxis to mammalian meat consumption and immediate anaphylaxis to tick bites, xenotransplantation, and certain drugs such as cetuximab [1–12]. Within the conflict and cooperation that drove the evolution of tick–host–pathogen interactions [13], humans evolved by losing the capacity to synthesize α-Gal to increase the protective immune response against pathogens with this modification on their surface while increasing the risk to develop the AGS [6]. This evolutionary adaptation suggested the possibility of developing vaccines and other interventions to induce the anti-α-Gal IgM/IgG protective response against pathogen infection to prevent or control major infectious diseases worldwide [14–20].

Recently, the C57BL/6 α1,3-Galactosyltransferase-knockout (α1,3-GalT-KO) mouse animal model was used to study the antibody response to the carbohydrate α-Gal and its potential for the control of infectious diseases such as malaria, leishmaniasis, Chagas disease, granulocytic anaplasmosis, and influenza caused by pathogens with this modification on their surface and/or by enhancing the protective immune response against these pathogens [15–22]. The results showed protection against pathogen infection in response to α-Gal-containing vaccine formulations [15,18–22]. However, the protective effect of the anti-α-Gal immune response for the control of tuberculosis caused by *Mycobacterium* spp. with α-Gal on their surface [17] and constituting one of the deadliest infectious diseases worldwide [23] has not been explored.

To address the possibility of using vaccination with α-Gal for the control of tuberculosis, in this study, we used the zebrafish *Danio rerio* (Hamilton, 1822) animal model. Zebrafish is a model organism for the study of immune mechanisms and new effective vaccines and control strategies against tuberculosis [24–28]. Additionally, zebrafish do not produce α-Gal and were recently shown to reproduce some features of the human immune response to this molecule as a model for the study of the AGS [29]. The results of this study showed that vaccination with α-Gal protects against mycobacterial infection in the zebrafish model of tuberculosis to further advance the possibility of developing a pan-vaccine for the simultaneous control of major infectious diseases worldwide [30]. Additionally, this vaccination strategy may be used for the control of fish mycobacteriosis or piscine tuberculosis affecting multiple freshwater and saltwater fish species and with human incidence worldwide [31].

2. Materials and Methods

2.1. Ethics Statement

Animal experiments were conducted in strict accordance with the recommendations of the European Guide for the Care and Use of Laboratory Animals. Animals were housed at and experiments were conducted at the experimental facility (IREC, Ciudad Real, Spain) with the approval and supervision of the Ethics Committee on Animal Experimentation of the University of Castilla La Mancha (PR-2018-06-13) and the Counseling of Agriculture, Environment, and Rural Development of Castilla La Mancha (ES130340000218).

2.2. Flow Cytometry Analysis of Mycobacterium marinum α-Gal Content

The *M. marinum* Aronson (ATCC 927) was cultured at 29 °C in 7H9 broth enriched with Middlebrook ADC (Becton Dickinson, Franklin Lakes, NJ, USA). The bacteria were washed twice in phosphate-buffered saline (PBS), centrifuges at 4000 g for 5 min, resuspended in PBS, fixed in 4% paraformaldehyde for 30 min at room temperature (RT), and washed once in PBS. The cells were incubated with 3% human serum albumin (HAS; Sigma-Aldrich, St. Louis, MO, USA) in PBS for 1 h at RT. Then, cells were incubated for 14 h at 4 °C with the α-Gal epitope (Galα1-3Galβ1-4GlcNAc-R) monoclonal antibody (M86, Enzo Life Sciences, Farmingdale, NY, USA) diluted 1:50 in 3% human serum

albumin (HAS)/PBS. Fluorescein isothiocyanate (FITC)-goat anti-mouse IgM (Abcam, Cambridge, UK) labelled antibody (diluted 1/200 in 3% HSA/PBS) was used as a secondary antibody and incubated for 1 h at RT. Samples were analyzed on a FAC-Scalibur flow cytometer equipped with CellQuest Pro software (BD Bio-Sciences, Madrid, Spain). The viable cell population was gated according to forward-scatter (FSC-H) and side-scatter (SSC-H) parameters. Aliquots of fixed and stained samples were used for immunofluorescence assays after air-drying and mounting in ProLong Antifade reagent containing 4′,6-diamidino-2-phenylindole (DAPI) (Molecular Probes, Eugene, OR, USA). The sections were examined using a Zeiss LSM 800 laser scanning confocal microscope (Carl Zeiss, Oberkochen, Germany) with oil immersion objectives (63×).

2.3. Zebrafish

Wild-type adult (6–8 months old) AB female and male zebrafish were kindly provided by Juan Galcerán Sáez from the Instituto de Neurociencias (IN-CSIC-UMH, Sant Joan d'Alacant, Alicante, Spain). These zebrafish were certified by Biosait Europe S.L. (Barcelona, Spain; https://biosait.com) as free of major fish pathogens such as *Mycobacterium* spp., *Pseudoloma neurophilia*, *Pseudocapillaria tomentosa*, and zebrafish retroviruses. The zebrafish were maintained in a flow-through water system at 27 °C with a light/dark cycle of 14 h/10 h and fed twice daily with dry fish feed (Premium food tropical fish, DAPC, Valladolid, Spain).

2.4. Zebrafish Caccination With α-Gal and Challenge with M. marinum

2.4.1. Experiment 1 (Figure 1A)

This experiment was designed to evaluate the effect of vaccination with bovine serum albumin (BSA) coated with α-Gal (BSA-α-Gal, thereafter named α-Gal; Dextra, Shinfield, UK) in combination with adjuvant Montanide ISA 71 VG (SEPPIC, Paris, France) and in comparison with BSA and adjuvant alone. For vaccine formulation, α-Gal was adjuvated as previously described [32] to a final concentration of 0.25 μg/μl in a vaccination dose volume of 20 μl. Fourteen fish were randomly allocated to vaccinated and control groups with a similar number of females and males. Fish were briefly anaesthetized by immersion in 0.02% tricaine methanesulfonate (MS-222) and vaccinated at weeks 0 (prime delivery) and 3 (boost delivery). Fish were vaccinated by intraperitoneal (IP) injection using a 30G insulin syringe with 50 μl of antigen composition. The *M. marinum* Aronson (ATCC 927) was cultured at 29 °C in 7H9 broth enriched with Middlebrook ADC (Becton Dickinson) and prepared for infection as previously described [27,33]. To verify the bacterial dose, *M. marinum* samples were diluted and plated on 7H10 agar enriched with Middelbrook OADC (Becton Dickinson) for counting bacterial colonies. Before challenge, fish were anaesthetized as described above and IP injected at week 5 with an infection dose equivalent to 50 ± 8 cfu of *M. marinum*, causing a chronic tuberculosis-like disease in zebrafish [27]. At week 8, fish were euthanized with immersion in 0.04% MS-222 and processed for analysis of antibody levels by ELISA, mycobacteria levels by qPCR, and expression of selected immune response gene markers by qRT-PCR. The zebrafish had weights of 333.0 ± 133.6 and 370.7 ± 91.2 mg at prime immunization and 344.2 ± 122.2 and 469.1 ± 106.0 mg at euthanasia for vaccinated and control groups, respectively.

2.4.2. Experiment 2 (Figure 1B)

In this experiment, the α-Gal antigen was formulated without adjuvant and used in comparison with PBS for vaccination of zebrafish treated with IP injection and mucosal exposure to PBS or *M. marinum* or left untreated. For vaccine formulation, α-Gal was diluted in PBS to a final concentration of 0.25 μg/μl in a vaccination dose volume of 20 μl. Controls were injected with a similar volume of PBS. A total of 87 fish were randomly allocated to uninfected/PBS, uninfected/α-Gal, vaccinated, and control groups with a similar number of females and males. Animals were vaccinated at weeks 0 and 3 as described in experiment 1. Then, at week 5 and before treatment (T1), fish from each group were

Vaccines **2020**, *8*, 195

euthanized as described above. Remaining fish were subjected to the different treatments at week 5 and euthanized at week 8 as described in experiment 1. These treatments included IP injection of PBS or *M. marinum* and mucosal exposure to PBS or *M. marinum*. IP injection was conducted as described above in experiment 1. Mucosal treatment was conducted as described before by immersion for 30 min in 500 ml water containing 56 ± 6 cfu/ml of *M. marinum*, while control animals were immersed in water with the same dose of PBS [28]. At week 8, fish were euthanized as described above in experiment 1 and processed for analysis of antibody levels by ELISA, granulomas by histopathology, mycobacteria levels by qPCR, proteome characterization by Sequential Windowed data independent Acquisition of the Total High-resolution Mass Spectra (SWATH), and expression of selected immune response gene markers by qRT-PCR (Figure 1B). The zebrafish had weights at prime immunization and euthanasia (T2), respectively, of 330.0 ± 132.0 and 345.9 ± 124.8 mg (PBS vaccination and treatment), 274.5 ± 137.3 and 357.9 ± 170.8 mg (α-Gal vaccination and no treatment), 258.3 ± 97.6 and 386.0 ± 78.3 mg (α-Gal vaccination and IP infection), 242.4 ± 117.9 and 323.4 ± 110.1 mg (α-Gal vaccination and mucosal infection), 279.4 ± 107.3 and 366.7 ± 149.3 mg (PBS vaccination and IP infection), and 340.4 ± 115.3 and 497.6 ± 84.0 mg (PBS vaccination and mucosal infection).

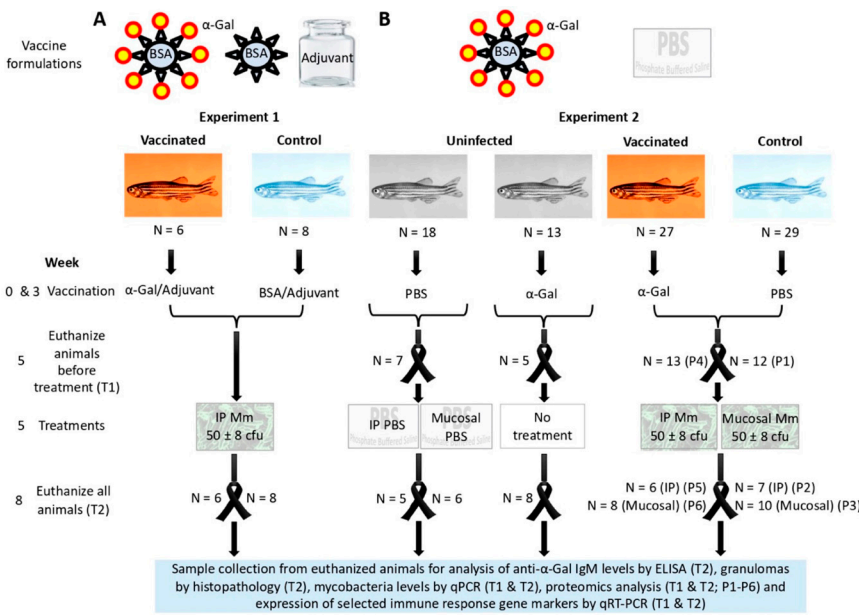

Figure 1. Experimental design: Two experiments were conducted to characterize the protective efficacy and mechanisms of vaccination with α-Gal in zebrafish infected with *M. marinum* (Mm). (**A**) In experiment 1, fish were parenterally (IP) vaccinated with α-Gal or bovine serum albumin (BSA) control with adjuvant and IP infected with Mm. Samples were collected after vaccination and treatment with Mm or PBS at the end of the experiment (T2). (**B**) Experiment 2 was conducted with IP vaccination with α-Gal without adjuvant in comparison with PBS-treated controls in fish infected with IP and mucosal Mm or left untreated. In experiment 2, samples were collected after vaccination and before treatment (T1) and at the end of the experiment (T2). Samples collected from euthanized fish were used for analysis of anti-α-Gal IgM levels by ELISA (T2), granulomas by histopathology (T2), mycobacteria levels by qPCR (T1 and T2), proteomics analysis (T1 and T2; P1–P6), and expression of selected immune response gene markers by qRT-PCR (T1 and T2).

2.5. Anti-α-Gal IgM Antibody Titers in Zebrafish

For ELISA, high absorption capacity polystyrene microtiter plates were coated with 100 ng of α-Gal per well in carbonate-bicarbonate buffer (Sigma-Aldrich). After an overnight incubation at 4 °C, coated plates were washed one time with 100 µl/well PBS/1% Triton X-100 (PBST) (Sigma-Aldrich), and then blocked with 100 µl/well of 1% HSA (Sigma-Aldrich) for 1 h at RT. A dilution curve with 1:10, 1:100, and 1:1000 fish serum peritoneal fluid samples was performed and then diluted (1:10, v/v) in blocking solution, and 100 µl/well was added into the wells of the antigen-coated plates and incubated for 1.5 h at 37 °C. Plates were washed three times with PBST and 100 µl/well of species-specific rabbit anti-zebrafish IgM antibodies diluted (1:1000, *v/v*) in blocking solution were added and incubated for 1 h at RT. Plates were washed three times with 300 µl/well of PBST. A goat anti-rabbit IgG-peroxidase conjugate (Sigma-Aldrich) was added diluted 1:3000 in blocking solution and incubated for 1 h at RT. After four washes with 100 µl/well of PBST, 100 µl/well of 3,3′,5,5′-Tetramethylbenzidine (TMB) (Promega, Madison, WI, USA) was added and incubated for 15 min at RT. Finally, the reaction was stopped with 50 µl/well of 2 N H_2SO_4 and the optical density (OD) was measured in a spectrophotometer at 450 nm. The OD at 450 nm was compared between different groups by Student's *t*-test with unequal variance ($p < 0.05$; experiment 1, $n = 6$ for vaccinated fish and $n = 8$ for controls; experiment 2, $n = 6$ for fish vaccinated and IP *M. marinum*, $n = 8$ for fish vaccinated and mucosal *M. marinum*, $n = 7$ for controls and IP *M. marinum*, and $n = 10$ for controls and mucosal *M. marinum*).

2.6. Histopathology

The analysis was conducted in animals collected from experiment 2 (Figure 1B). Zebrafish were sectioned sagittally, and half of them were immediately fixed in 10% neutral buffered formalin for 24 h at 21 °C, dehydrated in a graded series of ethanol, immersed in xylol, and embedded in paraffin wax using an automatic processor. Sections were cut at 4 µm and stained with haematoxylin and eosin (HE) and Ziehl–Neelsen (ZN) staining following standard procedures [27,28]. The small size of the zebrafish and the sagittal sections to divide them in two portions for molecular and histopathological studies permitted a histological assessment only in central nervous system, branchial arches, muscle, skin, liver, intestine, and gonads. Tuberculous granulomas were evaluated and classified according to their components (a) in early granuloma composed of an epithelioid macrophages infiltrate positive to mycobacteria and without or early necrosis and (b) in mature granuloma well-organized and infiltrated of epithelioid macrophages with areas of partial and complete central necrosis and acid-fast bacilli and insulated from the surrounding tissue by a fibrotic and/or cellular cuff. The quantitative assessment of the granulomas consisted of identifying and counting the organs with granulomas per zebrafish. Pathological findings were graded by a numerical score based on the number of granulomas, the type of granulomas, and the number of regions and/or organs involved by granulomatous disease in each fish. Histopathology and ZN staining for mycobacteria were used for the quantification of granuloma lesion scores in the studied organs. The granuloma lesion scores were compared between groups by Student's *t*-test with unequal variance and by a one-way ANOVA test (https://www.socscistatistics.com/tests/anova/default2.aspx) and the number of early tuberculosis-like granulomas with epithelioid macrophages infiltrates surrounding scattered mycobacteria, and well-organized granulomas with partial and complete necrosis were compared between α-Gal vaccinated and not vaccinated zebrafish by Student's t-test with unequal variance ($p = 0.05$; $n = 5$ for fish PBS vaccinated and IP PBS, $n = 6$ for fish PBS vaccinated and mucosal PBS, $n = 7$ for fish α-Gal vaccinated and untreated, $n = 5$ for fish vaccinated and IP *M. marinum*, $n = 8$ for fish vaccinated and mucosal *M. marinum*, $n = 7$ for controls and IP *M. marinum*, and $n = 9$ for controls and mucosal *M. marinum*).

2.7. Extraction of Total DNA, RNA, and Proteins from Zebrafish

Total DNA, RNA, and proteins were isolated from the intestine of euthanized fish using the AllPrep DNA/RNA/Protein (Qiagen, Hilden, Germany).

2.8. Characterization of M. marinum DNA Levels by qPCR

The DNA levels of *M. marinum* were determined by qPCR using the KAPA SYBR FAST one-step universal kit (Sigma-Aldrich) in the Rotor-Gene Q (Qiagen, Inc. Valencia, CA, USA) thermocycler following manufacturer's recommendations with specific primers and conditions for *M. marinum 16S ribosomal RNA* (*16S rRNA*; Genbank accession number: AF456240.1) (16SForward-F: 5'-ACTGAGATACGGCCCAGACT-3', 16SReverse-R: 5'- TCACGAACAACGCGACAAAC-3', annealing 56 °C, 30 sec). A dissociation curve was run at the end of the reactions to ensure that only one amplicon was formed and that the amplicon denatured consistently in the same temperature range for every sample [34]. The DNA Ct values were normalized against *D. rerio glyceraldehyde-3-phosphate dehydrogenase* (*gapdh*; NM_001115114.1) (GAPDHF: 5'-CGTGGTGCCAGTCAGAACAT-3', GAPDHR: 5'-AGTCAGTGGACACAACCTGG-3', annealing 56 °C, 30 sec) using the genNormddCT method [35]. *M. marinum* DNA-normalized Ct levels were compared between groups by Student's *t*-test with unequal variance ($p = 0.05$; experiment 1, $n = 6$ for vaccinated fish, $n = 8$ for controls; experiment 2 at T2, $n = 6$ for fish vaccinated and IP *M. marinum*, $n = 8$ for fish vaccinated and mucosal *M. marinum*, $n = 7$ for controls and IP *M. marinum*, and $n = 10$ for controls and mucosal *M. marinum*; experiment 2 at T1 vs. T2, $n = 7$ for PBS vaccinated uninfected fish, $n = 5$ for α-Gal vaccinated uninfected fish, $n = 13$ for α-Gal vaccinated infected fish, $n = 12$ for PBS vaccinated infected fish and T2, $n = 5$ for fish PBS vaccinated and IP PBS, $n = 6$ for fish PBS vaccinated and mucosal PBS, $n = 8$ for fish α-Gal vaccinated and untreated, $n = 6$ for fish vaccinated and IP *M. marinum*, $n = 8$ for fish vaccinated and mucosal *M. marinum*, $n = 7$ for controls and IP *M. marinum*, and $n = 10$ for controls and mucosal *M. marinum*). A Spearman's Rho correlation analysis (https://www.socscistatistics.com/tests/spearman/Default2.aspx) was performed between normalized *M. marinum* DNA levels and anti-α-Gal IgM antibody levels (experiment 1, $n = 6$ for vaccinated fish, $n = 8$ for controls, $\rho = -0.565$, two-tailed $p = 0.03$; experiment 2, $n = 14$ for α-Gal vaccinated fish and IP/mucosal infection at T2, $\rho = -0.515$, two-tailed $p = 0.004$, $n = 17$ for PBS controls and IP/mucosal infection at T2, $n = 6$ for α-Gal vaccinated fish and IP infection at T2, $n = 7$ for PBS controls and IP infection at T2, $\rho = -0454$, two-tailed $p = 0.12$, and $n = 8$ for α-Gal vaccinated fish and mucosal infection at T2, $n = 10$ for PBS controls and mucosal infection at T2, $\rho = -0522$, two-tailed $p = 0.03$).

2.9. Characterization of mRNA Levels of Selected Zebrafish Immune Response Genes by qRT-PCR

To characterize the expression of selected genes previously shown to be involved in vaccine protective mechanisms [36] and/or fish immune response to infection [37], a qRT-PCR was performed for the analysis of *D. rerio tumor necrosis factor-alfa* (*tnf alpha*; NM_212859.2), *chemokine receptor type 4a* (*cxcr4a*; NM_131882.3), *chemokine receptor 6a* (*ccr6a*; NM_001099991.1), *toll-like receptor 2* (*TLR2*; NM_212812.1), *toll-like receptor 4* (*TLR4*; NM_001328605), *interleukin 1-beta* (*IL-1β*; NM_212844.2), *akirin 1* (*akr1*; NM_001007186.2), *akirin 2* (*akr2*; NM_213294.2), and *complement component 3* (*C3*; NM_131243.1) genes in zebrafish in response to vaccination and mycobacterial infection. The qRT-PCR was performed using the KAPA SYBR FAST one-step universal kit (Sigma-Aldrich) in the Rotor-Gene Q (Qiagen) with specifics forward (F) and reverse (R) primers and conditions following manufacturer's recommendations (Table 1). A dissociation curve was run at the end of the reactions to ensure that only one amplicon was formed and that the amplicon denatured consistently in the same temperature range for every sample [34]. The mRNA Ct values were normalized against *D. rerio gapdh* as described above for the qPCR using the genNormddCT method [35]. The mRNA-normalized Ct values were compared between groups by Student's *t*-test with unequal variance ($p = 0.05$) and then represented as the ratio between normalized Ct values in fish α-Gal-vaccinated and PBS control IP infected with *M. marinum* at T2 ($n = 6$ for fish α-Gal vaccinated and $n = 7$ for controls), the ratio between normalized Ct values in fish α-Gal-vaccinated and PBS control with mucosal infection with *M. marinum* at T2 ($n = 8$ for fish α-Gal vaccinated and $n = 10$ for controls), and the ratio between normalized Ct values at T1 and T2 (T1, $n = 7$ for PBS vaccinated uninfected fish, $n = 5$ for α-Gal vaccinated uninfected fish, $n = 13$ for α-Gal vaccinated infected fish, $n = 12$ for PBS vaccinated infected fish; T2, $n = 5$ for fish PBS vaccinated and IP

PBS, $n = 6$ for fish PBS vaccinated and mucosal PBS, $n = 8$ for fish α-Gal vaccinated and untreated, $n = 6$ for fish α-Gal vaccinated and IP *M. marinum*, $n = 8$ for fish α-Gal vaccinated and mucosal *M. marinum*, $n = 7$ for controls and IP *M. marinum*, and $n = 10$ for controls and mucosal *M. marinum*).

Table 1. Oligonucleotide primer sequences and annealing conditions.

Gene	Oligonucleotide Primers	Annealing Conditions
tnf alpha	F: 5′-GCTTATGAGCCATGCAGTGA-3′ R: 5′-TGCCCAGTCTGTCTCCTTCT-3′	56 °C, 30 sec
ccr6a	F: 5′-AGCTTCTGCGTGGCATCTAT-3′ R: 5′-CAGACGGCTGCACAAACTAA-3′	56 °C, 30 sec
TLR4	F: 5′-TCACCTGGACAGCAAGAATG-3′ R: 5′-CGATTGACTTCCCTGCTTGA-3′	56 °C, 30 sec
IL-1β	F: 5′-GCATGTCCACATATGCGTCG-3′ R: 5′-GCTGGTCGTATCCGTTTGGA-3′	58 °C, 30 sec
akr1	F: 5′-AGTTTGAGGCCCTTCTCAGC-3′ R: 5′-AAGTGCCTTCATGTCTGGGG-3′	58 °C, 30 sec
TLR2	F: 5′-TGAATGGGTCGAGGAGATTC-3′ R: 5′-CACAAAGTGCTCCGACAGAA-3′	56 °C, 30 sec
cxcr4a	F: 5′-TGTACAGCAGCGTCCTCATC-3′ R: 5′-ACCCAGGTGACAAACGAGTC-3′	58 °C, 30 sec
C3	F: 5′-ACGCTCTCTGGATTGAAACA-3′ R: 5′-TGCCTTCTTGCATGGCAATC-3′	56 °C, 30 sec
akr2	F: 5′-ACTATGGACTTCGATCCGCT-3′ R: 5′-GCTCTGTGGTGAGTGCTGAA-3′	56 °C, 30 sec

2.10. Characterization of Zebrafish Proteome in Response to Vaccination and Infection

Isolated proteins were resuspended in 10 mM PBS with 2% SDS and protein concentration was determined using the BCA Protein Assay (Thermo Scientific) using bovine serum albumin (BSA) as standard. Proteins (100 µg per sample) were methanol/chloroform precipitated; resuspended in 30 µl 50 mM Tris-HCl pH 7.5, 2% SDS, 50 mM dithiothreitol (DTT); and boiled for 5 min at 95 C. Proteins were trypsin digested using the filter aided sample preparation (FASP) protocol using the FASP Protein Digestion Kit (Expedeon, San Diego, CA, USA) following manufacturer recommendations. The resulting peptides were desalted onto OMIX Pipette tips C18 (Agilent Technologies), dried-down; and stored at −20 °C until mass spectrometry analysis (MS) by SWATH-MS.

2.10.1. Proteome Analysis by SWATH-MS

The desalted protein digests were resuspended in 2% acetonitrile and 5% acetic acid in water and analyzed by reverse phase liquid chromatography mass spectrometry (RP-LC-MS/MS) using an ekspertTM nanoLC 415 system coupled on line with a 6600 TripleTOF® mass spectrometer (AB SCIEX; Framingham, MA, USA) through Information-Dependent Acquisition (IDA) followed by SWATH. Four micrograms of each protein digest of the different control and vaccinated groups from experiment 2 (four animals per group) were used for the generation of the reference spectral ion library as part of SWATH-MS analysis. The peptides were concentrated using a 0.1 × 20 mm C18 RP precolumn (Thermo Scientific), and then separated using a 0.075 × 250 mm C18 RP column (New Objetive, Woburn, MA, USA) operating at 0.3 ml/min. Peptides were eluted using a 120-min gradient from 5%–30% solvent B in solvent A followed by 15-min gradient from 30%–60% solvent B in solvent A (Solvent A: 0.1% formic acid in water, solvent B: 0.1% formic acid in acetonitrile) and directly injected into the mass spectrometer for analysis. For IDA experiments, the mass spectrometer was set to scanning full spectra (350–1400 m/z) using 250 ms accumulation time per spectrum, followed by up to 50 MS/MS scans

Vaccines **2020**, *8*, 195

(100–1500 *m*/*z*). Candidate ions with a charge state between +2 and +5 and counts per second above a minimum threshold of 100 were isolated for fragmentation. One MS/MS spectrum was collected for 100 ms, before adding those precursor ions to the exclusion list for 15 sec (mass spectrometer operated by Analyst TF 1.7; ABSciex). Dynamic background subtraction was turned off. MS/MS analyses were recorded in high-sensitivity mode with rolling collision energy on and a collision energy spread of 5. For SWATH quantitative analysis, twenty-two independent samples (four biological replicates from each PBS-vaccinated and α-Gal-vaccinated fish without treatment and with mucosal and IP *M. marinum* in experiment 2; Figure 1B) (8 μg each) were subjected to the cyclic data independent acquisition (DIA) of mass spectra using the SWATH variable windows calculator (V 1.0, AB SCIEX) and the SWATH acquisition method editor (AB SCIEX), similar to previously established methods [38]. A set of 50 overlapping windows was constructed (containing 1 *m*/*z* for the window overlap), covering the precursor mass range of 400–1250 *m*/*z*. For these experiments, a 50 -ms survey scan (350–1400 *m*/*z*) was acquired at the beginning of each cycle and SWATH-MS/MS spectra were collected from 100–1500 *m*/*z* for 70 ms at high-sensitivity mode, resulting in a cycle time of 3.6 sec. Collision energy for each window was determined according to the calculation for a charge +2 ion-centered upon the window with a collision energy spread of 15.

2.10.2. Library Generation/Protein Identification, Data Processing, and Relative Quantitation

To create a spectral library of all the detectable peptides in the samples, the IDA MS raw files were combined and subjected to database searches in unison using ProteinPilot software v. 5.0.1 (AB SCIEX) with the Paragon algorithm [39]. Spectra identification was performed by searching against the *Danio rerio* Uniprot database (62,016 entries in February 2020) with the following parameters: iodoacetamide cysteine alkylation, trypsin digestion, identification focus on biological modification, and thorough ID as search effort. The detected protein threshold was set at 0.05. An independent False Discovery Rate (FDR) analysis, using the target-decoy approach provided by Protein Pilot (AB SCIEX), was used to assess the quality of identifications. Positive identifications were considered when identified proteins reached a 1% global FDR. For SWATH processing, up to 10 peptides with seven transitions per protein were automatically selected by the SWATH Acquisition MicroApp 2.0 in the PeakView 2.2 software (AB SCIEX) with the following parameters: 15 ppm ion library tolerance, 5 min extracted-ion chromatogram (XIC) extraction window, 0.01 Da XIC width, and considering only peptides with at least 99% confidence and excluding those which were shared or contained modifications. However, to ensure reliable quantitation, only proteins which had 3 or more peptides available for quantitation were selected for XIC peak area extraction and exported for analysis in the MarkerView 1.3 software (AB SCIEX). Global normalization was performed according to the total area sums of all detected proteins in the samples. In order to identify proteins that were significantly differentially represented between samples, a Student's *t*-test ($p = 0.05$) was used to perform two-sample comparisons between the averaged area sums of all the transitions derived for each protein across the four replicate runs for each sample under comparison. Gene ontology (GO) annotations were obtained using the Blast2GO software (http://www.blast2go.org). Raw proteomics data was deposited at the PeptideAtlas repository (http://www.peptideatlas.org/) with the dataset identifier PASS01545.

3. Results

3.1. Experimental Design and Rationale

The experimental design used in this study addressed the protective efficacy of vaccination with α-Gal for the control of mycobacterial infection in the zebrafish model of tuberculosis using adjuvated (experiment 1; Figure 1A) and not adjuvated (experiment 2; Figure 1B) vaccine formulations. The rationale for using zebrafish is supported by constituting a validated model for tuberculosis [24–28] and the role of this species as an animal model for the study of the AGS [29]. The main objectives of the study were to characterize the effect of vaccination with α-Gal on mycobacterial infection

Vaccines **2020**, *8*, 195

and the immune mechanisms putatively involved in vaccine efficacy. To address these objectives, vaccinated and control zebrafish were infected with α-Gal-positive *M. marinum* [17], treated with PBS via IP or mucosal routes, or left untreated. Fish samples collected before and after treatment with *M. marinum* or PBS were used for analysis of IgM antibody levels by ELISA, granulomas by histopathology, mycobacteria levels by qPCR, proteomics analysis and expression of selected immune response gene markers by qRT-PCR (Figure 1A,B).

3.2. Zebrafish Antibody Response to Vaccination with α-Gal Correlates with Reduction in Mycobacterial Infection

In experiment 1 (Figure 1A), the anti-α-Gal IgM antibody levels significantly ($p = 0.02$) increased after vaccination with adjuvated α-Gal vaccine formulation when compared to controls (Figure 2A,B). The analysis of *M. marinum* DNA levels by qPCR showed a significant ($p = 0.04$) decrease in vaccinated when compared to control zebrafish (Figure 2C). A significant negative correlation ($p = 0.03$) was obtained between *M. marinum* DNA levels and anti-α-Gal IgM antibody titers (Figure 2D), thus providing evidence for the role of antibody response against α-Gal in the control of mycobacteriosis in vaccinated fish. In experiment 2 (Figure 1B), the results also showed a significant increase in the anti-α-Gal IgM antibody levels in both mucosal ($p = 0.004$) and IP ($p = 0.02$)-infected zebrafish when compared to controls (Figure 3A). The antibody response increased after vaccination (week 5, T1; $p = 0.01$) and remained higher than in untreated zebrafish (T0) until week 8 (T2; $p = 0.004$) (Figure 3B). The *M. marinum* DNA levels significantly increased after infection (T1 vs T2) only in unvaccinated PBS-treated and untreated control zebrafish for both mucosal ($p = 0.04$) and IP ($p = 0.01$) infection routes (Figure 3C). These results translated into a significant decrease in *M. marinum* DNA levels in α-Gal-vaccinated zebrafish when compared to controls infected via mucosal ($p = 0.001$) or IP ($p = 0.002$) routes (Figure 3D). As in experiment 1 but with a larger number of animals, a significant negative correlation ($p = 0.004$) was obtained between *M. marinum* DNA levels and anti-α-Gal IgM antibody titers (Figure 3E), thus providing additional support for the protective role of anti-α-Gal antibody response against mycobacterial infection in zebrafish.

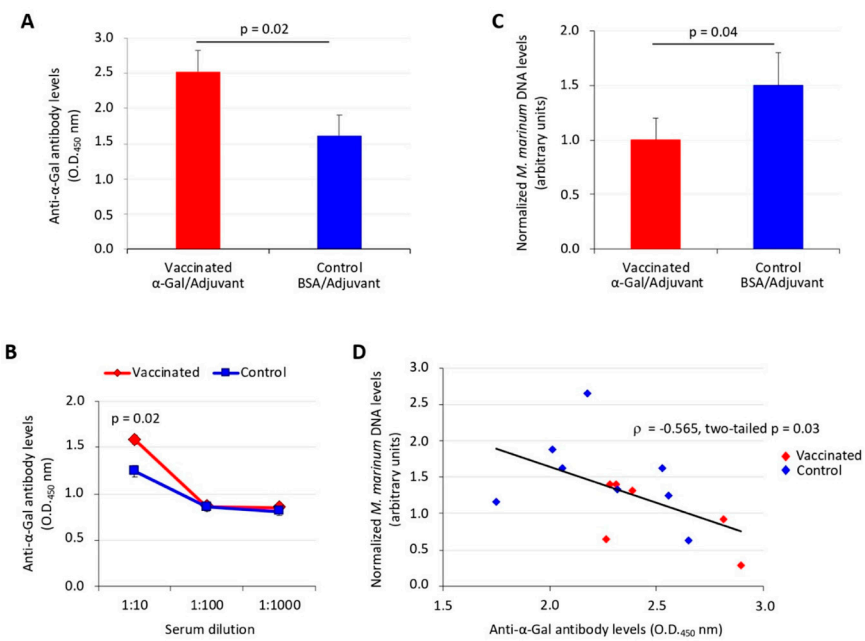

Figure 2. Experiment 1, effect of vaccination on the antibody response and mycobacterial infection

levels in zebrafish. (**A**) The IgM antibody titers against α-Gal were determined by ELISA in fish vaccinated with adjuvated α-Gal or BSA alone as control and challenged with IP *M. marinum*. Antibody titers in vaccinated and control fish were represented as the average + SD of the OD_{450nm} ($OD_{antigen}$ − $OD_{PBS\ control}$), and the mean of the duplicate values were compared between vaccinated and control groups by Student's *t*-test with unequal variance ($p < 0.05$). (**B**) ELISA dilution curve for IgM antibody titers against α-Gal in fish vaccinated with adjuvated α-Gal or BSA alone as control and challenged with *M. marinum*. Antibody titers were determined, represented, and analyzed as in (**A**) ($p < 0.05$). (**C**) *M. marinum* DNA levels were characterized by qPCR in vaccinated and control infected fish, normalized against *D. rerio gapdh*, represented as average + SD, and compared between groups by Student's *t*-test with unequal variance ($p < 0.05$). (**D**) Spearman's Rho correlation analysis between normalized *M. marinum* DNA levels and anti-α-Gal IgM antibody levels. Correlation rank coefficient (ρ) and *p*-value are shown. In all experiments, $n = 6$ for vaccinated fish and $n = 8$ for controls.

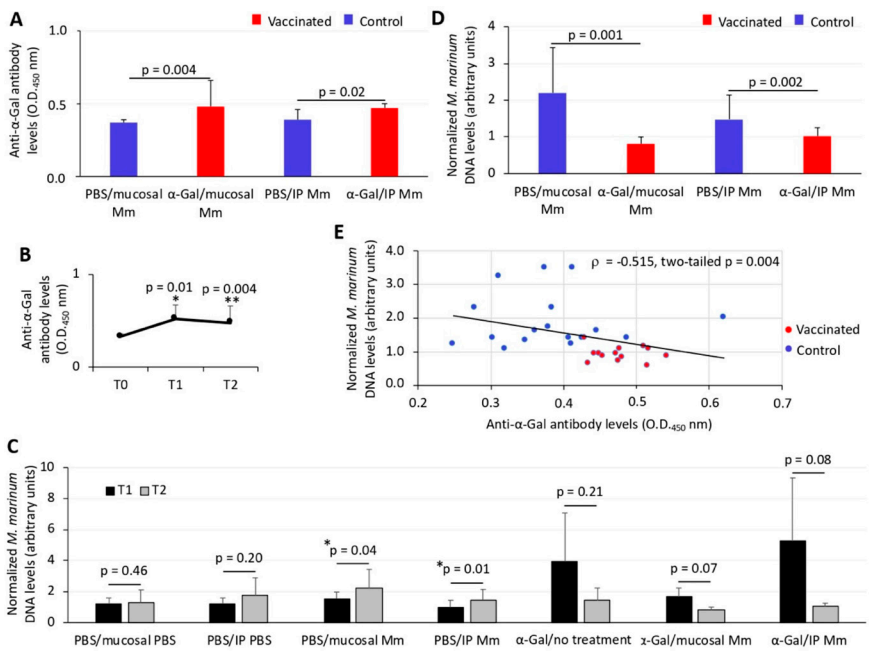

Figure 3. Experiment 2, effect of vaccination on the antibody response and mycobacterial infection levels in zebrafish. (**A**) The IgM antibody titers against α-Gal were determined by ELISA at T2 in fish vaccinated with α-Gal and PBS-treated controls infected with mucosal or IP *M. marinum* (Mm). Antibody titers in vaccinated and control fish were represented as the average + SD of the OD_{450nm} ($OD_{antigen}$ − $OD_{PBS\ control}$), and the mean of duplicate values were compared between vaccinated and control groups by Student's *t*-test with unequal variance ($p < 0.05$; $n = 6$ for fish vaccinated and IP Mm, $n = 8$ for fish vaccinated and mucosal Mm, $n = 7$ for PBS controls and IP Mm, and $n = 10$ for PBS controls and mucosal Mm). (**B**) The IgM antibody titers against α-Gal were determined by ELISA at different time points in PBS-treated uninfected fish (T0 before vaccination, $n = 18$), vaccinated with α-Gal and uninfected fish (T1, $n = 18$) and vaccinated with α-Gal and untreated fish (T2, $n = 8$). Antibody titers were determined and represented as in (A) and compared by Student's *t*-test with unequal variance (* $p = 0.01$, T1 vs. T0; ** $p = 0.004$, T2 vs. T0). (**C**) *M. marinum* DNA levels were characterized by qPCR at T1 and T2 in fish vaccinated with α-Gal and PBS-treated controls uninfected and infected with mucosal or IP Mm, normalized against *D. rerio gapdh*, represented as average + SD, and compared between T1

and T2 by Student's *t*-test with unequal variance (* $p < 0.05$; T1: $n = 7$ for PBS vaccinated uninfected fish, $n = 5$ for α-Gal vaccinated uninfected fish, $n = 13$ for α-Gal vaccinated infected fish, $n = 12$ for PBS vaccinated infected fish; T2: $n = 5$ for fish PBS vaccinated and IP PBS, $n = 6$ for fish PBS vaccinated and mucosal PBS, $n = 8$ for fish α-Gal vaccinated and untreated, $n = 6$ for fish vaccinated and IP Mm, $n = 8$ for fish vaccinated and mucosal Mm, $n = 7$ for controls and IP Mm, and $n = 10$ for controls and mucosal Mm). (**D**) *M. marinum* DNA levels were characterized by qPCR at T2 in fish vaccinated with α-Gal and PBS-treated controls infected with mucosal or IP Mm, normalized against *D. rerio gapdh*, represented as average + SD, and compared between groups by Student's t-test with unequal variance ($p < 0.05$; $n = 6$ for fish vaccinated and IP Mm, $n = 8$ for fish vaccinated and mucosal Mm, $n = 7$ for controls and IP Mm, and $n = 10$ for controls and mucosal Mm). (**E**) Spearman's Rho correlation analysis between normalized *M. marinum* DNA levels and anti-α-Gal IgM antibody levels (experiment 2, $n = 14$ for α-Gal vaccinated fish and IP/mucosal infection at T2 and $n = 17$ for PBS controls and IP/mucosal infection at T2). Correlation rank coefficient (ρ) and *p*-value are shown.

3.3. The Tuberculous Granuloma Lesion Scores Decrease in Zebrafish Vaccinated with α-Gal and IP Infected with Mycobacteria

None of the animals in any group presented tuberculosis-like lesions at T0 and T1 of the experiment; neither did the animals from the *M. marinum* uninfected groups at T2. However, tuberculous-like granulomas were observed in 100% ($IC_{95\%}$: 61.2%–100%) of the animals from IP *M. marinum*-infected groups at T2 and in 50% ($IC_{95\%}$: 21.5%–78.4%) and 60% ($IC_{95\%}$: 31.2%–83.1%) of the zebrafish in mucosal *M. marinum*-infected groups vaccinated and not vaccinated with α-Gal, respectively. Fish vaccinated with α-Gal and infected IP with *M. marinum* had a significantly lower mean number of tuberculous granuloma lesion score (2 ± 3) when compared to unvaccinated animals (5 ± 1) ($p = 0.03$), while no significant differences between groups were observed in zebrafish infected by mucosal *M. marinum* (2 ± 2 vs. 2 ± 3; $p > 0.40$) (Figure 4A). However, all *M. marinum*-infected groups presented a similar granuloma distribution of affected tissues, with the liver and gonads the organs more affected followed by intestine (Figure 4B), whereas mycobacteria were not detected in the brain, branchial arches, muscle, and skin. ZN staining confirmed the presence of mycobacteria in the cytoplasm of macrophages within granulomas of all zebrafish with tuberculous-like lesions (insets in Figure 4B(a) and (c)).

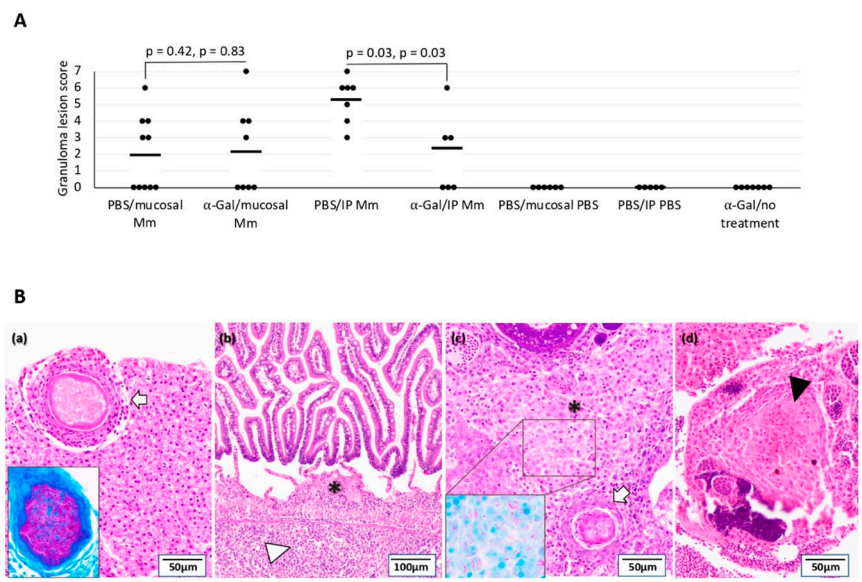

Figure 4. Effect of vaccination on tuberculous granulomas: The quantitative assessment of the

granulomas consisted of identifying and counting the organs with granulomas per zebrafish. Pathological findings were graded by a numerical score based on the number of granulomas, the type of granulomas, and the number of regions and/or organs involved by granulomatous disease in each fish. (**A**) Histopathology and Ziehl–Neelsen (ZN) staining for mycobacteria were used for the quantification of granuloma lesion scores in the studied organs. The granuloma lesion scores were compared between groups by Student's *t*-test with unequal variance and by a one-way ANOVA test (https://www.socscistatistics.com/tests/anova/default2.aspx) ($p < 0.05$; $n = 5$ for fish PBS vaccinated and IP PBS, $n = 6$ for fish PBS vaccinated and mucosal PBS, $n = 7$ for fish α-Gal vaccinated and untreated, $n = 5$ for fish vaccinated and IP *M. marinum*, $n = 8$ for fish vaccinated and mucosal *M. marinum*, $n = 7$ for controls and IP *M. marinum*, and $n = 9$ for controls and mucosal *M. marinum*). (**B**) Representative histopathology of zebrafish infected with *M. marinum*. (a) Liver tissue infected with *M. marinum* exhibiting tuberculosis-like mature granulomatous formation well-organized and surrounded by a capsule of connective tissue with complete central necrosis (white arrow). (b) Intestine from *M. marinum*-infected zebrafish presenting an early tuberculosis-like granuloma composed of epithelioid macrophages grouped loosely in lamina propia (asterisk *) and a diffuse epithelioid macrophages infiltrate in submucosa (white arrowhead). (c) Ovary tissue infected with *M. marinum* exhibiting an early tuberculosis-like granuloma composed of an epithelioid macrophage infiltrate (asterisk *) as well as a mature granuloma with well-defined border of macrophages and central necrosis (white arrow). (d) Testicle tissue from *M. marinum*-infected zebrafish showing a mature granuloma well-defined with early central necrosis (black arrowhead). A high acid-fast bacilli numbers were present in the central necrotic core of mature granulomas positive to ZN staining ((a), inset), while a lower bacterial number was observed residing within macrophages in early granulomas ((c), inset).

Early tuberculosis-like granulomas with epithelioid macrophage infiltrates surrounding scattered mycobacteria were predominant in *M. marinum*-infected zebrafish in unvaccinated groups with respect to fish vaccinated with α-Gal, although no significant differences were observed in zebrafish infected by mucosal *M. marinum* (36.7% and 50.0% for vaccinated and unvaccinated groups, respectively; $p = 0.69$) and IP *M. marinum* (38.3% and 52.3% for vaccinated and unvaccinated groups, respectively; $p = 0.46$). Accordingly, a higher numbers of well-organized granulomas with partial and complete necrosis were present in not vaccinated and *M. marinum*-infected zebrafish but without significant differences within each group (25.8% and 50.0% for vaccinated and not vaccinated mucosal infected groups ($p = 0.37$) and 31.7% and 42.0% for vaccinated and not vaccinated IP infected groups ($p = 0.53$)). The acid-fast bacilli were found predominantly in necrotic areas and were in greater numbers in fully necrotic than in partially necrotic zones.

3.4. The α-Gal Content Varies among M. marinum Bacteria

As previously shown [17], *M. marinum* has α-Gal on its surface (Figure 5A). However, the α-Gal content in *M. marinum* varied from negative or very low levels (37.56% of mycobacteria) to high levels (3.25% of mycobacteria) of α-Gal (Figure 5B,C). These results showed that not all mycobacteria have the same α-Gal content with possible functional implications.

Vaccines **2020**, *8*, 195

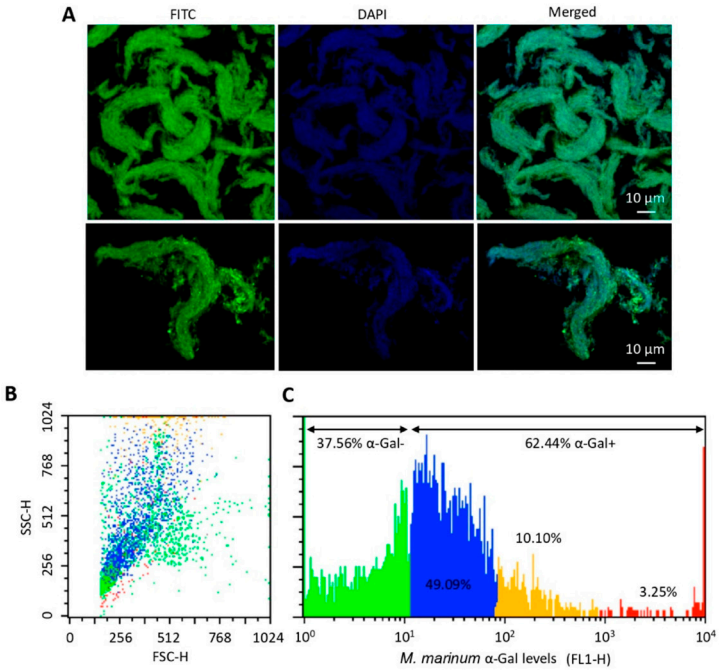

Figure 5. The α-Gal content in *M. marinum*: (**A**) Representative immunofluorescence images of *M. marinum* Aronson (ATCC 927) reference strain. (**B**) Density plot representing *M. marinum* that were gated by forward (FSC-H) and side (SSC-H) scatter. (**C**) Mycobacteria are represented in a histogram to evaluate the relative α-Gal levels (FL1-H). Cells were incubated with the α-Gal epitope monoclonal antibody M86. FITC-goat anti-mouse IgM-labelled antibody was used as a secondary antibody. Samples were analyzed on a FAC-Scalibur flow cytometer equipped with CellQuest Pro software. The viable cell population was gated according to forward-scatter (FSC-H) and side-scatter (SSC-H) parameters. Aliquots of fixed and stained samples were used for immunofluorescence assays after air-drying and mounting in ProLong Antifade reagent containing DAPI. The sections were examined using a Zeiss LSM 800 laser scanning confocal microscope with oil immersion objectives (63×; bars, 10 µm).

3.5. The B-Cell Maturation and TLR2/NF-kB-Mediated Immune Responses Play a Role in Mycobacterial Infection and Protective Response to α-Gal in Zebrafish

The expression of selected genes previously shown to be involved in vaccine protective mechanisms and/or fish immune response to infection was characterized by qRT-PCR in experiment 1 at T2 (after vaccination and treatment/IP infection) and in experiment 2 at T1 (after vaccination and before treatment/infection) and T2 (after vaccination and treatment/IP or mucosal infection) (Figure 6A–D and Figure S1A,B). The combined effect of vaccination and treatment/infection at T2 showed that the IP infection with *M. marinum* mostly upregulated the expression of selected genes with a higher effect on fish vaccinated with the adjuvant-containing α-Gal formulation (Figure 6A). In contrast, combined vaccination with mucosal *M. marinum* infection resulted in the downregulation or no effect of these genes (Figure 6B). In experiment 2, the effect of vaccination with α-Gal when compared to PBS-treated zebrafish at T1 resulted in significant ($p < 0.05$) upregulation of *IL-1β*, *akr2*, *TLR2*, *ccr6a*, and *akr1* (Figure 6C). In zebrafish infected with IP or mucosal *M. marinum*, the effect of infection when compared to PBS-treated controls at T2 showed a significant ($p < 0.05$) downregulation in response to infection for *tnf alpha* and *akr1* (mucosal infection) and *ccr6a* (IP infection) genes (Figure 6D).

Vaccines **2020**, *8*, 195

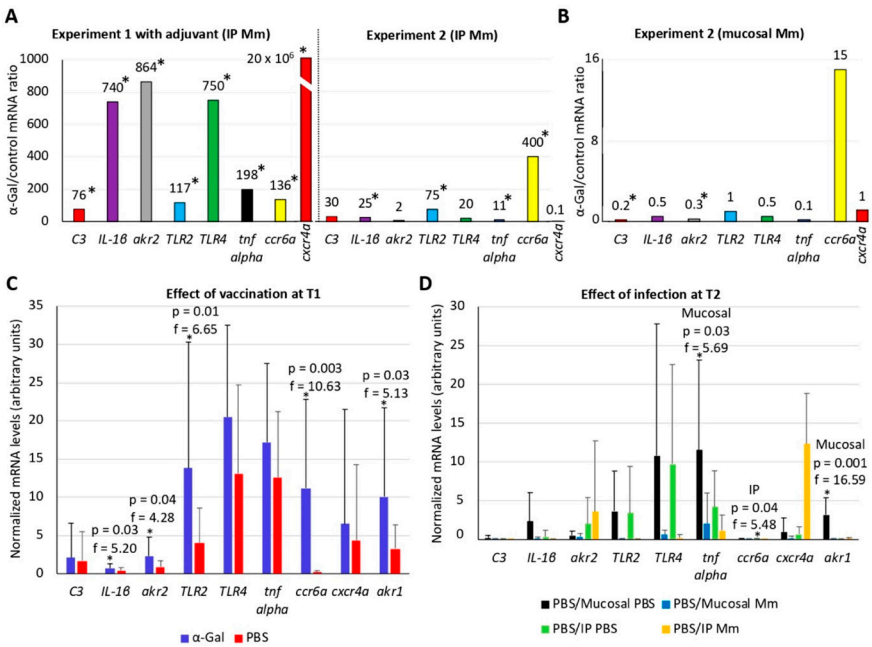

Figure 6. Effect of vaccination with α-Gal and mycobacterial infection on the expression of zebrafish immune response genes: The expression of selected immune response genes was characterized by qRT-PCR in zebrafish in response to vaccination with α-Gal or PBS and IP/mucosal infection with *M. marinum* (Mm). The mRNA levels were normalized against *D. rerio gapdh*, and normalized Ct values were compared between groups by Student's *t*-test with unequal variance (* $p < 0.05$; Figure S1A,B) and then represented as (**A**) the ratio between normalized Ct values in fish α-Gal-vaccinated and PBS or BSA control IP infected with Mm at T2 (experiment 1, $n = 6$ for fish α-Gal vaccinated and $n = 8$ for controls; experiment 2, $n = 6$ for fish α-Gal vaccinated and $n = 7$ for controls) and (**B**) the ratio between normalized Ct values in fish α-Gal-vaccinated and PBS control with mucosal infection with Mm at T2 ($n = 8$ for fish α-Gal vaccinated and $n = 10$ for controls). (**C**) The normalized mRNA levels were compared between zebrafish vaccinated with α-Gal ($n = 18$) and PBS ($n = 19$) to evaluate the effect of vaccination at T1 by a one-way ANOVA test (https://www.socscistatistics.com/tests/anova/default2.aspx) (* $p < 0.05$). (**D**) The normalized mRNA levels were compared between zebrafish vaccinated with PBS and treated by mucosal or IP route with PBS or Mm to evaluate the effect of infection at T2 by a one-way ANOVA test (https://www.socscistatistics.com/tests/anova/default2.aspx) (* $p < 0.05$; $n = 6$ PBS/mucosal PBS, $n = 10$ PBS/mucosal Mm, $n = 5$ PBS/IP PBS, $n = 7$ PBS/IP Mm).

To further evaluate the combined effect of vaccination and infection with *M. marinum* on zebrafish immune response genes, the mRNA levels of selected genes were compared at T1 and T2 in experiment 2 (Figures S2 and S3). The results showed that, as expected, the T1 = T2 mRNA ratio evidences no effect on immune response genes in fish vaccinated with PBS and treated with IP or mucosal PBS, thus validating the experimental design and analysis (Figures S2 and S3). The analysis of the different mRNA profiles showed that most genes had T1 = T2 and T1 > T2 profiles, thus suggesting no differences or a decrease in the mRNA levels after infection or no treatment in vaccinated fish (Figure S3).

After proteomics analysis, a total of 1777 proteins were identified in the zebrafish intestine (Table S1). Of them, differentially represented proteins after quantitation and comparative analysis by SWATH ($p < 0.05$) corresponded to 635 proteins (314 overrepresented and 321 underrepresented in P1 vs. P2, effect of IP infection at T2), 706 proteins (302 overrepresented and 404 underrepresented in P1 vs. P3, effect of mucosal infection at T2), 836 proteins (446 overrepresented and 390 underrepresented in

Vaccines **2020**, *8*, 195

P1 vs. P4, effect of vaccination at T1), 780 proteins (191 overrepresented and 589 underrepresented in P4 vs. P5, effect of vaccination and IP infection at T2), and 790 proteins (216 overrepresented and 574 underrepresented in P4 vs. P6, effect of vaccination and mucosal infection at T2) (Table S1). Although proteins encoded by most of the genes analyzed at the mRNA level were not identified in the proteomics analysis probably due to relatively low protein levels, these results showed an effect of the vaccination with α-Gal and/or mycobacterial infection in more than 60% of the identified proteins, suggesting a major impact on fish intestine proteome.

Proteomics analysis was focused on the immune system process proteins with special attention to those significantly represented ($p < 0.05$) in response to infection and vaccination (Figure 7A,B, Figure 8, Figures S4–S6). The effect of *M marinum* after IP (Figure 7A and Figure S4) and mucosal infection (Figure 7B and Figure S5) showed common overrepresented (e.g., ribosomal proteins, lysine-tRNA ligase, and leukotriene A4 hydrolase LTA4H) and underrepresented (e.g., complement components including C3, annexin, and tropomyosin alpha-1) proteins in response to infection (Figure 7A,B). Other proteins such as interferon (IFN)-g-inducible lysosomal thiol reductase, cathepsin L1, and heat shock protein 9 (HSP9) were differentially represented in response to either IP or mucosal infection (Figure 7A,B). The effect of vaccination with α-Gal evidenced the overrepresentation of proteins such as HSP9 and LTA4H, while complement components including C3, tropomyosin alpha-1, and annexin were underrepresented (Figure 8 and Figure S6). Other proteins such as ribosomal proteins were either under- or overrepresented in response to vaccination (Figure 8). Proteins such as DEAD (Asp-Glu-Ala-Asp) box polypeptide 41 (DDX41) and Rac family small GTPase 2 were underrepresented or overrepresented, respectively, in response to vaccination but did not change in response to infection (Figure 7A,B and Figure 8).

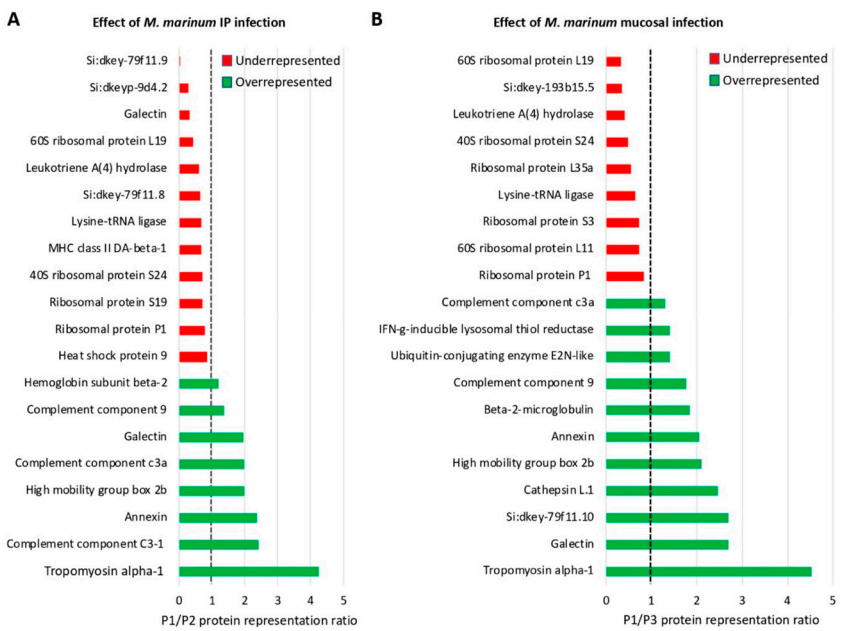

Figure 7. Proteomics analysis of immune system process proteins in response to *M. marinum* infection: Proteins annotated by Gene ontology (GO) using the Blast2GO software in the immune system process and significantly differentially represented between samples (Student's *t*-test; $p < 0.05$, $n = 4$) were included. (**A**) Effect of *M. marinum* IP infection on protein representation (P1/P2 ratio) after comparison

Vaccines **2020**, *8*, 195

between PBS-vaccinated (P1 at T1; Figure 1B) and IP-infected (P2 at T2; Figure 1B) zebrafish. (**B**) Effect of *M. marinum* mucosal infection on protein representation (P1/P3 ratio) after comparison between PBS-vaccinated (P1 at T1; Figure 1B) and mucosal-infected (P3 at T2; Figure 1B) zebrafish.

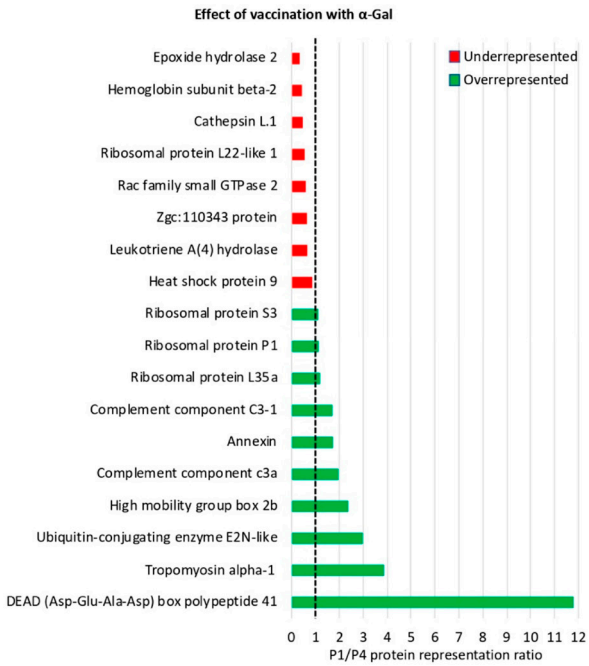

Figure 8. Proteomics analysis of immune system process proteins in response to vaccination with α-Gal: Proteins annotated by GO using the Blast2GO software in the immune system process and significantly differentially represented between samples (Student's *t*-test; $p < 0.05$, $n = 4$) were included. Effect of vaccination with α-Gal on protein representation (P1/P4 ratio) after comparison between PBS-vaccinated (P1 at T1; Figure 1B) and α-Gal-vaccinated (P4 at T1; Figure 1B) zebrafish.

The analysis of the mRNA profiles showed that, while *C3* and *cxcr4a* mRNA levels did not change throughout the experiment, *ccr6a*, *akr2*, and *IL-1β* levels increased after vaccination with α-Gal and remained unchanged after infection (Figure 9). However, the mRNA levels for *TLR4*, *tnf alpha*, *akr1*, and *TLR2* remained unchanged or increased after vaccination but decreased after infection (Figure 9). The profiles of immune response proteins relevant for mycobacterial infection showed that LTA4H and cathepsin L1 levels increased in response to vaccination or vaccination and infection (Figure 9). However, the representation profile of DDX41 and lysine-tRNA ligase decreased and increased only in response to vaccination or infection, respectively (Figure 9). In contrast, the representation profile for complement components including C3, annexin, and tropomyosin alpha-1 decreased in response to vaccination and both IP and mucosal *M. marinum* infection (Figure 9). In summary, these results showed that the mRNA/protein levels of immune response markers involved in B-cell maturation (e.g., *ccr6a*) and TLR2/NF-kB-mediated response (e.g., *TLR2*, *akr1*, *akr2*, *tnf alpha/IL-1β*, LTA4H, and cathepsin L1) are downregulated/underrepresented, are overrepresented, or do no change in response to mycobacterial infection while upregulated/overrepresented in response to vaccination with α-Gal. The C3 protein levels showed underrepresentation in response to both vaccination and mycobacterial infection, a result that correlated with no effect on gene regulation (Figure 9).

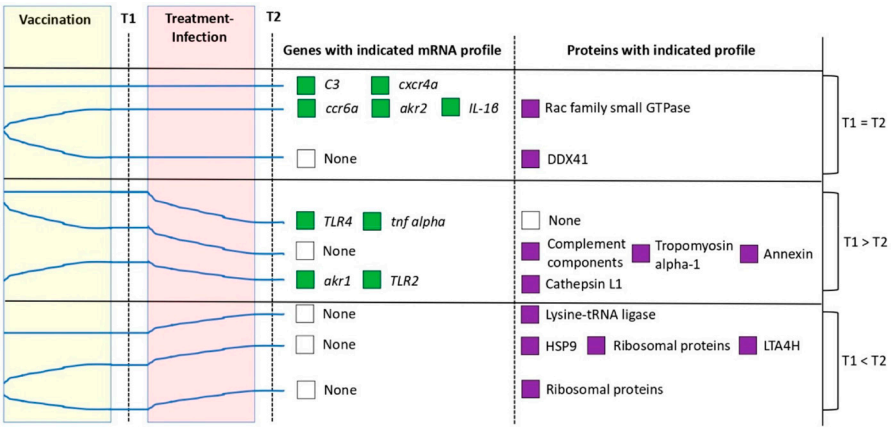

Figure 9. Summary mRNA and protein profiles of selected immune markers in response to vaccination and infection: The mRNA and protein profiles of selected immune response genes in response to vaccination at T1 and to treatment-infection at T2 are shown by tendency lines, which were associated to the corresponding genes or proteins. The results were compiled from qRT-PCR (Figure 6 and Figure S3) and proteomics (Figure 7A,B and Figure 8) analyses for experiment 2 at T1 and T2 (Figure 1B). Only statistically significant differences ($p < 0.05$) in mRNA and protein levels were considered. The results showed that the mRNA/protein levels of immune response markers involved in B-cell maturation (e.g., *ccr6a*), macrophage response (e.g., annexin), and TLR2/NF-kB-mediated response (e.g., *TLR2*, *akr1*, *akr2*, *tnf alpha/IL-1β*, DDX41, and Lysine-tRNA ligase) are downregulated by mycobacterial infection and upregulated in response to vaccination with α-Gal.

4. Discussion

The possibility of using the antibody-mediated immune response against α-Gal for the control of infectious diseases caused by pathogens with this modification on their surface in hosts such as humans, birds, and fishes that do not have the capacity to synthesize α-Gal was initially suggested by results in the malaria mouse model [15]. Then, results in leishmaniasis and Chagas disease further supported this possibility [18–20], leading to proposing the possibility of development of a single-antigen pan-vaccine for the control of major infectious diseases worldwide [11,16,17,30]. Pathogens causing infectious diseases with high incidence worldwide and with α-Gal modifications include *Plasmodium*, *Mycobacterium*, *Leishmania*, *Trypanosoma*, *Anaplasma*, *Borrelia*, and *Aspergillus* species and viruses such as human immunodeficiency virus (HIV), measles virus, vaccinia virus, paramyxovirus, vesicular stomatitis virus, Sindbis virus, and retroviruses [6,9,14,15,17–21].

The mechanisms behind the possibility of using α-Gal for developing a single-antigen pan-vaccine for the control of infectious diseases caused by pathogens with this modification on their surface include pathogen opsonization by anti-α-Gal IgM/IgG-type antibodies and boosting the non-pathogen-specific protective immune mechanisms [10,14–21]. The immunization with α-Gal will increase the levels of the natural anti-α-Gal IgM/IgG-type antibodies produced in response to gut microbiota [15] and do not cause an increase in the IgE-type allergic response to tick saliva, which are involved in triggering the AGS [1–12,15,40]. Therefore, in principle, the α-Gal-based vaccines could be applied to all hosts that do not produce α-Gal, but the immune response could be affected by different factors including the ABO blood groups [17].

In this study, we provided additional support for this proposal by characterizing the protective effect of the anti-α-Gal immune response for the control of tuberculosis caused by *Mycobacterium* spp. using the zebrafish model. The zebrafish model of tuberculosis has been used in our laboratory for the characterization of the protective response elicited after vaccination with heat inactivated *M. bovis* (IV) [27,28]. In these experiments, we showed a reduction of mycobacteriosis in vaccinated

Vaccines **2020**, *8*, 195

fish and suggested that the innate immune response mediated by the C3 pathway activated through TLR-AKR2-IL-1β and other proinflammatory cytokines acted as the protective mechanism against infection. Herein, the results showed some similarities and differences in the immune mechanisms activated by vaccination with IV and α-Gal.

The results suggested that *M. marinum* affects the zebrafish immunity by downregulating the expression of immune response genes with a stronger effect after mucosal infection that reproduces better the natural infection conditions. However, alternative innate immune mechanisms may be activated in response to mycobacterial infection [41]. Similar to vaccination with IV [27,28], the upregulation of proinflammatory cytokines through the TLR/NF-kB-AKR pathway was shown to be an α-Gal-induced putative protective mechanism to mycobacterial infection [42–44] (Figure 10). The use of adjuvant-containing α-Gal formulation showed higher levels of immune response genes in response to vaccination and infection when compared to α-Gal alone, thus suggesting that adjuvants may be considered to improve vaccine efficacy. However, the C3 pathway proposed to be involved in protective response to IV was not activated in α-Gal-vaccinated zebrafish. These results suggested that mycobacterial α-Gal may be like glycolipids that antagonize TLR2-mediated response (Figure 10). Cell envelope glycolipids and particularly sulfoglycolipids has been shown to inhibit NF-κB/AKR activation and subsequent cytokine production by acting as competitive antagonists of TLR2, thereby inhibiting the recognition of mycobacteria by this receptor [45].

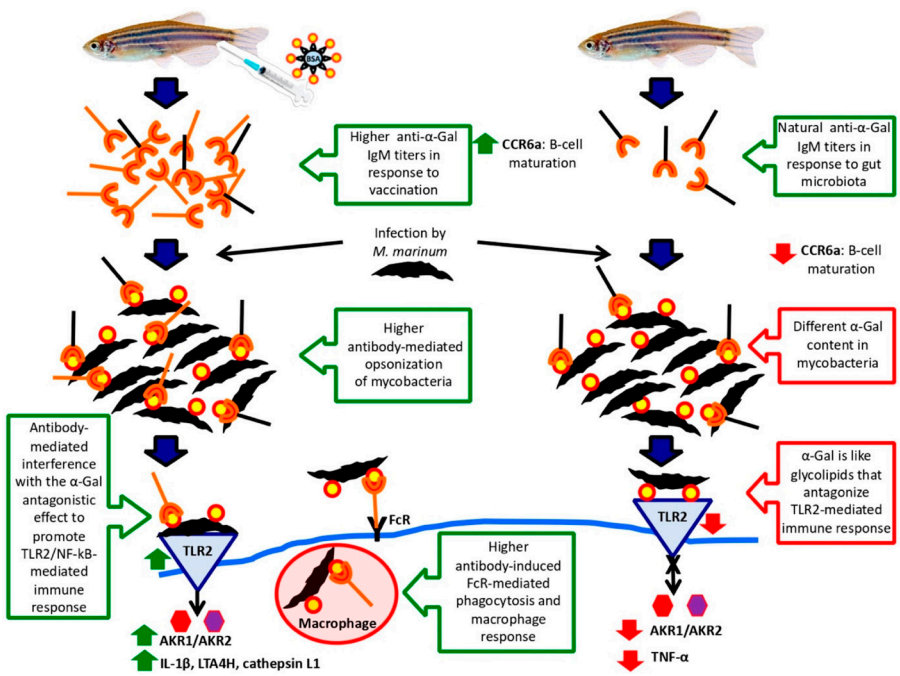

Figure 10. Immune mechanisms involved in mycobacterial infection and protective response to α-Gal in zebrafish: Zebrafish naturally produce anti-α-Gal IgM antibodies in response to gut microbiota with α-Gal modifications. However, vaccination with α-Gal results in higher anti-α-Gal IgM antibody levels. Additionally, while infection with *M. marinum* results in *ccr6a* downregulation, vaccination with α-Gal upregulates this gene to promote B-cell maturation and antibody production. Differences in α-Gal content between different mycobacteria may be an adaptive mechanism to prevent the anti-α-Gal IgM-mediated bacterial opsonization, which nevertheless will be more effective in vaccinated zebrafish.

This mechanism will also interfere with the α-Gal antagonistic effect to TLR2-mediated immune response. In this way, while mycobacterial infection interferes with the TLR2/NF-kB pathway, the induction of the TLR2/NF-kB pathway in response to vaccination will promote the immunity and the FcR-mediated phagocytosis and macrophage response in vaccinated zebrafish to control mycobacteriosis.

The previously shown role of antibodies against mycobacterial surface-exposed antigens in the control of tuberculosis [46] was also supported by results of our study. Zebrafish are α-Gal negative and have natural anti-α-Gal antibodies in response to gut microbiota [29]. Mycobacteria contain α-Gal on their surface, and therefore, antibodies against this antigen can opsonize *M. marinum* and promote Fc-receptor (FcR)-mediated phagocytosis and macrophage response with a higher effect in vaccinated zebrafish with higher anti-α-Gal antibody levels (Figure 10). The expression of the gene coding for the CCR6a beta chemokine receptor, which has been implicated in B-lineage maturation and antigen-driven B-cell differentiation and humoral immunity [47], was downregulated in response to infection but upregulated in vaccinated zebrafish, thus promoting the production of anti-α-Gal antibodies (Figure 10). Furthermore, *tnf alpha* was downregulated by *M. marinum* infection but not after vaccination with α-Gal, thus supporting a role for this cytokine in augmenting cell-mediated immunity in vaccinated zebrafish [46] (Figure 10). Antibody-mediated macrophage activation increases TNF-α secretion, which plays a major role in macrophage recruitment to the infection site during the initial and long-term control of tuberculosis [48]. Remarkably, the results showed that not all mycobacteria have the same α-Gal content, which may constitute an adaptation to escape from the anti-α-Gal antibody protective response in infected hosts. Nevertheless, higher anti-α-Gal antibody levels in vaccinated fish may mediate the interference with the α-Gal antagonistic effect to promote TLR2-mediated immune response (Figure 10).

Despite the finding that fish vaccinated with α-Gal showed a decrease in *M. marinum* infection levels, only animals infected with IP *M. marinum* had a significantly lower number of tuberculous granuloma lesions when compared to unvaccinated animals, and all *M. marinum*-infected groups showed a similar granuloma distribution of affected tissues. The chemokine receptor CXCR4 promotes granuloma formation and induction of angiogenesis by *M. marinum* [49]. Furthermore, *cxcr4* mRNA levels increase in patients with tuberculosis whereas amelioration of disease reduces receptor expression in vivo [50]. The C3 cleavage fragments modulate CXCR4-mediated response [51,52]; TNF-α, which stimulates the production of C3 [53], is also important in granuloma formation; and its neutralization results in the loss of granuloma structure [47]. In zebrafish, *cxcr4* mRNA levels did not change in response to vaccination with α-Gal and infection with *M. marinum*, and *tnf alpha* was downregulated in response to infection (Figure 6A–D and Figure 7). These results supported that vaccination with α-Gal decreases mycobacterial infection by mechanisms not mediated by the C3 pathway that has been proposed to be involved in protective response to vaccination with IV [27,28,36,54].

5. Conclusions

Vaccination with α-Gal protected against mycobacteriosis in the zebrafish model of tuberculosis. The results provided evidence that the protective mechanisms in response to vaccination with α-Gal include B-cell maturation, antibody-mediated opsonization of mycobacteria, FcR-mediated phagocytosis, macrophage response, interference with the α-Gal antagonistic effect of the TLR2/NF-kB-mediated immune response, and upregulation of pro-inflammatory cytokines. These mechanisms result in the decrease of mycobacteria levels through the activation of the humoral and cellular immune responses. These results provided additional evidence supporting the role of the α-Gal-induced immune response in the control of infections caused by pathogens with this modification on their surface and the possibility of using this approach for the control of multiple infectious diseases. The fact that vaccination with IV and α-Gal activate different immune protective mechanisms suggested that it may be possible to combine these antigens in future experiments to increase vaccine efficacy against mycobacterial infection.

Supplementary Materials: The following are available online at http://www.mdpi.com/2076-393X/8/2/195/s1, Figure S1: Effect of zebrafish vaccination with α-Gal and mycobacterial infection on the expression of immune response genes in experiments 1 (Figure S1A) and 2 (Figure S1B), Figure S2: Effect of different treatments/vaccination and mycobacterial infection on the T1 to T2 mRNA ratio of immune response genes, Figure S3: mRNA profile of immune response genes in response to different treatments/vaccination and mycobacterial infection, Figure S4: Differentially represented proteins in response to mycobacterial IP infection at T2, Figure S5: Differentially represented proteins in response to mycobacterial mucosal infection at T2, Figure S6: Differentially represented proteins in response to vaccination with α-Gal at T1, Table S1: Proteomics results.

Author Contributions: Conceptualization, J.d.l.F., M.V., A.C.-C., and C.G.; methodology, J.d.l.F. and M.V.; validation, I.P., M.C., and P.A.; formal analysis, J.d.l.F.; investigation, I.P., M.C., M.V., M.A.R., and P.A.; data curation, I.P., and M.V.; writing—original draft preparation, J.d.l.F.; writing—review and editing, J.d.l.F., M.V., A.C.-C., and C.G.; visualization, J.d.l.F. and M.V.; supervision, J.d.l.F. and M.V.; project administration, J.d.l.F., M.V., and C.G.; funding acquisition, J.d.l.F., M.V., and C.G.; All authors have read and agreed to the published version of the manuscript.

Funding: This study was supported by the Consejería de Educación, Cultura y Deportes, JCCM, Spain, projects CCM17-PIC-036 (SBPLY/17/180501/000185) and SBPLY/19/180501/000174. M.V. was supported by the University of Castilla La Mancha, UCLM, Spain, and the Fondo Europeo de Desarrollo Regional, FEDER, EU.

Acknowledgments: We thank Juan Galcerán Sáez (IN-CSIC-UMH, Spain) for providing zebrafish and Almudena González García and David Fernández (IREC, Spain) for technical assistance with the fish experimental facility.

Conflicts of Interest: The authors declare no conflicts of interest.

References

1. Van Nunen:, S.; O'Connor, K.S.; Clarke, L.R.; Boyle, R.X.; Fernando, S.L. The association between *Ixodes holocyclus* tick bite reactions and red meat allergy. *Intern. Med. J.* **2007**, *39*, A132.
2. Commins, S.P.; Satinover, S.M.; Hosen, J.; Mozena, J.; Borish, L.; Lewis, B.D.; Woodfolk, J.A.; Platts-Mills, T.A. Delayed anaphylaxis, angioedema, or urticaria after consumption of red meat in patients with IgE antibodies specific for galactose-alpha-1,3-galactose. *J. Allergy Clin. Immunol.* **2009**, *123*, 426–433. [CrossRef] [PubMed]
3. Steinke, J.W.; Platts-Mills, T.A.; Commins, S.P. The alpha-gal story: Lessons learned from connecting the dots. *J. Allergy Clin. Immunol.* **2015**, *135*, 589–596. [CrossRef] [PubMed]
4. Platts-Mills, T.A.; Schuyler, A.J.; Tripathi, A.; Commins, S.P. Anaphylaxis to the carbohydrate side chain alpha-gal. *Immunol. Allergy Clin. North. Am.* **2015**, *35*, 247–260. [CrossRef] [PubMed]
5. Mateos-Hernández, L.; Villar, M.; Moral, A.; Rodríguez, C.G.; Arias, T.A.; de la Osa, V.; Brito, F.F.; Fernández de Mera, I.G.; Alberdi, P.; Ruiz-Fons, F.; et al. Tick-host conflict: Immunoglobulin E antibodies to tick proteins in patients with anaphylaxis to tick bite. *Oncotarget* **2017**, *8*, 20630–20644. [CrossRef] [PubMed]
6. Galili, U. Evolution in primates by "Catastrophic-selection" interplay between enveloped virus epidemics, mutated genes of enzymes synthesizing carbohydrate antigens, and natural anticarbohydrate antibodies. *Am. J. Phys. Anthropol.* **2019**, *168*, 352–363. [CrossRef]
7. Hilger, C.; Fischer, J.; Wölbing, F.; Biedermann, T. Role and mechanism of galactose-alpha-1,3-galactose in the elicitation of delayed anaphylactic reactions to red meat. *Curr. Allergy Asthma Rep.* **2019**, *19*, 3. [CrossRef]
8. Cabezas-Cruz, A.; Valdés, J.; de la Fuente, J. Cancer research meets tick vectors for infectious diseases. *Lancet Infect. Dis.* **2014**, *10*, 916–917. [CrossRef]
9. Cabezas-Cruz, A.; Hodžić, A.; Román-Carrasco, P.; Mateos-Hernández, L.; Duscher, G.G.; Sinha, D.K.; Hemmer, W.; Swoboda, I.; Estrada-Peña, A.; de la Fuente, J. Environmental and molecular drivers of the α-Gal syndrome. *Front. Immunol.* **2019**, *10*, 1210. [CrossRef]
10. De la Fuente, J.; Pacheco, I.; Villar, M.; Cabezas-Cruz, A. The alpha-Gal syndrome: New insights into the tick-host conflict and cooperation. *Parasit. Vectors* **2019**, *12*, 154. [CrossRef]
11. Platts-Mills, T.A.E.; Commins, S.P.; Biedermann, T.; van Hage, M.; Levin, M.; Beck, L.A.; Diuk-Wasser, M.; Jappe, U.; Apostolovic, D.; Minnicozzi, M.; et al. On the cause and consequences of IgE to galactose-α-1,3-galactose: A report from the National Institute of Allergy and Infectious Disease workshop on understanding IgE-mediated mammalian meat allergy. *J. Allergy Clin. Immunol.* **2020**, *S0091-6749*, 30190–30191. [CrossRef] [PubMed]
12. Iweala, O.I.; Choudhary, S.K.; Addison, C.T.; Batty, C.J.; Kapita, C.M.; Amelio, C.; Schuyler, A.J.; Deng, S.; Bachelder, E.M.; Ainslie, K.M.; et al. Glycolipid-mediated basophil activation in alpha-gal allergy. *J. Allergy Clin. Immunol.* **2020**, *S0091-6749*, 30258–30260. [CrossRef] [PubMed]

13. De la Fuente, J.; Villar, M.; Cabezas-Cruz, A.; Estrada-Peña, A.; Ayllón, N.; Alberdi, P. Tick-host-pathogen interactions: Conflict and cooperation. *PLoS Pathog.* **2016**, *12*, e1005488. [CrossRef]
14. Hodžić, A.; Mateos-Hernández, L.; Frealle, E.; Román-Carrasco, P.; Alberdi, P.; Pichavant, M.; Risco-Castillo, V.; Le Roux, D.; Vicogne, J.; Hemmer, W.; et al. Infection with *Toxocara canis* inhibits the production of IgE antibodies to α-Gal in humans: Towards a conceptual framework of the hygiene hypothesis? *Vaccines* **2020**, *8*, 167. [CrossRef]
15. Yilmaz, B.; Portugal, S.; Tran, T.M.; Gozzelino, R.; Ramos, S.; Gomes, J.; Regalado, A.; Cowan, P.J.; d'Apice, A.J.; Chong, A.S.; et al. Gut microbiota elicits a protective immune response against malaria transmission. *Cell* **2014**, *159*, 1277–1289. [CrossRef]
16. Cabezas Cruz, A.; Valdés, J.J.; de la Fuente, J. Control of vector-borne infectious diseases by human immunity against α-Gal. *Expert Rev. Vaccines* **2016**, *15*, 953–955. [CrossRef]
17. Cabezas-Cruz, A.; Mateos-Hernández, L.; Alberdi, P.; Villar, M.; Riveau, G.; Hermann, E.; Schacht, A.; Khalife, J.; Correia-Neves, M.; Gortazar, C.; et al. Effect of blood type on anti-α-Gal immunity and the incidence of infectious diseases. *Exp. Mol. Med.* **2017**, *49*, e301. [CrossRef]
18. Iniguez, E.; Schocker, N.S.; Subramaniam, K.; Portillo, S.; Montoya, A.L.; Al-Salem, W.S.; Torres, C.L.; Rodriguez, F.; Moreira, O.C.; Acosta-Serrano, A.; et al. An α-Gal-containing neoglycoprotein-based vaccine partially protects against murine cutaneous leishmaniasis caused by *Leishmania major*. *PLoS Negl. Trop. Dis.* **2017**, *11*, e0006039. [CrossRef]
19. Moura, A.P.V.; Santos, L.C.B.; Brito, C.R.N.; Valencia, E.; Junqueira, C.; Filho, A.A.P.; Sant'Anna, M.R.V.; Gontijo, N.F.; Bartholomeu, D.C.; Fujiwara, R.T.; et al. Virus-like particle display of the α-Gal carbohydrate for vaccination against *Leishmania* infection. *ACS Cent. Sci.* **2017**, *3*, 1026–1031. [CrossRef]
20. Portillo, S.; Zepeda, B.G.; Iniguez, E.; Olivas, J.J.; Karimi, N.H.; Moreira, O.C.; Marques, A.F.; Michael, K.; Maldonado, R.A.; Almeida, I.C. A prophylactic α-Gal-based glycovaccine effectively protects against murine acute Chagas disease. *NPJ Vaccines* **2019**, *4*, 13. [CrossRef]
21. Hodžić, A.; Mateos-Hernández, L.; Leschnik, M.; Alberdi, P.; Rego, R.O.M.; Contreras, M.; Villar, M.; de la Fuente, J.; Cabezas-Cruz, A.; Duscher, G.G. Tick bites induce anti-α-Gal antibodies in dogs. *Vaccines* **2019**, *7*, 114. [CrossRef] [PubMed]
22. Yan, L.M.; Lau, S.P.N.; Poh, C.M.; Chan, V.S.F.; Chan, M.C.W.; Peiris, M.; Poon, L.L.M. Heterosubtypic protection induced by a live attenuated Influenza virus vaccine expressing galactose-α-1,3-galactose epitopes in infected cells. *mBio* **2020**, *11*, e00027-20. [CrossRef] [PubMed]
23. Salazar-Austin, N.; Dowdy, D.W.; Chaisson, R.E.; Golub, J.E. 70 years of TB prevention: Efficacy, effectiveness, toxicity, durability and duration. *Am. J. Epidemiol.* **2019**, *188*, 2078–2085. [PubMed]
24. Ramakrishnan, L. Looking within the zebrafish to understand the tuberculous granuloma. *Adv. Exp. Med. Bio.* **2013**, *783*, 251–266.
25. Cronan, M.R.; Tobin, D.M. Fit for consumption: Zebrafish as a model for tuberculosis. *Dis. Mod. Mec.* **2014**, *7*, 777–784. [CrossRef]
26. Van Leeuwen, L.M.; van der Sar, A.M.; Bitter, W. Animal models of tuberculosis: Zebrafish. *Cold Spring Harb. Perspect. Med.* **2015**, *5*, a018580. [CrossRef]
27. López, V.; Risalde, M.A.; Contreras, M.; Mateos-Hernández, L.; Vicente, J.; Gortázar, C.; de la Fuente, J. Heat-inactivated *Mycobacterium bovis* protects zebrafish against mycobacteriosis. *J. Fish Dis.* **2018**, *41*, 1515–1528. [CrossRef]
28. Risalde, M.A.; López, V.; Contreras, M.; Mateos-Hernández, L.; Gortázar, C.; de la Fuente, J. Control of mycobacteriosis in zebrafish (*Danio rerio*) mucosally vaccinated with heat-inactivated *Mycobacterium bovis*. *Vaccine* **2018**, *36*, 4447–4453. [CrossRef]
29. Contreras, M.; Pacheco, I.; Alberdi, P.; Díaz-Sánchez, S.; Artigas-Jerónimo, S.; Mateos-Hernández, L.; Villar, M.; Cabezas-Cruz, A.; de la Fuente, J. Allergic reactions and immunity in response to tick salivary biogenic substances and red meat consumption in the zebrafish model. *Front. Cell. Infect. Microbiol.* **2020**, *10*, 78. [CrossRef]
30. Cabezas-Cruz, A.; de la Fuente, J. Immunity to α-Gal: Towards a single-antigen pan-vaccine to control major infectious diseases. *ACS Cent. Sci.* **2017**, *3*, 1140–1142. [CrossRef]
31. Aubry, A.; Mougari, F.; Reibel, F.; Cambau, E. Mycobacterium marinum. *Microbiol. Spectr.* **2017**, *5*. [CrossRef]

32. Contreras, M.; Alberdi, P.; Fernández De Mera, I.G.; Krull, C.; Nijhof, A.; Villar, M.; de la Fuente, J. Vaccinomics approach to the identification of candidate protective antigens for the control of tick vector infestations and *Anaplasma phagocytophilum* infection. *Front. Cell. Infect. Microbiol.* **2017**, *7*, 360. [CrossRef]
33. Cosma, C.L.; Swaim, L.E.; Volkman, H.; Ramakrishnan, L.; Davis, J.M. Zebrafish and frog models of *Mycobacterium marinum* infection. *Curr. Protoc. Microbiol.* **2006**, *10*, 10B.2.
34. Ririe, K.M.; Rasmussen, R.P.; Wittwer, C.T. Product differentiation by analysis of DNA melting curves during the polymerase chain reaction. *Anal. Biochem.* **1997**, *245*, 154–160. [CrossRef]
35. Livak, K.J.; Schmittgen, T.D. Analysis of relative gene expression data using real-time quantitative PCR and the 2(-Delta Delta C(T)) Method. *Methods* **2001**, *25*, 402–408. [CrossRef]
36. Beltrán-Beck, B.; de la Fuente, J.; Garrido, J.M.; Aranaz, A.; Sevilla, I.; Villar, M.; Boadella, M.; Galindo, R.C.; Pérez de la Lastra, J.M.; Moreno-Cid, J.A.; et al. Oral vaccination with heat inactivated *Mycobacterium bovis* activates the complement system to protect against tuberculosis. *PLoS ONE* **2014**, *9*, e98048. [CrossRef]
37. Benard, E.L.; Rougeot, J.; Racz, P.I.; Spaink, H.P.; Meijer, A.H. Transcriptomic approaches in the zebrafish model for tuberculosis-insights into host- and pathogen-specific determinants of the innate immune response. *Adv. Genet.* **2016**, *95*, 217–251.
38. Gillet, L.C.; Navarro, P.; Tate, S.; Röst, H.; Selevsek, N.; Reiter, L.; Bonner, R.; Aebersold, R. Targeted data extraction of the MS/MS spectra generated by data-independent acquisition: A new concept for consistent and accurate proteome analysis. *Mol. Cell. Proteom.* **2012**, *11*, O111.016717. [CrossRef]
39. Shilov, I.V.; Seymour, S.L.; Patel, A.A.; Loboda, A.; Tang, W.H.; Keating, S.P.; Hunter, C.L.; Nuwaysir, L.M.; Schaeffer, D.A. The paragon algorithm, a next generation search engine that uses sequence temperature values and feature probabilities to identify peptides from tandem mass spectra. *Mol. Cell. Proteom.* **2007**, *6*, 1638–1655. [CrossRef]
40. Villar, M.; Pacheco, I.; Merino, O.; Contreras, M.; Mateos-Hernández, L.; Prado, E.; Barros-Picanco, D.K.; Francisco Lima-Barbero, J.; Artigas-Jerónimo, S.; Alberdi, P.; et al. Tick and host derived compounds modulate the biochemical properties of the cement complex substance. *Biomolecules* **2020**, *10*, 555. [CrossRef]
41. Lim, H.X.; Jung, H.J.; Lee, A.; Park, S.H.; Han, B.W.; Cho, D.; Kim, T.S. Lysyl-transfer RNA synthetase induces the maturation of dendritic cells through MAPK and NF-κB pathways, strongly contributing to enhanced Th1 cell responses. *J. Immunol.* **2018**, *201*, 2832–2841. [CrossRef]
42. Maji, A.; Misra, R.; Kumar Mondal, A.; Kumar, D.; Bajaj, D.; Singhal, A.; Arora, G.; Bhaduri, A.; Sajid, A.; Bhatia, S.; et al. Expression profiling of lymph nodes in tuberculosis patients reveal inflammatory milieu at site of infection. *Sci. Rep.* **2015**, *5*, 15214. [CrossRef]
43. Haeggström, J.Z.; Tholander, F.; Wetterholm, A. Structure and catalytic mechanisms of leukotriene A4 hydrolase. *Prostaglandins Other Lipid Mediat.* **2007**, *83*, 198–202. [CrossRef]
44. Rodriguez, A.R.; Yu, J.J.; Guentzel, M.N.; Navara, C.S.; Klose, K.E.; Forsthuber, T.G.; Chambers, J.P.; Berton, M.T.; Arulanandam, B.P. Mast cell TLR2 signaling is crucial for effective killing of *Francisella tularensis*. *J. Immunol.* **2012**, *188*, 5604–5611. [CrossRef]
45. Blanc, L.; Gilleron, M.; Prandi, J.; Song, O.R.; Jang, M.S.; Gicquel, B.; Drocourt, D.; Neyrolles, O.; Brodin, P.; Tiraby, G.; et al. *Mycobacterium tuberculosis* inhibits human innate immune responses via the production of TLR2 antagonist glycolipids. *Proc. Natl. Acad. Sci. USA* **2017**, *114*, 11205–11210. [CrossRef]
46. Jacobs, A.J.; Mongkolsapaya, J.; Screaton, G.R.; McShane, H.; Wilkinson, R.J. Antibodies and tuberculosis. *Tuberculosis* **2016**, *101*, 102–113. [CrossRef]
47. Lee, A.Y.S.; Körner, H. The CCR6-CCL20 axis in humoral immunity and T-B cell immunobiology. *Immunobiology* **2019**, *224*, 449–454. [CrossRef]
48. Lin, P.L.; Plessner, H.L.; Voitenok, N.N.; Flynn, J.L. Tumor necrosis factor and tuberculosis. *J. Investig. Dermatol. Symp. Proc.* **2007**, *12*, 22–25. [CrossRef]
49. Torraca, V.; Tulotta, C.; Snaar-Jagalska, B.E.; Meijer, A.H. The chemokine receptor CXCR4 promotes granuloma formation by sustaining a mycobacteria-induced angiogenesis programme. *Sci. Rep.* **2017**, *7*, 45061. [CrossRef]
50. Hoshino, Y.; Tse, D.B.; Rochford, G.; Prabhakar, S.; Hoshino, S.; Chitkara, N.; Kuwabara, K.; Ching, E.; Raju, B.; Gold, J.A.; et al. Mycobacterium tuberculosis-induced CXCR4 and chemokine expression leads to preferential X4 HIV-1 replication in human macrophages. *J. Immunol.* **2004**, *172*, 6251–6258. [CrossRef]

51. Ratajczak, M.Z.; Reca, R.; Wysoczynski, M.; Yan, J.; Ratajczak, J. Modulation of the SDF-1-CXCR4 axis by the third complement component (C3)-implications for trafficking of CXCR4+ stem cells. *Exp. Hematol.* **2006**, *34*, 986–995. [CrossRef]
52. Ratajczak, M.Z.; Serwin, K.; Schneider, G. Innate immunity derived factors as external modulators of the CXCL12-CXCR4 axis and their role in stem cell homing and mobilization. *Theranostics* **2013**, *3*, 3–10. [CrossRef]
53. Sheerin, N.S.; Zhou, W.; Adler, S.; Sacks, S.H. TNF-alpha regulation of C3 gene expression and protein biosynthesis in rat glomerular endothelial cells. *Kidney Int.* **1997**, *51*, 703–710. [CrossRef]
54. De la Fuente, J.; Gortázar, C.; Juste, R. Complement component 3: A new paradigm in tuberculosis vaccine. *Expert Rev. Vaccines* **2016**, *15*, 275–277. [CrossRef]

Supplementary material. Chapter 3a

Supplementary material not included from **Pacheco, I.,** Contreras, M., Villar, M., Risalde, M.A., Alberdi, P., Cabezas-Cruz, A., Gortazar, C., de la Fuente, J. (2020). Vaccination with alpha-Gal protects against mycobacterial infection in the zebrafish model of tuberculosis. Vaccines 8, 195.

https://www.mdpi.com/2076-393X/8/2/195

- Table S1. Proteomics results.

Chapter 3b. Probiotic bacteria with high alpha-Gal content protect zebrafish against mycobacteriosis

Pacheco, I., Díaz-Sánchez, S., Contreras, M., Villar, M., Cabezas-Cruz, A., Gortázar, C., de la Fuente, J. (2021). Probiotic bacteria with high alpha-Gal content protect zebrafish against mycobacteriosis. Pharmaceuticals 14, 635. https://doi.org/10.3390/ph14070635

pharmaceuticals

MDPI

Article

Probiotic Bacteria with High Alpha-Gal Content Protect Zebrafish against Mycobacteriosis

Iván Pacheco [1,†], Sandra Díaz-Sánchez [1,†], Marinela Contreras [2,†], Margarita Villar [1,3], Alejandro Cabezas-Cruz [4], Christian Gortázar [1] and José de la Fuente [1,5,*]

[1] SaBio, Instituto de Investigación en Recursos Cinegéticos IREC-CSIC-UCLM-JCCM, Ronda de Toledo 12, 13005 Ciudad Real, Spain; ivan.pacheco@uclm.es (I.P.); sandra.dsan@gmail.com (S.D.-S.); margaritam.villar@uclm.es (M.V.); christian.gortazar@uclm.es (C.G.)
[2] Interdisciplinary Laboratory of Clinical Analysis, Interlab-UMU, Regional Campus of International Excellence Campus Mare Nostrum, University of Murcia, Espinardo, 30100 Murcia, Spain; marinelacr@hotmail.com
[3] Biochemistry Section, Faculty of Science and Chemical Technologies and Regional Centre for Biomedical Research (CRIB), University of Castilla-La Mancha, 13071 Ciudad Real, Spain
[4] UMR BIPAR, INRAE, ANSES, Ecole Nationale Vétérinaire d'Alfort, Université Paris-Est, 94700 Maisons-Alfort, France; alejandro.cabezas@vet-alfort.fr
[5] Department of Veterinary Pathobiology, Center for Veterinary Health Sciences, Oklahoma State University, Stillwater, OK 74078, USA
* Correspondence: jose_delafuente@yahoo.com or josedejesus.fuente@uclm.es
† Equal contribution.

Abstract: Mycobacteriosis affects wild fish and aquaculture worldwide, and alternatives to antibiotics are needed for an effective and environmentally sound control of infectious diseases. Probiotics have shown beneficial effects on fish growth, nutrient metabolism, immune responses, disease prevention and control, and gut microbiota with higher water quality. However, the identification and characterization of the molecules and mechanisms associated with probiotics is a challenge that requires investigation. To address this challenge, herein we used the zebrafish model for the study of the efficacy and mechanisms of probiotic interventions against tuberculosis. First, bacteria from fish gut microbiota were identified with high content of the surface glycotope Galα1-3Galβ1-(3)4GlcNAc-R (α-Gal) that has been shown to induce protective immune responses. The results showed that probiotics of selected bacteria with high α-Gal content, namely *Aeromonas veronii* and *Pseudomonas entomophila*, were biosafe and effective for the control of *Mycobacterium marinum*. Protective mechanisms regulating immunity and metabolism activated in response to α-Gal and probiotics with high α-Gal content included modification of gut microbiota composition, B-cell maturation, anti-α-Gal antibodies-mediated control of mycobacteria, induced innate immune responses, beneficial effects on nutrient metabolism and reduced oxidative stress. These results support the potential of probiotics with high α-Gal content for the control of fish mycobacteriosis and suggested the possibility of exploring the development of combined probiotic treatments alone and in combination with α-Gal for the control of infectious diseases.

Keywords: probiotic; alpha-Gal; tuberculosis; fish; mycobacteriosis; immunology; vaccine; metabolism; antibody

Citation: Pacheco, I.; Díaz-Sánchez, S.; Contreras, M.; Villar, M.; Cabezas-Cruz, A.; Gortázar, C.; de la Fuente, J. Probiotic Bacteria with High Alpha-Gal Content Protect Zebrafish against Mycobacteriosis. *Pharmaceuticals* **2021**, *14*, 635. https://doi.org/10.3390/ph14070635

Academic Editors: Yuhei Nishimura and Martin Distel

Received: 26 May 2021
Accepted: 28 June 2021
Published: 30 June 2021

1. Introduction

The increasing incidence of infectious diseases associated with intensive aquaculture and water contamination is a major limitation for economics in aquaculture [1,2]. In particular, freshwater and marine fish mycobacteriosis caused by *Mycobacterium marinum* and other related *Mycobacterium* species affects wild fish and aquaculture [3,4]. Associated to it, the use of antibiotics has resulted in a growing prevalence of antibiotic-resistant pathogens, damage to the environment, reduced fish immunity due to effects on gut microbiota and risks associated with contaminated food [5–7]. Therefore, probiotics and

postbiotics are considered an environmentally sustainable alternative to antibiotics for the prevention and control of infectious diseases in aquaculture.

Probiotics are live microorganisms that guide molecular interactions with potential beneficial effects to the host [8,9]. Probiotics have shown beneficial effects on fish growth, nutrient metabolism, immune responses, disease prevention and control, and gut microbiota with higher water quality [10,11]. Most probiotics used in aquaculture are lactic acid or *Bacillus* spp. due to their safety for mammalian species and production of hydrolytic enzymes that increase nutrient utilization [12–14]. However, recently, other criteria, such as species-specificity, pathogenicity, antibiotic resistance, extracellular enzyme production and antagonistic activity [15], have been applied for the identification of new probiotic bacteria, such as *Shewanella xiamenensis*, *Aeromonas veronii* [12], *Chromobacterium aquaticum* [16], *Streptomyces flavotricini* [17] and *Pediococcus acidilactici* [18]. Regarding fish pathogenic *Mycobacterium* spp., probiotics have shown reduction in mycobacterial levels [19,20].

One of the main challenges associated with probiotics is the identification and characterization of the molecules and mechanisms associated with its function [9]. Recently, research has been focused on the characterization of probiotic bacteria-derived postbiotic biomolecules, such as cell-wall peptidoglycans, because they are safer while retaining the beneficial effects on fish host [21]. The oligosaccharide Galα1-3Galβ1-(3)4GlcNAc-R (α-Gal) is a glycan linked to proteins and lipids in prokaryotic and eukaryotic organisms and with potential for the control of infectious diseases [22,23]. The potential of the surface glycotopes, such as α-Gal, to induce protective immune responses makes them an effective target for the development of vaccines and probiotic/postbiotic interventions [22–26].

The zebrafish (*Danio rerio* Hamilton 1822) has been previously validated as a fish model for the study of tuberculosis, vaccines against mycobacteriosis, fish immunity, gut microbiota and probiotics efficacy on boosting nutrient metabolism and innate immunity against pathogen infection [16,18,24,27–36]. To address the potential of α-Gal-rich probiotics for the control of mycobacteriosis, in this, study zebrafish were used for the identification and characterization of bacterial microbiota α-Gal content. Then, selected bacteria with high α-Gal content, *Aeromonas veronii* and *Pseudomonas entomophila*, were used as probiotics for the control of *Mycobacterium marinum* and the study of associated microbiota and immune-mediated mechanisms. The results showed that treatment with α-Gal and probiotics with high α-Gal content modified fish gut microbiota composition and activated protective mechanisms regulating immunity and metabolism.

2. Results and Discussion

2.1. Zebrafish Gut Microbiota Contains Potential Probiotic Bacteria with High α-Gal Content

A methodological approach was developed for the identification and characterization of zebrafish native gut potential probiotic bacteria (Figure 1). After incubation, each morphologically distinct colony (form, color, texture, elevation and margin) was encoded. From each sampling plate, two representatives of each colony were randomly selected and subcultured on a separate blood agar and isolated for downstream analyses. A total of two different bacterial community phenotypes were observed under the identification criteria, aerobic and anaerobic bacteria in both LRZ and PSZ groups (Table 1). Sanger sequencing and BLASTN searches of the V3/V4 16S rDNA of five bacterial isolates resulted in 98.4% to 99.8% identity to bacteria previously reported in zebrafish gut microbiota [37–39] (Table 2). Of them, entries with maximum identity corresponded to *P. entomophila* (99.8%), *S. xiamenensis* (99.8%) and *A. veronii* (99.3%) (Table 2). These bacteria were then selected for the characterization of α-Gal content and glycan structure (Figure 2A–D).

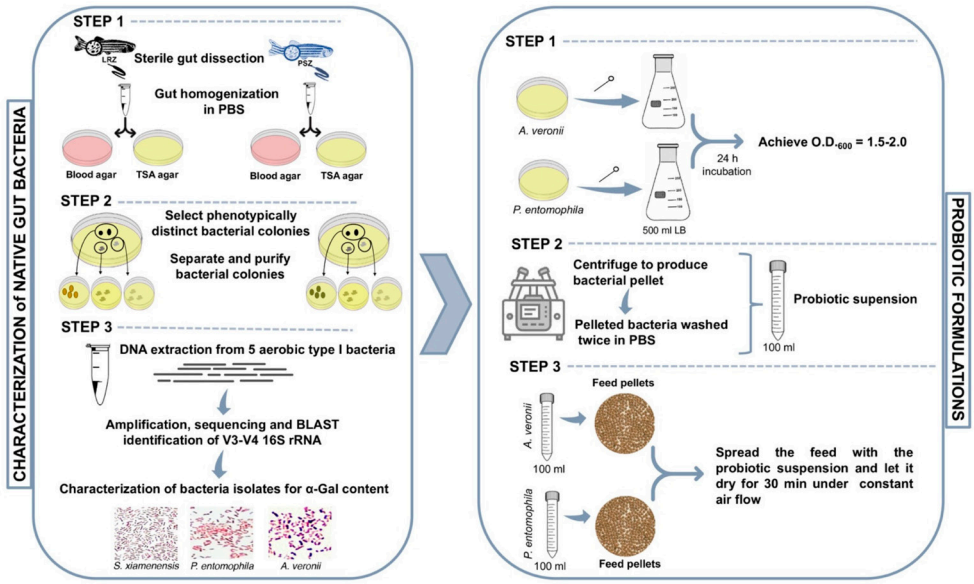

Figure 1. Methodology for the identification and characterization of zebrafish native gut potential probiotic bacteria. Adult female and male wild-type AB laboratory-reared zebrafish (LRZ) and pet-store zebrafish (PSZ) were used for analysis. Potential probiotic bacteria were isolated from the gut or gastrointestinal tract, and bacteria identified with high α-Gal content, namely *A. veronii* and *P. entomophila*, were used for probiotic formulations.

Table 1. Phenotypic characteristics and classification of cultured bacteria isolated from zebrafish gut microbiota.

Organism	Colony Description	Classification
Aerobic	circular, pink, raised, punctiform bacterial colonies	Type I
	circular, creamy white, raised, bacterial colonies (≤5 mm)	Type II
	irregular, dry white, flat colonies (≤5 mm)	Type III
Anaerobic	circular, creamy white, raised colonies (≤5 mm)	Type Ib
	circular, white, raised, punctiform colonies	Type IIb

Table 2. BLAST results of *16S rRNA* gene sequences from aerobic bacterial type I colony isolates.

ID	BLAST Match to 16S rRNA	Max Score, Total Score, Query Cover, Identity, E-Value	Genebank Accession Number	References in Zebrafish
PSZ1	*Aeromonas veronii* strain JCM 7375	813, 813, 91%, 99.3%, 0.0	NR_112838.1 NR_118947.1 NR_044845.1	[37–39]
PSZ4	*Microbacterium mitrae* strain M4-8	773, 773, 91%, 99.1%, 0.0	NR_104520.1	[37]
PSZ9	*Dyadobacter alkalitolerans* strain 12116	778, 778, 92%, 98.4%, 0.0	NR_044476.1	[39]
LRZ3	*Shewanella xiamenensis* strain S4	826, 826, 91%, 99.8%, 0.0	NR_116732.1	[37,39]
LRZ9	*Pseudomonas entomophila* L48	826, 826, 92%, 99.8%, 0.0	NR_102854.1	[37–39]

The maximum identities of all V3/V4 16S rRNA gene sequences were searched by using the GenBank DNA sequence database and the BLASTN.

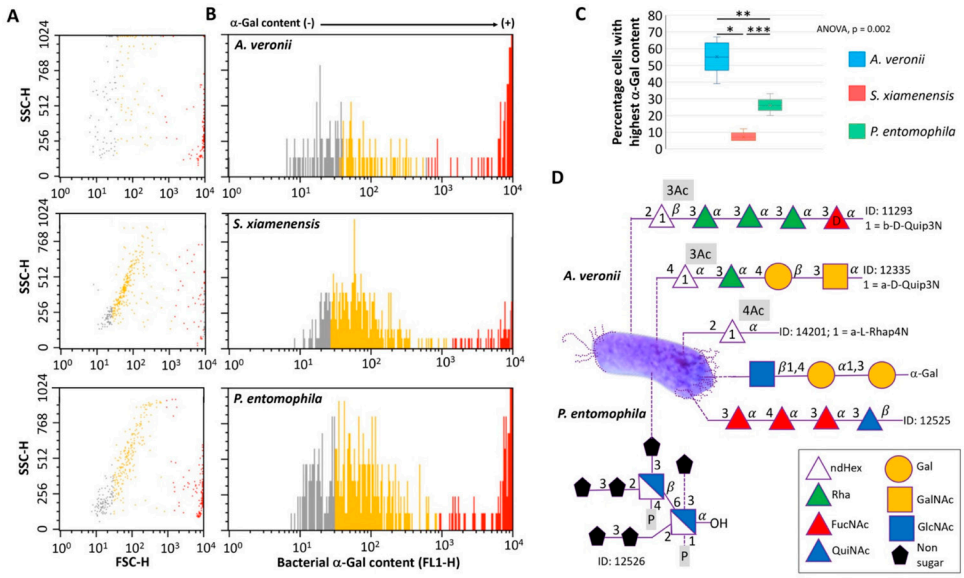

Figure 2. The carbohydrate structure and α-Gal content in potential probiotic bacteria. (**A**) Density plot representing bacteria that were gated by forward (FSC-H) and side (SSC-H) scatter. (**B**) Bacteria are represented in a histogram to evaluate the relative α-Gal levels (FL1-H). Cells were incubated with the α-Gal epitope monoclonal antibody M86. FITC-goat anti-mouse IgM-labeled antibodies were used as a secondary antibody. Samples were analyzed on a FAC-Scalibur flow cytometer equipped with CellQuest Pro software v.4. The viable cell population was gated according to forward-scatter (FSC-H) and side-scatter (SSC-H) parameters. (**C**) The percentage of viable cell population with highest α-Gal content (with mean fluorescence intensity >10^3 FSC-H; red marks) was compared between different bacteria by one-way ANOVA test ($p < 0.005$) followed by post hoc Holm multiple comparisons (* $p = 0.002$, ** $p = 0.02$, *** $p = 0.04$, $n = 5$ biological replicates). (**D**) The bacterial carbohydrate structure for bacteria identified in the zebrafish microbiota with highest α-Gal content, namely *A. veronii* and *P. entomophila*, was characterized by using the Bacterial Carbohydrate Structure Database. The α-Gal was included as reported here in both bacteria. Compound IDs are shown. IUPAC condensed terms are disclosed in Materials and Methods.

The results showed that all three bacteria have α-Gal on its surface (Figure 2A,B) with significantly highest relative levels (>10^3 FSC-H) in *A. veronii* (55% cells) and *P. entomophila* (26% cells) when compared to *S. xiamenensis* (7%) (Figure 2C). As a reference, published data for *M. marinum* showed 3.2% cells with highest α-Gal content [24]. These results correlated with the reported carbohydrate structure in these bacteria, in which *A. veronii* but not *P. entomophila* contain galactose in addition to α-Gal in compound ID 12335 [-4)-a-D-Quip3NAc-(1–3)-a-L-Rhap-(1-4)-b-D-Galp-(1–3_-a-D-GalpNAc-(1-] [40] (Figure 2D).

Among fish-associated bacteria, *A. veronii* is found in fresh water in association with vertebrates and invertebrates with virulence factors such as enterotoxin, flagella and outer membrane proteins that affect fishes and other aquatic animals with high mortality rate and economic losses [41–48]. *Pseudomonas entomophila* is commonly found in insects and soil and is closely related to *P. putida* [49]. Together with *Aeromonas* spp., *Pseudomonas* spp. are among the most pathogenic Gram-negative bacteria in fish with resistance to multiple antibiotics commonly used in aquaculture [50,51]. However, *A. veronii* and *Pseudomonas* spp. are also symbionts with possible beneficial effects for the host [12,42,52].

2.2. Bacteria from Zebrafish Gut Microbiota with High Alpha-Gal Content Are Not Toxic

A basic requirement for probiotics is the safety in treated organisms. To assess this requirement, the toxicity of bacteria from the zebrafish gut microbiota with highest α-Gal content, namely *A. veronii* and *P. entomophila*, was evaluated by intraperitoneal injection of different bacterial doses. The results suggested low pathogenicity and toxicity of these potential probiotic bacteria even at high doses of 1×10^6 CFU per fish (100% and 90% survival rate for *P. entomophila* and *A. veronii*, respectively; Figure 3A). The only symptom observed in treated fish before dead was abnormal behavior pattern. These results support the use of these bacteria for probiotic treatments in fish.

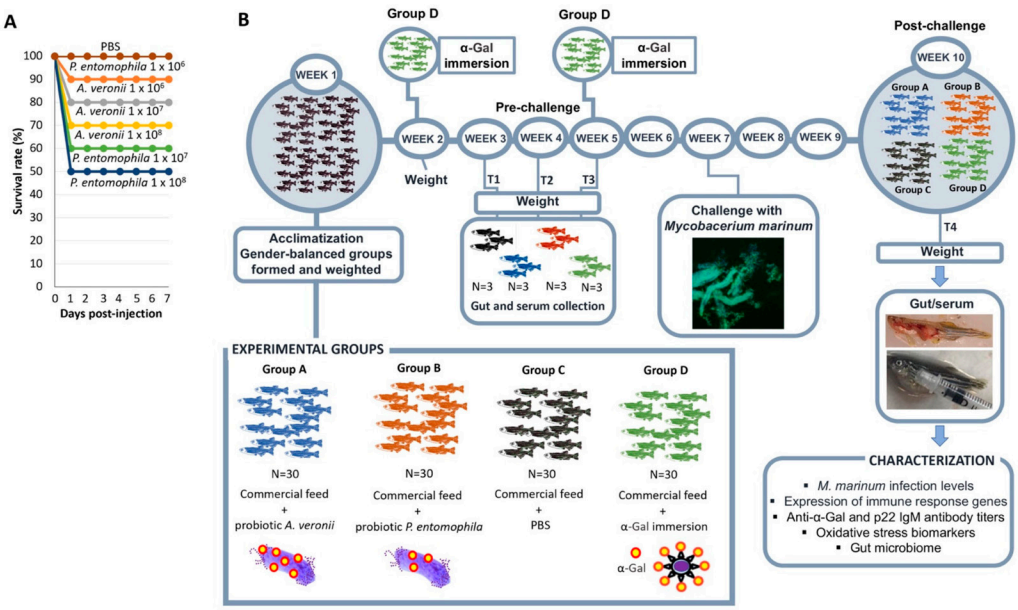

Figure 3. Evaluation of proposed probiotic bacteria in zebrafish. (**A**) Evaluation of bacterial biosafety. Ten fish per group were injected intraperitoneally with 1×10^6, 1×10^7 and 1×10^8 CFU per fish for both *A. veronii* and *P. entomophila*, separately. Fish injected with PBS buffer were used as controls. Bacterial toxicity was evaluated by recording signs and symptoms of infection and mortality of the injected fish daily for 7 days. (**B**) Experimental design for protective response against *M. marinum*. The effect of immunization with zebrafish gut candidate probiotic bacteria was evaluated with α-Gal and PBS used as positive and negative controls, respectively. Thirty LRZ were randomly allocated to Group A, commercial diet with probiotic *A. veronii*; Group B, commercial diet with probiotic *P. entomophila*; Group C, commercial diet with PBS; and Group D, commercial diet with α-Gal immersion. Fish were weighted at the weeks 1–5 and 10 at the end of the experiment. Gut and sera were collected at weeks 3 (T1), 4 (T2) and 5 (T3) and at the end of the experiment (week 10; T4) and processed for gut and serum collection for analysis of antibody levels by ELISA, mycobacteria levels by RT-qPCR, expression of selected immune response gene markers by RT-qPCR, oxidative stress biomarkers and gut microbiome.

2.3. Bacteria from Zebrafish Gut Microbiota with High Alpha-Gal Content Protect Fish against Mycobacteriosis

Bacteria from the zebrafish gut microbiota with highest α-Gal content and nontoxic were used as probiotics in fish challenged with *M. marinum* for the characterization of protective immune and oxidative stress responses and gut microbiome (Figure 3B).

The effect of probiotic treatment and challenge with *M. marinum* was characterized on the zebrafish mycobacterial infection levels and antibody response (Figure 4A–C and Figure 5). High animal-to-animal variations in the *M. marinum* infection determined by mycobacteria RNA levels were observed in the group treated with the *A. veronii* probiotic (Figure 4A). Consequently, a significant difference in mycobacterial infection when compared to control fish was observed only in groups treated with the *P. entomophila* probiotic (44% decrease) and α-Gal (38% decrease) (Figure 4A). However, the IgM antibody levels against *Mycobacterium* P22 and α-Gal were significantly lower and higher in all probiotics or α-Gal treated groups when compared to controls, respectively (Figure 4B). Accordingly, anti-P22 antibody titers significantly increased from T1 (before *M. marinum* infection) to T4 (after infection) only in the control group while anti-α-Gal antibody levels increased only in treated groups (Figure 5). These results suggested that the previously demonstrated protective antibody response to α-Gal [23,24] increased in response to probiotics and α-Gal treatments, which translated into lower anti-P22 antibody levels likely reflecting reduction in mycobacterial infection. In support to this finding, a correlation analysis was conducted between antibody titers and *M. marinum* infection RNA levels to show a significant positive and negative correlation for anti-P22 and anti-α-Gal antibody titers, respectively (Figure 4C). The results of this trial supported that *A. veronii* and *P. entomophila* may be used as probiotics against fish mycobacteriosis.

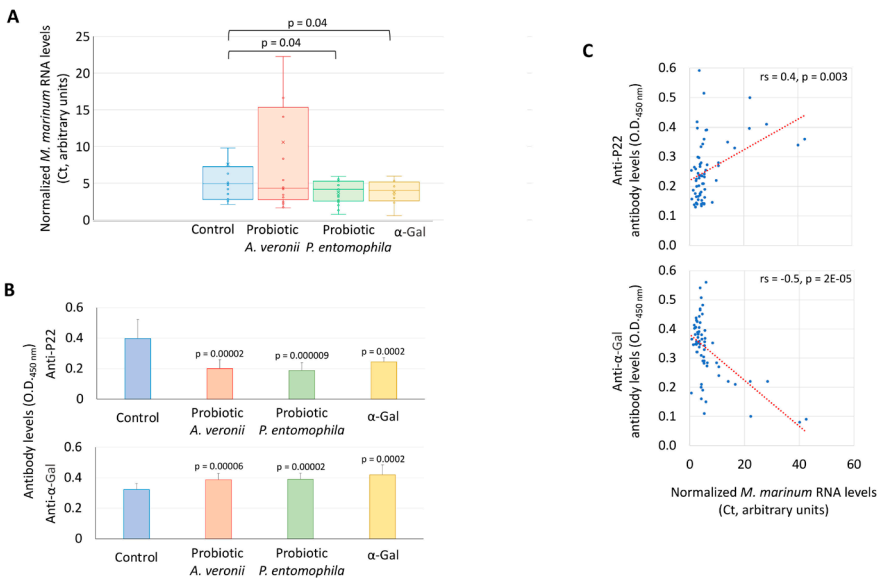

Figure 4. Effect of probiotic treatment and challenge with *M. marinum* on the zebrafish mycobacterial infection levels and antibody response. (**A**) *Mycobacterium* RNA levels were characterized by RT-qPCR in immunized and control PBS zebrafish challenged with *M. marinum*, normalized against *D. rerio gapdh*. The normalized Ct values were compared between treated and negative PBS control groups by Student's *t*-test with unequal variance ($p < 0.05$; $n = 10–17$/group). (**B**) Anti-α-Gal and P22 IgM antibody titers were characterized by ELISA in immunized and control PBS zebrafish challenged with *M. marinum*. The o.d. at 450 nm (mean of the duplicate well values of o.d. P22 or α-Gal–o.d. PBS control plus standard deviation, SD) were compared between treated and negative PBS control groups at T4 by Student's *t*-test with unequal variance ($p < 0.005$; $n = 12–20$/group). (**C**) Spearman's Rho correlation analysis between antibody titers and *M. marinum* infection RNA levels ($p < 0.005$).

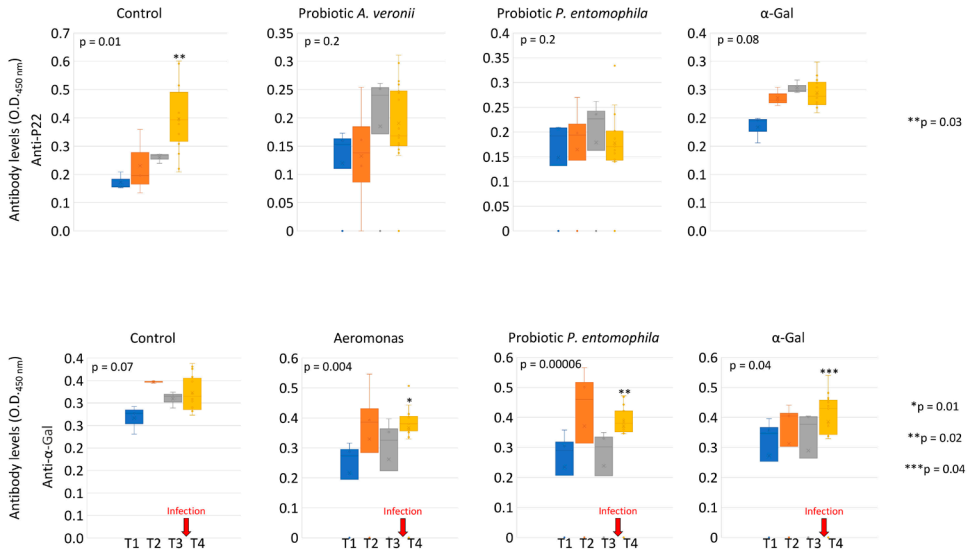

Figure 5. Anti-α-Gal and P22 IgM antibody titers in immunized and control PBS zebrafish challenged with *M. marinum*. Anti-α-Gal and P22 IgM antibody titers were characterized by ELISA. The o.d. at 450 nm (mean of the duplicate well values of o.d. P22 or α-Gal – o.d. PBS control) was compared between different time points (T1 to T4) by one-way ANOVA test ($p < 0.05$), followed by post hoc Holm multiple comparisons between T1 and T4 (* $p < 0.01$, ** $p < 0.04$, *** $p < 0.05$, n = 3–20/group). The time of infection challenge with *M. marinum* is shown with red arrows.

2.4. Treatment with Probiotic Bacteria with High α-Gal Content Induce the Expression of Immune Response and Nutrient Metabolism Genes

For the characterization of probiotic-induced mechanisms, immune response (*ccr6a*, *tlr2*, *akr2*, *IL-1ß*, *C3*, *IL-6*, *tnf-α* and *NF-kB*) and nutrient metabolism (*hk-1*) genes were selected, as they were previously shown to be involved in zebrafish immune protective mechanisms and response to immunization with α-Gal and probiotics [16,24,32,53] (Figure 6A,B). The expression of selected genes was characterized in the gut involved in both innate and adaptive fish immunity [35,53,54]. The effect of treatment with probiotics or α-Gal and *M. marinum* infection at the end of the trial (T4) corroborated previous results in α-Gal-immunized zebrafish [24] with upregulation of *ccr6a*, *tlr2*, *ak2* and *IL-1ß* (Figure 6A). The characterization of the effect of probiotics/α-Gal treatments before (T1/T3) and after (T4) infection with *M. marinum* showed upregulation of *hk-1* and *IL-6* in response to α-Gal treatment and upregulation of *hk-1*, *IL-6*, *tnf-α* and *NF-kB* in response to α-Gal treatment and *M. marinum* infection (Figure 6B; Supplementary Materials Figure S1). The treatment with probiotic *A. veronii* resulted in the upregulation of *ccr6a* and *tnf-α* before and after mycobacterial infection, respectively (Figure 6B; Supplementary Materials Figure S1). However, the *ccr6a* and *tlr2* mRNA levels decreased after treatment with probiotic *A. veronii* and *M. marinum* infection (Figure 6B; Supplementary Materials Figure S1). The treatment with *P. entomophila* upregulated *tnf-α* before infection and *tnf-α*, *IL-6* and *hk-1* after infection (Figure 6B). Gene expression levels did not vary in control zebrafish (Figure 6B; Supplementary Materials Figure S1), thus supporting those changes in gene mRNA were not in response to mycobacterial infection only.

Table 3. List of significant differentially represented bacterial taxa in zebrafish microbiota.

α-Gal vs. Control at Pre-Challenge						
Taxon	**Diff.btw**	**Diff.win**	**Effect**	**Overlap**	**We.ep**	**We.eBH**
Roseomonas	13.542346	2.9935668	4.663723	0.000233886	3.212340e-04	0.02402259
Tabrizicola	5.322295	0.9551066	5.490361	0.000233886	1.855949e-05	0.00295325
***P. entomophila* Probiotic Treatment vs. Control at Post-Challenge**						
Taxon	**Diff.btw**	**Diff.win**	**Effect**	**Overlap**	**We.ep**	**We.eBH**
Barnesiella	−2.124928	0.4827484	−3.883899	0.000140345	0.0003810454	0.02501155
Defluviicoccus	−2.790908	0.9249851	−3.087608	0.000140345	0.0003750165	0.02514513
Arenimonas	−1.797804	0.6606933	−2.640389	0.000140345	0.0006246535	0.03367145
Bradyrhizobium	−1.208369	0.5903415	−2.048345	0.000140345	0.0017745113	0.04961546
Gemmobacter	12.002481	3.4395137	3.290789	0.000140345	0.0019083535	0.04779711
Rubrivivax	10.355734	2.8742810	3.437225	0.000140345	0.0017269486	0.03403588
Dinghuibacter	8.695993	2.4873367	3.648279	0.000140345	0.0027296612	0.04676323
Candidatus Berkiella	9.832489	2.5879052	3.665712	0.000140345	0.0016078763	0.03464549
Tabrizicola	10.649151	2.5152927	4.325241	0.000140345	0.0020747599	0.03980276

The results were obtained by using the AlDEx2 algorithms. Abbreviations: diff.btw, median difference between groups on a log base 2 scale; diff.win, largest median variation within groups; effect, effect size of the difference, median of diff.btw/diff.win; overlap, confusion in assigning and observation; we.ep, expected value of the Welch Test value; we.eBH, expected value of the Benjamini–Hochberg corrected *p*-value.

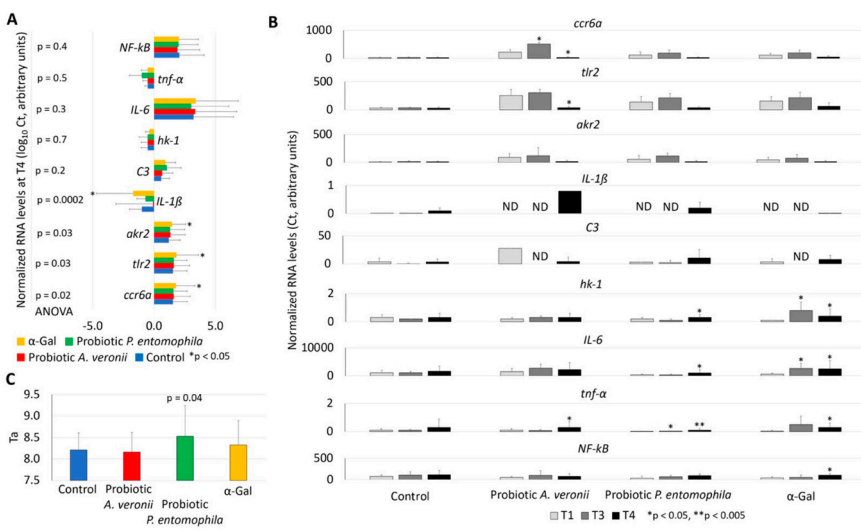

Figure 6. Expression of zebrafish immune-response genes in response to α-Gal and probiotic bacteria. The RT-qPCR was performed for the analysis of gene mRNA levels, using specific primers and conditions (Table 3). (**A**) The RNA normalized Ct values were compared between groups at T4 (end of the trial) by one-way ANOVA test followed by post hoc Holm multiple comparisons (https://astatsa.com/OneWay_Anova_with_TukeyHSD/; * $p < 0.05$, n = 3–20/group). (**B**) The RNA normalized Ct values were compared between T1 and T3/T4 by Student's *t*-test with unequal variance (* $p < 0.05$, ** $p < 0.005$; n = 12–20/group). Abbreviation: ND, not detected. High-resolution graphs are shown in Supplementary Materials Figure S1. (**C**) Antioxidant capacity in serum (Ta) was determined by using the potassium permanganate method and Ta values were compared between treated and control groups at T4 by Student's *t*-test with unequal variance ($p < 0.05$; n = 14–20/group). Data are shown as mean + SD.

2.5. Treatment with Probiotic Bacteria with High α-Gal Content Reduces Oxidative Stress in Fish

The serum total antioxidant capacity (Ta) was used to evaluate the effect of probiotics with high α-Gal content on fish oxidative stress (Figure 6C). The results showed a significant increase in Ta in fish treated with probiotic *P. entomophila* (Ta = 8.528 ± 0.711 vs. 8.210 ± 0.396 in control group). This Ta value is high when using human sera from young individuals as a reference [55] and supports an effect of probiotic *P. entomophila* on reducing the oxidative stress in treated fish. Probiotic treatments have resulted in increased serum total antioxidant capacity to facilitate prevention of oxidative stress that causes cellular damage and affects immune response in fish [56–59]. Furthermore, modulation of oxidative defenses has been correlated with protection against mycobacteriosis in fish [60,61].

2.6. Microbiota Composition Varies in Response to Treatment with Probiotic Bacteria and α-Gal

Immune training by fish gut microbiota is a core mechanism for the activation of protective responses against pathogen infection [31]. In humans, the composition of gut microbiota and microbiome driven immunomodulation affect protection against tuberculosis [62]. However, in fish these mechanisms are poorly understood.

Our study characterized the zebrafish gut microbiota to explore the effect of *A. veronii* and *P. entomophila* probiotics and α-Gal treatments on microbial populations and the immune response to *M. marinum*. Following *16S rRNA* gene sequencing and filtering a total of 8922 amplicon sequence variants (ASVs) were assigned and distributed into 39 phyla, 93 classes, 205 orders, 311 families and 646 genera (Supplementary Materials File S1: Data S1), using the DADA2 algorithm. For further analysis, ASVs with low counts and those with prevalence lower than 0.01% were filtered to remove spurious ASVs in the bacterial dataset. The results showed that the zebrafish gut microbiota in all experimental groups and at each time point (pre-challenge and post-challenge) is dominated by members of the phylum Proteobacteria (genera *Aeromonas*, *Acinetobacter, Gemmobacter* and *Plesiomonas*) followed by Bacteroidota (genera *Cloacibacterium*), Firmicutes, Actinobacteria and Planctomycetota phyla (Supplementary Materials File S1: Figures S2–S4). These microbial composition trends have been previously reported in the zebrafish gut microbiota [37,63].

To examine the dissimilarities in community composition between experimental groups at each time point (pre-challenge and post-challenge), beta diversity metric was assayed by using Bray–Curtis dissimilarity in univariable PERMANOVA models. The results showed significant differences between experimental groups (*A. veronii* probiotic treatment, *P. entomophila* probiotic treatment, and α-Gal) and controls at the pre-challenge stage ($p = 0.004$, $R^2 = 0.18$), but not at the post-challenge stage ($p = 0.128$, $R^2 = 0.19$) (Figure 7A). These results suggested that before *M. marinum* challenge the gut zebrafish microbial community differences observed might be attributed to the effect of treatments (*A. veronii* probiotic, *P. entomophila* probiotic and α-Gal) (Figure 7A). However, the challenge with *M. marinum* likely resulted in the disturbance of gut microbiota in all experimental groups (Figure 7A). From the taxonomic assignments, we observed that the genera *Aeromonas*, *Pseudomonas* and *Mycobacterium* are present in all experimental groups at both pre-challenge and post-challenge time points (Figure 7B), thus providing evidence of their ubiquity within the zebrafish microbial community. At the pre-challenge stage, the relative abundance of the genus *Aeromonas* in the *A. veronii* probiotic, α-Gal and control groups was higher than the genus *Pseudomonas* (Figure 7B). This finding could be associated with differences in the colonization rates and gut adaptation requirements for each bacterium and as the result of competitive microbial interactions [63,64]. In response to the *M. marinum* challenge, a decrease in the relative abundance of the genera *Aeromonas* and *Pseudomonas* occurred throughout all the experimental groups (Figure 7B).

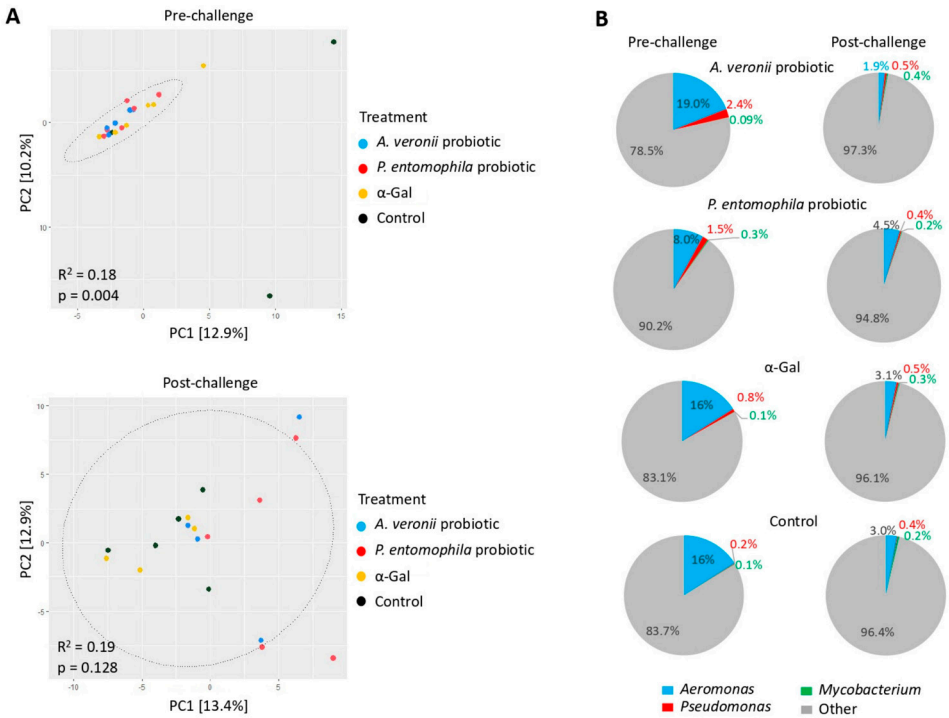

Figure 7. Zebrafish gut microbiota composition in response to probiotic and α-Gal treatments. (**A**) Principal component analysis of zebrafish gut microbiota grouped by treatment at pre-challenge and post-challenge stages. PCA ordination is based on the Bray–Curtis dissimilarity calculated with randomly rarefied data with no replacement applied to the centered-log transformed clr counts. The percentage of variation is explained by the principal components in the axis, PC1 and PC2. Ellipses indicate 95% confidence intervals. Each point represents one sample, and colors represent treatments/control groups. The closer the points are to one another, the more similar the microbiome composition of the samples are and vice versa. Adonis function in R software was used for PERMANOVA test to evaluate differences between groups. (**B**) Pie charts display the relative abundance of the genera *Aeromonas*, *Pseudomonas*, *Mycobacterium* and other found on each treatment group at pre-challenge and post-challenge stages. Relative abundance (%) of each genus was calculated from the ASVs raw counts obtained with DADA2 and normalized by total sum scaling.

Then, we further explored whether the gut microbiota differences observed between the experimental groups are induced by changes in the abundance of specific taxa. The differentially abundant taxa of the zebrafish gut microbiota are displayed in the effect size plots shown in Figure 8A,B for *A. veronii* and *P. entomophila* probiotics and α-Gal treatment groups in comparison to controls at pre-challenge and post-challenge stages. The effect size plots showed the presence of differential taxa at both pre-challenge and post-challenge stages (Figure 8A,B). We filtered the list of significantly different taxa found in the effect size plots of both groups generated with ALDEx2 to show only those taxa for which the expected Benjamini–Hochberg *p*-value was less than 0.05 (Table 3). From these results, we can conclude that, at pre-challenge stage, the *A. veronii* and *P. entomophila* probiotic treatments do not affect to the whole structure of the zebrafish gut microbiota, as no differential abundant taxa were found in in those groups. Based on our identification of bacteria with high α-Gal content in Zebrafish gut microbiota (Figure 2 and Table 2), this is an expected result, as *A. veronii* and *P. entomophila* are natural resident bacteria of

zebrafish (Table 2) and other fish species [12]. Therefore, no disturbance was observed at the pre-challenge stage for treatments with these probiotic bacteria. In contrast, at the pre-challenge stage the comparison of α-Gal treatment and control groups resulted in few differential taxa (Figure 8A), a result that supports a role for α-Gal glycan in shaping the microbiota composition [25,65,66]. However, at the post-challenge stage differentially abundant taxa were observed only in the *P. entomophila* probiotic treatment when compared to the control group (Figure 8B). These results suggested a change in the gut microbial community composition in zebrafish treated with *P. entomophila* probiotic and infected with *M. marinum*. Nevertheless, whether these observed differential taxa were directly related to *M. marinum* infection by means of competition and/or activation of immune system pathways needs to be further explored.

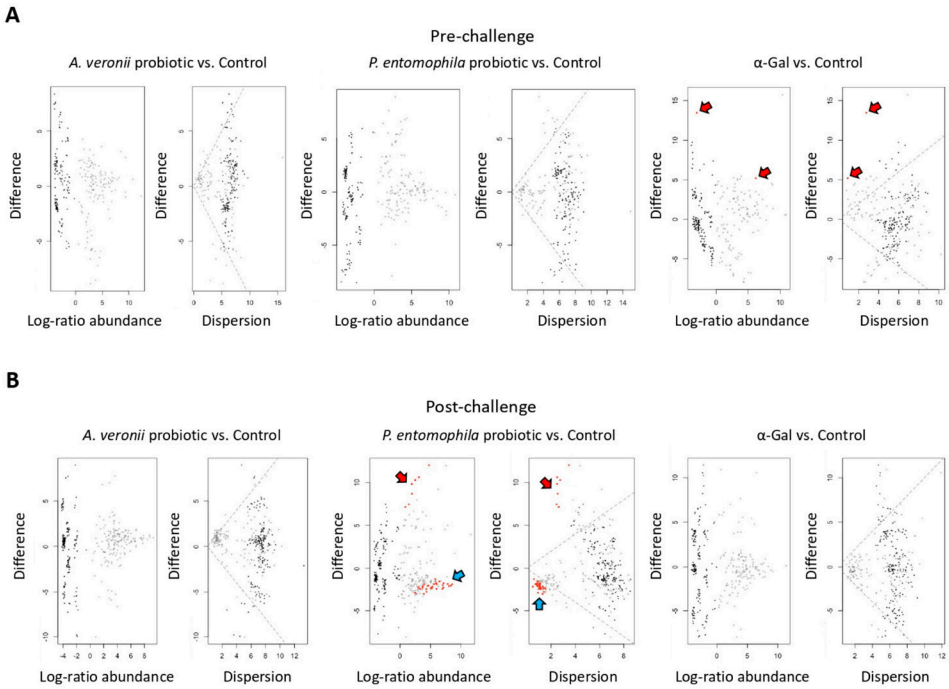

Figure 8. Differential abundance of bacterial taxa in zebrafish gut microbiota. (**A**) Taxa differential abundance of each treatment group vs. control at pre-challenge stage. (**B**) Taxa differential abundance of each treatment group vs. control at post-challenge stage. Taxa differential abundance was calculated with ALDEx2 and summarized in the effects size plots. The left MA plots (log-ratio abundance) show the relationship between abundance (log-ratio abundance is the clr value of each feature) on the *x*-axis and difference on the *y*-axis. The right plot (dispersion) is an effect plot that shows the relationship between difference and dispersion through the expected value of the log-difference between groups on the *y*-axis and the maximum within-group dispersion on the *x*-axis. In both plots, each point represents an individual ASV from the dataset at genus level. Taxa that are not significant are represented by gray or black points. Taxa that are statistically significant are represented by red points (Welch's test, $p < 0.05$). Points marked with red arrows are more abundant in α-Gal treatment samples at pre-challenge stage or in *P. entomophila* probiotic treatment samples at post-challenge stage when compared to controls. Points marked with blue arrows are more abundant in control than in *P. entomophila* probiotic treatment samples at post-challenge stage.

To characterize a possible association between the zebrafish gut microbiota and the IgM antibody response to α-Gal and *Mycobacterium* P22, a correlation analysis was performed between the abundance of bacterial taxa at genus level and antibody titers. We observed a pattern of significantly correlated taxa with anti-α-Gal IgM in all the experimental groups when compared at the pre-challenge and post-challenge time points, with a notable increase of significant taxa that correlate positively at the post-challenge time point in the α-Gal treatment group (Figure 9A). It has been demonstrated that certain bacteria from the zebrafish gut microbiota contain α-Gal on its surface (Table 2) [35], and thus the immunity induced in response to α-Gal treatment may negatively affect the zebrafish gut microbiota bacteria containing α-Gal [67,68]. In contrast, we did not observe a clear pattern of the significantly correlated taxa with anti-P22 IgM antibody titers (Figure 9B).

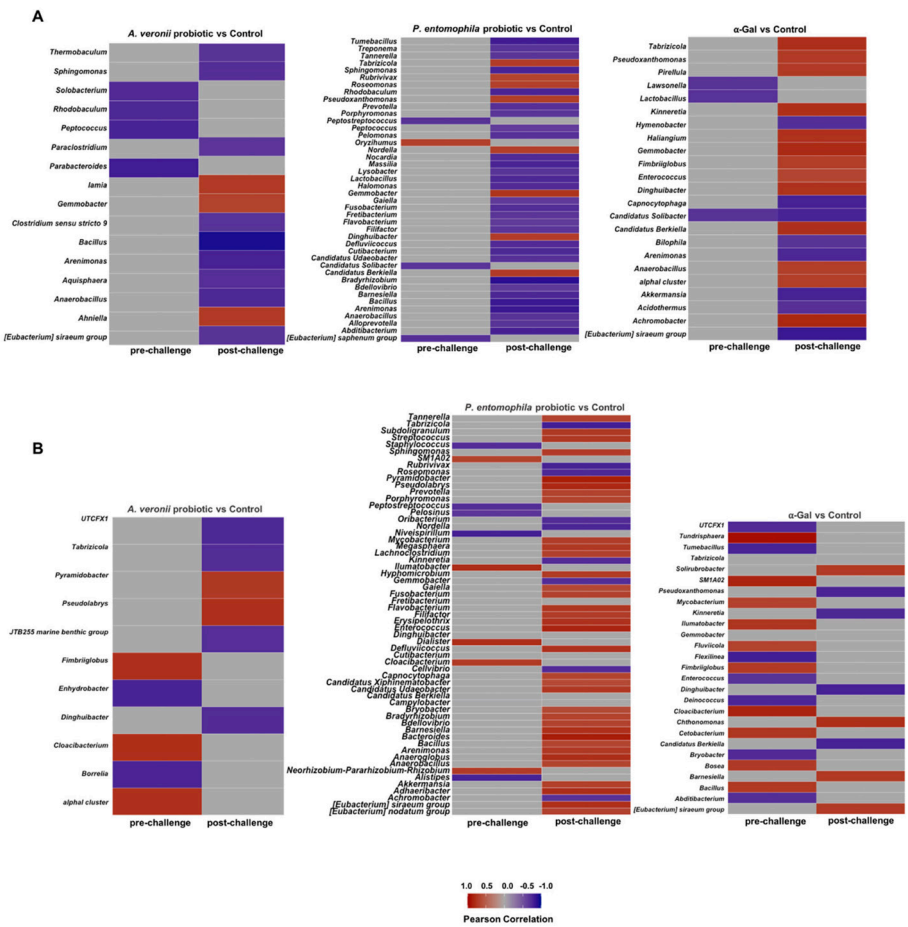

Figure 9. Correlation between zebrafish gut microbiota and antibody response. Heatmaps of the significantly correlated taxa with (**A**) anti-α-Gal and (**B**) anti-P22 IgM titers for each experimental group and at each stage (pre-challenge, post-challenge). Pearson correlations between zebrafish gut microbiota and anti-α-Gal and P22 IgM antibody titers were calculated with ALDEx2, using the aldex.corr function analysis, as implemented in R.

2.7. Mechanisms Mediating Protection against Mycobacteriosis by Probiotics with High α-Gal Content

Based on the results of this study together with previous findings in fish immunized with α-Gal or heat-inactivated *M. bovis* and protected against mycobacteriosis [24,32,33], we proposed mechanisms regulating immunity and metabolism induced by probiotic bacteria with high α-Gal content (Figure 10). These mechanisms included B-cell maturation, anti-α-Gal antibodies-mediated control of mycobacteria, induced innate immune responses and beneficial effects on nutrient metabolism and oxidative stress. Additionally, in the zebrafish model, the results suggested a role of immune system pathways in response to probiotics and α-Gal that are related to the microbiota composition [69–71].

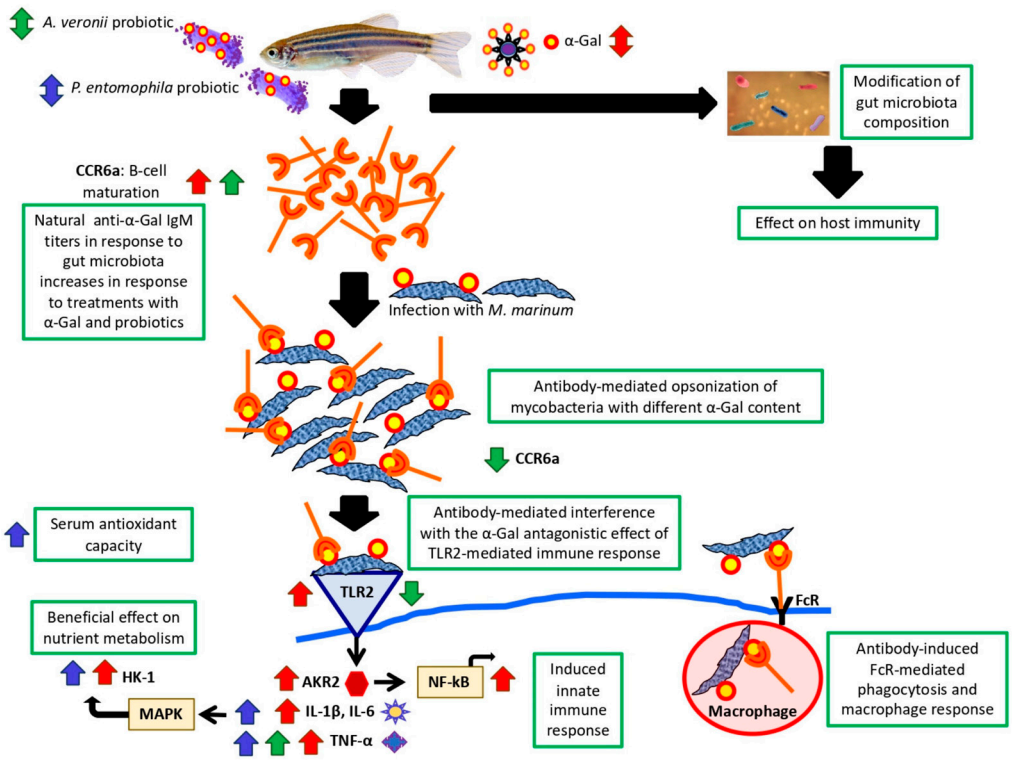

Figure 10. Protective mechanisms activated in response to α-Gal and probiotics with high α-Gal content. Mechanisms regulating immunity and metabolism induced by α-Gal and probiotic bacteria with high α-Gal content included modification of gut microbiota composition, B-cell maturation, anti-α-Gal antibodies-mediated control of mycobacteria, induced innate immune responses, beneficial effects on nutrient metabolism and reduced oxidative stress. Probiotics activated different mechanisms associated with the response to α-Gal.

Mycobacteria contain α-Gal on their surface, and zebrafish, similar to humans, evolved as α-Gal negative and produce natural anti-α-Gal antibodies in response to bacteria in the gut microbiota with this modification [24,35]. Therefore, the increase in the antibody levels to α-Gal in response to probiotics support a protective mechanism by antibody-mediated opsonization of mycobacteria through interactions with surface-exposed antigens and promotion of Fc-receptor (FcR)-mediated phagocytosis [24,72]. In accordance with

these results, the expression of the CCR6a beta chemokine receptor coding gene that is implicated in B-lineage maturation and antigen-driven B-cell differentiation and humoral immunity [73], was upregulated in response to α-Gal and probiotic *A. veronii* to promote the production of anti-α-Gal antibodies. To interfere with protective responses induced by treatment with probiotic *A. veronii*, *M. marinum* infection downregulated the expression of *ccr6* and *tlr2*.

The upregulation of proinflammatory cytokines (ILs and TNF-α) through the TLR/NF-kB-AKR innate immune pathway has been implicated in the α-Gal-induced protective mechanism to mycobacterial infection [24,72,74–77]. The activation of macrophages by anti-α-Gal antibodies increases TNF-α secretion which may promotes macrophage recruitment to the infection site with a role during the initial and long-term control of tuberculosis [24,78]. Additionally, α-Gal on mycobacterial membrane may be similar to glycolipids that antagonize TLR2-mediated response to inhibit NF-kB/AKR activation and subsequent cytokine production, a process which may be interfered by the anti-α-Gal antibodies [24,77].

In fish as in other organisms the enzyme HK-1 has a role in glycolysis [79]. Higher expression levels of *hk-1* in response to treatment with α-Gal and probiotic *P. entomophila* suggested a beneficial effect of α-Gal-containing probiotic bacteria on nutrient metabolism. Similar results have been reported in fish treated with xylanase-producing probiotics [16,34,80]. Additionally, proinflammatory cytokines such as TNF-α and IL-6, upregulated here by α-Gal and probiotic *P. entomophila*, have been implicated in the regulation of HK-1 through the mitogen-activated protein kinase (MAPK) pathway [81].

Probiotic *A. veronii* and *P. entomophila* specific signatures showed differences associated with these treatments (Figure 10). *A. veronii* with higher α-Gal content was the only probiotic inducing B-cell maturation, which was reverted by *M. marinum* infection, a finding that together with *tlr2* downregulation may explain the absence of significant differences in mycobacterial infection levels in these fish (Figure 4A). In contrast, probiotic *P. entomophila* was the only upregulating IL-6 resulting in the MAPK-mediated induction of HK-1-associated beneficial effect on nutrient metabolism. Probiotic *P. entomophila* was also the only treatment resulting in an increase of serum total antioxidant capacity, which facilitates immune response by preventing the oxidative stress in these fish. Finally, both probiotic bacteria induced innate immune response trough TNF-α upregulation. Other mechanisms associated with TLR2, AKR2, NF-kB and IL-1ß were regulated only in response to α-Gal and induced modifications in gut microbiota composition may enhance the protective response to infection.

3. Materials and Methods

3.1. Zebrafish

Wild-type adult (6–8 months old) AB female and male laboratory-reared zebrafish (LRZ) were kindly provided by Juan Galcerán Sáez from the Instituto de Neurociencias (IN-CSIC-UMH, Sant Joan d'Alacant, Alicante, Spain). These zebrafish were certified by Biosait Europe S.L. (Barcelona, Spain; https://biosait.com) as free of major fish pathogens, such as *Mycobacterium* spp., *Pseudoloma neurophilia*, *Pseudocapillaria tomentosa* and zebrafish retroviruses. Pet-store zebrafish (PSZ) female and male adults (6–8 months old) were purchased from a pet store in Ciudad Real (Spain) and transported to the microbiology laboratory installations at the IREC for immediate processing. The zebrafish were maintained in a flow-through water system at 27 °C, with a light/dark cycle of 14 h/10 h, and fed twice daily with dry fish feed (Premium food tropical fish, DAPC, Valladolid, Spain). Experiments were conducted in strict accordance with the recommendations of the European Guide for the Care and Use of Laboratory Animals. Animals were housed and experiments conducted at the experimental facility (IREC, Ciudad Real, Spain) with the approval and supervision of the Ethics Committee on Animal Experimentation of the University of Castilla La Mancha (PR-2018-06-13) and the Counseling of Agriculture, Environment, and Rural Development of Castilla La Mancha (ES130340000218).

3.2. Sampling and Bacterial Culture from Zebrafish Gut Microbiota

Potential probiotic bacteria were isolated from the gut of LRZ and PSZ (n = 10 each) (Figure 1). The culturable microbiota was sampled as previously described [38]. The ventral belly surface of freshly euthanized fish was opened with sterilized microsurgical blade and forceps under a light source. The intestinal system was transferred to 1.5 mL tubes containing 200 µL sterile PBS. The intestines were homogenized with a motorized pestle and disposable plastic loops were used to streak four serial dilutions on 5% chicken blood agar (Rockland antibodies and assays, Rockland Immunochemicals, Inc., Limerick, PA, USA) and TSA agar (Sigma-Aldrich, St. Louis, MO, USA) bacteriological plates for isolation of aerobic and anaerobic bacteria, respectively. The plates were incubated at 28 ºC and followed by inspections every day for up to 1 week. After incubation, each morphologically distinct colony (form, color, texture, elevation and margin) was encoded. From each sampling plate, two representatives of each colony were randomly selected, subcultured on separate blood agar and isolated for downstream analyses. A total of 5 phenotypes of different bacterial colonies were isolated in both LRZ and PSZ groups and classified (Table 1).

3.3. Bacterial DNA Extraction and 16S rRNA Gene Amplification and Sequencing

Genomic DNA was extracted from 5 different aerobic bacterial type I colony isolates (Figure 1 and Table 1) from LRZ and PSZ, using the direct boiling method [82]. The amplification of the 16S rRNA gene V3/V4 regions was carried out by PCR, using the primers 16S-341F: 5′-TCGTCGGCAGCGTCAGATGTGTATAAGAGACAGCCTACGGGNGGCWGCAG-3′ and 16S_805R: 5′-GTCTCGTGGGCTCGGAGATGTGTATAAGAGACAGGACTACHVGGGTATCTAATC-3′ in a final volume 25 µL (2 µL of DNA template (20 ng), 16 µL H_2O, 0.5 µL of dNTPs (10 nM), 2.0 µL of MgCl2 (25 mM), 0.1 µL AmpliTaq Gold DNA polymerase (Life Technologies, UK), 1 µL of each primer (10 nM) and 2.5 µL PCR Gold Buffer (Life Technologies, Carlsbad, CA, USA). An initial denaturation step at 95 °C for 10 min was followed by 35 cycles of pre-amplification at 94 °C for 30 s, 55 °C for 30 s and 72 °C for 30 s, followed by a final elongation step at 72 °C for 10 min. All PCR products were purified by using the ExoSap-IT PCR Product Clean-Up kit (Applied Biosystems, Foster City, CA, USA) following the manufacturer's instructions and Sanger sequenced, using the ABI PRISM® 3730 platform (Applied Biosystems) at the Genomic Unit (Campus Moncloa, University Complutense of Madrid, Madrid, Spain; https://www.ucm.es/english/genomics-and-proteomics). All the V3/V4 16S rRNA gene sequences were edited by using SnapGene software (https://www.snapgene.com, accessed on 30 June 2020) and the maximum identities were searched by using the GenBank DNA sequence database and the Nucleotide Basic Local Alignment Search Tool (BLASTN; https://blast.ncbi.nlm.nih.gov/Blast.cgi, accessed on 30 June 2020) (Table 2).

3.4. Analysis of Bacterial α-Gal Content

The analysis of α-Gal content was conducted in selected aerobic type I bacteria with maximum 16S rRNA gene sequence identity (99.3–99.8%; Table 2) (Figure 1). The *P. entomophila* (type strain, DSM 28517), *S. xiamenensis* (type strain, DSM 22215) and *A. veronii* (type strain, DSM 7386) were obtained from the German Collection of Microorganisms and Cell Culture (DSMZ Leibniz Institute, Braunschweig, Germany; https://www.dsmz.de). The flow cytometry analysis of bacterial α-Gal content was conducted as previously described [24,35]. Bacteria were washed in PBS, fixed and permeabilized with the Intracell fixation and permeabilization kit (Immunostep, Salamanca, Spain) following manufacturer's recommendations. The cells were incubated with 3% human serum albumin (HSA, Sigma-Aldrich) in PBS, for 1 h, at room temperature (RT). Then, cells were incubated for 14 h at 4 °C with the α-Gal epitope monoclonal antibody (M86, Enzo Life Sciences, Farmingdale, NY, USA) diluted 1:50 in 3% HSA/PBS. FITC-goat anti-mouse IgM (Abcam, Cambridge, UK) labelled antibody (diluted 1/200 in 3% HSA/PBS) was used as a secondary antibody and incubated for 1 h, at RT. Samples were analyzed on a FAC-Scalibur

flow cytometer equipped with CellQuest Pro software v.4 (BD Bio-Sciences, Madrid, Spain). The viable cell population was gated according to forward-scatter (FSC-H) and side-scatter (SSC-H) parameters. The viable cell population was gated according to forward-scatter (FSC-H) and side-scatter (SSC-H) parameters. The percentage of viable cell population with highest α-Gal content (mean fluorescence intensity $>10^3$ FSC-H) was compared between different bacteria by one-way ANOVA test ($p < 0.005$) followed by post hoc Holm multiple comparisons (https://astatsa.com/OneWay_Anova_with_TukeyHSD/; $p < 0.05$, $n = 5$ biological replicates).

3.5. Bacterial Carbohydrate Structure

The bacterial carbohydrate structure for bacteria identified in the zebrafish microbiota with highest α-Gal content, namely *A. veronii* and *P. entomophila*, was characterized by using the Bacterial Carbohydrate Structure Database (http://csdb.glycoscience.ru/bacterial/main.html) [83–86]. Symbol nomenclature for glycans is disclosed at the database (http://csdb.glycoscience.ru/database/index.html?help=eog). The International Union of Pure and Applied Chemistry (IUPAC; https://iupac.org) condensed terms for the glycan structure are ndHex (Deoxy-hexose; http://www.monosaccharidedb.org/display_monosaccharide.action?name=deoxy-HEX), Rha (L-Rhamnose; http://www.monosaccharidedb.org/display_monosaccharide.action?name=?LRhap), FucNAc (*N*-acetyl-L-fucosamine; http://www.monosaccharidedb.org/display_monosaccharide.action?name=LFucpNAc), QuiNAc (*N*-acetyl-D-quinovasomine; http://www.monosaccharidedb.org/display_monosaccharide.action?name=DQuipNAc), Gal (D-galactose; http://www.monosaccharidedb.org/display_monosaccharide.action?name=?DGalp), GalNAc (*N*-acetyl-D-galactosamine; http://www.monosaccharidedb.org/display_monosaccharide.action?name=DGalpNAc) and GlcNAc (*N*-acetylglucosamine; https://pubchem.ncbi.nlm.nih.gov/compound/*N*-Acetyl-D-Glucosamine). All databases were accessed in 28 February 2021.

3.6. Probiotic Bacteria

Bacteria identified in the zebrafish microbiota with highest α-Gal content, *A. veronii* (type strain, DSM 7386) and *P. entomophila* (type strain, DSM 28517) were used for probiotoic preparation (Figure 1). The strains were inoculated on Luria broth (LB) agar plates for pure culture by using bacterial incubator to provide appropriate temperature to bacterial growth at 37 ºC for *A. veronii* and 28 °C for *P. entomophila* for 24 h. The strains cultured on LB agar plates were stored at 4 °C for use. Bacteria were cultured on LB agar plates repeatedly every 1 to 2 days to keep them viable. Moreover, the cultures were also stored in LB liquid medium containing sterile 50% glycerol at −80 °C for long-stem storage.

3.7. Toxicity Assessment of A. veronii and P. entomophila

Toxicity of probiotic bacteria was assessed as previously described [16]. Adult female and male PSZ (6–8 months old; $n = 80$) with an average weight of 266 ± 59 mg were acclimatized for 7 days as described above (Section 3.1). A total of 10 fish per group were injected intraperitoneally with 10 µL of the diluted bacterial solution of 1×10^6, 1×10^7 and 1×10^8 CFU per fish for both *A. veronii* and *P. entomophila*, separately. Fish injected with PBS buffer were used as controls. Bacteria were cultured in LB broth for 24 h, at 37 and 28 °C for *A. veronii* and *P. entomophila*, respectively, and centrifuged at 4600× *g* for 20 min at 4 °C. The cell pellets were then suspended in an appropriate volume of PBS. Bacterial toxicity was evaluated by recording signs and symptoms of infection and mortality of the injected fish daily for 7 days.

3.8. Probiotic Formulation and Feed Administration

The probiotic formulation was prepared by using the coating and drying procedure [87] with some modifications (Figure 1). The probiotic suspension was prepared in 500 mL of fresh LB to grow *A. veronii* and *P. entomophila* for 24 h at 37 and 28 °C, respectively, and achieving an o.d. 600 of 1.5–2.0. Then, cultures were centrifuged at 4600× *g*

for 20 min at 4 °C to produce the bacterial pellet. Pelleted bacteria were then washed twice in 1 mL sterile PBS and approximately 2 g of cell mass were diluted in 100 mL of sterile PBS to make the final probiotic suspension. The probiotic suspension was prepared freshly every week during the duration of the experiment. The probiotic suspension prepared for *A. veronii* and *P. entomophila* was manually spread in petri dishes to coat the feed and let it dry for 30 min under constant airflow. Finally, the probiotic-treated groups received a commercial staple food consisting of soft granules with 4% insect meal (Sera Vipagran Nature, D52528, Heinsberg, Germany) containing the probiotic bacteria tested at a final concentration of 10^8 CFU/g. The probiotic bacterium was mixed into the diet before feeding and prepared freshly every day during the duration of the experiment. The viability of the probiotic suspension was monitored in the probiotic diet by plate count from 1 g of the probiotic suspension coated feed incubated for 5 min in 9 mL of sterile PBS, gently homogenized and serial dilutions cultured for 24 h on LB agar at 37 °C or 28 °C for *A. veronii* and *P. entomophila* probiotic suspension, respectively. All fish received a quantity of food ranging from 1.5% to 2% of their body weight per day during the experiment.

3.9. Zebrafish Treatment with Probiotics and Challenge with M. marinum

The experiment was designed to evaluate the effect of treatment with zebrafish gut candidate probiotic bacteria. Bovine serum albumin (BSA) coated with α-Gal (α-Gal; Dextra, Shinfield, UK) and PBS were used as positive and negative controls, respectively (Figure 3). Thirty LRZ were randomly allocated to different experimental groups with a similar number of adult females and males (Group A: commercial feed with probiotic *A. veronii*, Group B: commercial feed with probiotic *P. entomophila*, Group C: commercial feed with PBS, Group D: commercial feed with α-Gal immersion). For α-Gal treatment, fish were immunized by immersion n 200 mL of water from the fish tanks where 5 µg of α-Gal was added per fish for 30 min at weeks 2 and 5 (Figure 3). PBS was added to the commercial diet at a proportion of 500 µL per gram feed. Fish were weighted at the weeks 1–5 and 10 at the end of the experiment. Gut and sera were collected at weeks 3 (T1), 4 (T2) and 5 (T3) (3 fish per group) and at the end of the experiment (week 10; T4). The *M. marinum* Aronson (ATCC 927) was cultured at 29 °C in 7H9 broth enriched with Middlebrook ADC (Becton Dickinson) and prepared for infection as previously described [24,27,32,33]. To verify the bacterial dose, *M. marinum* samples were diluted and plated on 7H10 agar enriched with Middelbrook OADC (Becton Dickinson) for counting bacterial colonies. Fish were mucosally infected at week 7 with a dose equivalent to 48±7 cfu of *M. marinum* per animal causing a chronic tuberculosis-like disease in zebrafish [24,33]. At week 10, fish were euthanized with immersion in 0.04% MS-222 and processed for gut and serum collection for analysis of antibody levels by ELISA, mycobacteria levels by RT-qPCR, expression of selected immune response gene markers by RT-qPCR, oxidative stress biomarkers and gut microbiome. The zebrafish had a weight of 614 ± 259 and 694 ± 152 mg (Group C: PBS control), 643 ± 269 and 540 ± 181 mg (Group A: probiotic *A. veronii*), 681 ± 300 and 771 ± 299 mg (Group B: probiotic *P. entomophila*), and 463 ± 215 and 593 ± 336 mg (Group D: α-Gal) at the beginning and end of the experiment, respectively.

3.10. Characterization of M. marinum RNA Levels by RT-qPCR

Total RNA was extracted from zebrafish gut samples by using the AllPrep DNA/RNA/Protein kit (Qiagen, Hilden, Germany). The *M. marinum* RNA levels were determined by real-time reverse transcription polymerase chain reaction (RT-qPCR), using the iTaq™ Universal SYBR Green One-Step Kit (BioRad, CA, USA) in the CFX96™ Real-Time System (Bio-Rad) thermocycler following manufacturer's recommendations with specific primers and conditions for *M. marinum heat-shock protein 65* gene (*hsp65*; Genebank accession number: AF547855.1) [88] (hsp65Forward-F: 5′-CAACCCGCTCGGTCTGAA-3′, hsp65Reverse-R: 5′-CGACCTCTTTGGCCGACTT-3′, annealing at 59 °C for 30 s). A dissociation curve was run at the end of the reactions to ensure that only one amplicon was formed and that the amplicon denatured consistently in the same temperature range for every sample [89]. The

RNA cycle threshold (Ct) values were normalized against *D. rerio glyceraldehyde-3-phosphate dehydrogenase* gene (*gadph*; NM_001115114.1) (gadphF: 5′-CGTGGTGCCAGTCAGAACAT-3′, gadphR: 5′-AGTCAGTGGACACAACCTGG-3′, annealing at 56 °C for 30 s), using the genNormddCT method [90]. Cross-reactivity of the primers with probiotic bacteria was discarded by in silico *hsp65* sequence alignment and RT-PCR. The *M. marinum* RNA normalized Ct values were compared between treated and negative PBS control groups by Student's *t*-test with unequal variance ($p < 0.05$; $n = 10–17$/group).

3.11. Characterization of Anti-α-Gal and P22 IgM Antibody Titers in Zebrafish

For ELISA, high absorption capacity polystyrene microtiter plates were coated with 100 ng per well of α-Gal or *M. bovis* P22, an immunopurified subcomplex of bovine purified protein derivative (bPPD) [91] in carbonate–bicarbonate buffer (Sigma-Aldrich). After an overnight incubation at 4 °C, coated plates were washed one time with 300 µL/well PBS/0.05% Tween 20 (PBST; Sigma-Aldrich), and then blocked with 100 µL/well of 1% HSA (Sigma-Aldrich) at RT for 1 h. A dilution curve with 1:10, 1:100 and 1:1000 fish serum peritoneal fluid samples was performed and then diluted (1:10, *v/v*) in blocking solution and 100 µL/well were added into the wells of the antigen-coated plates and incubated for 1.5 h at 37 °C. Plates were washed three times with PBST and 100 µL/well of species-specific rabbit anti-zebrafish IgM antibodies diluted (1:1000, *v/v*) in blocking solution were added and incubated at RT for 1 h. Plates were washed three times with 300 µL/well of PBST. A goat anti-rabbit IgG-peroxidase conjugate (Sigma-Aldrich) was added diluted 1:3000 in blocking solution and incubated at RT for 1 h. After four washes with 100 µL/well of PBST, 100 µL/well of 3,3′,5,5′-tetramethylbenzidine (TMB) one solution (Promega, Madrid, Spain) were added and incubated for 15 min at RT. Finally, the reaction was stopped with 50 µL/well of 2 N H_2SO_4, and the o.d. was measured in a spectrophotometer at 450 nm. The o.d. at 450 nm (mean of the duplicate well values of o.d. P22 or α-Gal – o.d. PBS control) were compared between treated and negative PBS control groups at T4 by Student's *t*-test with unequal variance ($p < 0.05$; $n = 12–20$/group) and between different time points (T1 to T4) by one-way ANOVA test followed by post hoc Holm multiple comparisons (https://astatsa.com/OneWay_Anova_with_TukeyHSD/; $p < 0.05$, $n = 3–20$/group). A Spearman's Rho correlation analysis was conducted between antibody titers and *M. marinum* infection RNA levels (https://www.socscistatistics.com/tests/spearman/; $p < 0.005$).

3.12. Characterization of mRNA Levels of Selected Zebrafish Immune Response and Nutrient Metabolism Genes by RT-qPCR

Total gut RNA extracted as descried above (Section 3.10) was used for analysis. Selected zebrafish genes included immune response *chemokine receptor 6a* (*ccr6a*; NM_001099991.1), *toll-like receptor 2* (*tlr2*; NM_212812.1), *interleukin 1-beta* (*IL-1ß*; NM_212844.2), *akirin 2* (*akr2*; NM_213294.2), *complement component 3* (*C3*; NM_131243.1), *interleukin-6* (*IL-6*; JN698962), *tumor necrosis factor-alpha* (*tnf-α*; BC165066), *nuclear factor-kB* (*NF-kB*; AY163838) and nutrient metabolism *hexokinase 1* (*hk-1*; BC067330.1) [16,24]. Sequences were obtained from NCBI nucletotide database (https://www.ncbi.nlm.nih.gov/nucleotide/, accessed on 30 November 2020) and the UCSC Genome Browser on Zebrafish May 2017 (GRCz11/danRer11) Assembly (http://genome.ucsc.edu/cgi-bin/hgTracks?db=danRer11&lastVirtModeType=default&lastVirtModeExtraState=&virtModeType=default&virtMode=0&nonVirtPosition=&position=chr19%3A27019529%2D27023771&hgsid=1072595985_aaRkNS7FkPbTrWiA6ZHMUkLZ1fRT, accessed on 30 November 2020). To characterize the expression of selected genes, an RT-qPCR was performed for the analysis of *D. rerio* mRNA levels. The RT-qPCR was performed, and data were normalized as described above for mycobacterial RNA levels, using specific primers and conditions following manufacturer's recommendations (Table 4). The RNA normalized Ct values were compared between groups at T4 by one-way ANOVA test followed by post hoc Holm multiple comparisons (https://astatsa.com/OneWay_Anova_with_TukeyHSD/; $p < 0.05$, $n = 3–20$/group) and between T1 and T3/T4 by Student's *t*-test with unequal variance ($p < 0.05$; $n = 12–20$/group).

Table 4. Oligonucleotide primer sequences an annealing condition.

Genes	Oligonucleotide Forward (F) and Reverse (R) Primers	Annealing Conditions	References
ccr6a	F: 5′-AGCTTCTGCGTGGCATCTAT-3′ R: 5′-CAGACGGCTGCACAAACTAA-3′	56 °C, 30 s	[24]
tlr2	F: 5′-TGAATGGGTCGAGGAGATTC-3′ R: 5′-CACAAAGTGCTCCGACAGAA-3′	56 °C, 30 s	[24]
akr2	F: 5′-ACTATGGACTTCGATCCGCT-3′ R: 5′-GCTCTGTGGTGAGTGCTGAA-3′	56 °C, 30 s	[24]
IL-1ß	F: 5′-GCATGTCCACATATGCGTCG-3′ R: 5′-GCTGGTCGTATCCGTTTGGA-3′	58 °C, 30 s	[24]
C3	F: 5′-ACGCTCTCTGGATTGAAACA-3′ R: 5′-TGCCTTCTTGCATGGCAATC-3′	56 °C, 30 s	[24]
IL-6	F: 5′-TCAACTTCTCCAGCGTGATG-3′ R: 5′-TCTTTCCCTCTTTTCCTCCTG-3′	56 °C, 30 s	[16]
tnf-α	F: 5′-AAGGAGAGTTGCCTTTACCG-3′ R: 5′-ATTGCCCTGGGTCTTATGC-3′	54 °C, 30 s	[16]
NF-kB	F: 5′-AAGAGGACCAAAATAAGCACAG-3′ R: 5′-AAGTCCAAGGTACATCGCCATGA-3′	58 °C, 30 s	[16]
hk-1	F: 5′-ACTTTGGGTGCAATCCTGAC-3′ R: 5′-AGACGACGCACTGTTTTGTG-3′f	56 °C, 30 s	[16]

3.13. Characterization of Serum Total Antioxidant Capacity

Serum total antioxidant capacity (Ta) was characterized by using the potassium permanganate method [55]. Sera were diluted (1:10, 1:20, 1:40, 1:80 and 1:160) with distilled water, and 20 µL per well was added to a 96-well ELISA plate with blank no serum control. Then, 100 µL of 5 mmol/L solution of $KMnO_4$ (79 mg $KMnO_4$ dissolved in 100 mL distilled water) was added to each well and mixed with serum samples. Plates were incubated for 30 min at 37 °C in a water bath, after which the o.d. was measured in a spectrophotometer at 570 nm. The Ta was calculated:

$$Ta = 100/(OD1 + 2 \times (OD2 + OD3 + OD4) + OD5) \quad (1)$$

where OD1 to OD5 are the o.d. at 1:10 to 1:160 serum dilutions. Ta values were compared between treated and control groups at T4 (end of the trial) by Student's *t*-test with unequal variance ($p < 0.05$; n = 14–20/group).

3.14. Characterization of The Zebrafish Gut Microbiome

3.14.1. DNA Extraction, Amplicon Preparation, and Sequencing

A total of 39 zebrafish gut samples were selected to obtain a representative sample of each group (Group A: commercial feed with probiotic *A. veronii*, n = 10; Group B: commercial feed with probiotic *P.* entomophila, n = 11; Group C: commercial feed with PBS, n = 8; Group D: commercial feed with α-Gal immersion, n = 10) at two different time points to test whether challenge with *M. marinum* has an impact on zebrafish gut microbiota (pre-challenge with *M. marinum* at weeks 3–5, n = 21; post-challenge with *M. marinum* at week 10, n = 18) (Table 5).

Table 5. Description of samples per treatment group and time point.

Time Point	Treatment			
	A. veronii	***P. entomophila***	**α-Gal**	**PBS Control**
Pre-Challenge (weeks 3–5)	$n = 6$	$n = 6$	$n = 6$	$n = 3$
Post-Challenge (week 10)	$n = 4$	$n = 5$	$n = 4$	$n = 5$

Genomic DNA was extracted from individual zebrafish gut samples by using the All-Prep DNA/RNA/Protein kit. DNA sequencing was performed at the Genomic Unit Campus Moncloa (University Complutense of Madrid, Madrid, Spain). An aliquot of each DNA sample was used to prepare the libraries to amplify the V3 and V4 hypervariable regions of the *16S rRNA* gene by using the pair of primers 341F: 5′ TCGTCGGCAGCGTCAGATGTGTATAAGAGACAGCCTACGGGNGGCWGCAG and 805R:5′GTCTCGTGGGCTCGGAGATGTGTATAAGAGACAGGACTACHVGGGTATCTAATCC and PCR amplification of the amplicon target following the manufacturer's recommendations. The expected size of the PCR products (approximately 550 bp) was verified on a Bioanalyzer DNA 1000 chip (Agilent Technologies, Santa Clara, CA, USA) and further purified by using AMPure XP beads (Beckman Coulter, Life Sciences, Pasadena, CA, USA) for further processing. Then, Illumina sequencing adapters and index barcodes, using Nextera XT DNA library preparation kit (Illumina, Inc., San Diego, CA, USA), were added to the amplicon target before libraries were pooled together for further sequencing. All cluster generation and paired-end sequencing were performed on the Illumina Next-Generation Sequencing MiSeq system, using Illumina MiSeq v2 2 × 300 cycle chemistry, following the manufacturer's protocols.

3.14.2. Downstream Data Analysis for 16S rRNA Sequencing Processing and ASVs Workflow

A total of 12,799,596 MiSeq reads passing filter were pair-end demultiplexed and fastq file generated, using the Illumina MiSeq Reporter software. The raw *16S rRNA* sequences were uploaded to the Sequence Read Archive (SRA) repository (https://www.ncbi.nlm.nih.gov/sra; BioProject ID PRJNA728442, accession numbers SAMN19079379–SAMN19079417). Sequence analysis was performed by using DADA2 inference algorithm on primer-free reads to correct sequencing errors and create the ASVs for the zebrafish gut microbial communities (v.1.12) in R (v.4.0.1) [92]. The reads were quality filtered by using the filterAndTrim (https://rdrr.io/bioc/dada2/man/filterAndTrim.html) function that truncated the forward and reverse reads at 280 bp and 255 bp for the zebrafish gut microbiota dataset. Then, reads with more than 2 errors in the forward and 2 errors in the reverse reads were removed. Reads were merged after inference of sequence variation with learnErrors (https://rdrr.io/bioc/dada2/man/learnErrors.html) and denoised by using dada (https://rdrr.io/bioc/dada2/man/dada.html) functions. Chimeric sequences were eliminated with removeBimeraDenovo (https://rdrr.io/bioc/dada2/man/removeBimeraDenovo.html), and taxonomy was assigned to ASVs by using the classify–learn naïve Bayes taxonomic classifier assignTaxonomy (https://rdrr.io/bioc/dada2/man/assignTaxonomy.html) based on the SILVA database (https://www.arb-silva.de; v.138) database [93]. Taxa count abundances were extracted from original outputs for each taxonomic level (Supplementary Materials File S1: Data S1). Microbial community profiles were constructed at kingdom, phylum, class, order, family, genus for further analysis. All algorithms and databases were accessed in 31 March 2021.

3.14.3. Statistical Analysis of Gut Zebrafish Microbial Communities

For the zebrafish gut microbiota dataset, the ASVs count table was generated. A total of 8922 ASVs were assigned to the 39 samples (Table 5) and at 6 taxonomic ranks (kingdom, phylum, class, order, family and genus). All the subsequent biological analyses were performed by using the phyloseq (https://bioconductor.org/packages/release/bioc/html/phyloseq.html; v.3.10) [94] package and ggplot2 (https://ggplot2.tidyverse.org) was

used for visualizations in R (v.4.0.1). All ASVs with low counts and those with prevalence lower than 0.01% were filtered to remove spurious ASVs in the bacterial dataset. Then the microbial community composition was represented in terms of relative abundance at phylum, family and genus levels, keeping the most abundant five featured taxa at each level by using the tax-glom function (https://rdrr.io/bioc/phyloseq/man/tax_glom.html) in the phyloseq package (v.3.10). For estimating microbial community dissimilarities, Bray–Curtis distances were calculated by phyloseq (v.3.10) and vegan (https://cran.r-project.org/web/packages/vegan/index.html; v.2.5.7) [94] package implemented in R (v.4.0.3). Data were normalized by rarefaction, with no replacement, using the phyloseq function rarefy_even_depht (https://rdrr.io/bioc/phyloseq/man/rarefy_even_depth.html) and clr transform, using the microbiome package (https://microbiome.github.io/tutorials/; v.1.12.0) prior to diversity measures. Further, principal component analysis (PCA) plots were constructed to visualize the categorical partition of the samples explained by Bray–Curtis dissimilarity. Adonis from vegan package (https://rdrr.io/rforge/vegan/man/adonis.html) in R was used for Permutational multivariate analysis of variance (PERMANOVA) test to evaluate differences among groups (number of permutations set at 999). The taxa differential abundance analyses were performed by using the function aldex in ALDEx2 (https://bioconductor.org/packages/release/bioc/html/ALDEx2.html; v.1.22.0) after technical filtering of ASVs with less than 5 reads in total and appearing in less than two samples [95]. Differential abundance in the zebrafish gut microbiome was assessed for all the experimental groups treated with *A. veronii* probiotic feed, *P. entomophila* probiotic feed and α-Gal versus the control group treated with PBA at each time point (pre-challenge and post-challenge). Correlations between zebrafish gut microbiota and anti-α-Gal and P22 IgM antibody titers were calculated with ALDEx2 (v.1.22.0), using the aldex.corr function analysis (https://rdrr.io/bioc/ALDEx2/man/aldex.corr.html) as implemented in R (v.4.0.3), and visualized by using the package ggplot2. All packages and algorithms were accessed on 30 March 2021.

4. Conclusions

Treatment with probiotics prepared with bacteria from the gut microbiota with high α-Gal content protected against mycobacteriosis in the zebrafish model of tuberculosis. This study provided the first evidence on the effect of probiotics with high α-Gal content on eliciting protection against mycobacteriosis. The main limitations of the study are the limited number of samples included in some analyses and the need to corroborate in future studies the suggested protective mechanisms elicited by probiotics with high α-Gal content. The results provided preliminary evidence that the protective mechanisms induced in response to probiotics with high α-Gal content include B-cell maturation, antibody-mediated opsonization of mycobacteria, FcR-mediated phagocytosis, macrophage response, interference with the α-Gal antagonistic effect of the TLR2/NF-kB-mediated immune response, and upregulation of pro-inflammatory cytokines and innate immunity. Additionally, a beneficial effect on nutrient metabolism was observed through upregulation of HK-1 likely in response to IL-mediated activation of MAPK. The activation of these humoral and cellular immune mechanisms reduces mycobacteria infection. Treatment with probiotic *A. veronii* and *P. entomophila* activated different mechanisms, but all associated with the response to α-Gal. While probiotic *A. veronii* with highest α-Gal content promoted B-cell maturation, only probiotic *P. entomophila* produced beneficial effects on nutrient metabolism through HK-1 and reduced oxidative stress. Remarkably, both probiotic bacteria induced innate immune response trough TNF-α upregulation. These results support the potential of probiotics with high α-Gal content for the control of fish mycobacteriosis and provided additional evidence of the role of immune response to α-Gal for the control of infectious diseases caused by pathogens with this modification on their surface. The suggested mechanisms activated in response to probiotics with high α-Gal content need to be corroborated by using other experimental approaches to characterize innate immunity or humoral and cellular immune response. Differences in the activated protective mechanisms and gut mi-

crobiota composition between probiotics and α-Gal suggested the possibility of exploring the development of combined probiotic treatments alone and in combination with α-Gal for the control of mycobacteriosis and other infectious diseases.

Supplementary Materials: The following are available online at https://www.mdpi.com/article/10.3390/ph14070635/s1. Figure S1: Expression of zebrafish immune-response genes in response to α-Gal and probiotic bacteria. File S1: Data S1. Raw counts of taxonomic assignments per sample generated with DADA2 and grouped by time point and treatment group. File S1: Figure S2. Relative abundance of the top 5 phyla. File S1: Figure S3. Relative abundance of the top 5 families. File S1: Figure S4. Relative abundance of the top 5 genera.

Author Contributions: Conceptualization, J.d.l.F., M.V., S.D.-S., A.C.-C. and C.G.; methodology, I.P., S.D.-S. and M.C.; software, S.D.-S.; validation, I.P., M.C. and S.D.-S.; formal analysis, I.P., S.D.-S., M.C. and J.d.l.F.; investigation, I.P., S.D.-S. and M.C.; data curation, S.D.-S.; writing—original draft preparation, J.d.l.F. and S.D.-S.; writing—review and editing, I.P., S.D.-S., M.C., C.G. and A.C.-C.; visualization, S.D.-S. and J.d.l.F.; supervision, J.d.l.F. and M.V.; project administration, J.d.l.F. and M.V.; funding acquisition, J.d.l.F. and M.V. All authors have read and agreed to the published version of the manuscript.

Funding: This research was funded by Junta de Comunidades de Castilla-La Mancha (JCCM), Spain, and EU-FEDER (grant GALINFEC SBPLY/17/180501/000185). MC was funded by the Ministerio de Ciencia, Innovación y Universidades, Spain (grant FJC-2018-038277-I).

Institutional Review Board Statement: Experiments were conducted in strict accordance with the recommendations of the European Guide for the Care and Use of Laboratory Animals. Animals were housed at and experiments were conducted at the experimental facility (IREC, Ciudad Real, Spain) with the approval and supervision of the Ethics Committee on Animal Experimentation of the University of Castilla La Mancha (PR-2018-06-13) and the Counseling of Agriculture, Environment, and Rural Development of Castilla La Mancha (ES130340000218).

Informed Consent Statement: Not applicable.

Data Availability Statement: The data presented in this study are available in the article and Sequence Read Archive (SRA) repository (https://www.ncbi.nlm.nih.gov/sra; BioProject ID PRJNA728442, accession numbers SAMN19079379-SAMN19079417).

Acknowledgments: We thank Pilar Alberdi (IREC, Spain) for technical assistance with flow cytometry and David Fernandez Castellanos (IREC, Spain) for assistance with the zebrafish experimental unit. Juan Galcerán Sáez (IN-CSIC-UMH, Spain) is acknowledged for providing zebrafish. MV was supported by UCLM and EU-FEDER.

Conflicts of Interest: The authors declare no conflict of interest.

References

1. Duremdez, R.; Al-Marzouk, A.; Qasem, J.A.; Al-Harbi, A.; Gharabally, H. Isolation of *Streptococcus agalactiae* from cultured silver pomfret, *Pampus argenteus* (Euphrasen), in Kuwait. *J. Fish. Dis.* **2004**, *27*, 307–310. [CrossRef]
2. Bebak, J.; Wagner, B.; Burnes, B.; Hanson, T. Farm size, seining practices, and salt use: Risk factors for *Aeromonas hydrophila* outbreaks in farm-raised catfish, Alabama, USA. *Prev. Vet. Med.* **2015**, *118*, 161–168. [CrossRef] [PubMed]
3. Decostere, A.; Hermans, K.; Haesebrouck, F. Piscine mycobacteriosis: A literature review covering the agent and the disease it causes in fish and humans. *Vet. Microbiol.* **2004**, *99*, 159–166. [CrossRef]
4. Jacobs, J.M.; Stine, C.B.; Baya, A.M.; Kent, M.L. A review of mycobacteriosis in marine fish. *J. Fish. Dis.* **2009**, *32*, 119–130. [CrossRef] [PubMed]
5. Liu, Y.; Zhou, Z.; Wu, N.; Tao, Y.; Xu, L.; Cao, Y.; Zhang, Y.; Yao, B. Gibel carp *Carassius auratus* gut microbiota after oral administration of trimethoprim/ sulfamethoxazole. *Dis. Aquat. Organ.* **2012**, *99*, 207–213. [CrossRef]
6. Romero, J.; Feijoo, C.G.; Navarrete, P. *Antibiotics in Aquaculture—Use, Abuse and Alternatives*; INTECH Open Access Publisher: London, UK, 2012. [CrossRef]
7. Skwor, T.; Shinko, J.; Augustyniak, A.; Gee, C.; Andraso, G. *Aeromonas hydrophila* and *Aeromonas veronii* predominate among potentially pathogenic ciprofloxacin- and tetracycline-resistant aeromonas isolates from Lake Erie. *Appl. Environ. Microbiol.* **2014**, *80*, 841–848. [CrossRef]
8. Gioacchini, G.; Rossi, G.; Carnevali, O. Host-probiotic interaction: New insights into the role of the endocannabinoid system by in vivo and ex vivo approaches. *Sci. Rep.* **2017**, *7*, 1261. [CrossRef] [PubMed]

9. Daliri, E.B.; Ofosu, F.K.; Xiuqin, C.; Chelliah, R.; Oh, D.H. Probiotic effector compounds: Current knowledge and future perspectives. *Front. Microbiol.* **2021**, *12*, 655705. [CrossRef]
10. Akhter, N.; Wu, B.; Memon, A.M.; Mohsin, M. Probiotics and prebiotics associated with aquaculture: A review. *Fish. Shellfish Immunol.* **2015**, *45*, 733–741. [CrossRef]
11. Borges, N.; Keller-Costa, T.; Sanches-Fernandes, G.; Louvado, A.; Gomes, N.; Costa, R. Bacteriome structure, function, and probiotics in fish larviculture: The good, the bad, and the gaps. *Annu. Rev. Anim. Biosci.* **2021**, *9*, 423–452. [CrossRef]
12. Hao, K.; Wu, Z.Q.; Li, D.L.; Yu, X.B.; Wang, G.X.; Ling, F. Effects of dietary administration of *Shewanella xiamenensis* A-1, *Aeromonas veronii* A-7, and *Bacillus subtilis*, single or combined, on the Grass Carp (*Ctenopharyngodon idella*) intestinal microbiota. *Probiotics Antimicrob. Proteins.* **2017**, *9*, 386–396. [CrossRef]
13. Ringø, E.; Hoseinifar, S.H.; Ghosh, K.; Doan, H.V.; Beck, B.R.; Song, S.K. Lactic acid bacteria in Finfish—An update. *Front. Microbiol.* **2018**, *9*, 1818. [CrossRef] [PubMed]
14. Kuebutornye, F.; Abarike, E.D.; Lu, Y. A review on the application of *Bacillus* as probiotics in aquaculture. *Fish. Shellfish Immunol.* **2019**, *87*, 820–828. [CrossRef] [PubMed]
15. Banerjee, G.; Ray, A.K. The advancement of probiotics research and its application in fish farming industries. *Res. Vet. Sci.* **2017**, *115*, 66–77. [CrossRef] [PubMed]
16. Yi, C.C.; Liu, C.H.; Chuang, K.P.; Chang, Y.T.; Hu, S.Y. A potential probiotic *Chromobacterium aquaticum* with bacteriocin-like activity enhances the expression of indicator genes associated with nutrient metabolism, growth performance and innate immunity against pathogen infections in zebrafish (*Danio rerio*). *Fish. Shellfish Immunol.* **2019**, *93*, 124–134. [CrossRef]
17. Huang, H.; Zhou, P.; Chen, P.; Xia, L.; Hu, S.; Yi, G.; Lu, J.; Yang, S.; Xie, J.; Peng, J.; et al. Alteration of the gut microbiome and immune factors of grass carp infected with *Aeromonas veronii* and screening of an antagonistic bacterial strain (*Streptomyces flavotricini*). *Microb. Pathog.* **2020**, *143*, 104092. [CrossRef] [PubMed]
18. Arani, M.M.; Salati, A.P.; Keyvanshokooh, S.; Safari, O. The effect of *Pediococcus acidilactici* on mucosal immune responses, growth, and reproductive performance in zebrafish (*Danio rerio*). *Fish Physiol. Biochem.* **2021**, *47*, 153–162. [CrossRef] [PubMed]
19. Standen, B.T.; Rodiles, A.; Peggs, D.L.; Davies, S.J.; Santos, G.A.; Merrifield, D.L. Modulation of the intestinal microbiota and morphology of tilapia, *Oreochromis niloticus*, following the application of a multi-species probiotic. *Appl. Microbiol. Biotechnol.* **2015**, *99*, 8403–8417. [CrossRef]
20. Ljubobratovic, U.; Kosanovic, D.; Vukotic, G.; Molnar, Z.; Stanisavljevic, N.; Ristovic, T.; Peter, G.; Lukic, J.; Jeney, G. Supplementation of lactobacilli improves growth, regulates microbiota composition and suppresses skeletal anomalies in juvenile pike-perch (*Sander lucioperca*) reared in recirculating aquaculture system (RAS): A pilot study. *Res. Vet. Sci.* **2017**, *115*, 451–462. [CrossRef]
21. Pyclik, M.; Srutkova, D.; Schwarzer, M.; Górska, S. Bifidobacteria cell wall-derived exo-polysaccharides, lipoteichoic acids, peptidoglycans, polar lipids and proteins—Their chemical structure and biological attributes. *Int. J. Biol. Macromol.* **2020**, *147*, 333–349. [CrossRef] [PubMed]
22. Astronomo, R.D.; Burton, D.R. Carbohydrate vaccines: Developing sweet solutions to sticky situations? *Nat. Rev. Drug Discov.* **2010**, *9*, 308–324. [CrossRef]
23. Hodžić, A.; Mateos-Hernández, L.; de la Fuente, J.; Cabezas-Cruz, A. α-Gal-based vaccines: Advances, opportunities, and perspectives. *Trends Parasitol.* **2020**, *36*, 992–1001. [CrossRef] [PubMed]
24. Pacheco, I.; Contreras, M.; Villar, M.; Risalde, M.A.; Alberdi, P.; Cabezas-Cruz, A.; Gortázar, C.; de la Fuente, J. Vaccination with alpha-Gal protects against mycobacterial infection in the zebrafish model of tuberculosis. *Vaccines* **2020**, *8*, 195. [CrossRef]
25. Urra, J.M.; Ferreras-Colino, E.; Contreras, M.; Cabrera, C.M.; Fernández de Mera, I.G.; Villar, M.; Cabezas-Cruz, A.; Gortázar, C.; de la Fuente, J. The antibody response to the glycan α-Gal correlates with COVID-19 disease symptoms. *J. Med. Virol.* **2021**, *93*, 2065–2075. [CrossRef] [PubMed]
26. De la Fuente, J.; Gortázar, C.; Cabezas-Cruz, A. Immunity to glycan α-Gal and possibilities for the control of COVID-19. *Immunotherapy* **2021**, *13*, 185–188. [CrossRef] [PubMed]
27. Cosma, C.L.; Swaim, L.E.; Volkman, H.; Ramakrishnan, L.; Davis, J.M. Zebrafish and frog models of *Mycobacterium marinum* infection. *Curr. Protoc. Microbiol.* **2006**, *3*, unit 10B.2, chapter 10. [CrossRef]
28. Cronan, M.R.; Tobin, D.M. Fit for consumption: Zebrafish as a model for tuberculosis. *Dis. Model Mech.* **2014**, *7*, 777–784. [CrossRef] [PubMed]
29. Van Leeuwen, L.M.; van der Sar, A.M.; Bitter, W. Animal models of tuberculosis: Zebrafish. *Cold Spring Harb. Perspect. Med.* **2014**, *5*, a018580. [CrossRef] [PubMed]
30. Myllymäki, H.; Bäuerlein, C.A.; Rämet, M. The zebrafish breathes new life into the study of tuberculosis. *Front. Immunol.* **2016**, *7*, 196. [CrossRef]
31. Masud, S.; Torraca, V.; Meijer, A.H. Modeling infectious diseases in the context of a developing immune system. *Curr. Top. Dev. Biol.* **2017**, *124*, 277–329. [CrossRef]
32. Risalde, M.A.; López, V.; Contreras, M.; Mateos-Hernández, L.; Gortázar, C.; de la Fuente, J. Control of mycobacteriosis in zebrafish (*Danio rerio*) mucosally vaccinated with heat-inactivated *Mycobacterium bovis*. *Vaccine* **2018**, *36*, 4447–4453. [CrossRef]
33. López, V.; Risalde, M.A.; Contreras, M.; Mateos-Hernández, L.; Vicente, J.; Gortázar, C.; de la Fuente, J. Heat-inactivated *Mycobacterium bovis* protects zebrafish against mycobacteriosis. *J. Fish Dis.* **2018**, *41*, 1515–1528. [CrossRef]

34. Lin, Y.S.; Saputra, F.; Chen, Y.C.; Hu, S.Y. Dietary administration of *Bacillus amyloliquefaciens* R8 reduces hepatic oxidative stress and enhances nutrient metabolism and immunity against *Aeromonas hydrophila* and *Streptococcus agalactiae* in zebrafish (*Danio rerio*). *Fish Shellfish Immunol.* **2019**, *86*, 410–419. [CrossRef] [PubMed]
35. Contreras, M.; Pacheco, I.; Alberdi, P.; Díaz-Sánchez, S.; Artigas-Jerónimo, S.; Mateos-Hernández, L.; Villar, M.; Cabezas-Cruz, A.; de la Fuente, J. Allergic reactions and immunity in response to tick salivary biogenic substances and red meat consumption in the zebrafish model. *Front. Cell. Infect. Microbiol.* **2020**, *10*, 78. [CrossRef] [PubMed]
36. Benard, E.L.; Rougeot, J.; Racz, P.I.; Spaink, H.P.; Meijer, A.H. Transcriptomic approaches in the zebrafish model for tuberculosis-insights into host- and pathogen-specific determinants of the innate immune response. *Adv. Genet.* **2016**, *95*, 217–251. [CrossRef]
37. Roeselers, G.; Mittge, E.K.; Stephens, W.Z.; Parichy, D.M.; Cavanaugh, C.M.; Guillemin, K.; Rawls, J.F. Evidence for a core gut microbiota in the zebrafish. *ISME J.* **2011**, *5*, 1595–1608. [CrossRef] [PubMed]
38. Cantas, L.; Sørby, J.R.; Aleström, P.; Sørum, H. Culturable gut microbiota diversity in zebrafish. *Zebrafish* **2012**, *9*, 26–37. [CrossRef] [PubMed]
39. Dahan, D.; Jude, B.A.; Lamendella, R.; Keesing, F.; Perron, G.G. Exposure to arsenic alters the microbiome of larval zebrafish. *Front. Microbiol.* **2018**, *9*, 1323. [CrossRef] [PubMed]
40. Turska-Szewczuk, A.; Duda, K.A.; Schwudke, D.; Pekala, A.; Kozinska, A.; Holst, O. Structural studies of the lipopolysaccharide from the fish pathogen *Aeromonas veronii* strain Bs19, serotype O16. *Mar. Drugs* **2014**, *12*, 1298–1316. [CrossRef]
41. Molinari, L.M.; Scoaris, D.O.; Pedroso, R.B.; Bittencourt, N.L.R.; Nakamura, C.V.; Nakamura, T.U.; Abreu Filho, B.A.; Dias Filho, B.P. Bacterial microflora in the gastrointestinal tract of Nile tilapia, *Oreochromis niloticus*, cultured in a semi-intensive system, *Acta Sci. Biol. Sci.* **2003**, *25*, 267–271. [CrossRef]
42. Silver, A.C.; Williams, D.; Faucher, J.; Horneman, A.J.; Gogarten, J.P.; Graf, J. Complex evolutionary history of the *Aeromonas veronii* group revealed by host interaction and DNA sequence data. *PLoS ONE* **2011**, *6*, e16751. [CrossRef]
43. Song, M.F.; Kang, Y.H.; Zhang, D.X.; Chen, L.; Bi, J.F.; Zhang, H.P.; Zhang, L.; Qian, A.D.; Shan, X.F. Immunogenicity of extracellular products from an inactivated vaccine against *Aeromonas veronii* TH0426 in koi, *Cyprinus carpio*. *Fish Shellfish Immunol.* **2018**, *81*, 176–181. [CrossRef]
44. Yang, B.; Zhang, D.; Wu, T.; Zhang, Z.; Raza, S.; Schreurs, N.; Zhang, L.; Yang, G.; Wang, C.; Qian, A.; et al. Maltoporin (LamB protein) contributes to the virulence and adhesion of *Aeromonas veronii* TH0426. *J. Fish. Dis.* **2019**, *42*, 379–389. [CrossRef]
45. Yang, B.; Song, H.; An, D.; Zhang, D.; Raza, S.; Wang, G.; Shan, X.; Qian, A.; Kang, Y.; Wang, C. Functional analysis of *preA* in *Aeromonas veronii* TH0426 reveals a key role in the regulation of virulence and resistance to oxidative stress. *Int. J. Mol. Sci.* **2019**, *21*, 98. [CrossRef] [PubMed]
46. Yang, B.; Chen, C.; Sun, Y.; Cao, L.; Zhang, D.; Sun, W.; Zhang, L.; Wang, G.; Shan, X.; Kang, Y.; et al. Comparative genomic analysis of different virulence strains reveals reasons for the increased virulence of *Aeromonas veronii*. *J. Fish Dis.* **2021**, *44*, 11–24. [CrossRef]
47. Volpe, E.; Mandrioli, L.; Errani, F.; Serratore, P.; Zavatta, E.; Rigillo, A.; Ciulli, S. Evidence of fish and human pathogens associated with doctor fish (*Garra rufa*, Heckel, 1843) used for cosmetic treatment. *J. Fish Dis.* **2019**, *42*, 1637–1644. [CrossRef] [PubMed]
48. Li, T.; Raza, S.; Yang, B.; Sun, Y.; Wang, G.; Sun, W.; Qian, A.; Wang, C.; Kang, Y.; Shan, X. *Aeromonas veronii* infection in commercial freshwater fish: A potential threat to public health. *Animals* **2020**, *10*, 608. [CrossRef] [PubMed]
49. Vodovar, N.; Vallenet, D.; Cruveiller, S.; Rouy, Z.; Barbe, V.; Acosta, C.; Cattolico, L.; Jubin, C.; Lajus, A.; Segurens, B.; et al. Complete genome sequence of the entomopathogenic and metabolically versatile soil bacterium *Pseudomonas entomophila*. *Nat. Biotechnol.* **2006**, *24*, 673–679. [CrossRef] [PubMed]
50. Thune, R.; Stanley, L.A.; Cooper, R.K. Pathogenesis of gram—Negative bacteria infections in warm-water fish. *Fish Annu. Rev. Fish. Dis.* **1993**, *3*, 37–68. [CrossRef]
51. Preena, P.G.; Dharmaratnam, A.; Swaminathan, T.R. Antimicrobial resistance analysis of pathogenic bacteria isolated from freshwater Nile Tilapia (*Oreochromis niloticus*) cultured in Kerala, India. *Curr. Microbiol.* **2020**, *77*, 3278–3287. [CrossRef]
52. Hasan, K.N.; Banerjee, G. Recent studies on probiotics as beneficial mediator in aquaculture: A review. *J. Basic Appl. Zool.* **2020**, *81*, 53. [CrossRef]
53. Gioacchini, G.; Giorgini, E.; Olivotto, I.; Maradonna, F.; Merrifield, D.L.; Carnevali, O. The influence of probiotics on zebrafish *Danio rerio* innate immunity and hepatic stress. *Zebrafish* **2014**, *11*, 98–106. [CrossRef]
54. Liu, X.; Wu, H.; Liu, Q.; Wang, Q.; Xiao, J.; Chang, X.; Zhang, Y. Profiling immune response in zebrafish intestine, skin, spleen and kidney bath-vaccinated with a live attenuated *Vibrio anguillarum* vaccine. *Fish Shellfish Immunol.* **2015**, *45*, 342–345. [CrossRef] [PubMed]
55. Zhang, M.; Liu, N.; Liu, H. Determination of the total mass of antioxidant substances and antioxidant capacity per unit mass in serum using redox titration. *Bioinorg. Chem. Appl.* **2014**, *2014*, 928595. [CrossRef] [PubMed]
56. Slaninova, A.; Smutna, M.; Modra, H.; Svobodova, Z. A review: Oxidative stress in fish induced by pesticides. *Neuro Endocrinol. Lett.* **2009**, *30* (Suppl. S1), 2–12.
57. Yadav, S.S.; Kumar, R.; Khare, P.; Tripathi, M. Oxidative stress biomarkers in the freshwater fish, *Heteropneustes fossilis* (Bloch) exposed to sodium fluoride: Antioxidant defense and role of ascorbic acid. *Toxicol. Int.* **2015**, *22*, 71–76. [CrossRef] [PubMed]
58. Lee, J.W.; Choi, H.; Hwang, U.K.; Kang, J.C.; Kang, Y.J.; Kim, K.I.; Kim, J.H. Toxic effects of lead exposure on bioaccumulation, oxidative stress, neurotoxicity, and immune responses in fish: A review. *Environ. Toxicol. Pharmacol.* **2019**, *68*, 101–108. [CrossRef] [PubMed]

59. Zamani, B.; Sheikhi, A.; Namazi, N.; Larijani, B.; Azadbakht, L. The effects of supplementation with probiotic on biomarkers of oxidative stress in adult subjects: A systematic review and meta-analysis of randomized trials. *Probiotics Antimicrob. Proteins.* **2020**, *12*, 102–111. [CrossRef]
60. Bernut, A.; Dupont, C.; Ogryzko, N.V.; Neyret, A.; Herrmann, J.L.; Floto, R.A.; Renshaw, S.A.; Kremer, L. CFTR protects against *Mycobacterium abscessus* infection by fine-tuning host oxidative defenses. *Cell Rep.* **2019**, *26*, 1828–1840.e4. [CrossRef]
61. Black, H.D.; Xu, W.; Hortle, E.; Robertson, S.I.; Britton, W.J.; Kaur, A.; New, E.J.; Witting, P.K.; Chami, B.; Oehlers, S.H. The cyclic nitroxide antioxidant 4-methoxy-TEMPO decreases mycobacterial burden in vivo through host and bacterial targets. *Free Radic. Biol. Med.* **2019**, *135*, 157–166. [CrossRef]
62. Wipperman, M.F.; Bhattarai, S.K.; Vorkas, C.K.; Maringati, V.S.; Taur, Y.; Mathurin, L.; McAulay, K.; Vilbrun, S.C.; Francois, D.; Bean, J.; et al. Gastrointestinal microbiota composition predicts peripheral inflammatory state during treatment of human tuberculosis. *Nat. Commun.* **2021**, *12*, 1141. [CrossRef] [PubMed]
63. Nadal, A.P.; Ikeda-Ohtsubo, W.; Sipkema, D.; Peggs, D.; McGurk, C.; Forlenza, M.; Wiegertjes, G.F.; Brugman, S. Feed, microbiota, and gut immnunity: Using the zebrafish model to understand fish health. *Front. Immunol.* **2020**, *11*, 114. [CrossRef] [PubMed]
64. Robinson, C.D.; Klein, H.S.; Murphy, K.D.; Parthasarathy, R.; Guillemin, K.; Bohannan, B.J.M. Experimental bacterial adaptation to the zebrafish gut reveals a primary role for immigration. *PLoS Biol.* **2018**, *16*, e2006893. [CrossRef]
65. Mateos-Hernández, L.; Obregón, D.; Maye, J.; Borneres, J.; Versille, N.; de la Fuente, J.; Estrada-Peña, A.; Hodžić, A.; Šimo, L.; Cabezas-Cruz, A. Anti-tick microbiota vaccine impacts *Ixodes ricinus* performance during feeding. *Vaccines* **2020**, *8*, 702. [CrossRef]
66. Bamgbose, T.; Anvikar, A.R.; Alberdi, P.; Abdullahi, I.O.; Inabo, H.I.; Bello, M.; Cabezas-Cruz, A.; de la Fuente, J. Functional food for the stimulation of the immune system against malaria. *Probiotics Antimicrob. Proteins.* **2021**, 1–13. [CrossRef]
67. Galili, U.; Rachmilewitz, E.A.; Peleg, A.; Flechner, I. A unique natural human IgG antibody with anti-α-galactosyl specificity. *J. Exp. Med.* **1984**, *160*, 1519–1531. [CrossRef]
68. Galili, U.; Mandrell, R.E.; Hamadeh, R.M.; Shohet, S.B.; Griffiss, J.M. Interaction between human natural anti-α-galactosyl immunoglobulin G and bacteria of the human flora. *Infect. Immun.* **1988**, *56*, 1730–1737. [CrossRef]
69. Koch, B.E.V.; Yang, S.; Lamers, G.; Stougaard, J.; Spaink, H.P. Intestinal microbiome adjusts the innate immune setpoint during colonization through negative regulation of MyD88. *Nat. Commun.* **2018**, *9*, 4099. [CrossRef] [PubMed]
70. Kanther, M.; Sun, X.; Mhlbauer, M.; MacKey, L.C.; Flynn, E.J.; Bagnat, M.; Jobin, C.; Rawls, J.F. Microbial colonization induces dynamic temporal and spatial patterns of NF-κB activation in the zebrafish digestive tract. *Gastroenterology* **2011**, *141*, 197–207. [CrossRef] [PubMed]
71. Cheesman, S.E.; Neal, J.T.; Mittge, E.; Seredick, B.M.; Guillemin, K. Epithelial cell proliferation in the developing zebrafish intestine is regulated by the Wnt pathway and microbial signaling via Myd88. *Proc. Natl. Acad. Sci. USA* **2011**, *108* (Suppl. S1), 4570–4577. [CrossRef]
72. Jacobs, A.J.; Mongkolsapaya, J.; Screaton, G.R.; McShane, H.; Wilkinson, R.J. Antibodies and tuberculosis. *Tuberculosis* **2016**, *101*, 102–113. [CrossRef]
73. Lee, A.Y.S.; Körner, H. The CCR6-CCL20 axis in humoral immunity and T-B cell immunobiology. *Immunobiology* **2019**, *224*, 449–454. [CrossRef]
74. Haeggström, J.Z.; Tholander, F.; Wetterholm, A. Structure and catalytic mechanisms of leukotriene A4 hydrolase. *Prostaglandins Other Lipid Mediat.* **2007**, *83*, 198–202. [CrossRef] [PubMed]
75. Rodriguez, A.R.; Yu, J.J.; Guentzel, M.N.; Navara, C.S.; Klose, K.E.; Forsthuber, T.G.; Chambers, J.P.; Berton, M.T.; Arulanandam, B.P. Mast cell TLR2 signaling is crucial for effective killing of *Francisella tularensis*. *J. Immunol.* **2012**, *188*, 5604–5611. [CrossRef] [PubMed]
76. Maji, A.; Misra, R.; Kumar Mondal, A.; Kumar, D.; Bajaj, D.; Singhal, A.; Arora, G.; Bhaduri, A.; Sajid, A.; Bhatia, S.; et al. Expression profiling of lymph nodes in tuberculosis patients reveal inflammatory milieu at site of infection. *Sci. Rep.* **2015**, *5*, 15214. [CrossRef] [PubMed]
77. Blanc, L.; Gilleron, M.; Prandi, J.; Song, O.R.; Jang, M.S.; Gicquel, B.; Drocourt, D.; Neyrolles, O.; Brodin, P.; Tiraby, G.; et al. *Mycobacterium tuberculosis* inhibits human innate immune responses via the production of TLR2 antagonist glycolipids. *Proc. Natl. Acad. Sci. USA* **2017**, *114*, 11205–11210. [CrossRef] [PubMed]
78. Lin, P.L.; Plessner, H.L.; Voitenok, N.N.; Flynn, J.L. Tumor necrosis factor and tuberculosis. *J. Investig. Dermatol. Symp. Proc.* **2007**, *12*, 22–25. [CrossRef] [PubMed]
79. Enes, P.; Panserat, S.; Kaushik, S.; Oliva-Teles, A. Nutritional regulation of hepatic glucose metabolism in fish. *Fish. Physiol. Biochem.* **2009**, *35*, 519–539. [CrossRef] [PubMed]
80. Saputra, F.; Shiu, Y.L.; Chen, Y.C.; Puspitasari, A.W.; Danata, R.H.; Liu, C.H.; Hu, S.Y. Dietary supplementation with xylanase-expressing B. amyloliquefaciens R8 improves growth performance and enhances immunity against *Aeromonas hydrophila* in Nile tilapia (*Oreochromis niloticus*). *Fish Shellfish Immunol.* **2016**, *58*, 397–405. [CrossRef]
81. Taneja, N.; Coy, P.E.; Lee, I.; Bryson, J.M.; Robey, R.B. Proinflammatory interleukin-1 cytokines increase mesangial cell hexokinase activity and hexokinase II isoform abundance. *Am. J. Physiol. Cell Physiol.* **2004**, *287*, C548–C557. [CrossRef]
82. Peng, X.; Yu, K.-Q.; Deng, G.-H.; Jiang, Y.-X.; Wang, Y.; Zhang, G.-X.; Zhou, H.-W. Comparison of boiling with commercial kits for extracting fecal microbiome DNA by Illumina sequencing of 16S RNA tags. *J. Microbiol. Methods* **2013**, *9*, 455–462. [CrossRef]
83. Toukach, P.V.; Knirel, Y.A. New database of bacterial carbohydrate structures. *Glycoconj. J.* **2005**, *22*, 216–217.

84. Toukach, P.V.; Egorova, K.S. Carbohydrate structure database merged from bacterial, archaeal, plant and fungal parts. *Nucleic Acids Res.* **2016**, *44*, D1229–D1236. [CrossRef] [PubMed]
85. Toukach, P.V.; Egorova, K.S. New Features of carbohydrate structure database notation (CSDB Linear), as compared to other carbohydrate notations. *J. Chem. Inf. Model.* **2020**, *60*, 1276–1289. [CrossRef] [PubMed]
86. Egorova, K.S.; Toukach, P.V. Glycoinformatics: Bridging isolated islands in the sea of data. *Angew. Chem. Int. Ed. Engl.* **2018**, *57*, 14986–14990. [CrossRef]
87. Wanka, K.M.; Damerau, T.; Costas, B.; Krueger, A.; Schulz, C.; Wuertz, S. Isolation and characterization of native probiotics for fish farming. *BMC Microbiol.* **2018**, *18*, 119. [CrossRef]
88. Meritet, D.M.; Mulrooney, D.M.; Kent, M.L.; Löhr, C.V. Development of quantitative real-time PCR assays for postmortem detection of *Mycobacterium* spp. common in zebrafish (*Danio rerio*) research colonies. *J. Am. Assoc. Lab. Anim. Sci.* **2017**, *56*, 131–141.
89. Ririe, K.M.; Rasmussen, R.P.; Wittwer, C.T. Product differentiation by analysis of DNA melting curves during the polymerase chain reaction. *Anal. Biochem.* **1997**, *245*, 154–160. [CrossRef]
90. Livak, K.J.; Schmittgen, T.D. Analysis of relative gene expression data using real-time quantitative PCR and the 2(-Delta Delta C(T)) Method. *Methods.* **2001**, *25*, 402–408. [CrossRef] [PubMed]
91. Infantes-Lorenzo, J.A.; Moreno, I.; Risalde, M.; Roy, Á.; Villar, M.; Romero, B.; Ibarrola, N.; de la Fuente, J.; Puentes, E.; de Juan, L.; et al. Proteomic characterisation of bovine and avian purified protein derivatives and identification of specific antigens for serodiagnosis of bovine tuberculosis. *Clin. Proteomics* **2017**, *14*, 36. [CrossRef]
92. Callahan, B.J.; McMurdie, P.J.; Rosen, M.J.; Han, A.W.; Johnson, A.J.A.; Holmes, S.P. DADA2: High-resolution sample inference from Illumina amplicon data. *Nat. Methods* **2016**, *13*, 581–583. [CrossRef] [PubMed]
93. Yarza, P.; Yilmaz, P.; Pruesse, E.; Glöckner, F.O.; Ludwig, W.; Schleifer, K.H.; Whitman, W.B.; Euzéby, J.; Amann, R.; Roselló-Mora, R. Uniting the classification of cultured and uncultured bacteria and archaea using 16S rRNA gene sequences. *Nat. Rev. Microbiol.* **2014**, *12*, 635–645. [CrossRef] [PubMed]
94. McMurdie, P.J.; Holmes, S. Phyloseq: An R package for reproducible interactive analysis and graphics of microbiome census data. *PLoS ONE* **2013**, *8*, e61217. [CrossRef] [PubMed]
95. Fernandes, A.D.; Reid, J.N.; Macklaim, J.M.; McMurrough, T.A.; Edgell, D.R.; Gloor, G.B. Unifying the analysis of high-throughput sequencing datasets: Characterizing RNA-seq, 16S rRNA gene sequencing and selective growth experiments by compositional data analysis. *Microbiome* **2014**, *2*, 15. [CrossRef]

Supplementary material. Chapter 3b

Supplementary material not included from **Pacheco, I.,** Díaz-Sánchez, S., Contreras, M., Villar, M., Cabezas-Cruz, A., Gortázar, C., de la Fuente, J. (2021). Probiotic bacteria with high alpha-Gal content protect zebrafish against mycobacteriosis. Pharmaceuticals 14, 635.

https://www.mdpi.com/1424-8247/14/7/635

- File S1: Data S1. Raw counts of taxonomic assingnations per sample generated with DADA2 and grouped by time point and treatment group.

GENERAL DISCUSSION

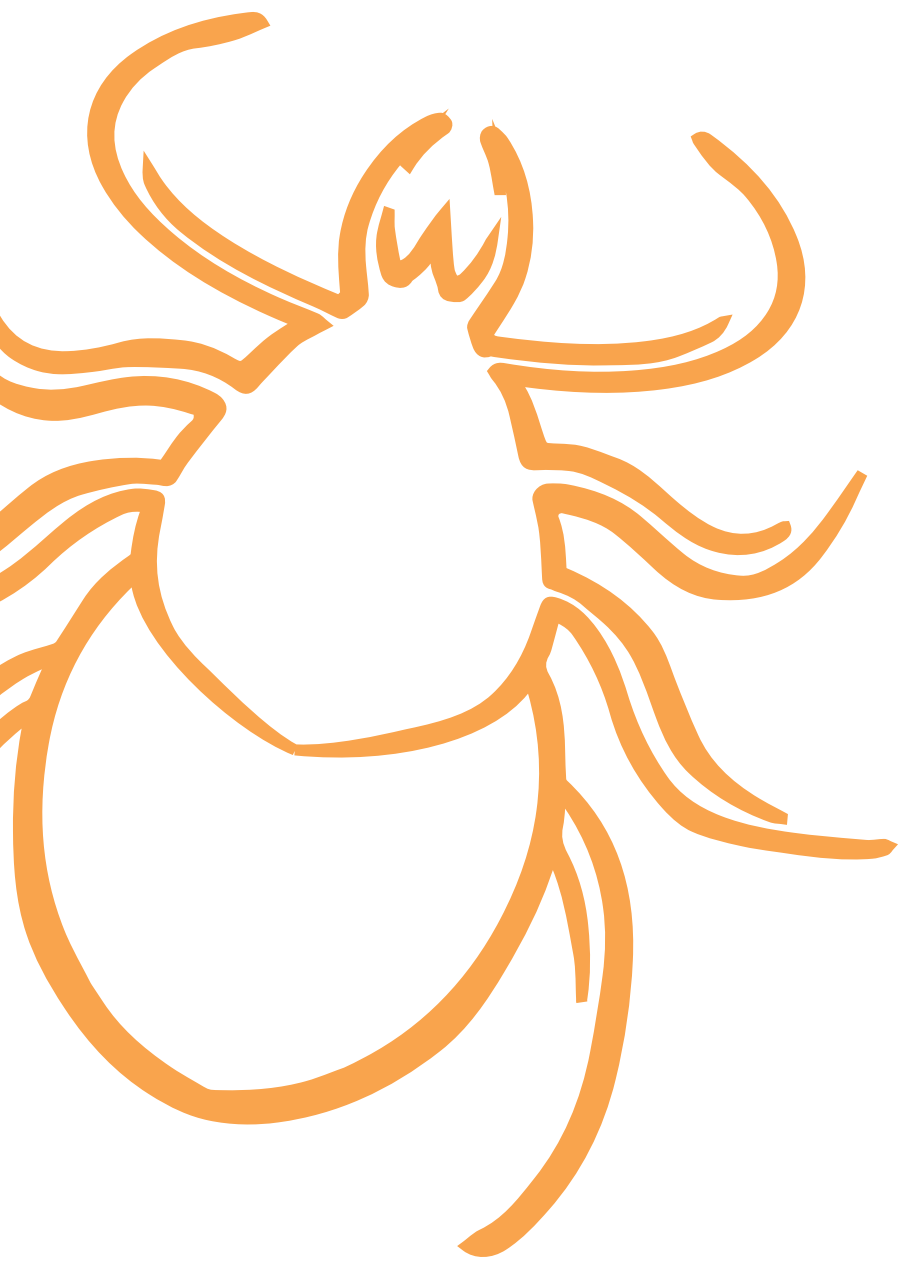

General Discussion

Ticks are blood-feeding ectoparasite vectors of pathogens as viruses, bacteria and protozoa, associated with the AGS and vector-borne diseases (VBDs) affecting human and animal health, representing a growing burden worldwide been part of the One Health concept. **(Dantas-Torres et al., 2012; de la Fuente et al., 2008; de la Fuente et al. 2017).**

Several approaches have been implemented to reduce the risk of vector-borne diseases (VBDs). This includes the use of chemical acaricides to control tick infestations and pathogen transmission, but is not yet fully effective due to generation of acaricide-resistant ticks and contamination of the environment. **(Eisen et al., 2016).**

Previous studies indicate a conflict and cooperation between tick-host-pathogens interactions, which may benefit the vector by increasing its survival and facilitating multiplication and transmission of the pathogen through feeding of the host. **(Chmelar et al., 2016a; 2016b; de la Fuente et al., 2016; Gulia-Nuss et al., 2016).**

The alpha-Gal is a carbohydrate present on tick salivary glycoproteins and tissues of non-catarrhine mammals, leading to the Alpha-Gal Syndrome (AGS). **(Steinke et al., 2015).**

Humans do not produce the α1,3-galactosyltransferase (α1,3GT or GGTA1) gene and as a consequence do not synthesize alpha-Gal epitopes, having a high susceptibility to contract the AGS **(Galili, 2015)**. The most common

symptoms of the AGS described in humans are a delayed anaphylaxis to red meat consumption and immediate anaphylaxis to tick bites, rejection of xenotransplantation and certain drugs such as cetuximab. **(Cabezas-Cruz et al., 2019; Hilger et al., 2019).** This syndrome is caused by tick species of the genera *Amblyomma, Ixodes, Rhipicephalus, Hyalomma* and *Haemaphysalis*, because they can synthesize α-Gal by themselves but it is also found in the host blood meal and the midgut microbiota of ticks. **(Cabezas-Cruz et al., 2021; Sharma et al., 2021).**

This is why the main objective of this thesis is to understand the mechanisms involved in the immune response to glycan alpha-Gal to prospectively control diseases related to the modification of this pathogen through different omics approaches.

In this matter, proteomic analysis identified tick saliva proteins with alpha-Gal modifications (alphagalactome) such as cytoglobin-1, 14-3-3 family chaperone and vitellogenin-1, secreted into saliva during feeding in tick species such as *Amblyomma americanum* and *Ixodes holocyclus*. These proteins play a putative role in the biological activity and the immune response to the AGS and other diseases. The results provided additional support for the tick origin of proteins with alpha-Gal and how these proteins may elicit a protective antibody response against tick infestations and pathogen infection. **(Chapter 1A)**.

The study of cementome of *Rhipicephalus microplus* female ticks through a proteomic approach has shed light on which are the main components of the tick cement at different feeding stages and what is its origin **(Chinery, 1973).** Results showed a high identification of tick and host derived proteins and biomolecules such as alpha-Gal in the tick cement as predominant components, which confirms that an interaction between both allows the prolongation of tick feeding and changes the tick cement composition **(Chapter 1B)**.

However, an effective diagnosis is essential to control the spread of vector-borne diseases. Tick bites induce high levels of anti-alpha-Gal IgE antibodies as an immune response in humans but also there are several risk factors to consider in the AGS as immune response markers and immunoreactive proteins, so it would be beneficial integrate all co-factors to predict the AGS **(Chapter 2A).**

It is also interesting the integration of a comparative analysis in a dataset of IgE, IgM, IgG and IgA antibody responses to alpha-Gal and blood groups, age and sex in healthy individuals and patients diagnosed with AGS, tick-borne allergies, GBS and COVID-19. It allowed to illustrate a determining factor in the lack of impact of AGS in blood group B/AB individuals due to the lower antibody titers **(Cabezas-Cruz et al., 2017; Chapter 2B**).

In **Chapter 2C**, a new risk factor that may affect the antibody response to alpha-Gal was explored resulting in a reduction of anti-alpha-Gal IgM and IgG antibody levels that may increase the susceptibility to allergic diseases such as AGS. In contrast, there were no significant changes in the IgE response, suggesting that both antibodies are independent in diagnosis of infectious and allergic diseases.

To further research, in the **Chapter 2D**, we studied the effect of saliva inoculation from ticks in a zebrafish model to simulate how it might affect humans. Tick saliva contains biomolecules such as PGE2 and alpha-Gal that affect host immune response and in this experimental approach we observed allergic hemorrhagic anaphylactic-type reactions and abnormal behavior patterns in zebrafish fed with red meat with alpha-Gal content after inoculation **(Franceschetti et al., 2009; Mihara et al., 2017; Haddad et al., 2018**). To identify the possible immune mechanisms associated with allergic reactions, we selected immune response and food allergy markers involved in Th1 and Th2 cell-mediated responses were characterized in the kidney and intestine of fish (**Huang et al., 2018; Lu et al., 2008; Martins et al., 2019; Liu et al., 2015**). Results confirm that these allergic reactions were associated with tissue-specific TLR-mediated responses in Th1 and Th2 cells with a possible

role for basophils in the immune response to tick saliva.

From another point of view, the tick-host-pathogen interactions were studied. We propose vaccines as the main solution to the conflict, at least the most effective and eco-sustainable known, to control ticks and vector-borne diseases (**de la Fuente et al., 2017**).

Chapter 3 give us a perspective of cooperation between all of them in a zebrafish model. The study presented in the **Chapter 3A** makes evident that vaccination with alpha-Gal increase the levels of TLR, AKR2, IL-1b and the natural anti-alpha-Gal IgM/IgG type antibodies and do not cause an increase in the IgE-type allergic response to tick saliva in zebrafish infected with *Mycobacterium marinum.* Therefore, the alpha-Gal-based vaccines could be applied to all hosts that do not produce alpha-Gal to protect against related diseases.

Thus, we developed the use of probiotics prepared with bacteria from the gut microbiota with high alpha-Gal content as a protective vaccine against mycobacteriosis in the zebrafish model. Treatment with probiotic *Aeromonas veronii* and *Pseudomonas entomophila* activated different humoral and cellular immune mechanisms, but all associated with the response to alpha-Gal **(Chapter 3B)**.

From my point of view, an increasingly optimal design of vaccines in the future must integrate the knowledge of continuous advances. Therefore, the new risk factors that are being discovered in the development of AGS and its consequences reported in **chapter 2** could address the progress that we mentioned above. In addition, it is crucial to continuously reinvent the use of new strategies when administering vaccines in their formulation, quantity and type, as we show in **chapter 3**. Thus, we could control multiple tick infestations and vector-borne diseases such as AGS.

In conclusion, analyzing the molecular mechanisms involved in tick-host-pathogen interactions by omics approaches and formulating more effective and economical vaccines that can be used worldwide, could be a good way to advance in the eradication of tick-borne diseases.

REFERENCES

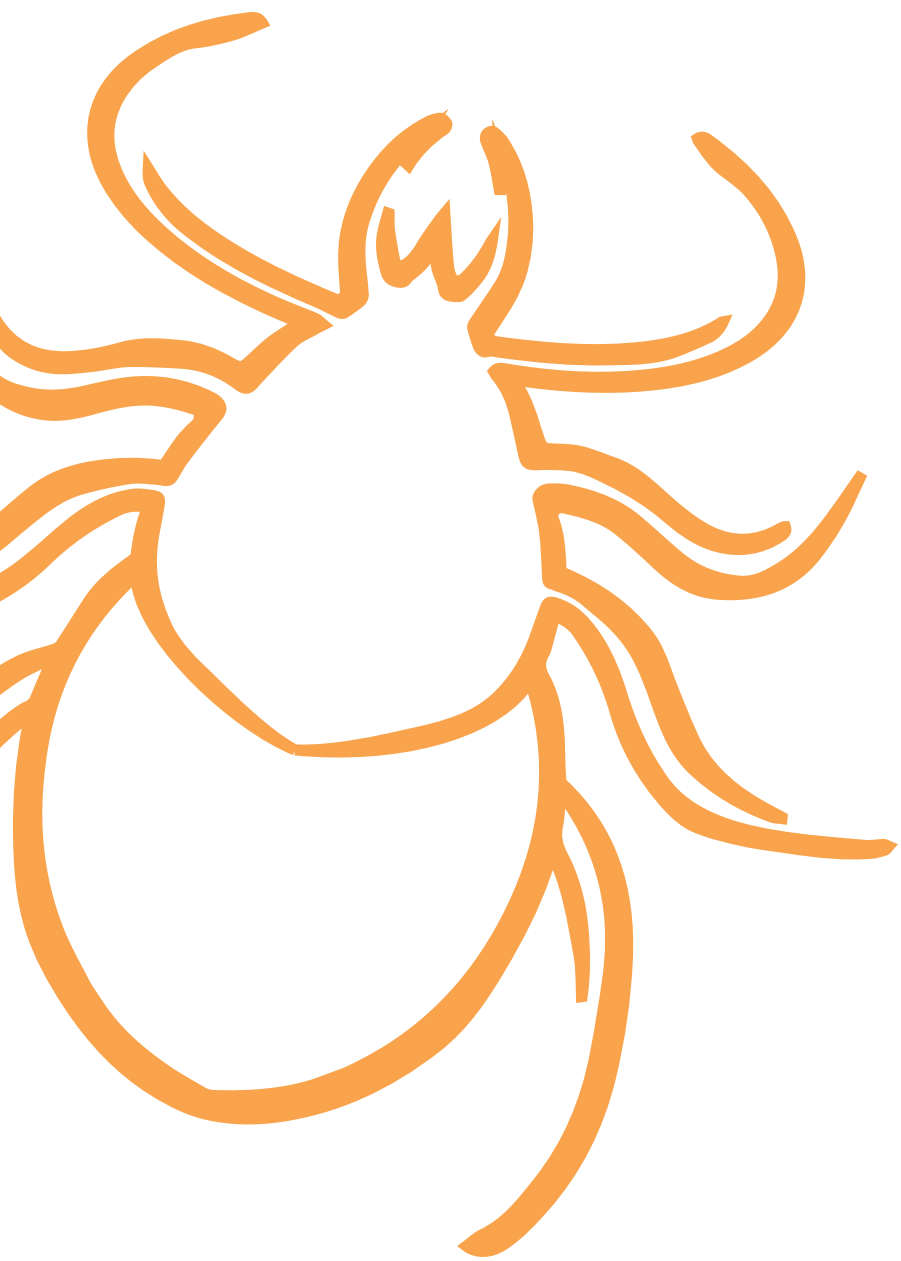

References

Cabezas-Cruz, A., Mateos-Hernández, L., Alberdi, P., Villar, M., Riveau, G., Hermann, E., Schacht, A. M., Khalife, J., Correia-Neves, M., Gortazar, C., de la Fuente, J. (2017). Effect of blood type on anti-α-Gal immunity and the incidence of infectious diseases. Exp Mol Med. 49(3), e301.

Cabezas-Cruz, A., Hodžic, A., Román-Carrasco, P., Mateos-Hernández, L., Duscher, G.G., Sinha, D.K., Hemmer,W., Swoboda, I., Estrada-Peña, A., de la Fuente, J. (2019). Environmental and molecular drivers of the alpha-Gal syndrome. Front Immunol. 10, 1210.

Cabezas-Cruz, A., Hodžić, A., Mateos-Hernández, L., Contreras, M., de la Fuente, J. (2021). Tick-human interactions: from allergic klendusity to the α-Gal syndrome. Biochem J. 478(9), 1783–1794.

Chinery,W.A. (1973). The nature and origin of the "cement" substance at the site of attachment and feeding of adult *Haemaphysalis spinigera* (Ixodidae). J Med Entomol. 10, 355–362.

Chmelař, J., Kotál, J., Karim, S., Kopacek, P., Francischetti, I.M., Pedra, J.H., Kotsyfakis, M. (2016a). Sialomes and mialomes: A systems-biology view of tick tissues and tick-host interactions. Trends Parasitol. 32(3),242–254.

Chmelař, J., Kotál, J., Kopecký, J., Pedra, J.H., Kotsyfakis, M. (2016b). All for one and one for all on the tick-host battlefield. Trends Parasitol. 32, 368-377.

Dantas-Torres, F., Chomel, B.B., Otranto, D. (2012). Ticks and tick-borne diseases: a One Health perspective. Trend Parasitol. 28 (10),437-446.

de la Fuente, J., Estrada-Peña, A., Venzal, J.M., Kocan, K.M., Sonenshine, D.E. (2008). Overview: ticks as vectors of pathogens that cause disease in humans and animals. Front Biosci. 13, 6938–6946.

de la Fuente, J., Villar, M., Cabezas-Cruz, A., Estrada-Peña, A., Ayllón, N., Alberdi, P. (2016). Tick-host-pathogen interactions: conflict and cooperation. PLoS Pathog. 12, e1005488.

de la Fuente J., Contreras M., Estrada-Peña, A., Cabezas-Cruz, A. (2017). Targeting a global health problem: vaccine design and challenges for the control of tick-borne diseases. Vaccine. 35, 5089–5094.

Eisen, L., Dolan, M.C. (2016). Evidence for personal protective measures to reduce human contact with blacklegged ticks and for environmentally based control methods to suppress host-seeking blacklegged ticks and reduce infection with Lyme disease spirochetes in tick vectors and rodent reservoirs. J Med Entomol. 53, 1063-1092.

Francischetti, I. M., Sa-Nunes, A., Mans, B. J., Santos, I. M., Ribeiro, J. M. (2009). The role of saliva in tick feeding. Front Biosci. 14, 2051–2088.

Galili, U. (2015). Significance of the evolutionary α1,3-Galactosyltransferase (*GGTA1*) gene inactivation in preventing extinction of apes and old world monkeys. J Mol Evol. 80, 1–9.

Gulia-Nuss, M., Nuss, A.B., Meyer, J.M., Sonenshine, D.E., Roe, R.M., Waterhouse, R.M., et al. (2016). Genomic insights into the *Ixodes scapularis* tick vector of Lyme disease. Nature Commun. 7, 10507.

Haddad, V. Jr, Haddad, M. R., Santos, M., and Cardoso, J. L. C. (2018). Skin manifestations of tick bites in humans. An Bras Dermatol. 93, 251–255.

Hilger, C., Fischer, J., Wölbing, F., Biedermann, T. (2019). Role and mechanism of galactose-alpha-1,3-galactose in the elicitation of delayed anaphylactic reactions to red meat. Curr Allergy Asthma Rep. 19, 3.

Huang, J., Liu, C., Wang, Y., Wang, C., Xie, M., Qian, Y., Fu, L. (2018). Application of in vitro and in vivo models in the study of food allergy. Food Sci Hum Wellness 7, 235–243.

Liu, X., Wu, H., Liu, Q., Wang, Q., Xiao, J., Chang, X., Zhang, Y. (2015). Profiling immune response in zebrafish intestine, skin, spleen and kidney bath-vaccinated with a live attenuated *Vibrio anguillarum* vaccine. Fish Shellfish Immunol. 45, 342–345.

Lu, M.W., Chao, Y.M., Guo, T.C., Santi, N., Evensen, O., Kasani, S.K., Hong, J.R., Wu, J.L.(2008). The interferon response is involved in nervous necrosis virus acute and persistent infection in zebrafish infection model. Mol Immunol. 45, 1146–1152.

Martins, R. R., Ellis, P. S., MacDonald, R. B., Richardson, R. J., Henriques, C.M. (2019). Resident immunity in tissue repair and maintenance: the zebrafish model coming of age. Front Cell Dev Biol. 7,12.

Mihara, M. (2017). Histopathologic study of the human skin in the early stage after a tick bite: a special reference to cutaneous tissue reaction to the cement substance of tick saliva. Yonago Acta Med. 60, 186–199.

Sharma, S.R., Karim, S. (2021). Tick saliva and the alpha-gal syndrome: finding a needle in a haystack. Front Cell Infect Microbiol. 11, 680264.

Steinke, J.W., Platts-Mills, T.A., Commins, S.P. (2015). The alpha-gal story: lessons learned from connecting the dots. J Allergy Clin Immunol. 135, 589–596.

CONCLUSIONS/ CONCLUSIONES

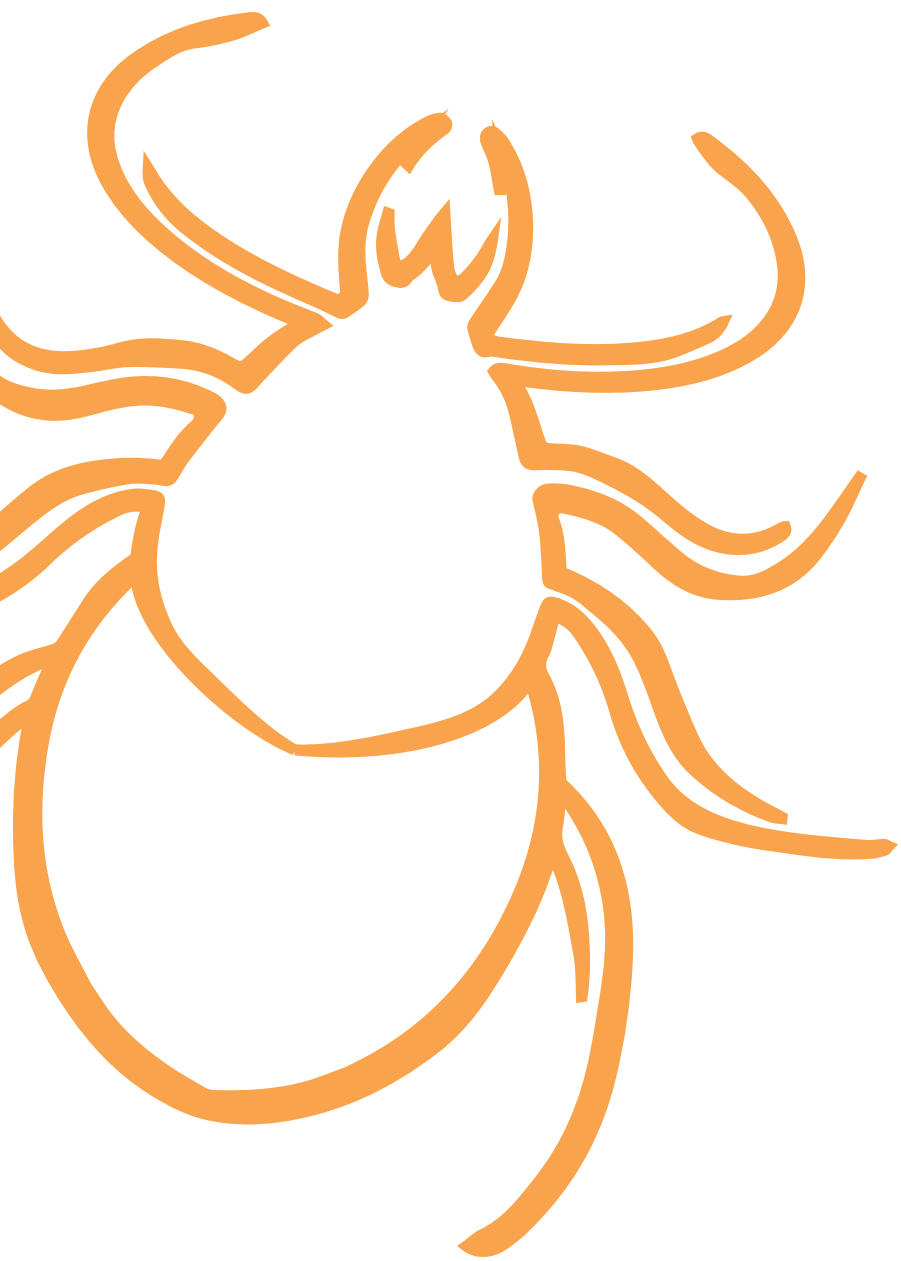

Conclusions/ Conclusiones

1. Characterization of tick-derived salivary proteins with alpha-Gal modifications using sera from AGS patients with severe symptomatology identified candidate disease biomarkers such as cytoglobin-1, 14-3-3 family chaperone and vitellogenin-1.

   La caracterización de proteínas derivadas de la saliva de garrapatas reactivas a sueros de pacientes con sintomatología grave del síndrome de alfa-Gal permitió identificar biomarcadores candidatos de la enfermedad tales como la citoglobina-1, chaperonas de la familia 14-3-3 y vitelogenina-1.

2. The application of proteomic approaches to the identification of tick and host derived proteins in the cementome of *Rhipicephalus microplus* revealed that a combination of them is an evolutionary adaptation to long-lasting ectoparasitic blood feeding.

   La aplicación de enfoques proteómicos para la identificación de proteínas derivadas de garrapatas y hospedadores presentes en el cementoma de Rhipicephalus microplus reveló que la combinación de ambas es una adaptación evolutiva a la alimentación con sangre durante largos períodos de tiempo por parte de estos ectoparásitos

3. A novel diagnostic method of the AGS based on measuring anti-alpha-Gal IgE titers and several cofactors such as blood type will facilitate an effective diagnosis of the syndrome.

Un novedoso método de diagnóstico del síndrome de alfa-Gal basado en la medición de títulos de IgE anti-alfa-Gal junto a otros cofactores determinantes como son los grupos sanguíneos facilitarán un diagnóstico eficaz del síndrome.

4. The immune pathways of anti-alpha-Gal IgM/IgG and IgE production are independent in AGS, GBS and allergy-type reactions to tick bites.

Las vías inmunitarias de producción de IgM/IgG e IgE anti-alfa-Gal son independientes en los síndromes de alfa-Gal y Guillain-Barré, así como en reacciones alérgicas a las picaduras de garrapatas.

5. Zebrafish is an animal model to simulate the allergic reactions that humans develop in response to tick saliva compounds.

El pez cebra es un modelo animal capaz de simular las reacciones alérgicas que desarrollan los humanos en respuesta a los componentes de la saliva de las garrapatas.

6. Alpha-Gal is a vaccine candidate antigen against pathogens with and without alpha-Gal modifications in hosts such as humans, birds and fishes that do not have the capacity to synthesize this molecule.

El alfa-Gal es un antígeno candidato para ser usado como vacuna frente a patógenos con y sin modificaciones de alfa-Gal en hospedadores como humanos, aves y peces que no tienen la capacidad de sintetizar esta molécula.

7. Novel use of probiotics prepared with bacteria with high alpha-Gal content induce protective mechanisms regulating immunity and metabolism in the zebrafish model against fish mycobacteriosis, being crucial for future research in the control of major infectious diseases worldwide.

El uso novedoso de probióticos preparados con bacterias con alto contenido de alfa-Gal induce mecanismos protectores que regulan la inmunidad y el metabolismo en el modelo de pez cebra frente a la micobacteriosis, siendo crucial para futuras investigaciones en el control de las principales enfermedades infecciosas en todo el mundo.

AGRADECIMIENTOS

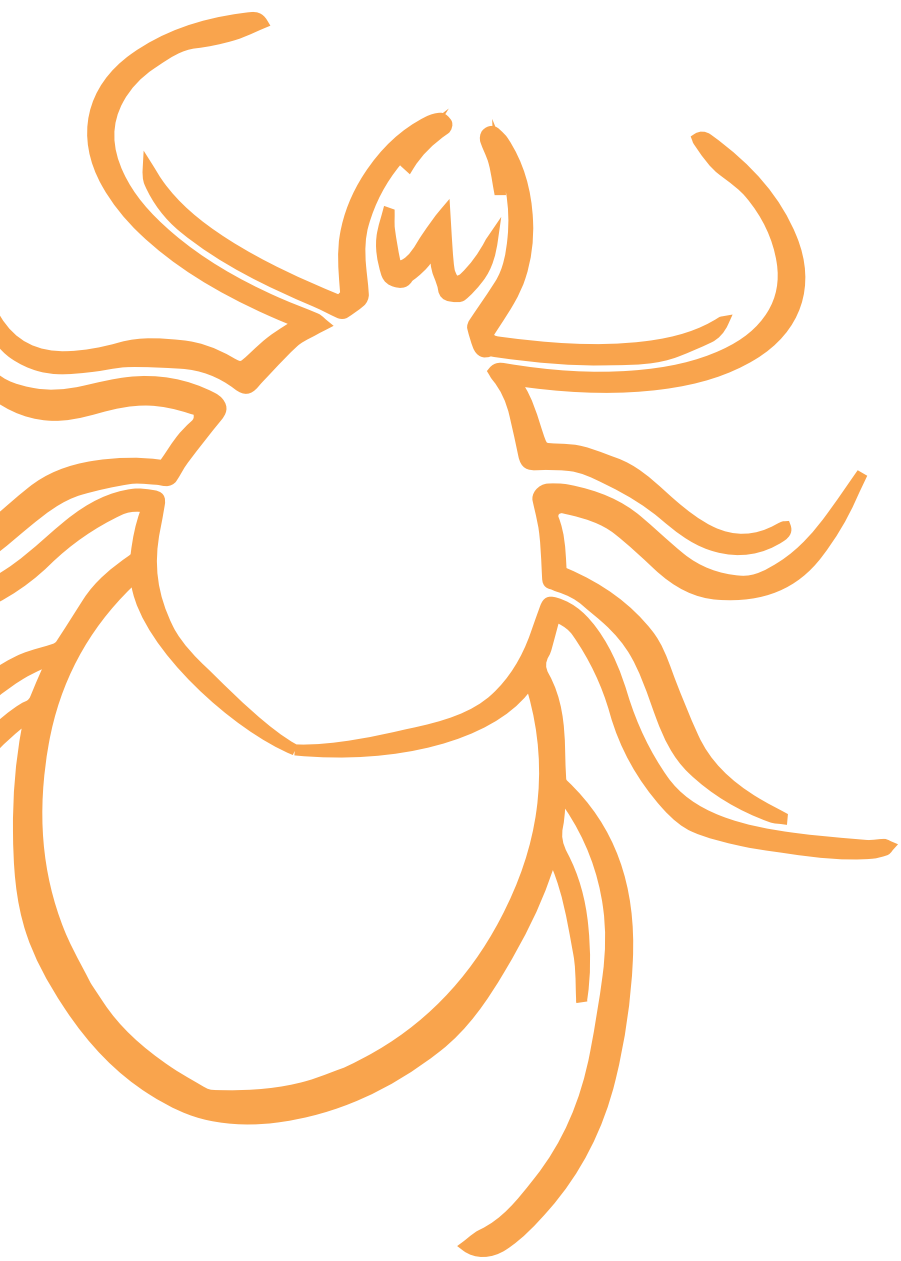

Agradecimientos

"Hace falta una vida para aprender a vivir"
Séneca

Presenta extraordinaria complejidad resumir en una serie de líneas todo aquello que debo agradecer, allá voy.

Primero, quisiera dar las gracias a toda la familia no biológica que ha llevado a cabo su papel de cicerone en mi etapa predoctoral. A Pepe, agradecerte con vehemencia la dedicación minuciosa en la dirección de mi tesis, por no dudar a la hora de incorporarme a tu grupo de investigación, por haberme tratado como si de un hijo se tratase; a tu hija Gaby y tu esposa Karelia, de las mujeres más amables que me he cruzado en la vida. Ojalá algún día os pueda dar buenas noticias.

A Marga, mi co-directora, amiga y compañera. Sin ti estas líneas jamás hubiesen sido escritas, aún recuerdo sin esfuerzo nuestro primer mail. Deseo que la vida te compense con el triple (al menos) de lo que tú aportas a los demás.

Agradecer la ayuda inmensa que he recibido por parte de Alejandro, mi co-director, tanto a nivel profesional como personal.

Especial mención merece el grupo de genómica del IREC, el escuadrón con el que he batallado vis a vis cada embolado y gozo. Comienzo por Marinela, Sara y Sandra, gracias por vuestra paciencia ingente, por darme vuestro tiempo y por haberme dado los mejores consejos y técnicas para perfeccionar

mi trabajo, sin vuestra ayuda mi avance estaría frustrado. Almudena, rubricas la frase anterior, más la atribución de ser mi protectora, amiga y apoyo fundamental. Angie, fuiste un pilar primordial en mi inicio, hasta el COVID me destinó a ocupar tu asiento y escritorio, no hubo día en el que no me acordase de ti al dirigirme hacia "nuestro rincón". Alberto, Isa, Marta, Pilar, Lourdes, Lorena, José Fran, Rubén, gracias por ayudarme siempre que lo he requerido. Paul, Part, Weronika, Hedvika, Gabriella, thank you for your kindness and fellowship in the lab. Por último, David, compañero de despacho de principio a fin, el único con el que he reído a carcajada limpia, el que me ha visto llorar en mis peores momentos, hemos saltado de alegría, brindado mil veces (y las que faltan), aconsejado otras tantas, empatizado el uno con el otro en cualquier situación; eres mi hermano no biológico, te voy a echar muchísimo de menos, de verdad, gracias eternas.

A todas las personas que forman parte del grupo SaBio y el conjunto del IREC. A Christian, Fran, Pelayo, Vidal, Bea, Úrsula, Encarni, Yolanda, Paqui, Pablo, Rafa, Olga, Mónica, entre otros investigadores. A Jon, uno de los mejores compañeros de despacho que se puedan tener, eres muy grande. A Sara, Alberto, Raúl, Patri, Saúl, Azahara, Chinchilla, Carmen, Elisa, Laia, Javitxa. Gracias a todos por prestarme vuestra ayuda.

A Ernesto, por su colaboración en los trabajos del síndrome de Guillain-Barré.

A Agustín, por ayudarme a identificar garrapatas y mil trabajos más.

A Edu, por adentrarme en el mundo de la microscopía electrónica.

A Jorge, un conserje fenomenal que lleva el humor allá donde va. Jamás se perdió nada de lo que pedí, por todo ello, millones de gracias.

A Ainhoa, que me hizo ver que una buena amistad no necesita mil años para forjarse, es de las que dan y dan, sin esperar nada a cambio. Te echo de menos.

Al personal de administración del IREC, que han tramitado todo aquello que he necesitado con la mejor voluntad y cariño. Carolina, Lucía, Pilar, Alicia, María y Ángela, os estoy muy pero que muy agradecido.

Mencionar la gran labor de Emilia, que no sólo desempeña su cargo, sino que además ha sido la única persona que logró subirme la autoestima a diario. Qué gran corazón.

Toca dar las gracias a amigos, compañeros de colegio, instituto, universidad, y conocidos varios, que me han encumbrado hasta escribir estas líneas: Antonio, Toñín, Kike, Seto, David, Patri, Puche, Diego, USA, Álvaro, Chema, Pardi, Ernesto, Chevy, María, José Manuel, Contreras, Carlos, Joselito, Rober, José Antonio, Vicente, Lourdes, Mari Ángeles, Olga, Pedro, Carlos Daniel, Leo, Nía, Ana, Esther, Paco, Blanca, Nevado, Josemaría, Inma, Fran, Germán, Alana, Carmen, Nando, Juanjo, Noelia, Kamila, Salomé, Simón, Soraya, Xyla, Chisco, Manu, Ismael, Miriam, Javier, Andrea, Maribel, Solomy, Esteban, Marilo, Iciar, Jesús, Xecar, Julian, Laura, Liz, Maria Fernanda, Manuel Vicente, Marina, Marta, Márquez, Mariate, Balao, Elías, Antoñiyo, Verónica, Miguel, Miriam, Miren, Silvia, Mari Loli, Naomi, Ramón, Reka, Rocío, Joky, Mer, Alberto, Guille, Chus, Santy, Sergio, Sonia, Virginia, Yai, Lauren, Isa… siento que me dejo a mucha gente en el tintero, pero intenté meteros a todos. A Osman, una de las mejores personas que conocí en UK, que siempre logra emocionarme y animarme; por supuesto, a Nico y Mia. A Ana, compañera de carrera, que ha sido mi mejor amiga en los momentos más importantes de la tesis, no tengo palabras. A Anita, que además de ser la mujer más guapa del planeta, también lo es su corazón. A Paquito, que me apoyó un montón en la carrera y a día de hoy ese afán perdura. A Sandra, que me ha dado los mejores consejos y sacado sonrisas cuando "pintaban bastos" en sentido figurado. A Víctor, cómo olvidarme de ti, que me has dado la vida que necesitaba en esta etapa, sólo tú consigues hacerme reír sin decir una palabra, gracias tron.

A los chicos del attica, cuantísimo voy a añorar vuestra presencia y las clases de spinning. A Cris, por ser la mejor profe posible. A Virtu, Elena, Anita, Víctor, Vicky, Maripaz, Javi, Rosana. Especialmente a Gonzalo, quien me ha acompañado cual guerrero hasta llegar a la meta. A Nuria y Rosi, que me han cuidado como si fuese un hermanito. A Fran, que día tras día me vio avanzar, mil gracias por tus consejos. Qué grandes sois.

A la gente de la playita, que tanta vida da, estén o no allí: Mari Carmen, Rafa, Puri, Blanca, Luis, Laura, Rafita, Andrea, Javi, María José, Noe, Benito, Marisa, Dori, Miquel, Mari Ángeles, Jaime, Teresa, Ignacio, Manolo, Enriqueta. Vicente, va por ti allá donde estés.

A la familia Agroborja S.L., que me abrió las puertas de su casa y gracias a ello aprendí a valorar el esfuerzo colectivo. A aquellas empresas de UK, que me brindaron la oportunidad de trabajar y abrirme al mundo.

A mis caseros de Granada, Jorge y Mari Carmen, que siempre han estado pendientes de mi y a día de hoy me muestran su cariño.

A mi casero de Ciudad Real, Pedro, que me trató genial en esta etapa.

A Agustina, que ha hecho posible que esta tesis luzca brillante.

Para acabar, agradecer al conjunto de mi familia todo ese apoyo recibido durante el transcurso de estos años. A mis tíos: Manolo, Alfonso, Olalli, Juanita, Reina, María Teresa y, especialmente, a Pedro, que va a vencer esa batalla, no me cabe la menor duda. A mis primos: Rafa, Ángel, Carmen Mari, José David, Manuel y, por último, a José Carlos, que dijo que quería ser científico como su primo; si llegas a leer estas líneas, me gustaría que tomases como referencia que si yo he llegado hasta aquí, tú puedes llegar todo lo lejos que seas capaz de proponerte, espero que nadie frene tus ilusiones, trabaja duro. A las parejas de mis primos y sus hijos. A mis abuelos que me ven desde el cielo.

Y, por último, pero no por ello menos especial, sino todo lo contrario, agradecer con toda mi energía y tesón todo lo que habéis hecho por mí desde que vi la luz en este mundo. A papá, mamá y mi hermano Josema, que sin vosotros siempre sería invierno, el azúcar tendría el gusto de la sal marina, y no conocería el significado del amor verdadero. Con vosotros todo, sin vosotros nada.

A Alba y a mi sobrina recién nacida, Roma, que traerá alegría y hará abuelita a mi mamá.

Llegados a este punto, he releído todo lo escrito en este apartado y, llevaba razón, era complicado sintetizar tanta bondad y buen hacer por vuestra parte.

Me llevo los buenos momentos y entierro los malos. Me llevo gente magnífica y una bonita experiencia.

Gracias a todos desde lo más profundo de mi corazón.

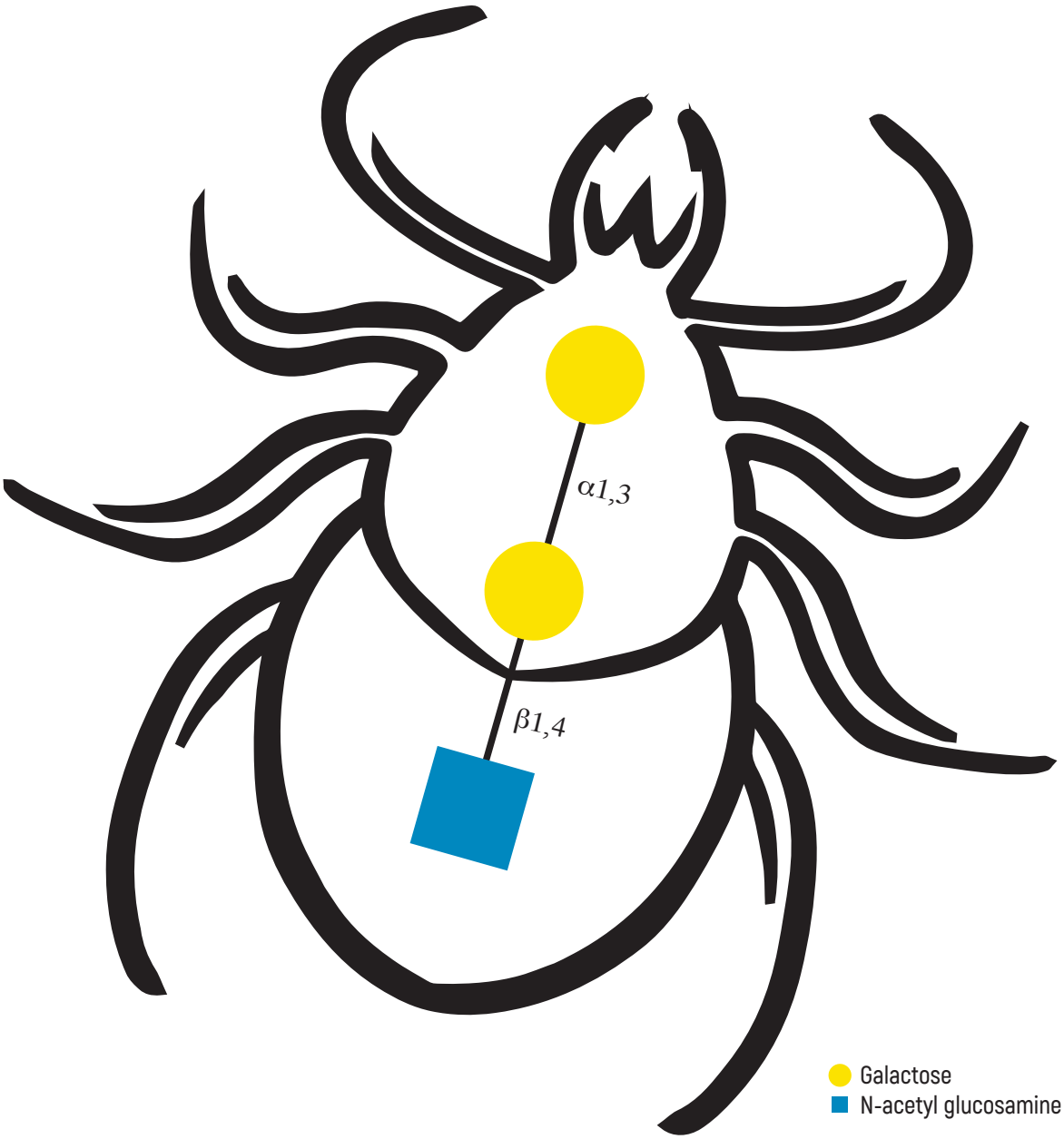

UNIÓN EUROPEA
Fondo Social Europeo
El FSE invierte en tu futuro

irec

CSIC
Consejo Superior de Investigaciones Científicas

Universidad de Castilla-La Mancha

Castilla-La Mancha